CLINICAL ANALYSIS OF LIVER FUNCTION

Development of a Novel Method for the Detection of Portosystemic Shunts

Todd James Matthews BHSc (Hons)

December 2013

Discipline of Surgery
School of Medicine
Faculty of Health Science

THE UNIVERSITY of ADELAIDE

An original thesis submitted in total fulfilment of the requirements of the degree of Doctor of Philosophy

Abstract

A portosystemic shunt (PSS) is defined as a congenital or acquired abnormal blood vessel that redirects blood around the liver without being filtered through hepatic parenchyma. PSS are thought to contribute to the distribution of isolated secondary metastases beyond the liver in 1.7 - 7.2% of all colorectal cancer patients without cirrhosis of the liver. No standardised clinical test for PSS yet exists and subsequently, the majority of PSS cases are detected incidentally through radiological means. To better identify PSS, a simple standardised clinical test for its detection is needed. The aim of this thesis was to develop a cost effective, non-invasive technique that can detect and measure PSS in a healthy liver model.

Methods

An artificial 8mm diameter PSS was created between the portal vein and the inferior vena in a pig model with a catheter inserted in the confluence of the hepatic veins for sample collection. A spectrum of compounds including indocyanine green (ICG), ^{13}C-methacetin, sorbitol and lignocaine, were injected into the portal system. To analyse the pharmacokinetic nature of the shunt and liver, Evans blue dye and ^{14}C-sucrose were also administered. ICG was measured via a LiMON® spectrometer attached to the pig's snout, while levels of the other indicators were measured by serial blood and breath sample collection over a 40 minute period. The process was repeated with the PSS clamped as the control.

Results

Of the administered compounds, only ICG had the potential to clearly identify and quantify the shunt due to the rapid serial sampling via the LiMON®. Further simulations using ICG demonstrated that the shunted fraction can be calculated using the transit times, including mean residence time, lag time and pharmacokinetic modelling.

Conclusion

Although this study has not yet provided a concise method for PSS detection available for immediate clinical use, it does provide a large foundation for further exploration into a quantitative technique. A future PSS test would allow an added risk assessment for secondary cancer, and consequently individual cancer therapy may be better targeted for individual patient care.

Thesis Declaration

I certify that this work contains no material which has been accepted for the award of any other degree or diploma in my name, in any university or other tertiary institution and, to the best of my knowledge and belief, contains no material previously published or written by another person, except where due reference has been made in the text. In addition, I certify that no part of this work will, in the future, be used in a submission in my name, for any other degree or diploma in any university or other tertiary institution without the prior approval of the University of Adelaide and where applicable, any partner institution responsible for the joint-award of this degree.

I give consent to this copy of my thesis, when deposited in the University Library, being made available for loan and photocopying, subject to the provisions of the Copyright Act 1968.

I also give permission for the digital version of my thesis to be made available on the web, via the University's digital research repository, the Library Search and also through web search engines, unless permission has been granted by the University to restrict access for a period of time.

Signed: _____

Date:_____

Preface

This thesis is the first stage toward portosystemic shunt (PSS) detection. Chapter 1 explores the range of PSS diagnosed in patients without liver disease and the associated method that was used for diagnosis, while also underlying the values for a need of a standardised clinical test. Chapter 2 replicates PSS by describing a surgical method to mimic a large PSS within a swine model. With an artificial PSS developed, chapter 3 describes the different practical dynamic techniques that may be plausible for PSS detection, with some viable techniques to be explored further. Chapter 4 studies the techniques chosen from chapter 3 in the PSS swine model and determines which technique is best suited for PSS identification and quantification. Chapter 5 reviews how the best technique from chapter 4 can quantify the shunt and what possible limits the shunt itself has with this technique. Finally, chapter 6 summarises this technique with a future outlook as to what PSS detection implications would have a clinical setting. This chapter also outlines the limitations and complications with the previous methods and what steps were used to overcome these problems. References and additional material can be found in chapters 7 and 8.

Acknowledgements

The author acknowledges the involvement of those who assisted with this study. Mr Mark Hamilton, Dr Nadia Blest and Dr Joe Dawson assisted in the surgical predication of a PSS. Dr Peng Li assisted in sample collection and analysis. Professor Simon Barry, Ms Betty Zacharakis and Ms Esther Burt assisted in breath sample analysis. Dr Timothy Kuchel and Mr Matthew Smith assisted in animal anaesthesia. Professor Guy Maddern supervised the entirety of this study. A special acknowledgment to Mr Markus Trochsler, who assisted in all aspects of this study.

Table of Contents

List of Tables, Figures and Equations

CHAPTER 1 Introduction

CHAPTER 2 Development of a Portosystemic Shunt in a Swine Model

CHAPTER 5 Determining Portosystemic Shunt Fractions

List of Abbreviations

Abbreviation	Definition
^{13}C-	[13]Carbon labelled
^{14}C-	[14]Carbon labelled
1-qQ	Difference of flow rate fraction
^{3}H-	3Hydrogen labelled
AUC	Area under curve
CF_4	Tetrafluromethane
CO^2	Carbon dioxide
CT	Computed tomography
CTA	Computer tomography angiography
CTC	Circulating tumour cells
CYP1A2	Cytochrome 1A2
D1	Drug administration site into the portal vein with the shunt closed (normal control).
D2	Drug administration site into the portal vein above the open shunt flowing into the liver only (control).
D3	Drug administration site directly into the start of the shunt.
D4	Drug administration site into the portal vein below the shunt.

E_{ICG}	Extraction of Indocyanine green
$E_{sorbitol}$	Extraction of sorbitol
f(t)	Inverse Gaussian distribution function
GLUTs	Glucose transporter
ICG	Indocyanine green dye
R15	Plasma disappearance rate at 15 minutes
IRMS	Isotope-ratio mass spectrometry
IVC	Inferior vena cava
MATEs	Mammalian multidrug and toxic compound extrusion
MEGX	Monoethylglycinexylidide
MRA	Magnetic resonance angiography
MRI	Magnetic resonance image
MRT	Mean residence time
MTT	Mean transit time
N2O	Nitrogen oxide
NTCP	Sodium-dependent taurocholate co-transporting protein
OATPs	Organic anion transporting polypeptides
OATs	Organic anion transporter

OCTs	Polyspecific organic cation transporters
Ost α and β	Organic solute or steroid transporter alpha and beta
PSS	Portosystemic shunt
PTFE	Polytetrafluroethylene
PV	Portal vein
Q	Flow rate
QC	Quality control
qQ	Fraction of flow
R^2	Correlation coefficient
RD	Relative dispersion
SD	Standard deviation
TIPS	Transjugular intrahepatic portosystemic shunt
TNM	Tumour node metastases staging system
TQEH	The Queen Elizabeth Hospital
TTD	Transit time
UV	Ultraviolet
VOC	Volatile organic compound

Publications, Presentations and Competitions

Publications, papers submitted for publication and conference presentations pertaining to results relating to the thesis are listed below. Abstracts, manuscripts and presentations can be found in Chapter 8: Appendices.

Published Abstracts and Conference Presentations

Matthews, T., Li , P., Hamilton, M., Trochsler, M., Butler, R., Roberts, M., and Maddern, G. J., *Clinical analysis of liver function: Can portosystemic shunts be measured?* , in *The Australiasian Surgical Research Society Meeting*. 2010, ANZ Journal of Surgery: Adelaide, South Australia. p. 11. (Appendix C)

Matthews, T., Li , P., Hamilton, M., Trochsler, M., Butler, R., Roberts, M., and Maddern, G., *Clinical analysis of liver function: Can portosystemic shunts be measured?*, in *The Australasian Surgical Research Society Meeting*. 2011, ANZ Journal of Surgery: Adelaide, South Australia. p. 8. (Appendix D)

Conference Presentations

Matthews, T., Li , P., Hamilton, M., Trochsler, M., Butler, R., Roberts, M., and Maddern, G. J., *Clinical analysis of liver function: Can portosystemic shunts be measured?* , in *The Queen Elizabeth Hospital Research Day*. 2011, The Hospital Research Foundation: Woodville South, South Australia. (Appendix E)

Matthews, T., Li , P., Hamilton, M., Trochsler, M., Butler, R., Roberts, M., and Maddern, G. J., *A novel non-invasive technique for the detection of portosystemic shunts*, in *The Queen Elizabeth Hospital Research Day*. 2012, The Hospital Research Foundation: Woodville South, South Australia. (Appendix F)

Competitions

Matthews, T. *Find that Shunt!* Three minute thesis competition. 2012. University of Adelaide, South Australia. (Appendix G)

Submitted Manuscripts

Matthews T, Trochsler M, Maddern G. Review of Incidentally diagnosed congenital and acquired portosystemic shunts in patients without cirrhotic liver disease: *a need for a standardised clinical test.* Submitted to British Journal of Surgery (Appendix H)

Matthews T, Trochsler M, Hamilton M, Maddern G. Creation of a portocaval shunt in pigs, with a method to estimating shunt fractions. Submitted to Journal of Surgical Research (Appendix I)

Matthews T, Barry S, Zacharakis B, Maddern G. Detrimental effect of isoflurane in gas chromatography. Submitted to Journal of Breath Research (Appendix J)

Matthews T, Kuchel T, Maddern G. Safe and inexpensive method for breath sampling and a technique for continuous intravenous anaesthesia in pigs. Submitted to Journal of Breath Research (Appendix K)

Matthews T, Weiss M, Li P, Trochsler M, Hamilton M, Roberts M, Maddern G. Portosystemic shunt fraction determination by pharmacokinetic modelling. Intended for publication (Appendix L)

CHAPTER 1

Introduction

1.1 Introduction

A portosystemic shunt (PSS) is defined as a congenital or acquired abnormal blood vessel that diverts a portion or all of the hepatic portal blood into the systemic venous system. Consequently the diverted blood does not pass through the liver sinusoidal parenchyma. Portosystemic shunts developing after birth may develop *de novo*, as a consequence of disease or as a result of human intervention, but still little is known about them. Normal human vascular anatomy does not contain any venous connections between intrahepatic portal branches and hepatic veins, nor are there any connections between superior mesenteric veins, splenic veins, extrahepatic portal veins and other systemic veins [1, 2]. PSS are often seen in patients with cirrhosis of the liver, but have also surprisingly been viewed in patients with functionally healthy liver, including patients without cirrhosis, fibrosis or hepatitis.

1.1.1 Classification

Portosystemic shunts are anatomically divided into two groups – extrahepatic (Figure 1.1) and intrahepatic (Figure 1.2). The English surgeon, John Abernethy FRS, first described extrahepatic vascular anomalies consistent with a PSS in the post mortem examination of a 10 month old infant in 1793 [3]. Consequently, these PSSs are now described as being of an "Abernethy" Type. Bellah *et al.* [4] were the first to image extrahepatic PSS, with more recent work by Morgan and Superina [5]

resulting in the description of Abernethy Types I and II (Figure 1.1). An Abernethy Type I PSS diverts all blood from the portal vein into the inferior vena cava (IVC) and the intrahepatic portal vein is absent. An Abernethy Type II PSS diverts a portion of the blood into the IVC with the portal vein being tortuous.

Few Abernethy Type I cases have been reported in detail with pathological examination, and therefore it is possible that an underdeveloped hypoplastic portal vein may still be present [6]. It is therefore suggested that the Abernethy classifications show variability, rather than definite clinical representation [2].

Doehner *et al.*[7] initially reported intrahepatic PSSs, however Mori *et al.* [8] was the first to image them and Park *et al.*[9] later categorised them into four types (Figure 1.2) based on their location in Coinaud's segments (Figure 1.3)[10, 11]. Park Type I is a single, constant diameter shunt from the intrahepatic portal vein to the IVC. In Park Type II, single or multiple shunts can be found between the intrahepatic portal branches and the hepatic veins within the same segment. Park Type III is a shunt, which has formed via a portal system aneurysm connecting to a hepatic vein, and in Park Type IV, there are multiple shunts between the portal branches and the hepatic veins in multiple segments.

There are several different classifications to describe PSSs. For the purpose of this thesis and to encourage standardisation of PSS classification, the Abernethy and Park descriptions will be used.

Table 1.1: Summary of Abernethy extrahepatic and Park intrahepatic portosystemic shunt definitions.

PSS	Type	Definition
Abernethy	I	All blood from the portal vein is diverted into the inferior vena cava, and the intrahepatic portal vein is absent.
	II	A portion of the blood from the portal vein is diverted into the inferior vena cava with the portal vein being thin and tortuous.
Park	I	A single, constant diameter shunt connecting the intrahepatic portal vein to the inferior vena cava.
	II	Single or multiple shunts can be found between the intrahepatic portal branches and the hepatic veins within the same segment.
	III	A shunt formed via a portal system aneurysm connecting to a hepatic vein.
	IV	Multiple shunts between the portal branches and the hepatic veins in multiple segments.

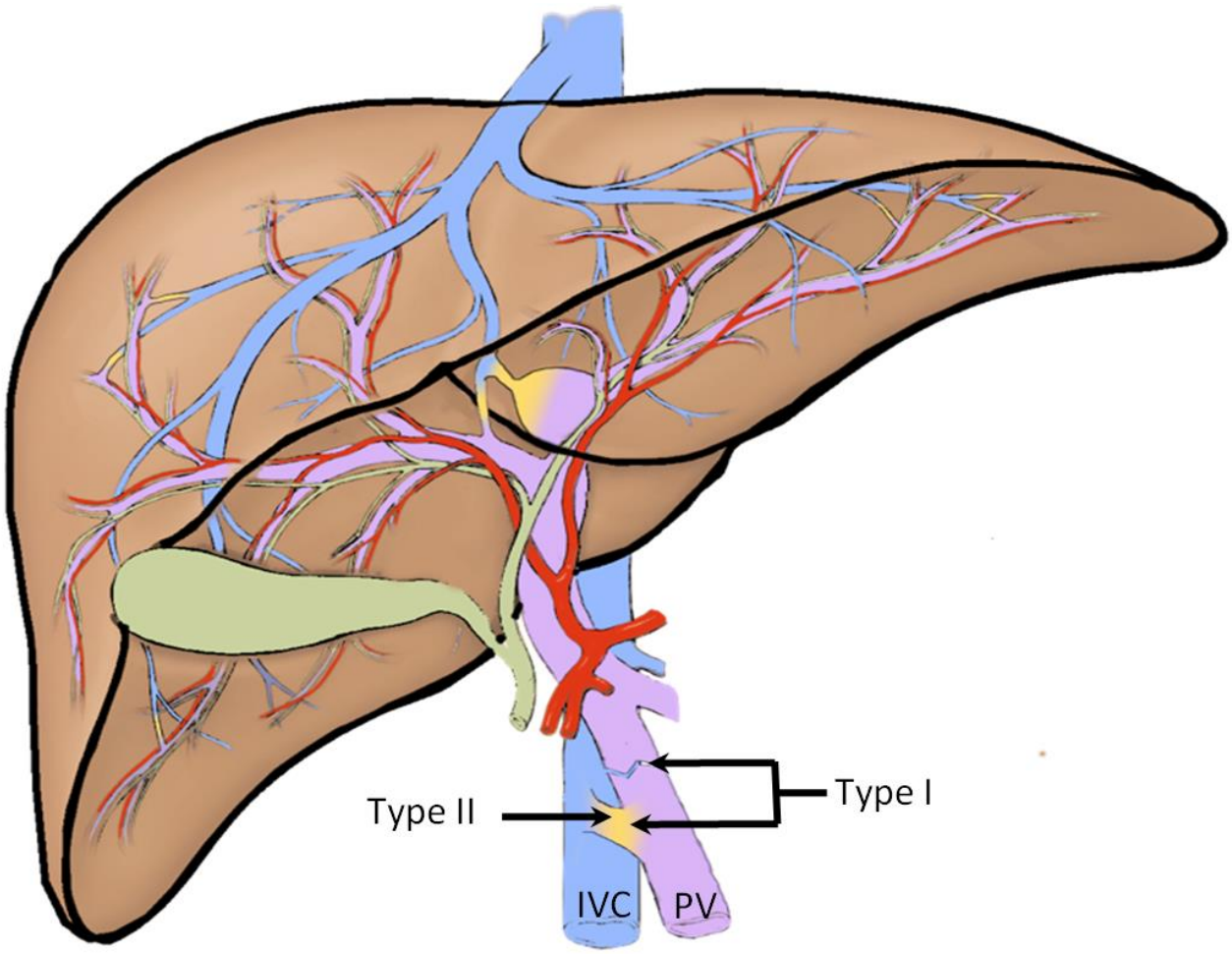

Figure 1.1: Extrahepatic Abernethy portosystemic shunts. Type I: All blood from the Portal Vein (PV) is diverted into the Inferior Vena Cava (IVC). Type II: a portion of blood diverted into the Inferior Vena Cava with the Portal Vein being patent, but tortuous.

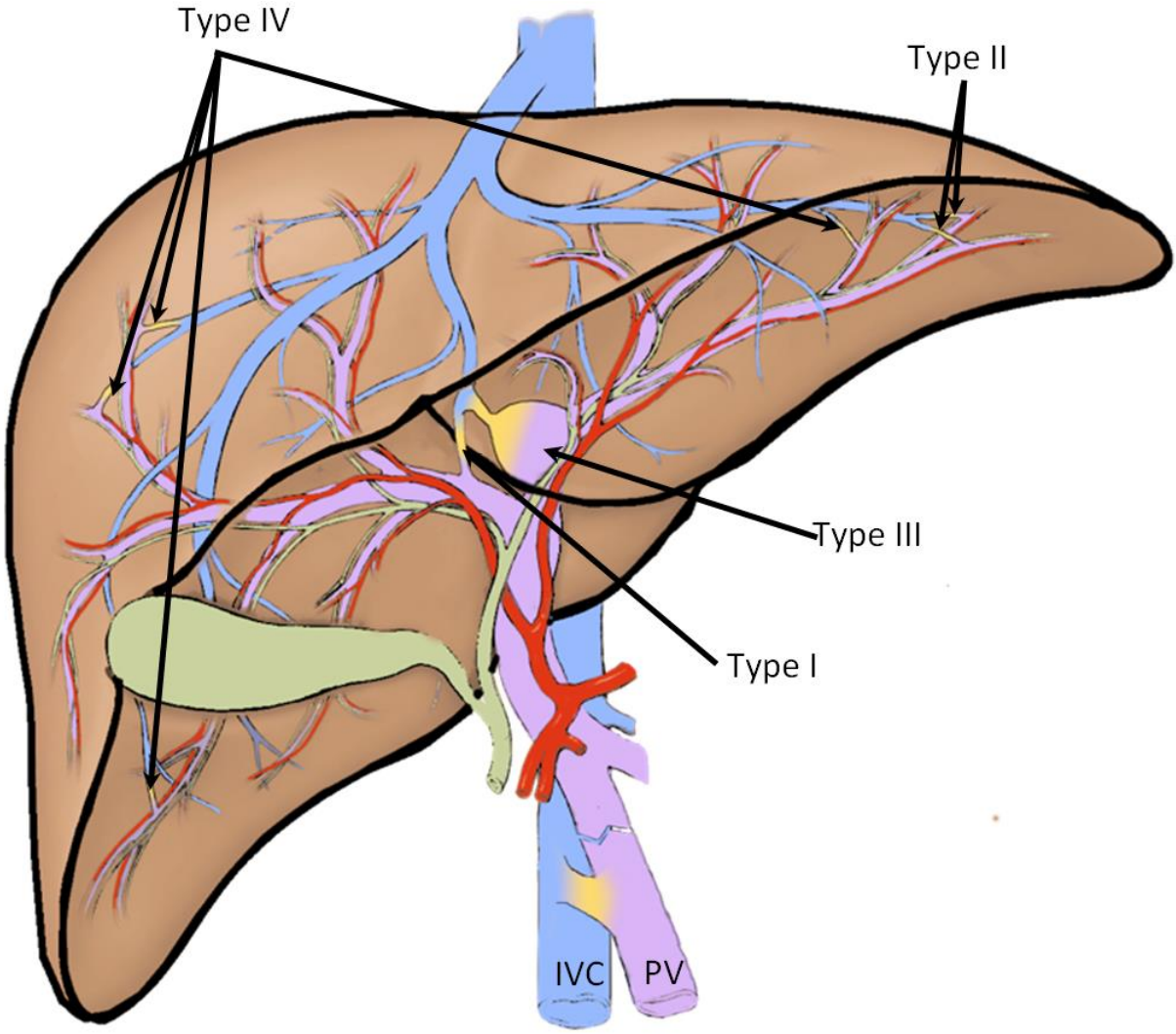

Figure 1.2: Park classification: Type I has a single, constant diameter shunt from the intrahepatic portal vein (PV) to the inferior vena cava (IVC). In Park Type II, single or multiple shunts can be found between the intrahepatic portal branches and the hepatic veins within the same segment. Park Type III has a shunt, which has formed via a portal system aneurysm connecting to a hepatic vein, and in Park Type IV, there are multiple shunts between the portal branches and the hepatic veins in multiple segments

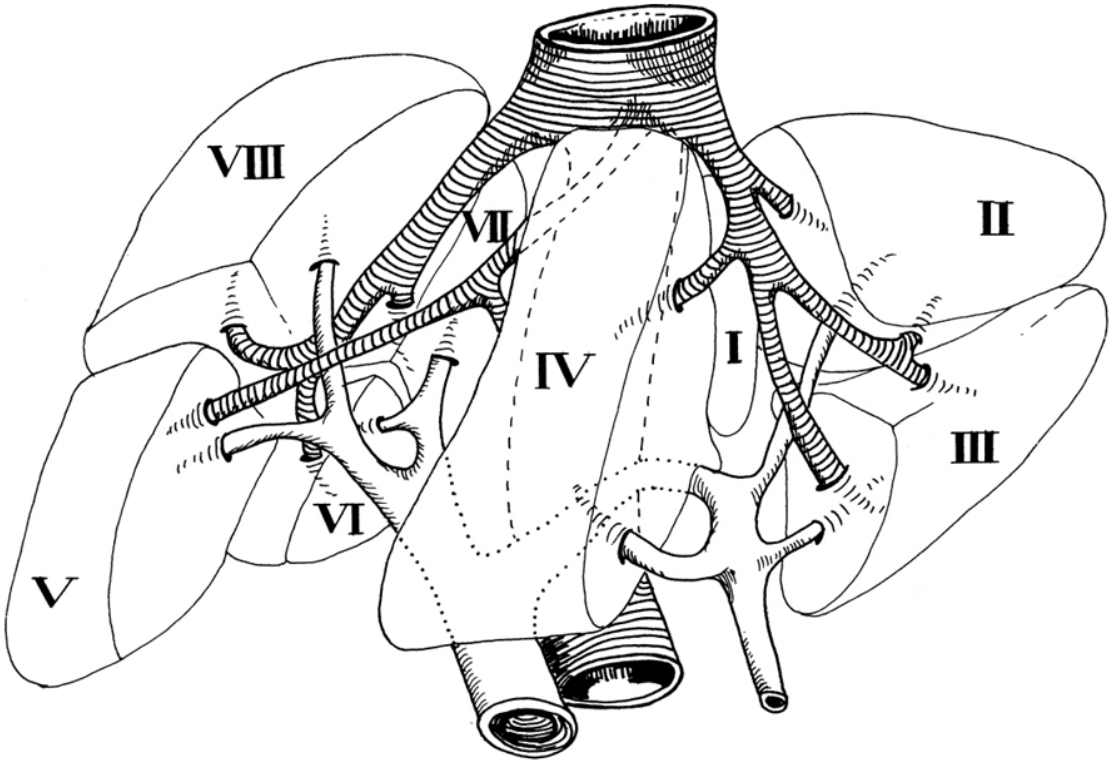

Figure 1.3: Human liver divided into segments according to Couinaud's nomenclature. The left lobe consists of segments I-IV, while the right lobe consists of segments V-VIII.

1.1.2 Portosystemic Shunt Variability Within The Classifications

Five types of classifications have been proposed for PSSs [12]. The Park and Abernethy classification is the most commonly used with some slight additions and variations. However, within the classification definitions, there is still some room for interpretation.

Abernethy and Banks [3] reported an abnormal IVC, however in most cases, the IVC is normal. A PSS may typically drain into the IVC anywhere between the level of the renal veins [13] to the confluence of the hepatic veins [14]. There are reports of a portal vein formed from the splenic and superior mesenteric veins ascending retrohepatically and connecting to the IVC above the confluence of the hepatic veins [15, 16]. There is also an additional report of a Type I PSS connecting directly the right atrium [5]. There cases reporting with variation when either the splenic or superior mesenteric vein join to another systemic vein, which are more commonly associated with Type I [2], or similarly the portal vein connects directly into a systemic vein other than the IVC. Other systemic veins may include left or right renal veins or azygos vein [6, 17-19]. Although rare, there are several reports of a shunt between the inferior mesenteric vein, or the superior rectal tributaries with the common left or right internal iliac vein [14, 20, 21].

In a typical Type II PSS, portal blood is partially shunted via the IVC posteriorly to the liver [22-24] and the intrahepatic portal vein is of normal appearance or

hypoplastic [24-26]. However, the shunt has been noted to be partly intrahepatic when traversing the caudate lobe [27]. Most cases note the hepatic artery and its' intrahepatic branches are enlarged [14, 23, 28], while the portal venules are small or not present [14, 15, 20]. However, some liver biopsies were reported as normal in appearance [29].

1.1.3 Incidence

Acquired PSSs are commonly recognised in patients with cirrhotic liver disease as a compensatory mechanism for the associated portal hypertension [30]. In contrast, congenital and naturally acquired PSSs are thought to be rarely recognised in healthy individuals or in patients with non-cirrhotic liver disease. It is speculated that PSSs only occur in 1/30,000 people, however this is based purely on a nationwide screening for galactosemia [12, 31]. Hypergalactosemia is a rare genetic disorder known to be associated with PSSs [32, 33]. Such PSSs have usually been serendipitously detected and more may be detected if there was a standardised clinical prognostic test. Neither the true incidence, the cause, nor the clinical effect of a PSS in healthy individuals or in patients with non-cirrhotic liver disease is known. The absence of a standard, simple, diagnostic procedure to detect and evaluate the entity contributes to this ignorance.

Abernethy Type I PSSs are more common in females [14, 23]. Abernethy Type II are thought to be more prevalent in males [23, 25], but this is not universally accepted

[6]. From 1971 to 2003, 61 cases of Abernethy extrahepatic PSSs were found, with a majority of Type I more commonly occurring in females [4-6, 13, 14, 16, 18, 20, 23, 34-53]. Although Type II extrahepatic PSS were not as common in these cases, the prevalence was similar in both males and females. PSSs have been reported at ages ranging from 31 weeks intrauterine life to 76 years (Type I) and 28 weeks intrauterine life to 69 years (Type II) [6].

Park Types I and II are far more common than Types III and IV [2]. A study by Glitzelmann *et al.* [54] in 145,000 infants, it was demonstrated that congenital PSS in infants are rare. A PSS was evident in only five infants through biochemical and ultrasound findings. Of these five infants, only one was documented in a case study. Although still rare, 34 Park Type PSSs and 17 Abernethy Type PSSs were identified [55]. However, more infants have been diagnosed with PSS in Japan than anywhere else in the world, and it is thought that the prevalence of congenital PSSs is higher in Japan as infants are routinely screened for hypergalactosemia [2, 25, 55].

1.1.4 Associated Malformations

Several congenital malformations are described in children with Abernethy PSSs. Cardiovascular anomalies including ventriculoseptal defect, coarctation of the aorta and atrioseptal defect are most prevalent in Abernethy Type I [5, 6, 13, 23, 25]. There are several further cases which report biliary atresia, some of which included splenic malformation syndrome (polysplenia, situs inversus and intestinal

malrotation) [5, 23]. Other uncommon associated conditions include multicystic dysplastic kidney, oculoauriculovertebral dysplasia, choledochal cysts, skeletal anomalies and cutaneous haemangioma [14-16, 56, 57].

Congenital malformations associated with Park Type PSSs are rarely seen, but biliary atresia, cutaneous haemangioma and congenital cardiac disease have been reported [54, 55, 58-60]. Congenital cardiac disease especially is thought to be linked to long durational PSS patency and aetiology [25, 61]. There are some reports that suggest there may be a general angiogenesis abnormality causing PSSs. Two patients with PSSs were reported, in association with multiple coronary artery fistulae [62], a left internal carotid-basilar anastomosis and absent vertebral arteries [60].

Fewer associated abnormalities and conditions have been reported in relation to Abernethy Type II, although they are similar to the associated conditions related to Type I [2]. These include pulmonary valve atresia, patent ductus arteriosus, oculoauriculovertebral dysplasia, polysplenia with IVC anomalies and Cornelia de Lange syndrome [6, 23-25, 63].

1.1.5 Symptoms and Complications

Few symptoms have been associated with Park Type PSSs, many cases of which are asymptomatic [2]. On occasion neonatal jaundice has been reported [2]. Two main

complications can occur as a result of PSSs. Firstly, hepatic encephalopathy is often a symptom of large PSS, and secondly PSSs may influence the development of intrahepatic tumours.

Hepatic encephalopathy is caused from circulating toxins affecting the cerebrum. These toxins are typically removed by the liver in a single pass, however a PSS avoids the metabolisation of the toxins. There can also be an increased concentration of bile acids, postprandial glucose, galactose, ammonia and nitrogenous substances, which may have an effect on the brain [55, 64]. Long standing PSSs can cause hypergalactosemia, which then may lead to cataract formation [64]. Often encephalopathy is related to the size and duration of the PSS [55], however, the vulnerability to hepatic encephalopathy increases with age [2].

The lack of, or severe reduction in intrahepatic portal blood flow may cause over arterialisation of the liver. This therefore can increase levels of hepatic growth factors such as insulin, glucagon or hepatocyte growth factor [65]. Any combination of these factors may encourage growth of benign hepatic tumours, such as focal nodular hyperplasia, nodular regenerative hyperplasia and adenoma [6, 14, 16, 20, 24, 41], or malignant hepatic tumours including hepatocellular carcinoma or hepatoblastoma [13, 56]. It is possible that these tumours may regress if PSSs are occluded, especially in patients with Abernethy Type II PSSs [2].

Experimental models and human patients have shown that reduced portal venous flow may cause some liver atrophy [66-68]. Animal models have also demonstrated that congenital PSSs in rats have developed hyperplastic nodules and hepatic atrophy [69, 70]. Portal venous blood supplies hepatotrophic factors from the digestive system including insulin and glucagon, which may cause decreased liver size due to a congenital PSS. However, other factors may be at play including an imbalance between liver regeneration and apoptosis [65, 67].

Other less common complications have been noted such as hyperandrogenism and hyperinsulinism due to an Abernethy Type I PSSs [71]. Hepatopulmonary syndrome was also seen in patients with Abernethy Type II [26, 72]. Some reports suggest that PSSs may cause fatty liver features, as these features disappeared after the PSS was occluded [73, 74].

1.1.6 Pathogenesis

Three different hypotheses have been proposed as a cause of extrahepatic shunts and two potentially for intrahepatic shunts. The congenital theory proposes that during the initial stages of foetal development, there are connecting venous networks between the subcardinal and vitelline venous systems, as well as between the portal branches and the caval tributaries, which may later form a PSS [75], similar to the intra-uterine circulation through the ductus venous. Most congenital PSSs will spontaneously self-occlude during the first 12 - 24 months of life, however

it is unknown how often this occurs [54, 58, 61, 64, 76, 77]. If the PSS does not occlude further complications can occur in adolescence and adulthood.

PSSs often occur in neonatal infants with a patent ductus venosus connecting the left portal vein to left hepatic vein via the umbilical recess of the liver [2]. Typically, this would start to occlude directly after birth with the liver being fully functional after 17 days [78-80]. It is thought that delayed closure may be the result of higher venous pressure and congenital heart disease [2]. The ductus venosus later forms the ligamentum venosum within the fissure between the caudate lobe and segment 3. Persistent patency of the ductus venous has only been diagnosed in 15 cases and was seen more in males than females [81]. Persistent patency is thought to be caused from or associated with either a genetic disorder [73, 82], or hypoplasia of the intrahepatic portal vein [81-83].

Development of Abernethy Type I has been associated with excessive involution of the periduodenal vitelline veins [15]. However, it is unknown if a PSS is the cause of a lack in development of the portal vein or if the lack of a portal vein causes the development of a PSS [2].

Moncure *et al.* [84] proposed the adhesion theory after a PSS was found at the site of intra-abdominal adhesion in a patient with mesenteric varices. A third theory

proposed by Akahoshi *et al*. [29] argues that PSSs are the natural result of idiopathic portal hypertension.

1.1.7 Detection and Assessment

Computed tomography (CT) and Doppler ultrasound scanning are the most frequently used imaging modalities for assessing the liver in adults, and therefore may account for the detection of most PSSs. These methods are commonly used to obtain images of vascular structures and there is considerable expertise required in their interpretation. However, there are several significant problems relating to the use of these techniques for the purpose of PSS detection. Both CT and Doppler ultrasound scanning can be time consuming when searching for a PSS. Furthermore, a simple CT scan of the abdomen has a similar amount of radiation (10mSv) to nine abdominal x-rays or 200 chest x-rays [85, 86] and therefore carries a significant radiation burden. Although Doppler ultrasound scanning does not involve any radiation, it can have a low sensitivity for some PSSs, especially if they are small. The efficacy of Doppler ultrasound scanning is dependent on the transducer used to identify the location and size of the PSSs and the skill of the operator [87]. Lisovsky *et al.* [88] reported that Doppler ultrasound scanning was unreliable in detecting PSSs, and suggested that PSSs are commonly undiagnosed.

It is possible that the lack of a portal vein is unseen via ultrasound due to decreased intrahepatic vascular visibility and decreased liver size [64]. Attempts to find an Abernethy Type I PSS, visual clues may include an enlarged hepatic artery and common bile duct at the hepatic hilum [64]. Similarly, a liver biopsy may indicate

the presence of an Abernethy Type I or possibly Type II PSS, with demonstration of absent portal venules, bile duct proliferation, arterialisation, and periportal fibrosis [82, 88]. However, these histological factors are not conclusive alone for a PSS [88]. With several indications, a CT would then be required to locate the Type I PSS.

1.1.8 Treatment

Surgical ligation or radiological occlusion can be used to treat PSS if it is surgically accessible [2]. Treatment is especially required if the PSS is the cause of hepatic encephalopathy or if there is a high risk of a benign hepatic tumour developing. Occlusion of PSS may not be safe in all cases especially if the portal vein is hypoplastic. Occlusion of the PSS may cause portal hypertension or hepatofugal flow. In some cases is may be deemed appropriate to surgically narrow the PSS and allow acclimatisation before occlusion [25]. For patients with an Abernethy Type I PSS, a liver transplant is currently the only viable treatment [5, 23, 89]. However, optimal treatment should be assessed separately for each patient.

Patients who are asymptomatic may not need treatment. In these cases, patients can be treated with a protein-free diet and regular administration of branched-chain amino acids and lactulose if any metabolic abnormalities occur [90].

1.2 Gastrointestinal Cancers

Colorectal cancer and associated secondary cancers are the third most common gastrointestinal cancer worldwide and the fourth most common cause of death. The most common sites for secondary gastrointestinal cancer can be identified liver and lung [91, 92]. Before the primary tumour has been discovered, between 15 - 20% of patients will have secondary metastases [93]. Over a four year period, 754 patients were diagnosed with gastrointestinal cancer, including 12% being diagnosed colorectal cancer. Interestingly, 6% of the colorectal cancer patients were also diagnosed with isolated secondary lung metastases [94]. Tan *et al.* [94] estimated that between 1.7 - 7.2% of colorectal cancer patients have isolated secondary lung metastases.

Veins from the gastrointestinal organ drain into the portal system (Figure 1.4) [95] and is therefore clearly understood as to how cancer may spread beyond the liver, without the liver obtaining metastases itself. Theoretically, cancers spreading via the bloodstream should be trapped by the liver, rather than progress further and generate distant metastases. One possible theory to this obscure metastatic distribution phenomenon is that PSSs play a role in facilitating the distribution of cancer, however this remains to be investigated.

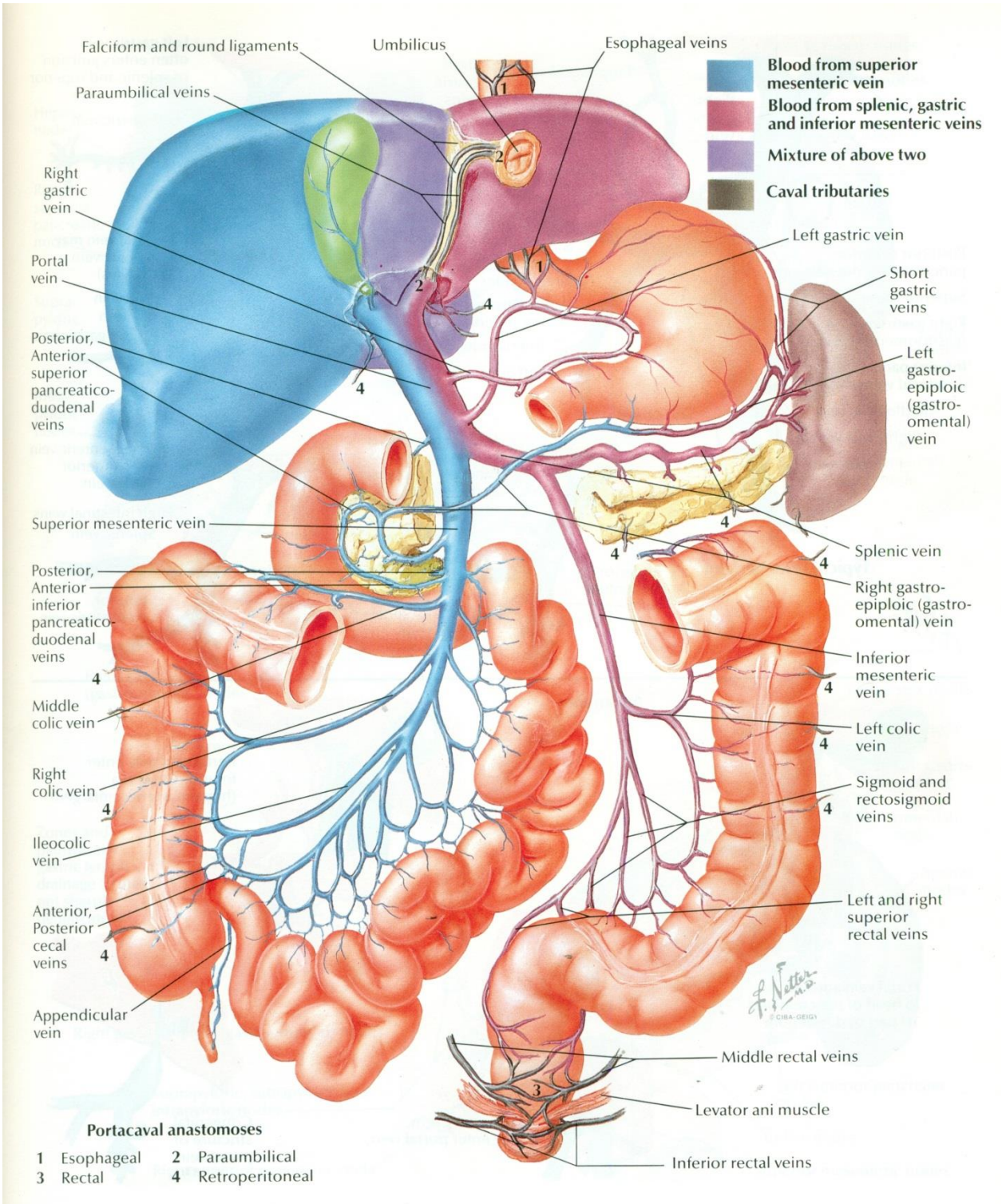

Figure 1.4: Gastrointestinal organs with venous drainage into the portal system [95].

1.2.1 Circulating Tumour Cells

Circulating tumour cells (CTC) are cancer cells that have originated from a primary tumour and circulating through the vascular system or lymphatic system [96]. The quantity of CTC that are released into the blood stream from a primary cancer is unknown [97] as their detection is difficult given there are only 1 to 10 CTC per millilitre of whole blood as compared to the millions of white blood cells and red blood corpuscles [98, 99]. It is speculated that CTC distribution mostly occurs from haematogenous dissemination [97, 100-103]. Dissemination into surrounding lymphatics of the primary tumour is often a dead end rather than the route of CTC metastasising and further spreading CTC [104]. It is estimated that only 0.01% of CTC will actually proliferate into a metastasis [105].

1.2.2 Metastases Distribution

A hypothesis, first proposed in 1958 by Lore *et al.* [106] and later studied by Saitoh *et al.* [107], suggested that PSSs could be one of the routes responsible for the distribution of gastrointestinal metastases to distant organs, for examples colorectal metastases into the lung rather than the liver. Theoretically, CTC from colorectal carcinomas should be 'trapped' by the liver, without further dissemination. However, according to this hypothesis, a PSS may act as a direct or indirect route for metastatic cancer cells to reach the pulmonary vascular system. If this hypothesis is correct, it is possible that detection and elimination of a naturally occurring PSS in cancer patients could prevent some forms of metastatic disease, or provide a prognostic indicator.

Wallace *et al*. [108] noted secondary metastases in two of their patients who had been implanted with artificial PSSs. Implantation of a transjugular intrahepatic portosystemic shunt (TIPS) was successfully performed in 37 patients. TIPS is an artificial shunt that has been more widely used within the last decade to treat portal hypertension and other complications [108]. Two of these patients who were previously diagnosed with pancreatic neuroendocrine tumours had been identified with thoracic metastases and <5 mm nodules in the lungs, ten months after the TIPS procedure without hepatic metastases. The TIPS is most similar to Park Types I or II PSSs, depending on the site of the stent. Although, PSS diameters may be different to that of TIPS, the effects remain similar. The report by Wallace *et al.* [108] is an example of cancer patients that are later diagnosed with pulmonary nodules (secondary tumours) which may be due to TIPS. Therefore, it is possible that metastases beyond the liver may occur via a PSS.

CTC may still pass through the liver without a PSS provided they are not detected by the hepatic immune system. CTC must pass via the vascular bed within the sinusoid wall, which contains phagocytes, called Kupffer cells and liver-resident macrophages. These Kupffer cells and macrophages are the first line of defence in removing unwanted cells and particles, including CTC [109-111]. For a CTC to be undetected and disseminate further ligands on the CTC membrane need to be modified through a multi-step process to give the 'appearance' of a normal cell.

The biophysics of endothelial cell and CTC interaction is still not entirely understood [112]. CTC undergo several stresses including shear hemodynamic stress, immune-

surveillance and anchorage-dependent survival signalling [113] during movement through the extracellular matrix and vascular system. With these stresses, CTC roll and adhere along the epithelium via selectins and their specific binding selectin-ligand. There are three types of selectins, L-, E- and P-selectin which are a type of glycoprotein found in the transmembrane that bind to corresponding glyconjugates or ligands on other cell membranes [112-115]. As the CTC move through the extracellular matrix and vascular system, they interact with different haemeopotoeic and endothelial cells, which consequently modifies their selectin ligands. This allows the CTC to acquire the potential to create site specific metastases [113]. Notably, colorectal carcinoma CTC injected into the portal system of E- and P-selectin knockout mice caused 84% fewer lung metastases as compared with normal mice [116]. This suggests that some CTC dispatched from colorectal carcinomas particularly acquire E- and P-selectin ligands, which are specific for the lung and still bypass the hepatic immune system.

Notwithstanding the strategies that CTC may employ to circumvent hepatic surveillance, the presence of a PSS may increase the concentration of colorectal carcinoma CTC reaching the lungs.

1.3 Summary

Naturally occurring and congenital PSSs are not a widely understood area, especially when found in patients without cirrhosis. Although, believed to be rare, it is possible that microscopic Park Type PSSs maybe still present in some patients.

Gastrointestinal cancers are far more common in adults, and it is debatable as to how these cancer patients have metastatic dissemination beyond the liver, without metastases in the liver. PSS may be one factor that increases the risk of secondary cancer occurring. However, there are no standardised clinical tests to detect PSS, which therefore limit the number of PSS studies.

This chapter further reviews the available literature regarding: (a) congenital or naturally acquired PSSs in adult patients with functionally healthy livers (without cirrhosis, hepatitis or fibrosis.); and (b) the allied methods used to diagnose and characterize these PSSs. Reports regarding surgical PSSs and children under the age of 18 years old were excluded from this review.

1.4 Objectives

1. To review the occurrence of congenital or acquired PSSs in adult patients, with normal liver function.
2. Explore similarities between patients including age at diagnosis and symptoms.
3. What methods have been able to incidentally detect these PSSs and which are the most prevalently used methods.

1.5 Question

In adults, with normal liver function and congenital or naturally acquired PSSs and no plausible associated cause, what is the most frequently used diagnostic procedure?

1.6 Methodology

1.6.1 Search Strategy

Inclusion and exclusion criteria were defined. Articles were included if the patient was human, patient(s) had a natural PSS, functionally healthy liver, were equal to or older than 18 years and the article was in English. Articles were excluded if the patient(s) had a surgical PSS, diseased liver including cirrhosis, fibrosis or hepatitis, were younger than 18 years, was an animal, or the article was not written in English.

PUBMED, EMBASE, MEDLINE and Cochrane Library searches were performed using the terms listed in Search Term 1.1 and has been formatted for a PUBMED search. Due to the numerous articles containing a surgical PSS, PSSs caused by liver disease, PSSs found in children and animals, a ‘NOT’ section was included, which excludes all articles containing elements of the exclusion criteria. If the patient could not be determined as an adult or the state of the patient's liver could not he clearly defined, the article was not included for review.

“portosystemic shunt OR portocaval shunt OR portasystemic shunt OR portacaval shunt[tw] OR porto systemic shunt[tw] OR porto caval shunt[tw] OR portal systemic shunt[tw] OR portal caval shunt[tw] OR mesocaval shunt[tw] OR splenorenal shunt[tw] OR portosystemic shunts[tw] OR portocaval shunts[tw] OR portasystemic shunts[tw] OR portacaval shunts[tw] OR porto systemic shunts[tw] OR porto caval shunts[tw] OR portal systemic shunts[tw] OR portal caval shunts[tw] OR mesocaval shunts[tw] OR splenorenal shunts[tw]”

“NOT (portasystemic shunt, surgical[mh] OR transjugular[tw] OR tips*[tw] OR dog[tw] OR dogs[tw] OR cat[tw] OR cats[tw] OR foetus[mh] OR umbilical veins[mh] OR caput medusa[tw] OR liver transplantation[mh] OR transplant*[tw] OR budd-chiari syndrome[tw] OR neonatal[tw] OR fibrosis[tw] OR fibrotic[tw] OR thrombosis[mh] OR prenatal[tw] OR foetus[tw]) AND (Humans[Mesh] AND English[lang] AND adult[MeSH])”

Search Term 1.1: Search terms formatted for PUBMED used to find naturally occurring or acquired portosystemic shunts in adults without cirrhosis.

1.6.2 Search Results

A total of 429 articles were identified from PubMed and Medline, from which 114 articles were included after reviewing the abstracts. An Embase search of the same keywords found a total of 266 articles. Following a review of the abstracts, 53 articles were included. A search for the term 'aneurysmal spontaneous portosystemic shunts' yielded 14 additional articles, of which eight were included. No articles were identified in the Cochrane Library. A total of 175 articles were selected for full text review. After reading through full texts, 80 of the 175 were deemed appropriate for inclusion in this review. Articles that were still found to contain patients with cirrhotic liver disease, patients who had a surgical PSSs or where data could not be clearly identified such as age were excluded from this review (Figure 1.5).

All but ten articles, which were retrospective cohort studies, were case studies. Data extracted from these 80 articles included age, sex, symptoms, medical history, PSS detection method, treatment, blood test results including ammonia levels and indocyanine green dye retention at 15 minutes (ICG R15) and Abernethy or Park Type PSS. If the article did not explicitly specify the Type of Abernethy or Park PSS, it was categorised into one of the Abernethy or Park Types according to its description. Splenorenal and gastrorenal shunts were categorised under Abernethy Type II.

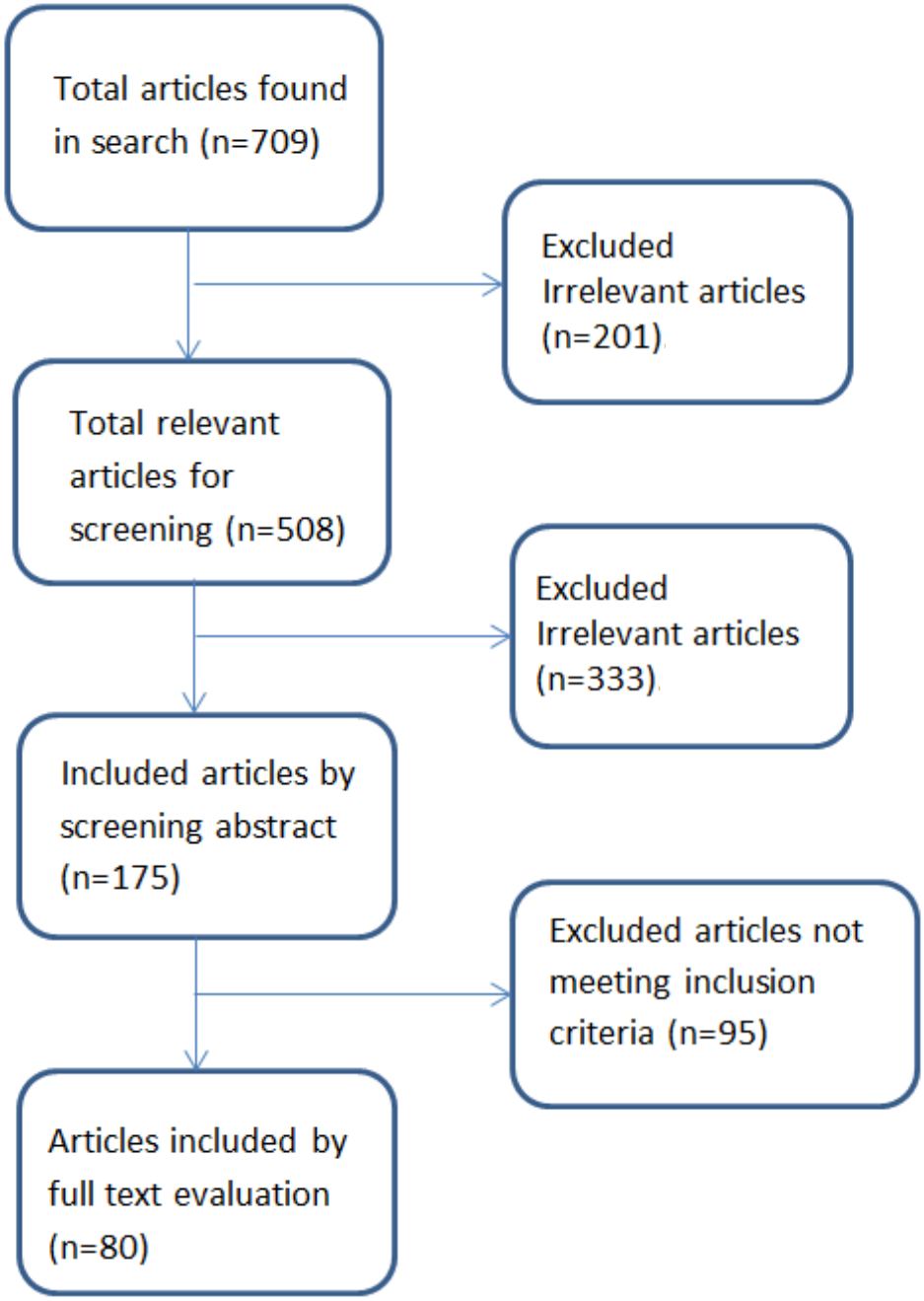

Figure 1.5. Flow chart of the systematic search strategy.

1.6.3 Demographics

In 80 clinical research articles, our analysis revealed that 112 patients were diagnosed with either an extrahepatic (Abernethy) or intrahepatic (Park) PSS. With regards to PSS sub-type, of these 112 PSS cases a total of 49 patients (43.8%) presented with extrahepatic Abernethy PSS and 61 patients (54.5%) were found to have intrahepatic Park PSS. In two patients the shunt type could not be specified (Table 1.2). Overall, PSSs were more prevalent in women than men (69 and 41 respectively). The exception to this finding was in the Abernethy Type I subset, where there were six males and two females.

Patients were commonly diagnosed with a PSS at a median (range) age of 51 (18 – 87) years for males and 55 (18 – 90) years for females (Table 1.3). The median age of patients with an Abernethy PSS was 50 (18 – 84) years, while the median age in patients with a Park PSS was 57 (18 – 90) years.

1.6.4 Frequency of Diagnostic Procedures

PSSs were detected and confirmed in 81 of the 112 patients (72.3%) using a single imaging method (Table 1.4). Doppler ultrasound scanning, computed tomography and computed tomography angiography (CT/A) were the most common with 26 and 24 patients respectively.

In 31 patients (27.6%) two or more imaging methods were required to confirm the presence of a PSS (Table 1.4). Of these combined methods, Doppler ultrasound and

CT were the most commonly used conjointly in 15 patients of the 26 patients that required a combination of two methods.

1.6.5 Symptomatology and Associated Conditions

Only 72 cases report on symptoms and associated conditions. The majority of the symptoms reported were neurological symptoms including encephalopathy, disorientation/ataxia, dysarthria and nausea (Table 1.5). Encephalopathy was the most common and reported in 27 cases. The next most common symptom and complaint were hyperammonemia in 18 patients and abdominal pain in 16 patients, while five patients did not report any symptoms.

Idiopathic portal hypertension and Osler-Weber-Rendu syndrome, also known as hereditary haemorrhagic telangiectasia, are both believed to be associated with PSSs, and were seen in eight and five patients respectively. However, in 34% of cases PSSs were an incidental finding while testing for indirect or non-associated diseases. Some of these diseases included ovarian, oesophageal, mammary, gastric, colon, urinary tract and rectal carcinomas.

1.6.6 Other Investigations:

Other clinical investigations reviewed included, blood ammonia levels, ICG R15 and reported PSS flow rates. Analysis of included studies revealed 26 patients (23.2%) with reported ammonia levels, ranging from 41.9 to 424 μg/dL. Of these 26 cases,

18 patients had above normal levels, 30 to 85 μg/dL with a median of 130 μg/dL, ranging from 89 to 424 μg/dL [117].

One study reported on ICG R15 in 14 patients, which is commonly used as a liver function test. A normal ICG R15 after 15 minutes is <10% [118]. In 11 cases, the ICG R15 was remarkably high, even though their liver was classified as 'healthy'. Normal ICG R15 is described in three patients, while the remaining 11 patients showed an elevated IGC R15 ranging from 13 to 47.5%, with a median of 39%. Of the three patients with normal ICG R15 levels, two were found to have a Park Type II PSS with a low shunting ratio of <9%. The third patient had a Park Type III PSS with a large 11 cm aneurysm with turbulent flow. The slow flow in the shunt may account for the normal ICG R15 results.

Seven cases reported the shunt ratio and/or flow rate as measured by Doppler ultrasound (Table 1.6). The shunted ratio ranged from 15.7 to 39.5%, with a median of 25.5% and the shunt flow rate ranged from 0.17 to 1.2 L/min with a median of 0.33 L/min. Three cases with Park Type III PSSs demonstrated 6 mmHg, 8 mmHg and 17 mmHg pressure gradients between the portal branches and hepatic veins [119-121].

Table 1.2: Prevalence of the type of shunt in male and female patients.

Shunt Type		**Males**	**Females**	**Total**
Abernethy	Type I	6	3	9
	Type II	17	23	40
Park	Type I	1	5	6
	Type II	6	17	23
	Type III	9	14	23
	Type IV	2	7	9
	Unknown	-	-	2
	Total	41	69	112

Table 1.3: Median age at diagnosis of shunts n=104 (no data reported in eight patients)

Shunt Type		Median (years)	Range (years)
Abernethy Type I			
	Male	51.5	24 - 63
	Female	33	28 - 42
	Both	42	24 - 63
Abernethy Type II			
	Male	48	20 - 67
	Female	51	18 - 84
	Both	50.5	18 – 8 4
Park Type I			
	Male	68	68
	Female	58	43 - 69
	Both	62.5	43 - 69
Park Type II			
	Male	53.5	24 - 67
	Female	59	22 - 90
	Both	56	22 - 90
Park Type III			
	Male	53	18 - 87
	Female	59	27 - 89
	Both	57	18 - 89
Park Type IV			
	Male	54.5	43 - 66
	Female	47	34 - 68
	Both	47	34 - 68

Table 1.4: Different methods used for detection of naturally occurring portosystemic shunts in patients without hepatic cirrhosis. CT/A – computed tomography/angiography. MRI/A – magnetic resonance imaging/angiography. n=number of patients.

PSS Type	**Abernethy**		**Park**						
Method	**Type I**	**Type II**	**Type I**	**Type II**	**Type III**	**Type IV**	**Unknown**	**Total**	**Reference**
Doppler Ultrasound	1	4	2	7	10	2	-	26	[118, 119, 122-136]
CT/A	1	10	1	5	2	3	2	24	[19, 75, 86, 137-153]
Angiography/X-ray	-	13	-	2	1	3	-	19	[8, 51, 117, 154-169]
Scintigraphy	-	6	-	1	-	1	-	8	[170-174]
MRI/A	1	2	-	1	-	-	-	4	[175-178]
Combination of 2 methods	3	5	3	6	8	-	-	25	[118, 121, 126, 134, 143, 167, 179-187]
Combination of 3 methods	2	1	-		1	-	-	4	[120, 143, 188, 189]
Combination of 4 methods	-	-	-	1	1	-	-	2	[25, 190]
Total single method	3	35	3	16	13	9	2	81	
Total combinations	5	6	3	7	10	-	-	31	
Total	8	41	6	23	23	9	2	112	

Table 1.5: Symptoms and pre-existing conditions in patients with Abernethy and Park type portosystemic shunts.

	Abernethy Type		Park Type				
Symptom	**I**	**II**	**I**	**II**	**III**	**IV**	**Total**
Neurological symptoms							
Encephalopathy	1	18	1	3	3	1	27
Disorientation/Ataxia	-	4	2	1	2	2	11
Dysarthria	-	3	1	-	1	-	5
Non-neurological symptoms							
Hyperammonemia	1	10	2	2	2	1	18
Abdominal pain	2	5	1	3	4	1	16
Fatigue	-	1	-	1	3	-	5
Jaundice	1	1	-	-	1	-	3
Other pain	1	2	-	-	-	-	3
Dyspnoea	-	1	-	-	-	-	1
Flapping tremor	-	-	-	-	1	-	1
Nausea	-	1	-	-	-	-	1
No symptoms		1	1	1	2	-	5
Not reported		2	-	4	2	-	8
Associated Conditions							
Osler-weber-rendu syndrome	-	-	-	1	-	4	5
Hypertension	-	6	1	-	2	-	9
Non-associated conditions							
Neoplastic diseases	1	1	-	5	4	-	11
Other	2	14	-	3	3	1	23

Table 1.6: Shunt flow rate and shunted ratio.

Patient	Shunt Type	Shunt flow rate (L/min)	Shunted ratio (%)	Reference
1	Park Type III	0.17	14.7	[118]
2	Park Type III	0.08	9	[118]
3	Park Type III	0.33	22	[118]
4	Park Type III	0.36	29	[118]
5	Park Type III	1.2	-	[119]
6	Park Type IV	-	68.1	[171]
7	Abernethy Type II	-	39.5	[129]

1.7 Discussion

Over a 29 year period (1982-2011), 112 adult patients were incidentally diagnosed with PSS, emphasizing the rarity of this vascular malformation. This rarity in PSS diagnosis may be due to the lack of a standardised, cost-effective, and safe clinical test given that most cases of PSSs in patients with functionally healthy livers remain unnoticed. Therefore, the frequency of PSSs could be higher than currently thought, either due to patients not being tested for PSS or the limitations of the available diagnostic techniques. The clinical implications of PSSs, including the effect on reduced rate of drug metabolism and questionable tumour metastases distribution, highlight a need for the development of a diagnostic technique.

There are several limitations with this review mainly due to the inconsistency of PSS terminology and how they are categorised [12]. It is also questionable as to what constitutes a congenital PSS and a spontaneous PSS. Congenital implies that the PSS is present from birth, however there are some articles which use it with a definition that is actually 'acquired PSS' or 'natural PSS'. Most PSSs are 'naturally acquired' unless there is a congenital vascular malformation from birth. Similarly with 'spontaneous PSSs', which implies that a PSS suddenly appears without cause, most articles reference 'spontaneous' as secondary to another problem, for example, an aneurysm. We have categorised the PSSs into Abernethy and Park Types as a means to encourage a standardised PSS categorisation system.

Eighty articles were reviewed describing 112 patients with PSSs, of which the majority were incidental findings while undergoing imaging tests. The pathogenesis of the PSSs in these adult patients remains still largely unknown, except in those with Park Type III PSS, and some patients with Park Type IV who have Osler-Weber-Rendu Syndrome. The hypothesis originally posed by Lore *et al.* [106] that PSSs could be one of the routes responsible for the distribution of gastrointestinal metastases to distant organs, deserves additional attention. Therefore the question can be asked "What is the frequency of PSSs in patients with pulmonary metastases from colorectal origin without liver metastasis?" Although there are still yet to be any studies which directly link metastatic distribution with PSSs, it has been reported that two pancreatic neuroendocrine cancer patients, who had a TIPS inserted, were diagnosed with pulmonary metastases several weeks after the intervention [108]. A plausible explanation is that the artificial shunt acted as a route for circulating tumour cells to bypass the liver. Therefore, PSSs may be a plausible explanation for patients present with pulmonary metastases from pulmonary origin and no secondary liver metastases [191].

The 112 patients included in this review, Doppler ultrasound scanning and CT scans were singularly the most frequently used methods to detect PSSs (23% and 21% respectively; Table 1.4). However, 31 patients required two or more different methods to confirm a PSS. Of these, 15 were diagnosed using a combination of both CT and Doppler ultrasound. This indicates that PSSs may be difficult to detect with just one method, or need confirmation with an additional imaging modality, thus

supporting the need for new detection techniques. Other methods, such as MRI, MRA, CTA, venography and angiography procedures can be used for validation, however these methods can be costly and sometimes more time consuming than using Doppler ultrasound or CT alone.

CT scanning is a commonly used procedure in many medical fields, but is associated with a significant radiation burden, particularly, abdominal scans where patients are susceptible to a large exposure of radiation [85, 86]. It is therefore advisable that the amount of received radiation a patient can have at any one time should be kept at a minimum.

Doppler ultrasound scanning, MRI and MRA do not have the same radiation hazard as CT, angiography or venography, but could be time consuming and expensive. Although Doppler ultrasound scanning is more commonly used, PSSs are extremely difficult to find unless they are large. Small PSSs could quite easily be missed with the wrong transducer [87], or if they are intrahepatic and without the use of a contrast [192]. MRI or MRA is a better choice for determining the presence of PSSs as there is no radiation. Although standard MRI cannot visualise blood flow in veins or arteries, the addition of a contrast dye makes it easier for the MRI to demonstrate the vein [193].

An additional concern with radiological PSS detection techniques is their sensitivity and specificity, which may be insufficient to detect small or microscopic PSSs. Angiography, CTA, and similarly scintigraphy may be better in detecting the smaller intrahepatic shunts as they can be visualised with a contrast dye or radioactive dye respectively [194]. Even if the PSS cannot be clearly identified by the dye, the connecting veins may still be visible, indicating the presence of a PSS. This may be especially useful for the detection of Park Type IV shunts.

Not all PSSs will have a similar size even across the different types. Many cases have reported the PSS to be 'large' or to have a diameter between 0.2 – 5 cm [8, 19, 51, 117, 129, 132, 134, 138, 144, 149, 154, 163, 169, 177, 178, 180, 181, 187]. There were ten Abernethy cases where the PSS was reported to be between 1 – 5 cm in diameter or as large/giant [19, 51, 117, 129, 144, 154, 163, 177, 180, 181], whereas there were eight Park cases that reported the PSS diameter to range between 2 – 7 mm in diameter and large or enormous in size [8, 132, 134, 138, 149, 169, 178, 187]. The larger diameter will increase the volume of flow to the heart, however this is not necessarily related to the severity of any associated symptoms.

Several reports using Doppler ultrasound scanning and scintigraphy went further to measure an associated shunt rate (Table 1.6). It has been suggested that encephalopathy is not associated with PSS, even in patients with cirrhotic livers if the shunted fraction is less than 24 – 30% [118, 129]. Although, children are less

likely to have hepatic encephalopathy even with shunt ratio of 60%. Elderly patients with a shunting ratio larger than 60% have the greatest risk of hepatic encephalopathy [15, 29, 73].

Few risk factors are actually distinguishable between age, sex, symptoms and pre-existing disease. Since the discovery of PSSs is often serendipitous, no clear conclusions can be made about the age it is acquired. Large PSS can be associated with a few symptoms, such as encephalopathy, disorientation or other neural and psychiatric disorders [195], idiopathic portal hypertension and Osler-Weber-Rendu disease [124, 138]. Pain itself has not been directly associated with PSSs. Disregarding patients with a pre-existing disease, what is interesting is the lack of symptoms in several cases. If a person is asymptomatic, then the chance of a PSS being discovered would be low. However, it is also possible that some symptoms may be attributed to the pre-existing condition and therefore it is still unlikely that a PSS will be discovered. Consequently, it is impossible to provide an incidence of PSSs in patients without cirrhosis.

Twenty patients reported to have high serum levels of ammonia. This is comparable to the findings in patients with cirrhotic liver disease and one of the known associations of PSS is high serum ammonia [30]. Ammonia plasma levels alone are not conclusive enough to determine the presence of a PSS, but it can be used as an indication of a PSS to indirectly determine the severity of the shunt [30, 195].

Fourteen patients were also tested for ICG R15. Eleven had retention up to four times higher than normal (<10%) ICG. These levels are similar to those seen in a cirrhotic patient. Typically, high ICG R15 levels indicate severe liver dysfunction, but if other tests, such as liver biochemistry blood test and biopsies, show no sign of liver failure, ICG R15 may well be a strong indicator of a PSS. Issues with both ammonia and ICG R15 tests are that, alone, they are neither conclusive nor quantitative. However, if the ammonia serum test is used in conjunction with ICG R15 test, integration of these two biomarkers could serve as a more conclusive test for a PSS, and would be indicative of the need for further imaging tests.

Depending on the severity and/or Type of PSS, treatment options may be limited. If the patient shows no symptoms and is in good health, then there may not be any need for treatment. In most cases, patients were treated for their symptoms of encephalopathy and pain, and not for the actual PSS. In some extreme cases, where a PSS was having a serious effect on the patient, the patient underwent surgical treatment for either an occlusion, ligation or embolization procedure [117, 142, 153, 160, 163, 164, 166, 177, 180].

1.8 Conclusion

Over 29 years, there were 112 cases of PSSs in adult patients with functionally healthy livers, which were critically reviewed in the literature. Most PSSs were serendipitously found with a high prevalence in middle aged patients and especially

in women. Doppler ultrasound and CT were more commonly used in the detection of PSSs. However these methods are not guaranteed to find a PSS and they could be easily missed. It is suggested that a combination of methods is used, which may decrease the chance of a PSS being missed, although more attention to this research area is required. Microscopic PSSs could easily be missed using any of the current techniques available, and therefore answering the question if PSSs have a role in metastatic distribution is currently not possible. A novel technique is needed that can quantify a PSS, which is less susceptible to the downfalls and limitations of radiological techniques in order to provide evidence in answering what role PSSs may play in metastatic distribution.

1.9 Significance

Currently, there is no standardised clinical test for PSS detection and they may be more common than first thought. These PSS are thought to be the reason behind the distribution of secondary metastases beyond the liver in 15-20% of all colorectal cancer patients with functionally healthy livers, that is patients without cirrhosis, fibrosis or hepatitis. Detection of PSSs could provide an early warning to the systemic spread of cancer, allowing for more appropriate medical treatment.

1.10 Aim

To develop a cost effective, non-invasive technique that can identify and measure portosystemic shunts in a functionally healthy liver.

CHAPTER 2

Development of a Portosystemic Shunt in a Swine Model

2.1 Introduction

Artificial grafts were first used experimentally in 1947, in an animal model, to replace the aorta [196]. Many different materials were studied as a suitable graft; however major problems were thrombogenicity and durability. Further research showed that the polyethylene terephthalate (Dacron) and polytetrafluoroethylene (PTFE) were far more durable and performed well provided the diameter of the graft was great than 6 mm [197]. When the graft is attached to tissue, many serum proteins including, albumin, fibrinogen and immunoglobulin, are absorbed into the graft immediately after it is exposed to blood flow and line the graft. The interaction between blood and the graft surface is dependent on surface charge, surface energy and friction. Positive surface charge will allow platelet adhesion, while negative charge will reduce the platelets affinity for adhesion.

PTFE was originally marketed in 1937 by DuPont as Teflon® [197]. The PTFE compound itself is hydrophobic, however through a process of heating, stretching and extruding, a microporous structure can be formed. This allows a better tissue adhesion, and as the surface is negatively charged, it reduces the chance of thrombosis [197]. The patency of PTFE has been demonstrated to be long lasting [198-200] and has also been used to create an artificial PSS for relief of portal hypertension [201, 202]. Currently, PTFE shunts are commonly used for vascular procedures in human medicine.

Surgical portosystemic shunts and TIPS are procedures which are sometimes performed in patients who generally have portal hypertension or are undergoing liver transplantation. A TIPS procedure is often used to relieve portal hypertension and decreases the chances of intestinal bleeding or ascites by creating a direct route between the intrahepatic portal vein and hepatic vein. The hepatic vein is then intubated with a specialised catheter via the peripheral jugular vein under radiologic guidance [203].

The size and length of natural PSS can range dramatically between individuals and also shunt type. In all of these cases, blood flow has been hepatopetal with the pressure difference between the portal vein and IVC being greatly different. There are some patients with a Park Type III PSS that have shown a pressure gradient of 6 to 17 mmHg between the portal branches and the hepatic veins [119-121]. It is known that fluid direction is always from high pressure to low pressure, however the rate of flow within the portal vein can change dramatically depending on heart rate, breathing rate, if food is being consumed, and even body position.

There have been some case studies in both Park and Abernethy PSSs that show the fraction of blood flowing through the shunt. The mean (range) fraction between these cases is 30.4% (9 – 68.1%) and the shunt flow rate mean was 0.428L/min (0.08 – 1.2 L/min) [118, 119, 129, 171]. This large range of blood bypassing the liver may have some serious consequences as outlined in Chapter 1.

For the experimental work in this thesis, there are three possible shunt materials that could be used, being polytetrafluoroethylene (PTFE), vein from a donor animal or silicon tubing. Scavenged vein and PTFE are commonly used in vascular procedures. Anastomoses can be quickly formed by a trained vascular surgeon; however blood clotting can quickly occur within silicon occluding the PSS if the blood is not well heparinised. PTFE has similar properties to arteries as it allows fluid movement across the wall, similar to a vein or artery, however PTFE can occlude over time. Scavenged vein is the optimal material for grafts as it is not a prosthetic material and is less likely to thrombose. However, vein grafts are technically difficult to perform and much care and time is needed to avoid excess bleeding and punctures.

One of the most common types of PSSs found in patients is the extrahepatic, Abernethy Type II PSSs. These shunts directly connect the portal vein and the IVC, external to the liver with the portal vein patent and are normally <7mm diameter [8, 19, 51, 117, 129, 132, 134, 138, 144, 149, 154, 163, 169, 177, 178, 180, 181, 187]. Based on these patients, it was decided to be the simplest PSS to mimic within a swine model.

A swine model was chosen as they have similar sized blood vessels and liver function to humans. The portal vein and IVC of a swine have a similar diameter and flow rates to that of a human with a liver size of approximately 1500 cm^3.

Previous PSS models within a pig have used TIPS with a focus of improving patency for patient care [204, 205]. Some earlier portocaval shunt models have been used to treat hypercholesterolemia [206] or measure cholesterol metabolism [207].

This study recreates an Abernethy Type II PSS in a swine model. Pigs were used as they have very similar anatomical organs, vascular size and function to those in humans, giving an optimal canvas to perform an Abernethy Type II anastomosis, whereby providing results that are applicable and relevant to a clinical setting.

2.2 Materials & Methods

This study was approved by the University of Adelaide Animal Ethics committee (No. M-2010-92a) and the Institute of Medical and Veterinary Science Animal Ethics committee (No. 96/10a). All procedures were performed at The Queen Elizabeth Hospital (TQEH) animal house (Woodville South, South Australia).

Eight pathogen free domestic female pigs were used in this study and were housed in TQEH animal house with 12 hour day/night cycles in a 24 degree Celsius temperature controlled room. Each pig was imported four days prior to surgery to acclimatise to TQEH animal house with an appropriate diet and water was provided ad libitum. Ethical guidelines were followed according to the National health and

Medical Research Council's Australian code of practice for the care and use of animals for scientific purposes [208].

Using a swine model, an extrahepatic portosystemic shunt was created between the portal vein, approximately 5 – 10 cm below the liver, to the IVC. Each shunt had a diameter of 8 mm and was made out of PTFE or scavenged swine iliac vein from another pig (diameter ranged 6-8 mm). Two trial pigs were used to pilot test the PTFE and iliac vein material. A further six pigs were used for the study using the material deemed most appropriate.

The median weight of the pigs was 45 kg, ranging 35 to 55 kg. Each pig was anesthetised by a trained veterinary technician with 0.5mg/kg ketamine followed by a continuous dose of 1.5% isoflurane in oxygen via an endotracheal tube for the duration of the surgery. Intravenous access was established. The animals were continuously monitored for change in heart rate and oxygen saturation for the duration of the procedure. After the surgery was completed and all samples collected the pig was euthanized with a lethal dose 100 mg/kg of sodium pentobarbitone.

2.2.1 Surgical Procedure

A 10 cm incision was made on the lower right side of the neck and the jugular vein was dissected and mobilised (Figure. 2.1A). A 16G x 1.25" Braun Introcan Safety® intravenous catheter was inserted into the jugular vein to allow for a 0.9% sodium chloride drip line. The catheter and drip line were secured to nearby epithelium (Figure 2.1B). A midline laparotomy was performed with an approximately 40 cm incision (Figure 2.2). The infrahepatic vena cava was exposed via visceral rotation and then mobilised in a cephalad fashion to a level at the confluence of the liver substance and the adventitia of the cava (Figure 2.3A). The portal vein was then identified and mobilised with separation of lymphatics and lymphatic nodes that surround the portal vein (Figure 2.3B). Each pig was initially heparinised with a weight appropriate dose of 80 units/kg of intravenous heparin, immediately followed by 5000 units of heparin added to each 1 L 0.9% saline bag.

The IVC was partially clamped using a side biting Satinsky clamp and a longitudinal venotomy was performed with local heparin/saline irrigation (Figure. 2.4A). An end-to-side anastomosis of the portosystemic shunt was performed using continuous 6/0 polypropylene suture (Ethicon™) and 8 mm diameter by 10-15cm PTFE tubing or scavenged iliac vein. The portal vein and IVC were prepared with a 16 mm elliptical excision and the shunt material, PTFE or iliac vein, was bevelled at each end for an acute angled connection to reduce turbulence. The anastomosis is first started at the 'heel' end with a suture running along each side to the middle. The 'toe' end is then started with sutures running along each side, meeting the other

suture from the heel in the middle with any excess trimmed before the join is complete (Figure 2.5) [209]. The shunt was flushed with heparinised saline and clamped. The portal vein anastomosis was similarly completed with partial occlusion clamping and end to side anastomosis using 6/0 suture material in continuous fashion (Figure. 2.4B).

The portal system and shunt were flushed with heparinised saline and the suture line was completed and haemostasis achieved. Antegrade portal circulation was achieved prior to release of the clamp on the shunt. A dual lumen Turbo-Flo® 4 French catheter (Cook Medical) was flushed with saline and inserted into the portal vein inferior to the liver, approximately 10 cm below the shunt. Another tri-lumen 5 French catheter was inserted into the IVC and guided up to the confluence of the hepatic veins. Each catheter has surrounding 6/0 purse string sutures to secure and avoid tearing of the veins. The shunt was then left to stabilise for five minutes (Figure. 2.6)

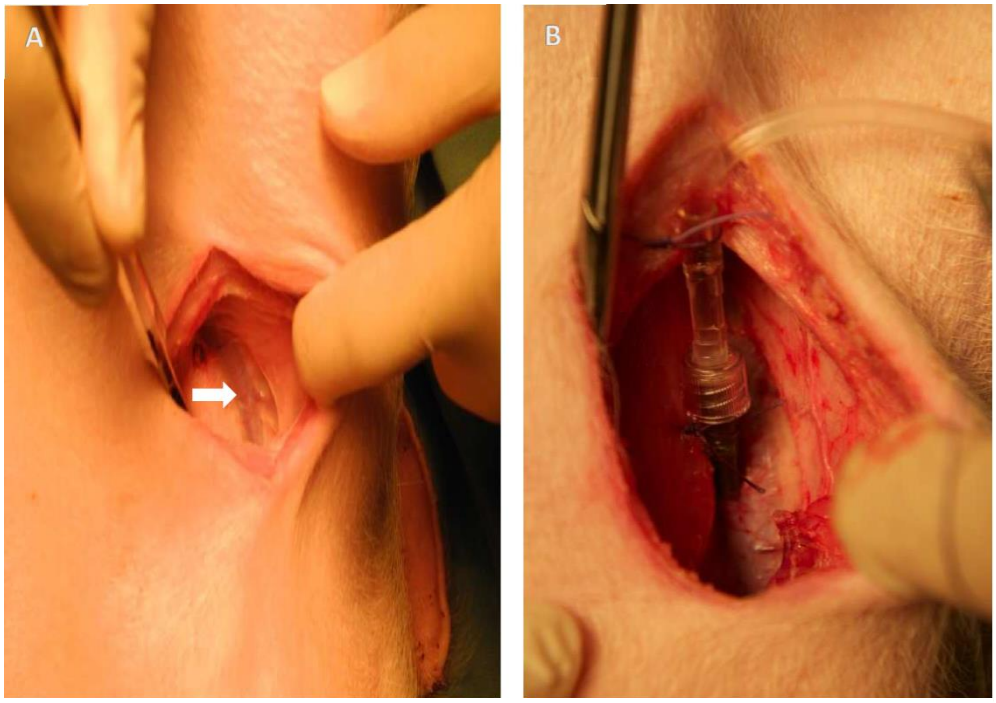

Figure 2.1: A 10 cm incision made on the lower right side of the neck. (**A**) The Jugular vein located (arrow). (**B**) Drip line inserted into the jugular vein with a 16G Braun Introcan Safety® needle.

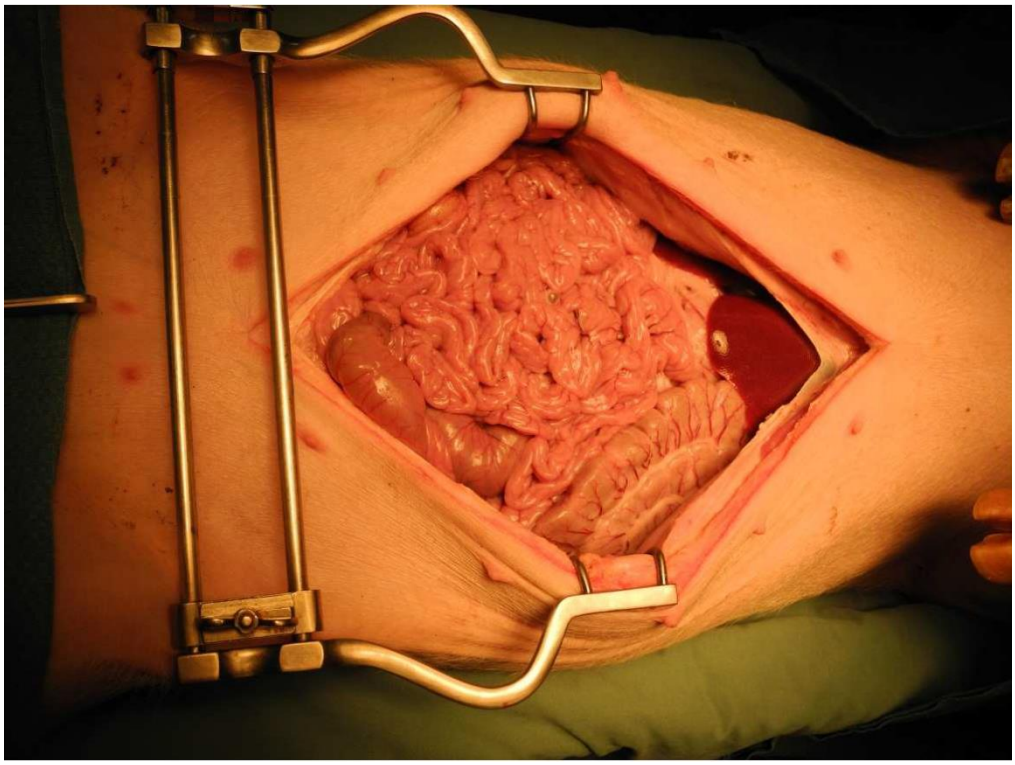

Figure 2.2: A 40 cm incision was made down the midline to expose abdominal organs and vessels.

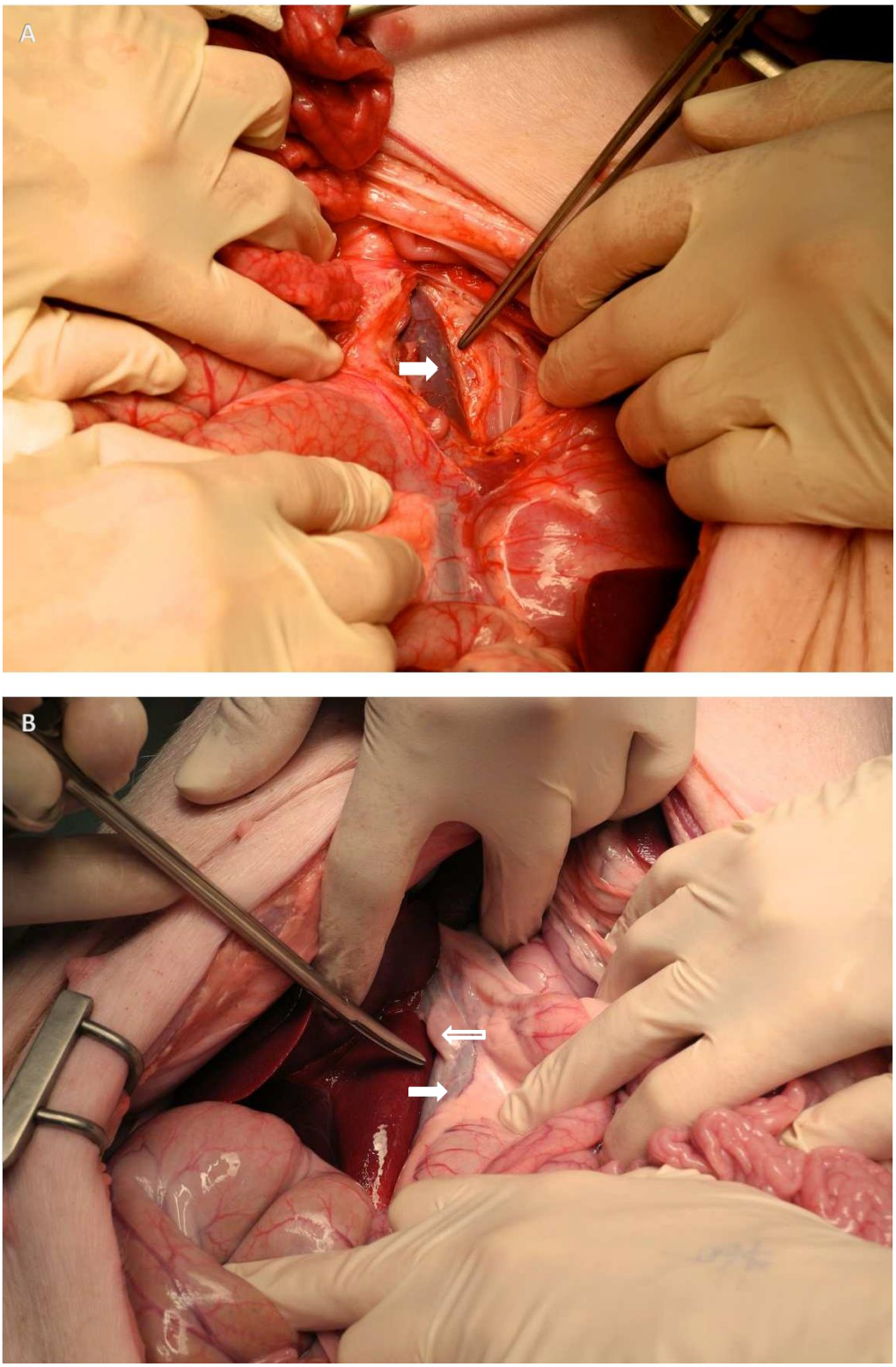

Figure 2.3: (**A**) The inferior vena cava (arrow) is located and mobilised to a level at the confluence of the liver. (**B**) The portal vein (solid arrow) was identified and mobilised with separation of lymphatics (hollow arrow) and nodes that surround the portal vein.

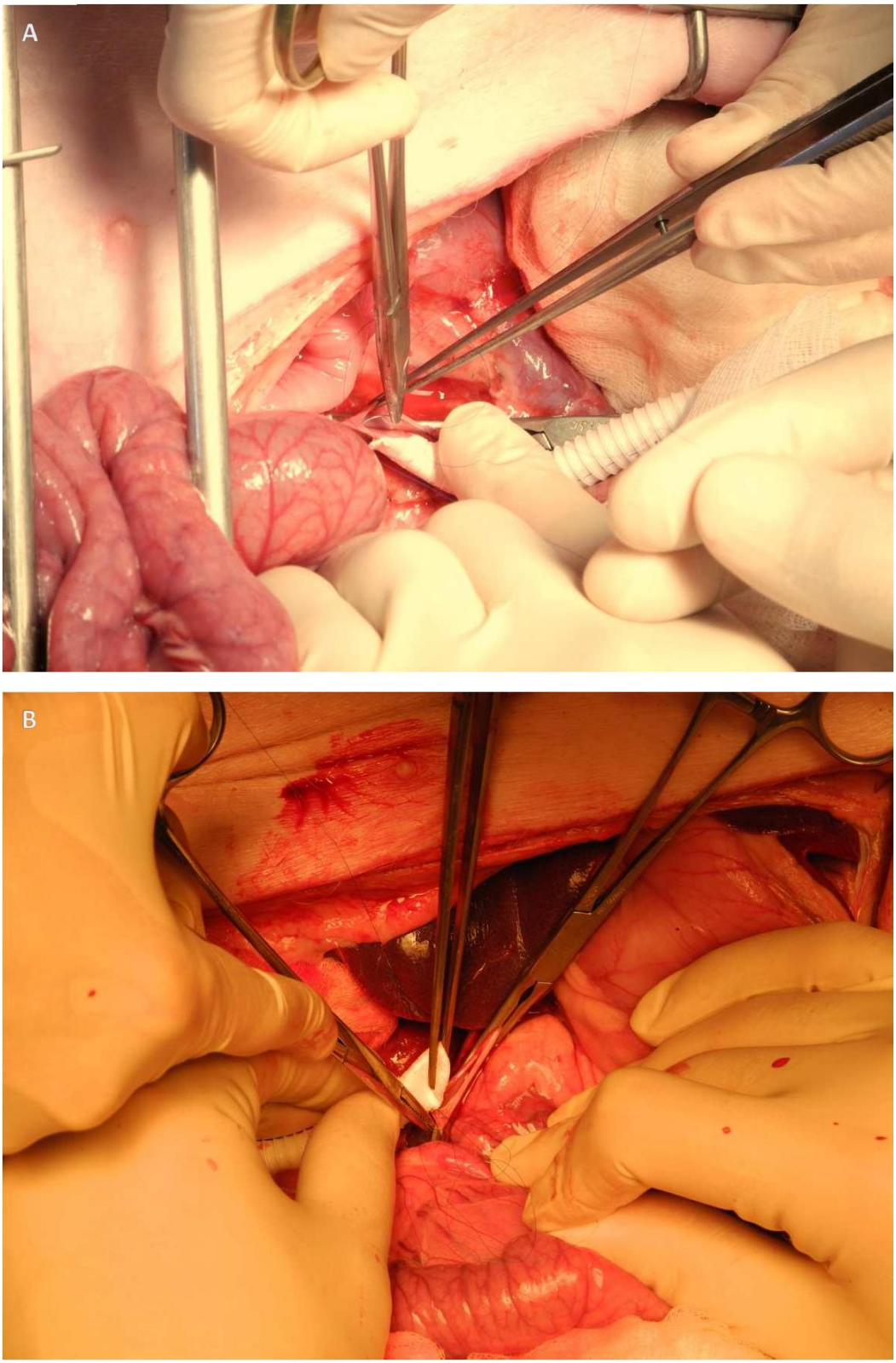

Figure 2.4: (A) The inferior vena cava (IVC) was partially clamped using a side biting satinsky clamp and a longitudinal venotomy was performed. An end to side anastomosis of the portosystemic shunt is performed using continuous 6/0 polypropylene suture and 8 mm diameter by 10-15 cm PTFE tubing. (B) The portal vein anastomosis was similarly completed with partial occlusion clamping and end-to-side anastomosis.

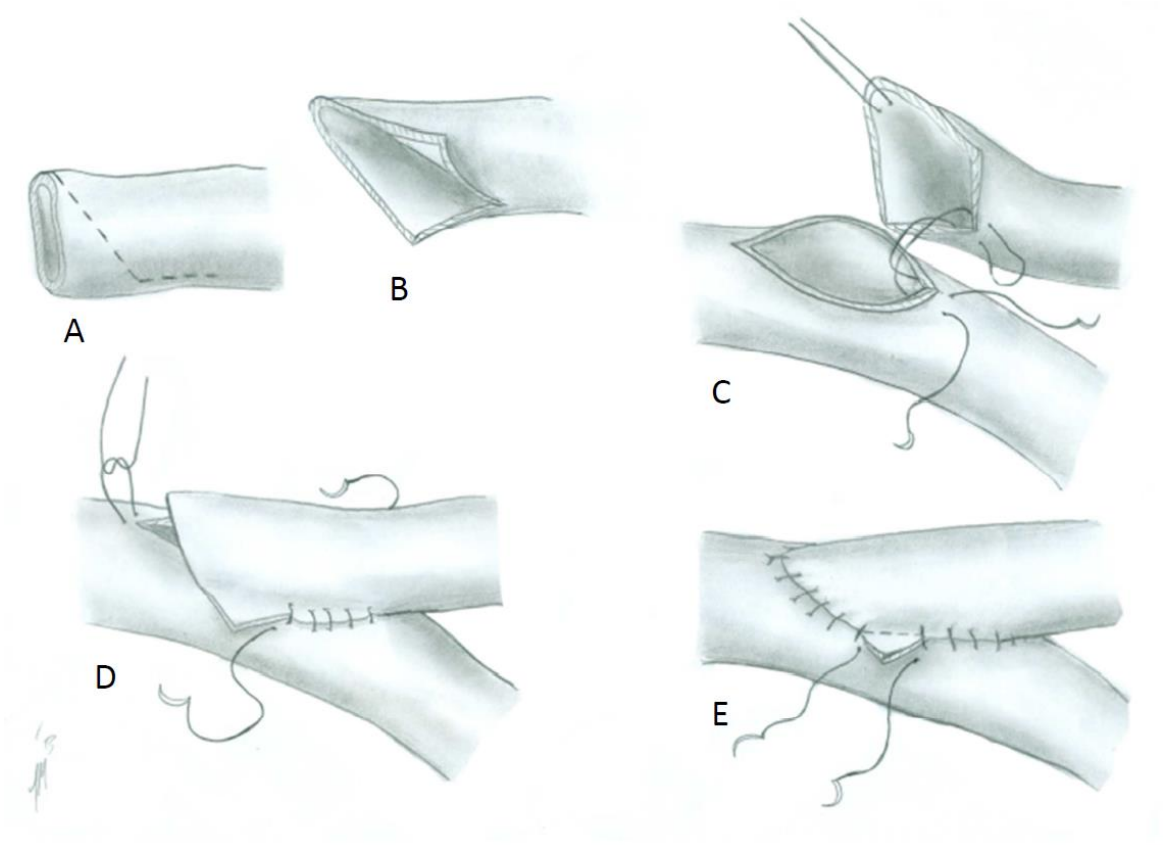

Figure 2.5: Schematic of an end-to-side anastomosis. (**A** and **B**) The graft material is trimmed. (**C**) A 16 mm elliptical excision is made into the portal vein or inferior vena cava with the suture starting at the 'heel'. (**D**) The 'heel' is sutured until half way, along both sides and then suturing is started from the toe. (**E**) Suture from the toe is joined in the middle with any excess edges removed.

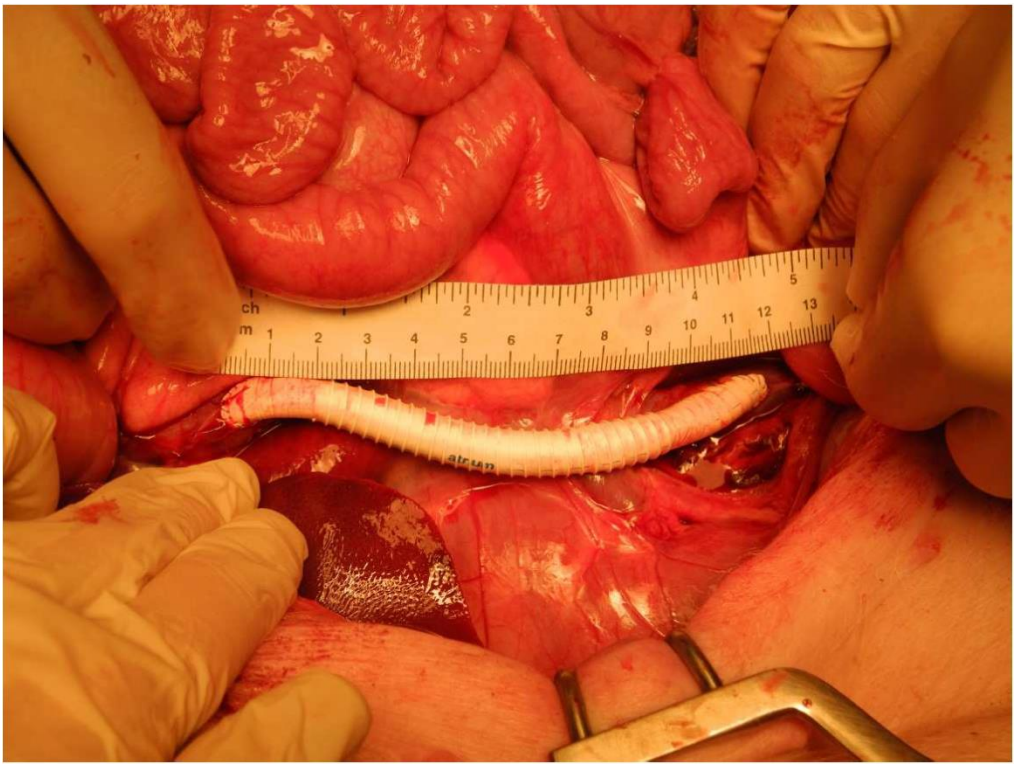

Figure 2.6: The end to side anastomosis of the portosystemic shunt is measured and allowed to stabilise for five minutes.

2.2.2 Shunt Flow Direction

Typically flow direction and velocity can be determined using Doppler ultrasound scanning with the appropriate transducer. A thermodilution technique could also be used to measure flow, however, the appropriate computer for thermodilution could not be obtained.

Doppler ultrasound was conducted with a SonoSite® Micromaxx and a HEFL38 13-6 Mhz transducer. This type of transducer is typically used in vascular surgery and for vascular imaging. After the anastomosis described in the previous section had stabilised, the transducer was placed directly on top of the anastomosis, portal vein and IVC. Due to the type, size and weight of the transducer, there was a tendency for the veins to collapse, hence imaging the vein and calculating its velocity was difficult. Due to the physical properties of PTFE, being made of a synthetic material that contains air pockets, ultrasound is poorly transmitted from air to water due to impedance mismatching and the ultrasound is virtually reflected. Further PSSs were soaked in 0.9% saline solution, in a modified vacuum container (Figure 2.7). However, the blood flow could still not be determined with a soaked PTFE anastomosis. This was believed to be due to a low flow rate and the type of transducer. Ideally, a more appropriate transducer would be a smaller 'hockey stick' shaped probe, for example the SonoSite® SLA 13-6 MHz. This probe is lighter, smaller and therefore unlikely to collapse the veins and due to the smaller scanning area, the transducer would have better spatial resolution. Due to the high costs of

Doppler ultrasound transducers, the 'hockey stick' probe could not be obtained for animal use.

Fluid dynamics state that fluids will always flow from high to low pressure, provided there are no obstructions. In humans, a typical portal vein pressure is 23 - 25 mmHg and the IVC pressure is 0 - 3 mmHg. Due to the animal being in supine position with an open abdominal cavity for the shunt procedure, there are no external forces on the portal vein and IVC, the pressure will be much less and will be mostly due to the force of the blood within the vessel. An ARGON® DTXPlus™ central venous pressure transducer was connected to the catheters previously inserted in the portal vein and in the IVC. The pressure transducer was fixed at the same height as the midline of the pig and connected to a 1 L bag of 0.9% saline solution in a pressure bag set to 300 mmHg. The lines were flushed of any air and the pressure is zeroed to atmospheric pressure via a three way tap. The line was then connected to the catheter in the portal vein or IVC and allowed to stabilise for one minute. Pressure measurements were taken for the portal vein with the shunt open and shunt closed, the IVC with the shunt open and closed, and in the portal vein with a clamp above the shunt for 100% shunting.

Figure 2.7: A vacuum container consisting of a 100 mL glass jar filled with 0.9% saline solution and a portion of PTFE. A BD Connecta™ three-way tap with luer-lock has been drilled and glued into the cap so air can be withdrawn from the jar using a syringe.

2.2.3 Shunted Blood

Since neither suitable Doppler ultrasound nor thermodilution equipment were available, an exact calculation of blood flow through the shunt could not be obtained.

Theoretically, flow rate can be calculated using a rearranged Hagan Poiseuille equation (Equation 2.1). Also, a new simplified equation developed in dogs was used to calculate PSS fraction (Equation 2.2)[210].

Kudo *et al.* [118] measured shunt ratio by dividing the blood flow volume of the shunt by that of the portal vein using Doper ultrasound. However, as Doppler ultrasound was not available, the PSS fraction was calculated using the ratio of total volume between the portal vein and the total volume of the anastomoses (Equation 2.3). The volume of each vessel can be calculated by π x radius^2 x length. Photographs were used to measure the length of the shunt and the diameter of the portal vein. Due to the difficulty of measuring the length of the portal vein, average lengths 6.5 ± 1.5 cm was used.

$$Flow\ rate = \frac{\text{Pressure difference}.\pi.\text{diameter of shunt\^{}4}}{128.\text{blood viscosity}.\text{length of shunt}}$$

Equation 2.1: Hagan Poiseuille equation rearranged to find the flow rate of the portosystemic shunt.

$$PSS\ fraction\ (\%) = 100 - \frac{100\ .\ \text{PVP (shunt)}}{\text{PVP (control)}}$$

Equation 2.2: A simplified equation to calculate the portosystemic shunt (PSS) fraction using the Portal vein pressure (PVP) when the shunt is open and closed. Adapted from Washizu et al. [210].

$$PSS\ fraction\ (\%) = 100\ .\frac{\text{PSS volume}}{\text{portal vein volume}}$$

Equation 2.3: Ratio of blood volume between the portosystemic shunt (PSS) volume and the portal vein volume.

2.3 Results

2.3.1 Anastomosis Material

Both scavenged iliac vein and PTFE work equally well as an anastomosis between the portal vein and IVC (Figure 2.8). However, due to time restraints, PTFE was a better option for several reasons. Firstly, using the iliac vein has several problems. The iliac vein is fragile and thus difficult to create a PSS in short lengths, and secondly, the procedure would take longer than two hours to complete by an experienced vascular surgeon. The iliac vein is also limited by the length that can be scavenged as this length may not be long enough to reach between the portal vein and IVC. The time taken to perform the anastomosis with PTFE was less than one hour, unless any accidental bleeding occurred. Apart from the surgical time advantage with PTFE, it maintains a constant diameter unlike the iliac vein and is not limited by length, although each shunt was created as short as possible (10-12cm). As the flow rate in the anastomosis could not be determined from Doppler ultrasound in either iliac vein or PTFE, PTFE was used for all remaining procedures due to its convenience.

Photographs of each pig shunt were taken to record the length of the PTFE and the width of the portal vein (Figure 2.9). The PTFE shunt lengths ranged from 9 to 13.5 cm, with a mean of 10.1 cm (Table 2.1). The shortest length possible was used, but was dependant on the visual location of the portal vein and IVC. The diameter of the portal vein was also recorded, with a mean of 14 mm, and was used to calculate

its volume. The ratio of the anastomosis volume to the portal vein volume estimates the expected volume of blood bypassing the liver, with a mean ranging between 39.5 - 56.4% (assuming portal vein lengths of 6.5 ± 1.5 cm) (Table 2.1).

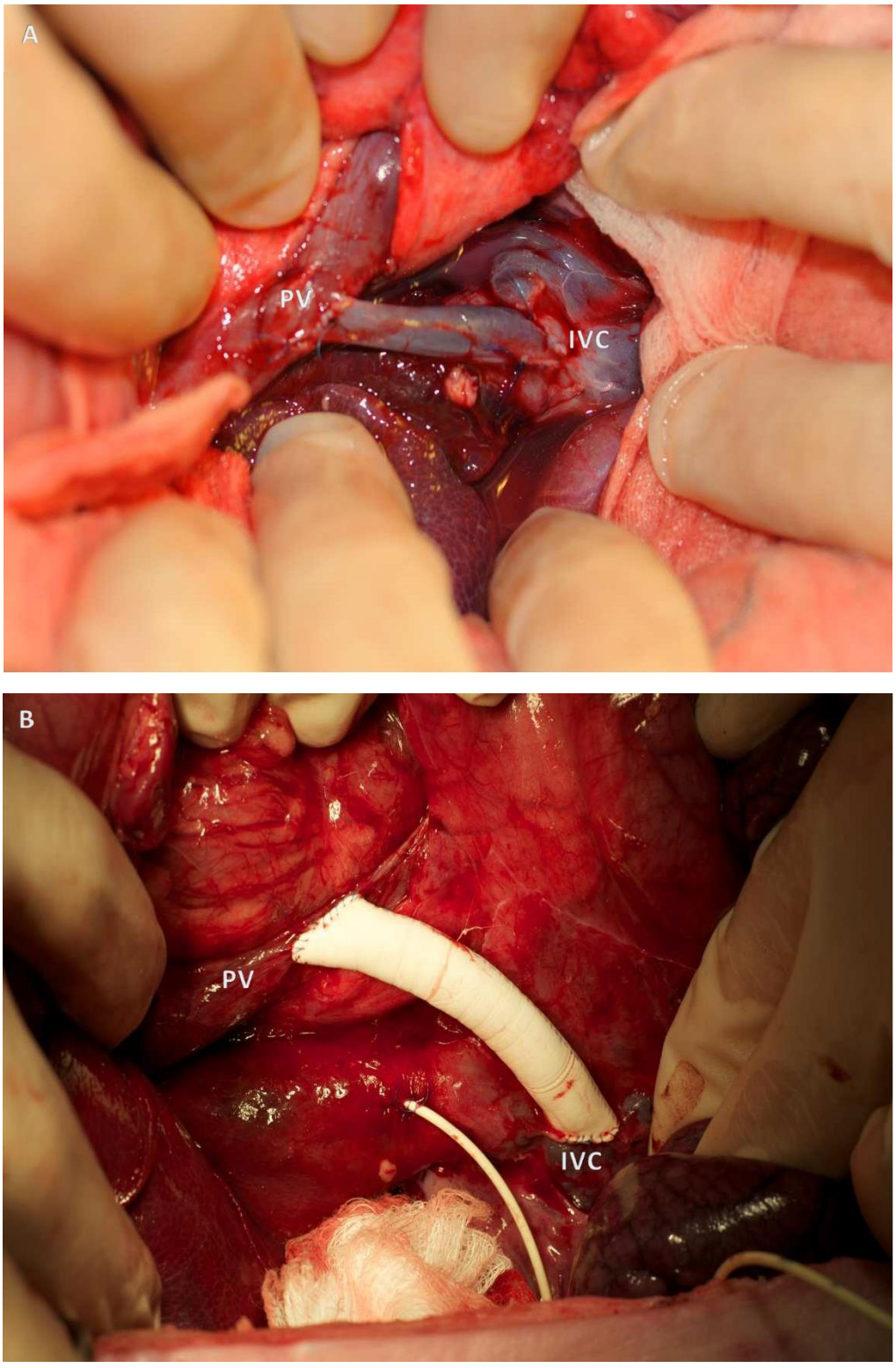

Figure 2.8: (**A**) scavenged iliac vein and (**B**) PTFE used to create an anastomosis between the portal vein (PV) and inferior vena cava (IVC).

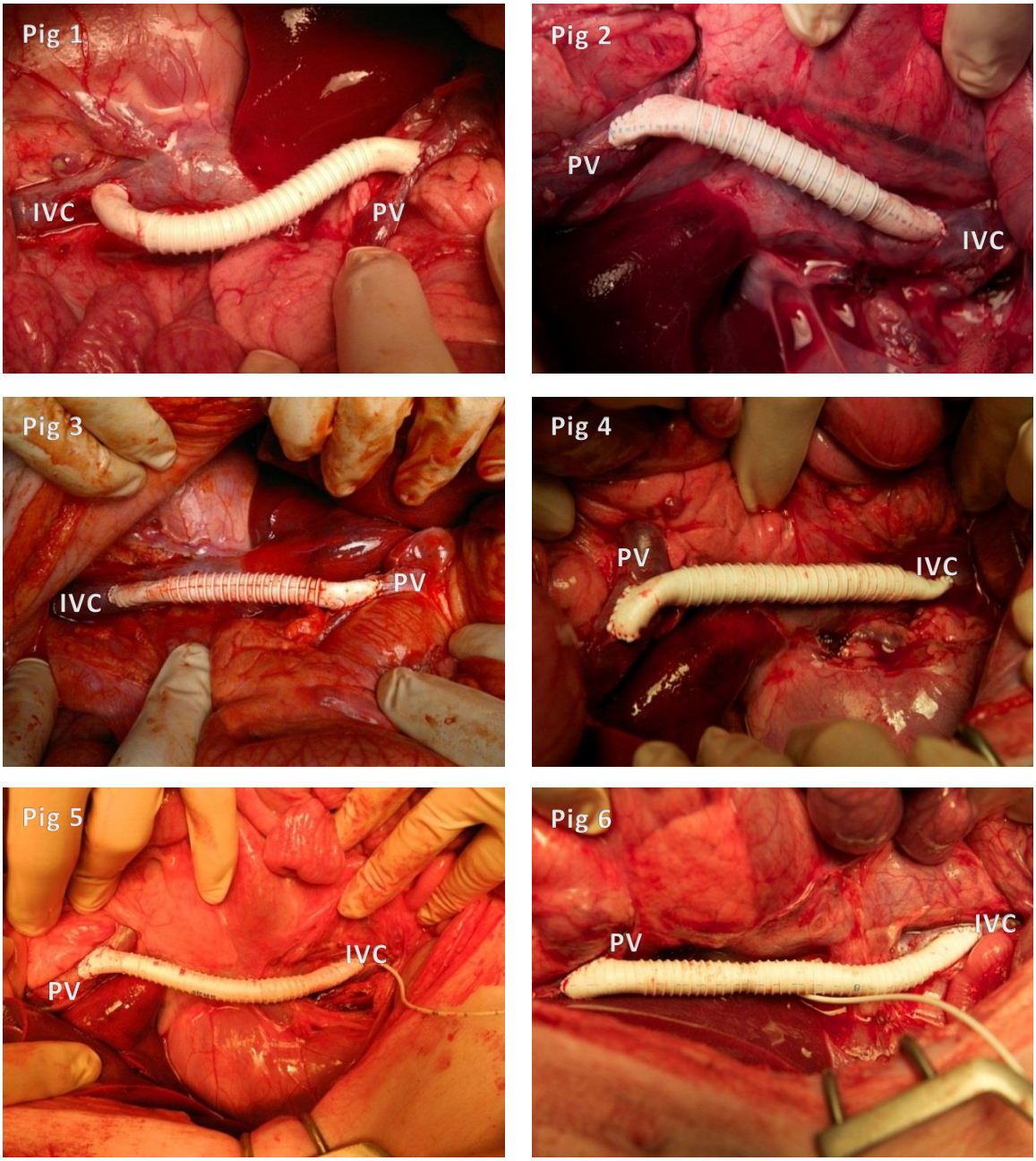

Figure 2.9: Images of all anastomoses inserted into each of the six pigs between the portal vein (PV) and inferior vena cava (IVC)

2.3.2 Pressure Gradient

There was a significant pressure difference towards the IVC from the portal vein when the shunt was closed ($p<0.001$) and also when the shunt was open ($p<0.001$) (Table 2.2), and can be assumed that flow direction is from the portal vein to the IVC. Due to the hemodynamic properties of blood, the actual flow rate is difficult to calculate using the Hagan-Poiseuille equation (Equation 2.1). Another simple equation was used to estimate the fraction of blood shunted, based on the difference of portal venous pressure when the shunt is open and closed (Equation 2.2)[210]. However, this equation requires a minimum of 1 mmHg pressure difference and fails to take into account the portal vein can expand, thus reducing pressure.

The portal vein was clamped above the anastomosis to allow 100% shunting. Pressure difference was recorded in the portal vein with 100% shunting and was compared against portal vein pressure with the shunt open. The mean pressure of 100% shunting was 4.5 mmHg, ranging from 1 to 7 mmHg and is significantly higher than normal flow with shunt open, mean of 1.83 mmHg, ranging 1 to 3 mmHg ($p=0.02$). This is to be expected as more blood is now forced through the shunt.

Table 2.1: Length of anastomoses that was inserted into each pig with the ratio between the portal vein (PV) and shunt (PSS) volumes. A range is given as the portal vein length was assumed of 6.5 ± 1.5cm.

Pig	Shunt Length (cm)	PV:PSS Ratio (%)
1	9	38.9 ± 9.7
2	8.5	42.15 ± 10.6
3	8.5	42.2 ± 10.5
4	10	43.2 ± 10.7
5	11	54.5 ± 13.6
6	13.5	66.9 ± 16.7
Mean ± SD	10.1 ± 1.9	47.9 ± 11.96

Table 2.2: Pressure differences (mmHg) between portal vein (PV) and inferior vena cava (IVC) with the shunt open (S) and when closed/control (C).

Pig	PV-C	IVC-C	Gradient	PV-S	IVC-S	Gradient
1	4	-5	9	2	-4	6
2	2	-5	7	2	-6	8
3	1	-3	4	1	-4	5
4	2	-6	8	1	-5	6
5	2	-3	5	2	-3	5
6	7	-2	9	3	-3	6
Mean ± SD	3 ± 1.1*	-4 ± 1.5	7 ± 2.1	1.8 ± 0.5**	-4.2 ± 1.2	6 ± 1.1

*Students T test between PV-C and IVC-C ($p<0.01$). ** Students T test between PV-S and IVC-S ($p<0.01$).

2.4 Discussion

Here we successfully recreated an extrahepatic Abernethy Type II PSS in a swine model. Due to the sheer size of the PSS, it can be classified as 'enormous' as it is 8 mm in diameter and slightly larger than what's been previously reported in patients with PSS is and without cirrhosis [8, 132, 134, 138, 149, 169, 178, 187].

The surgical PSS procedure used is similar to what would be used for a liver transplant or any other type of shunt surgery and the end-to-side anastomosis is commonly used for vein and artery reconstructive vascular surgery [209]. It is classified as the safest technique due to sound haemostasis throughout the connection, even at the 'heel' and the suture placement reduces narrowing at the 'toe'.

There are several limitations with using pigs in this scenario. Pigs are known to be susceptible to anaesthetics and may prematurely die. In this study, the total time each pig was anaesthetised was over five hours, but no pigs prematurely died or were prematurely euthanized. Pigs three and five started breathing on their own, which can be out of synchronisation with the respirator and could potentially result in suffocation of the animal. An increase of isoflurane usually resolved this issue. The independent breathing reflex can also have an affect the venous blood flow by increasing its pressure and rate of flow. This may have caused some erratic flow rates through the anastomoses. The swine venous system is extremely delicate and

can be easily punctured if due care is not taken. In pig 1 and 3, the catheter inserted into the portal vein came out, causing extra tearing and excessive bleeding. Therefore, not all data could be collected from these pigs.

Measuring the pressure difference between the portal vein and IVC would ideally been more appropriate if the measurement was taken at either end of the anastomosis. However, for this to occur, two more catheters would need to be inserted into the portal vein and IVC. Although theoretically possible, due to the fragile nature of the vascular system, there runs a high risk of tearing and bleeding and therefore was not practical. As a consequence, pressures of the portal vein and IVC were measured and using Bernoulli's principle, it can be concluded that flow is from portal vein to IVC.

At any given point in time, the ratio of blood shunted is the same irrespective of actual flow rate, which can change. The total volume of the portal vein and the total volume of the shunt is the same ratio as the percentage shunted. Although this technique is not completely accurate, it does show a good estimate of shunting rate and can be used when other equipment is not available.

A section of the PTFE was removed after each pig was euthanized to check for patency. The first two trial pigs demonstrated that a large single dose of heparin was not adequate to keep the shunt patent. Hourly top up doses of heparin helped

reduce the anastomosis thrombosing, but this still restricted the flow. A constant flow of heparin through a heparinised saline drip maintained the patency of the anastomosis. The downside of this was if bleeding did occur, it was extremely difficult to stop without partial clamping.

2.5 Conclusion

Using techniques based from human surgery, it was possible to create and mimic a PSS in a swine model. Due to time restraints and difficulty of the surgery, PTFE was seen as the optimal material to perform the anastomosis. The anastomosis is large enough to allow adequate flow into the IVC, but still allow hepatopetal flow in the portal vein. This type of shunt could potentially also mimic the same fraction of blood diverting around the liver as other types of large PSS, being Abernethy or Park.

CHAPTER 3

Practical Methods for Portosystemic Shunt Detection

3.1 Introduction

The liver is the largest internal organ, weighing approximately 2% of adult body weight and is histologically divided into four lobes, two larger left and right lobes and two smaller, quadrate and caudate lobes [211]. The liver's blood is supplied from both the hepatic portal vein (75%) and the hepatic artery (25%). The hepatic artery carries the oxygenated blood to the liver and mixes with the deoxygenated blood from the portal vein, in the sinusoids prior to reaching the hepatocytes. Once the blood has passed through the lobule to the central vein, it then flows through the liver into the IVC. Couinaud [10, 11] later anatomically separated the liver into eight segments for surgical use with each segment having its own terminal branch of the portal vein, hepatic artery and drained by the hepatic veins.

This multifunction organ has an important role in uptake, stoage and distribution of nutrients and vitamins, regulation of very low density lipoproteins, degradation of toxic substances and has exocrine and endocrine-like functions. The liver absorbs and breaks down the majority of the substances from the portal vein including, nutrients, toxic substances from the intestine, blood cells and endocrine secretions from the pancreas, and organisms from the gastrointestinal tract [211].

One of the major functions of the liver is the metabolism and excretion of drugs [212]. Drugs are taken up into the hepatocytes either passively or actively through a range of transporters and are then metabolised through the phase I cytochrome

P450 (CYP) system [213, 214] and phase II conjugating enzymes [213, 214]. Polar or ionised compounds require uptake into hepatocytes through either a single or several active transporters [214-216] (Figure 3.1). Some of these include the sodium-dependent taurocholate co-transporting protein (NTCP), organic anion transporting polypeptides (OATPs), organic anion transporters (OATs), the polyspecific organic cation transporters (OCTs), organic solute or steroid transporter alpha and beta (Ost α and β) [216] and glucose transporter (GLUTs). Once the drug is metabolised, it's substrate is then excreted into the sinusoid or bile canaliculi through multidrug resistance proteins (MRPs), breast cancer resistance protein (BCRP) and the bile export pump (BSEP) [216, 217].

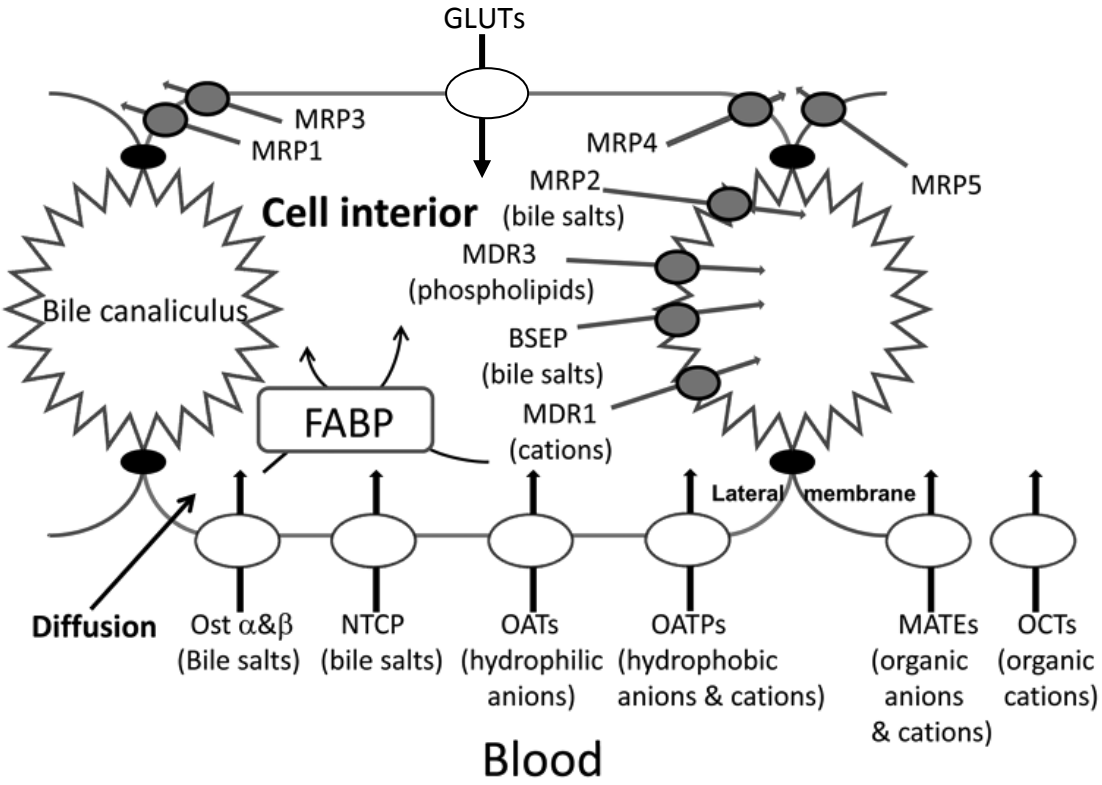

Figure 3.1: Schematic of a hepatocyte with the location of drug transporters. The drug transporters illustrated include the sodium-dependent taurocholate co-transporting protein (NTCP), organic anion transporting polypeptides (OATPs), organic anion transporters (OATs), the polyspecific organic cation transporters (OCTs), organic solute or steroid transporter alpha and beta (Ost α and β), Mammalian multidrug and toxic compound extrusion (MATEs) proteins and glucose transporter (GLUTs) (Adapted from Li *et al* [216]*;* published with permission see Appendix M)

3.1.2 Possible Portosystemic Shunt Detection Techniques

3.1.2.1 Microspheres

Microspheres are microscopic beads that have been used to measure portosystemic shunts. In a study on rats, conventional physiological indices found intrahepatic shunts with diameters up to 80-90 µm [218, 219]. In these studies, the microspheres were used as an intrahepatic portal blockade, which emphasised shunting as shown by reduced uptake of glucose [220-222].

Radio-labelled microspheres have been used to measure shunt fractions [223, 224]. They are administered into the portal vein and the pulmonary recovery is recorded, however, the size of radio-labelled microspheres is limited to 15 µm in diameter [220]. Hence, any blood flow through shunts smaller than 15 µm is excluded. In a study conducted rats by Li *et al*. [220] 15 µm microspheres were injected into rodents to enhance hepatic hypertension. In the control group, it was found that 2.1% of blood flow naturally passed through shunts. With the administration of microspheres and hepatic ligation, the shunt size dramatically increased, allowing 95.9% of blood flow to be shunted.

3.1.2.2 Biomarkers

It has been suggested that administering sorbitol and ICG together and measuring the difference in extraction fractions it will indicate the presence of a PSS [225]. However, this view is not universally agreed upon [226]. The extraction fraction is the rate that a substrate can cross a sinusoidal membrane into a hepatocyte, where 1.0 is the fastest extraction fraction. The extraction fraction E [equivalent to 1 – (hepatic venous concentration /arterial concentration)] can be measured (Equation 3.1) in one sinusoid by permeability of a substrate (P, litres per minute per square centimetre), surface area (S, square centimetres) and the flow through the sinusoid (F, litres per minute) [226].

(**A**) $Ex=1-e^{-PxS/F}$ (**B**) $Px.S = -F.In(1-Ex)$

Equation 3.1: Kety-Renkin-Crone equation (**A**) to find the extraction rate (E) of a substrate in a sinusoid, *x* denotes the measurement is specific to the substrate. Rearranged Kety-Rekin-Crone equation (**B**) to determine the linear relationship between two substrates [226].

Generally, in a healthy liver the extraction of sorbitol is great that the extraction of ICG, therefore the hepatocyte uptake of sorbitol is also greater than the uptake of ICG. . However, theoretically in patients with liver disease who may have a PSS, the flow will increase causing the extraction to decrease. Although, in some studies little change in E has been seen in patients with cirrhosis and acute liver failure [226, 227]. Originally Molino *et al.* [225] described that measuring the fraction of blood shunted equalled 1 – $E_{sorbitol}$ and blood 'shunted' via capillarisation could be measured by the equation $E_{ICG} - E_{sorbitol}$. However, Molino assumed that the correlation between E_{ICG} and $E_{sorbitol}$ was linear (directly proportional), and the curved relationship shown was due to capillarisation. Ott *et al.* [226] also found a curved relationship between E_{ICG} and $E_{sorbitol}$, suggesting the two are indirectly proportional, therefore measuring shunts is more complicated than using just these equations.

Many pharmacological agents, or biomarkers have been used to test for liver function, but none have been exclusively tested to measure PSS. To test for PSS, a pharmacological agent must be extensively metabolised by the liver and have low intravenous bioavailability, thus have a high (close to 1) extraction fraction, hence a high first-pass hepatic clearance. It is also advisable to use compounds with different uptake transporters as so there is little to no competition between uptake, which may reduce the overall first pass clearance. The half-life of the compound is also crucial; a low half-life is preferred (i.e. <2hrs) as this will reduce the testing time on patients.

3.1.3 Aims & Hypothesis

Due to the high risk of microspheres, it is highly unlikely that this method at this point intime will be a practical option. Many pharmacological agents are readily available in a clinical setting to test for liver function or used in general practice; it is therefore hypothesized that a deviation in the pharmacokinetics can demonstrate the presence of a PSS. Therefore, this chapter aimed to identify suitable compounds or pharmacological agents, with a short half-life and fast hepatic uptake (>0.8) that may be used as a PSS marker.

3.2 Methods

A search for pharmacological agents and other compounds was made in the Australian Medicines Handbook [228] and PubMed for any agents commonly used within a clinical setting or for liver function assessment. The noted compounds were selected based on an inclusion criteria of half-life <2 hours and high hepatocyte extraction (>80%). From the compounds that met the inclusion criteria, only one per hepatic uptake transporter was chosen so as not to compete and cause saturation.

3.3 Results

A total of 110 compounds were found that had a high hepatocyte uptake. However, only six had a short half-life, high extraction faction and had different hepatic

uptake pathways (Figure 3.2; see Appendix A for full list of searched drugs and compounds). ICG was added to the list (Table 3.1) due to the very short half-life and availability of a pulse spectrophotometry, LiMON® (Pulsion®, Germany) which measures ICG non-invasively. A final list of compounds and agents that met the inclusion criteria can be found in Table 3.1 and their corresponding dose in Table 3.2. To measure liver dispersion, two further control compounds were chosen, ^{14}C-sucrose and Evans blue as they are not metabolised by the liver.

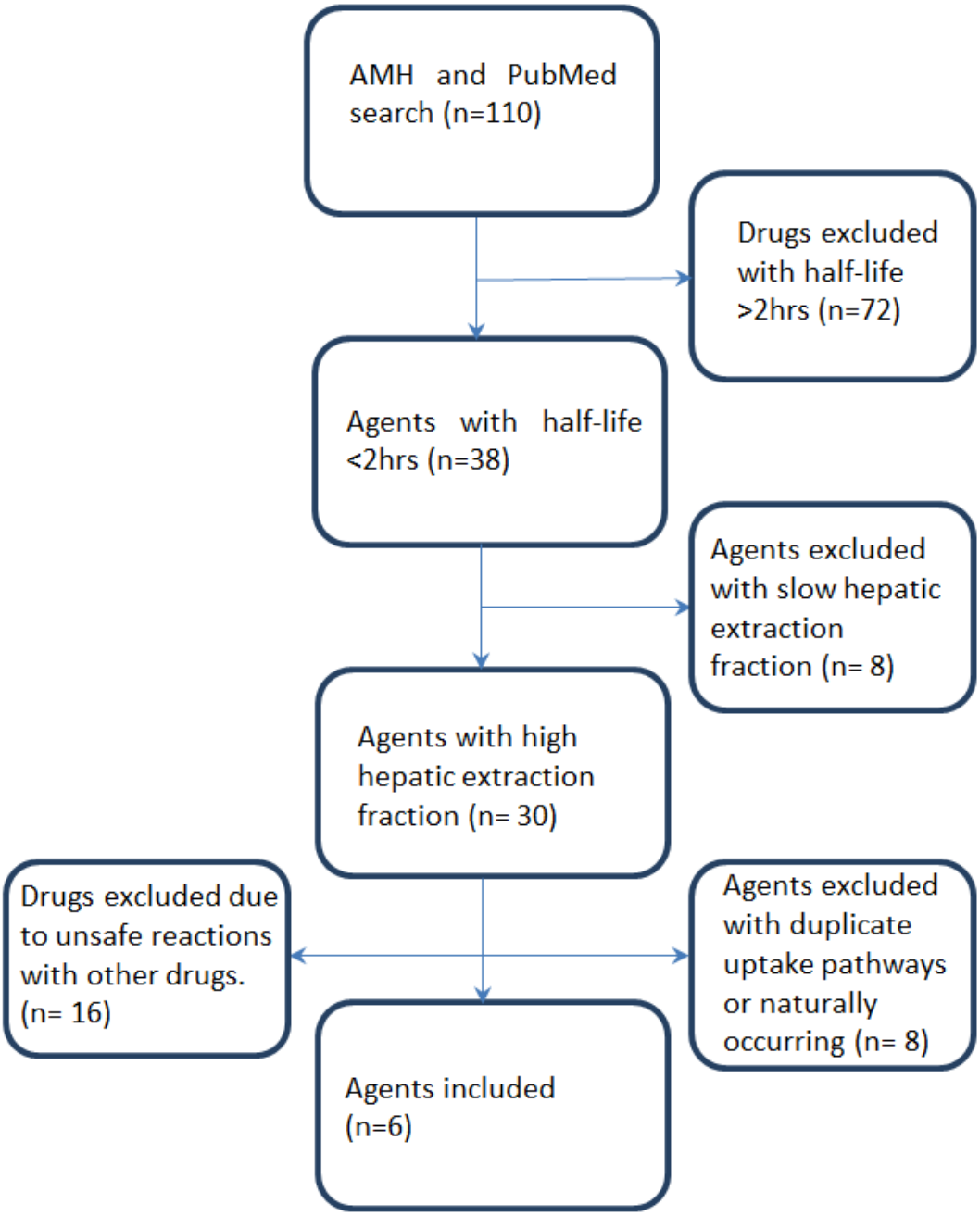

Figure 3.2: Flow chart of pharmacological agents and compounds that may be suitable for detection of portosystemic shunts.

Table 3.1: List of pharmacological agents and compounds that may be used as a portosystemic marker.

Name	Half-life (mins)	Extraction fraction (%)	Uptake transporters
Lignocaine	90	99	Passive
Sorbitol	0.5	96	GLUT 4
Fructose	20	99	GLUT 2/5
^{13}C-methacetin	60	99	Passive
^{3}H-taurocholate	30	99	NTCP, OATP, OAT2, OST
Ethanol	-	*15mL/100mL/hr	Passive
Indocyanine green	3	66	OAT7

*clearance rate.

NTCP - sodium-dependent taurocholate co-transporting protein.

OATPS - organic anion transporting polypeptides.

OATs - organic anion transporters the polyspecific.

OCTs - organic cation transporters.

Ost - organic solute or steroid transporter.

GLUTs- proteins and glucose transporter.

Table 3.2 List of pharmacological agents and compounds with respective doses.

Drug	Dose (mg/kg)	Reference
Lignocaine	1	[229]
Sorbitol	2	[230]
Fructose	100	[231]
^{13}C-methacetin	2	[232]
^{3}H-Tauracholate	1.5 x 106 dpm	[233]
Ethanol	600	[234]
Indocyanine green	0.25	[235]
Evans Blue*	1 mg/Kg	[236]
^{14}C-Sucrose*	3 x 106 dpm	[233]

*Compounds used to measure liver dispersion

3.4 Discussion

The pharmacological agents which matched the inclusion criteria were lignocaine, sorbitol, ethanol, fructose, ^{13}C-methacetin and ^{3}H-taurocholate. ICG has an extraction fraction of 0.66, but is also another possible option as it is completely metabolised by the liver, and can be non-invasively sampled by pulse spectrometry. The general theory to measure a PSS is to intravenously inject these agents directly into the portal system and then measure their concentration in the blood once it has passed through the liver. If there is any significant remnant in the blood, it may suggest that a PSS is present. Due to the high risk of microspheres, it will not be further investigated in this thesis.

3.4.1 Lignocaine and Monoethylglycinxylidide (MEGX)

Lignocaine is a local anaesthetic which is passively uptaken into the hepatocyte and 97% metabolised by the cytochrome P450 pathway, into monoethylglycinexylidide (MEGX) [237]. Lignocaine has previously been used to measure liver function by monitoring MEGX levels at a series of time points up to six hours after lignocaine administration [238]. A previous study has shown that the metabolism of lignocaine can be correlated to the severity of cirrhotic livers, where the MEGX levels are inverse with ICG clearance and alanine transaminase activity [239]. However this test is based on metabolism and results may be inconsistent due to metabolic variation between patients. Also, MEGX is limited to and dependent on hepatic flow

and metabolism rate, which further can be affected by drugs which may increase or decrease this flow [240, 241].

Due to the short half-life of 1.5 hours and a high extraction fraction of 0.995 [237], lignocaine may be suitable to measure PSS. The volume of blood shunted can be measured by determining the ratio of lignocaine : MEGX. If a shunt is present, the ratio of lignocaine : MEGX will be much higher than normal.

3.4.2 Sorbitol, Fructose and Ethanol

Sorbitol is a non-absorbable sugar alcohol that was synthesised for use as an artificial sweetener [242] and fructose is natural sugar found in most foods. Sorbitol and fructose uptake into the hepatocyte is via GLUT 7 and GLUT 2/5 respectively and due to sorbitol's high extraction fraction of 0.96 [243] and fructose being 99% metabolised in the liver, they may be suitable for measuring PSS. Ethanol is slightly different from the other pharmacological agents described as it does not have a half-life, but rather a linear clearance rate of 15 mL per 100 mL blood flow per hour. If the dosage of ethanol is less than the clearance rate, then it may be used to measure a PSS. Fructose and ethanol were removed from this study for several reasons. A high sensitivity assay for fructose could not be obtained. Low sensitivity assays are available however, there was the possibility of glucose cross-contamination, since glucose is commonly found in plasma. Assay equipment was

not readily available for ethanol. Also, the volume of plasma required for assaying off-site was more than could be collected (see *Chapter 4: 4.2.3 Sample Collection*).

3.4.3 ^{3}H-taurocholate

Taurocholate is a bile salt that has a high extraction fraction of 0.9 and maybe a suitable compound to test for a PSS as it transported into the bile instead of re-entering the vascular system. Taurocholate uses active transport (ATP-dependent transport) to cross the canalicular hepatocyte membrane into the hepatocytes [244] via NTCP , OAT, OATP and Ost [233]. Taurocholate is then excreted into the bile via the bile salt export pump (BSEP) virtually unchanged [28]. As taurocholate can be radio-labelled [^{3}H], it is easily detectable in blood, thus may be a suitable compound for measuring PSSs. However, due to the large expense per dose, ^{3}H-taurocholate (approximately AU$1,200 per dose) was not deemed as a sustainable option at this time.

3.4.4 13C-methacetin

^{13}C-methacetin has been used as a liver function assessment by measuring the ratio and decay of $^{13}CO_2$ in the breath. Methacetin is passively taken up into the hepatocyte and is entirely metabolised by cytochrome 1A2 (CYP1A2) [245], which has been directly linked to assessing the function of the liver. CYP1A2 metabolises methacetin into acetaminophen (paracetamol) and CO_2 [232]. The $^{13}CO_2$ breathed out, measured in liver function tests, may not match the amount of ^{13}C-methacetin

injected, which could be due to either the diffusion process in the blood [246] or from the presence of a PSS, allowing methacetin to directly bypass the hepatocytes. As methacetin is exclusively metabolised in the liver and has a high extraction fraction, methacetin may be used to measure PSS by finding the ratio of methacetin and its metabolite in blood samples. PSSs may also be indicated by measuring the rate of $^{13}CO_2$ decay in the breath.

3.4.5 Indocyanine Green and the LiMON® System

Indocyanine green (ICG) is a water soluble compound, which has been used to measure liver function in a clinical setting. Hepatic blood circulation, energy reserve [247] and functional hepatic mass [248] can also be measured by ICG clearance. ICG easily binds to albumin in plasma and then is completely taken up via OAT7 and transferred to the biliary system [249]. ICG remains unchanged as it does not enter the intestine, whereby avoiding enterohepatic recirculation [250].

ICG clearance tests involve measuring serum samples at several time points post intravenous administration of ICG, with liver function capacity (ICG retention) best seen at 15 minutes after administration (R-15). A normal ICG retention rate ranges from 3.5% to 10.6% at R-15 [251]. Non-invasive pulse infrared spectroscopy (i.e. LiMON® system, Pulsion Medical Systems, Munich, Germany) is also used to measure ICG uptake and elimination. The LiMON system monitors the ICG clearance continuously and gives a final clearance rate after 20 minutes [252, 253].

There has been some discrepancy in liver function tests between Okochi *et al*. [254], de Liguori Carino *et al.* [235] and Sugimoto *et al.* [252]. This may be due to a range of variables including individual patient metabolic rate or the severity of an individual's liver disease.

In a standard LiMON® test, each patient is intravenously injected with 0.25 mg/kg of ICG-PULSION® dye in 5 mL of saline solution. ICG plasma clearance and retention is then measured continuously for 20 minutes [235]. As ICG has a low extraction fraction of 0.61 [255] and concentrations are measured constantly, it is hypothesized that the presence of a PSS may be shown graphically. When ICG is injected directly into the portal vein, ICG will quickly bypass the liver through a PSS and theoretically form an early peak on the LiMON® machine followed by a slower secondary peak from the ICG that has passed through the liver. This may be visually demonstrated by double peaks shown in an ICG concentration versus time graph. The size of the first peak is dependent on the size of the PSS. However, if the PSS is small, it may be visually demonstrated as a broad parabolic graph. It is unknown if extremely small anatomical shunts, i.e. kinetic shunts [226] or capillarisation will be visually shown in these results.

3.5 Conclusion

There are many more pharmacological agents, other than those discussed, that have a high extraction fraction and short half-life (such as glyceryl trinitrate,

nimodipine and lovastatin), however these generally have severe side effects when used in addition with other drugs and may cause harm. Four compounds were chosen to be used in this study to measure and detect PSSs, those being lignocaine, sorbitol, ^{13}C-methacetin and ICG. ^{13}C-methacetin and ICG have the advantage as ^{13}C-methacetin's metabolite $^{13}CO_2$ can be measured non-invasively via breath testing and ICG can be measured by pulse spectrometry, both are relatively inexpensive.

CHAPTER 4

Analytical Methods and Results

4.1 Introduction

In this study, four compounds, ICG, ^{13}C-methacetin, sorbitol and lignocaine were chosen for assessment based on the fact that they are quickly metabolised by the liver, and therefore it is possible to obtain a snap shot of liver function in a short period of time (see *Chapter 3: Possible Methods for Portosystemic Shunt Detection*). An additional two compounds Evans blue dye and ^{14}C-sucrose were used as a comparative measure as these are not metabolised by the liver.

It was postulated that a deviation in the rate of metabolisation and transit times for a given compound could identify and quantify a PSS. Particular focus was given to ^{13}C-methacetin and ICG for their ability to be measured non-invasively via breath testing and percutaneous spectrophotometry respectively. This chapter aims to determine which of the selected compounds has the most potential for PSS detection and quantification.

4.1.1 LiMON ® Spectrophotometry

The ICG retention and elimination has been well established as a liver function test and there are many different techniques to detect ICG in the blood. One ICG detection technique is the use of pulse spectrophotometry [256-259], which was first developed in 1967 [260]. Currently, the LiMON® system (Pulsion®, Germany) is

the only spectrophotometry device, used for the detection of ICG available in Australia (Figure 4.1) [261]. The LiMON® system detects approximately 25 to 30 data points per second and determines the ICG plasma disappearance rate (PDR) and the retention rate at 15 minutes (R15). The R15 score can be integrated with a risk score or used on its own as a measure of liver function [261-263]. More recently, the LiMON® system has been used with ^{13}C-methacetin [264], for the prediction of post-hepatectomy liver failure [235]. The LiMON® system was chosen for this study due to it being non-invasive, inexpensive and for possessing a fast sampling rate (see *Chapter 3: 3.4.5 Indocyanine green and the LiMON® system*).

It was hypothesised that an early peak or double peak may occur in the presence of a shunt. The mean residence time (MRT) lag time; the time taken for the ICG concentration to reach a threshold, are reduced in the presence of a shunt.

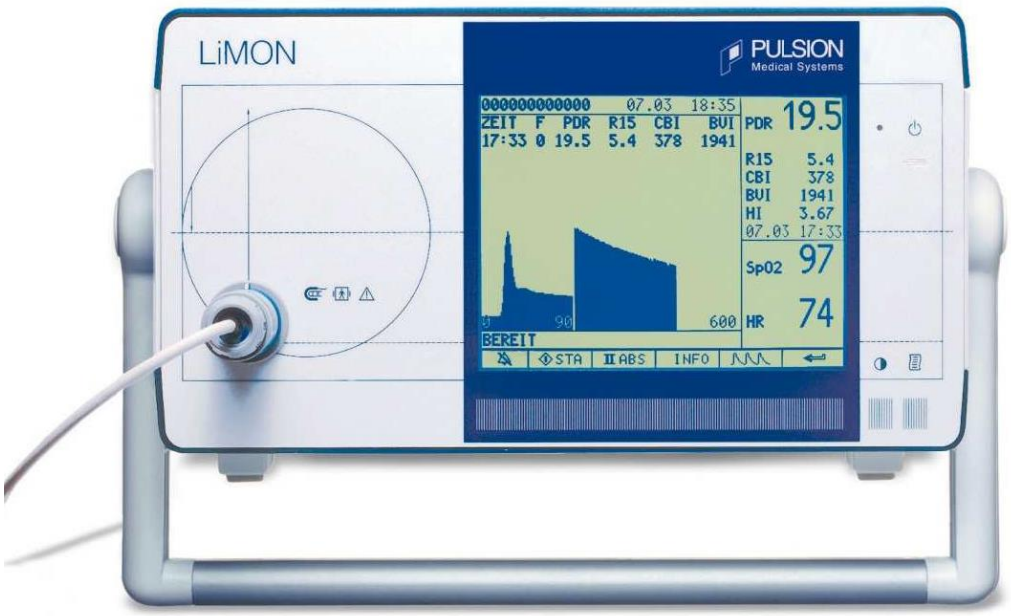

Figure 4.1: LiMON machine by Pulsion® Medical Systems (Germany) that uses spectrophotometry to detect Indocyanine Green dilution and retention in the systemic system (Source: http://www.pulsion.com/index.php?id=2189 Accessed: 11-02-2013)

4.1.2 Breath Testing

Breath testing with 13-carbon labelled [^{13}C] compounds has been used for a range of tests including the detection of *Helicobacter pylori* using ^{13}C-urea [265-267], lung cancer detection [268-270], gastric emptying using ^{13}C-acetic acid and ^{13}C-lactose ureide [271] and liver function using ^{13}C-phenylaline, ^{13}C-lucine or ^{13}C-methacetin [232, 272]. In particular ^{13}C-methacetin has been used to predict liver failure post-hepatectomy [264] and post-liver transplantation [273]. However, despite the advantages of non-invasive breath testing, ^{13}C labelled compounds are not widely used in a clinical setting mostly due to a lack of understanding of the ^{13}C-methacetin and $^{13}CO_2$ metabolic process [274]. For this study ^{13}C-methacetin was used as it is exclusively taken up and metabolised by the liver, and its metabolite $^{13}CO_2$ can be non-invasively collected in vials and assayed by isotope-mass spectrometer (IRMS) (see *Chapter 3: 3.4.4 ^{13}C-methacetin*).

4.1.3 Plasma Sampling

Lignocaine, also known as lidocaine or xylocaine, is a local anaesthetic used in many surgical procedures or for post-operative analgesia [275]. Typically, lignocaine is injected subcutaneously as local anaesthesia, but can also be intravenously injected to treat ventricular arrhythmia [276]. The rate of Lignocaine metabolisation is dependent on hepatic blood flow [241]. Therefore, a PSS would change the hepatic haemodynamics and therefore rate of lignocaine metabolisation and MEGX production is inversely proportional to the size of the PSS (see *Chapter 3: 3.4.1*

Lignocaine and Monoethylglycinxylidide (MEGX)). Lignocaine was used in this study due to its rapid uptake into the liver and short half-life, and was deemed safe for intravenous injection at a low dose.

Sorbitol is found in fruit [277] and is commonly used as an artificial sweetener [242]. It is not typically used in a clinical setting, however sorbitol has ben used previously used as an agent to measure liver function [243]. Sorbitol is normally used as an artificial sweetener.Sorbitol was used in this study due to its high uptake into the liver, despite a slow metabolism rate [243] (see *Chapter 3: 3.4.2 Sorbitol, Fructose and Ethanol*).

4.2 Methods

4.2.1 Procedure Overview

Chapter 2 provides full details of the PSS surgical procedure. Briefly, under general anaesthesia administered by a trained veterinary technician, a midline laparotomy was undertaken. Visceral rotation was then performed to allow exposure of the infrahepatic vena cava. Following from this, the vena cava was mobilised in a cephalad fashion to a level at the confluence of the liver substance and the adventitia of the infrahepatic vena cava. The portal vein was identified and mobilised with separation of lymphatics and nodes surrounding the portal vein. The swine were systemically heparinised with a weight appropriate dose of IV Heparin (80 units/kg). Thereafter partial clamping using a side biting/Satinsky clamp was performed on the cava. A longitudinal venotomy was then performed with local heparinised saline irrigation. An end-to-side anastomosis of the portosystemic shunt was performed using continuous 6/0 polypropylene suture. The shunt was then flushed with heparinised saline and clamped and the portal anastomosis is similarly completed under partial occlusion clamping, with end to side anastomosis using 6/0 suture material. The shunt and portal system were flushed with heparinised saline, with the suture line completed and haemostasis achieved. Antegrade portal circulation was achieved prior to releasing the clamp on the shunt. Cannulae were introduced with surrounding 6/0 purse string sutures into the portal circulation and infrahepatic vena cava. Flow direction is confirmed with pressure differences between the portal vein and infrahepatic vena cava.

A LiMON® disposable sensor was attached to the bottom lip of the pig and reinforced with surgical tape. The LiMON® machine was left to stabilise for several minutes until 'ready' was shown on the display. The machine was then connected to a computer so the raw data files could be recorded. The marker injection was connected to the large lumen (16G) catheter which was previously inserted into the portal vein. The LiMON® machine was started with a 10 second count down and the bolus of markers were injected at the end of the countdown, followed by 5 mL of saline to flush the catheter.

Bolus injections were prepared containing ICG, ^{13}C-methacetin, lignocaine and sorbitol (Table 4.1). A second bolus was prepared containing Evans Blue and ^{14}C-sucrose (Table 4.1). All injections were stored in a dark and warm environment until time of administration (See *4.2.2 Marker Preparation*).

The first bolus was injected (Table 4.1) in the following scenarios. 1) Portal vein with shunt open. 2) Portal vein with shunt closed (control). 3) Jugular vein (peripheral site) with shunt closed. 4) Jugular vein with shunt open. Each bolus was injected in less than 2 seconds with sampling collected for the following 40 minutes (see *4.2.3 Sample Collection*). The animal was allowed to stabilise for 5 minutes before the next injection. The following two injections using bolus 2 (Table 4.1) were both made into the portal vein with the shunt open and then again closed.

Sampling for Evans blue dye and ^{14}C-sucrose in the latter two injections were collected for three minutes each. All blood samples were immediately centrifuged for 10 minutes and the plasma was separated and stored at -80°C until ready for analysis. Breath samples were stored away from UV light at room temperature until time for analysis (see 4.2.3 Sample Collection).

4.2.2 Marker Preparation

Indocyanine green (25 mg vial, PULSION®), ^{13}C-methacetin (Cambridge Isotope Laboratories Inc., MA), D-Sorbitol (Optigen Scientific, Australia) and Lignocaine (2%, 100 mg in 5 mL, Pfizer Australia) were combined as a bolus injection in a single 20 mL syringe with the doses listed in Table 4.1. Prior to injection, each compound had to be made into a stock solution. The two ICG bottles were prepared by filling the bottle with 5 mL double distilled H_20 and kept away from light. ^{13}C-methacetin was prepared by dissolving 500 mg in 10 mL of 100% ethanol and agitated for 10 minutes or until dissolved in a 35°C water bath to speed up the process. The solution was then kept in a 30°C water bath to prevent precipitation. Sorbitol was prepared by dissolving 6g in 10mL of double distilled H_2O.

A second injection set was prepared by dissolving 100 mg of Evans blue (Sigma-Aldrich) in 2 mL double distilled H_2O and agitating until dissolved. A small amount of ^{14}C-sucrose (10 µL, 3 x 10^6 dpm) was added to the Evans blue solution. The tube was then wrapped in cling-film and stored in another larger tube to reduce

radiation exposure. This sample was prepared by a licenced laboratory technician with radioactive substance training. Neither Evans blue dye or ^{14}C-sucrose is metabolised by the liver, and is therefore administered as control compounds to show the limits of the shunt and hepatic system.

Table 4.1: Dose and stock solution of each compound used as marker for portosystemic shunts.

Drug	Dose (mg/kg)	Stock Solution Concentration (mg/mL)
Bolus 1		
Lignocaine	1	20
^{13}C-methacetin	2	50
Sorbitol	30	600
ICG	0.25	5
Bolus 2		
^{14}C-sucrose	3 x 10^6 dpm	-
Evans Blue	1	50

ICG – iIndocyanine green

4.2.3 Sample Collection

Blood samples were collected from the large lumen catheter (16G) inserted into the IVC. Samples were rapidly collected at a rate of 1 mL every ten seconds for two minutes using 2 mL syringes, then every two minutes until 20 minutes elapsed, and then every five minutes until 40 minutes elapsed. Blood samples were then transferred into 1.5 mL microtubes with approximately 20 µL heparin. All samples were agitated for five seconds then centrifuged for ten minutes at 15,000 rpm (~25,000 x g). The supernatant was separated and placed in new 1.5 mL microtubes for storage at -80^{o}C. Simultaneously, the LIMON® collected the density of ICG via a spectrometer placed on the bottom lip. At the same time the blood samples were taken, breath samples were also collected in duplicate every two minutes until 40 minutes had elapsed. Breath samples were collected in vacuum sealed 12 mL Exetainer® vials with a rubber septa (138W, Labco®) using a modified blood transfer device (Terumo® Venoject holder with Venoject male luer adapter) (Figure 4.2). Two BD Conneta™ three way taps with Leur-Lock were joined and connected between the sample line for the anaesthetics machine and respirator. Blood transfer devices were then connected to the free end of the three way tap. The Exetainers® were then manually pressed down in the transfer device (Figure 4.2), piercing the septa in time with the respirator.

After all four sample sets were collected a bolus injection of Evans blue and ^{14}C-sucrose was injected into the portal vein with the anastomosis open and closed

(control). Blood samples were taken every 10 seconds for two minutes and every 20 seconds until three minutes had elapsed. No breath samples were taken.

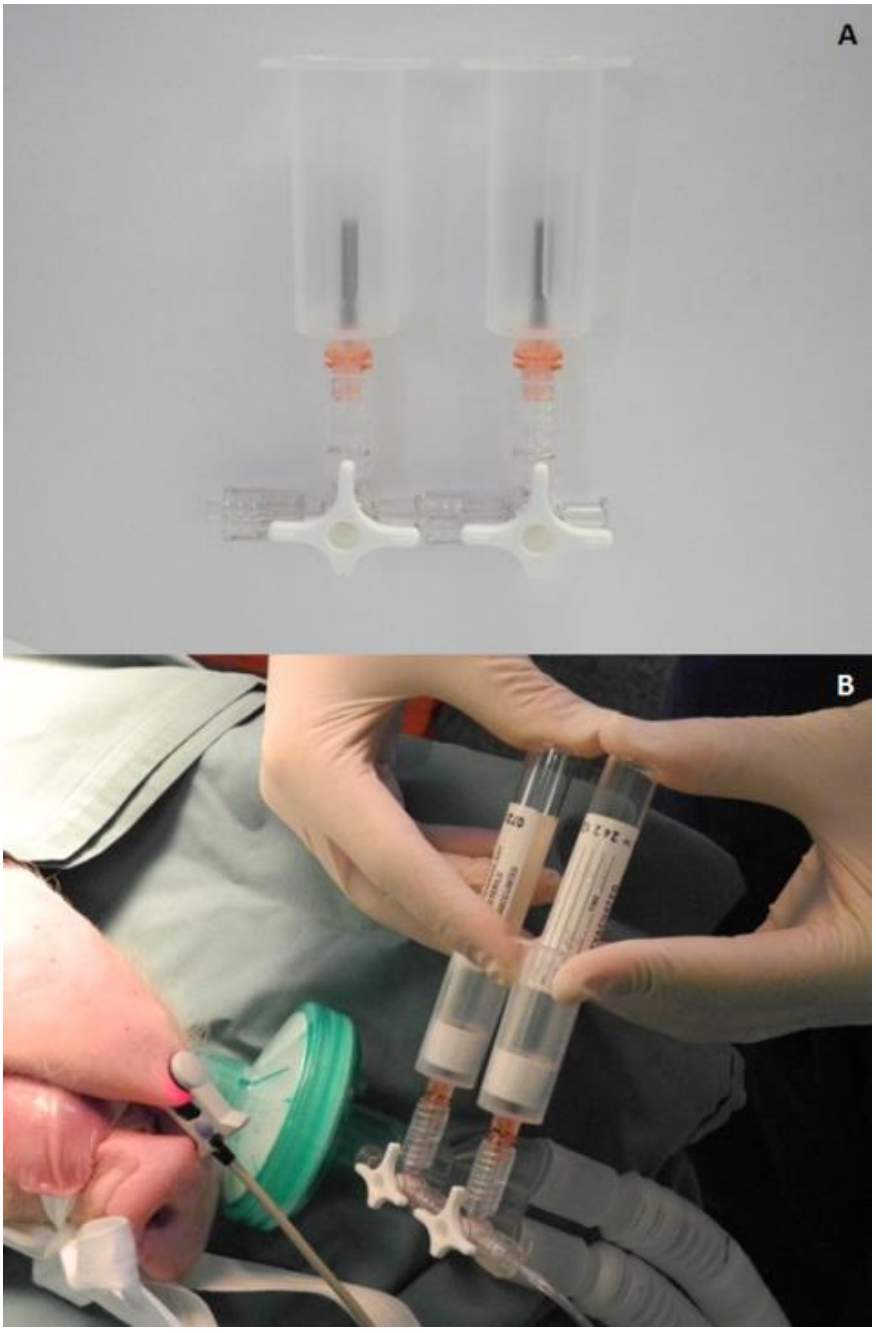

Figure 4.2: (A) Breath sample collecting apparatus consisting of two blood transfusers and two three way taps that **(B)** connect to the sample line of the anaesthesia machine.

4.2.4 Analytical Methods

4.2.4.1 High Performance Liquid Chromatography (HPLC) Equipment

Two HPLC systems were used. The HPLC system consisted of a Waters 616 quaternary pumping system (Waters, Milford, MA) with a Waters pump controller module II, a Waters 717-plus auto injector, a Waters symmetry C18 5 µm 3.9 x 150 mm steel cartridge column with a Securityguard™ (Phenomenex®) column guard and a waters 996 photo diode array detector. This was used for the analysis of methacetin, lignocaine and sorbitol. The second HPLC system consisted of a Shimadzu SCL-10A VP system controller, SPD-10A UV-VIS spectrophotometric detector, LC-10AT pump controller and Gastorr GT-102 pump. This system was used to analyse ICG. The same Waters symmetry C18 and guard column was used.

4.2.4.2 Sample Preparation for HPLC

The compounds ICG, methacetin, lignocaine and sorbitol were assayed via high-performance liquid chromatography HPLC. Samples were prepared by adding 900 µL of 99% HPLC grade methanol (Scientific Optigen, Australia) to 300 µL plasma sample in a micro centrifugation tube. These samples were agitated for 20 seconds to ensure complete coagulation of the proteins. The prepared sample was then centrifuged for 10 minutes at 15,000 rpm (25,000 x g). The 200 µL supernatant was then transferred to the auto-sampler vials for HPLC assay.

Sample preparation for sorbitol required several steps so it was detectable via the HPLC machine [278]. This required combining 70 µL plasma sample, 20 µL of 1 M phosphate buffer and 15 µL of 8M sodium hydroxide followed by agitating for five minutes. To stop the reaction 15 µL of 1M phosphoric acid was added and then agitated for a further 60 seconds. To coagulate the proteins 100µL of the prepared samples was combined with 300µL of methanol, agitated for 30 seconds and then centrifuged for 10 minutes at 15,000 rpm (25,000 x g).

A standard curve for each compound was made using the same sample preparation for each of the compounds with known concentrations of 0, 5, 10, 20, 50, 100 µg/mL.

4.2.4.3 Methacetin HPLC Method

The methacetin assay was based on a phenacetin assay [279] and performed on the Waters HPLC machine. The mobile phase for methacetin was made up of 30% methanol and 70% 2 mM phosphate buffer, pH3.8. The methanol and phosphate buffer were pre-mixed and sonicated for five minutes to remove any gas. The wavelength was initially set to a range of 200-300 nm to find the optimal wavelength. The optimal wavelength was found to be 247 nm with an expected retention time of five minutes when the flow rate of mobile phase is set to 1 mL/min.

4.2.4.4 Indocyanine Green HPLC Method

The HPLC method for ICG was based and modified from Soons *et al.* [280]. The optimised method used 45% acetonitrile and 55% 2 mM phosphate buffer, pH6 as the mobile phase. The UV detector wavelength was set at 790 nm and the retention time of ICG was four minutes.

4.2.4.5 Lignocaine and MEGX HPLC Method

The HPLC method for lignocaine and MEGX was based on Chen *et al.* [281] ,Abraham *et al.* [282] and Wusbucju *et al.* [283], and adapted to the HPLC equipment available. The mobile phase contained 5% methanol and 95% 0.05M phosphate buffer at pH 4.5 at a rate of 1.6mL/min. The wavelength for the detector was set at 210nm and the expected retention time was 22 minutes for MEGX and 35 minutes for Lignocaine.

4.2.4.6 Sorbitol HPLC Method

The HPLC method for sorbitol was based from Richmond *et al.* [284] and Kwang-Hyok *et al.* [278], and adapted to the HPLC equipment available. The mobile phase contained 70% acetonitrile. The wavelength for the detector was set at 228 nm and the expected retention time was 23 minutes.

No data could be extracted from the sorbitol assay. No peak could be seen between the positive control and background. This, however was thought to be an issue with the sample preparation as the sorbitol compound itself doesn't have an active component that can be detected and therefore requires a benzoic ring to be attached. Due to time restrictions together with the unreliable and lengthy preparation assaying technique it was decided that sorbitol would no longer be assayed.

4.2.4.7 ^{14}C-sucrose and Evans Blue Analytical Methods

^{14}C-sucrose was assayed via scintillation. A plasma sample of 100µL was combined with 2 mL of scintillation buffer and agitated for 15 seconds in scintillation tubes. A MINIMAX beta TRICARB 4000 series liquid scintillation counter (Packard Instruments, Meriden, CT) was used and recorded for three minutes in each vial.

To assay Evans blue, 100µL of plasma was inserted into each of the wells of a Cellstar® F-bottom 96 well plate (Greiner Bio-one). The colour density was determined by absorbance on a Fluostar OPTIMA (BMG Labtech) at a wavelength 625nm.

4.2.4.8 $^{13}CO_2$ Breath Analysis Method

Breath samples were sent to the Gastroenterology department at the Women's and Children's Hospital (North Adelaide, South Australia) for analysis. Breath samples were analysed using an isotope ratio mass spectrometer (IRMS). The machine used was an Automated Breath ^{13}Carbon Analyser (ABCA, SerCon®), an ABCA auto-sampler and SC8400 carbosieve G 60/80 mesh packed column. The IRMS was first calibrated with 5 ± 0.5% CO_2 in nitrogen. The breath samples in the exetainers were then loaded into the auto-sampler with a 5 ± 0.5% reference gas placed in every 10th position. The data was then analysed using the provided software (SerCon, ABCA ^{13}Carbon Isotope Ratio Analyser: Version 500.7.4 2004).

Breath samples were analysed from a trial animal showing a reduced concentration of $^{13}CO_2$ in the breath in the shunted model as would be expected (Figure 4.3). However as further breath samples that were assayed, increased inconsistency and inaccuracy were shown by a quality control standard (see *6.2.2 Breath Sampling*). Therefore further breath samples not be analysed as the data would not be accurate. Briefly, it was thought that the isoflurane used to anaesthetise the animals was present in the breath samples combined with components within the gas chromatography column. Isoflurane slowly blocked the column causing the retention time of $^{13}CO_2$ to decrease and missing the analysis window. No previous literature has reported this issue. Several potential solutions were researched including use of a silica zeolite filter, however one downfall of this procedure is that it also removes CO_2 from the breath [285]. A further procedure was also attempted

without success: heating the column to 100°C to ‘unblock’ the column. To prevent this from happening again, all animals from this point forward were anaesthetised via intravenous administration only.

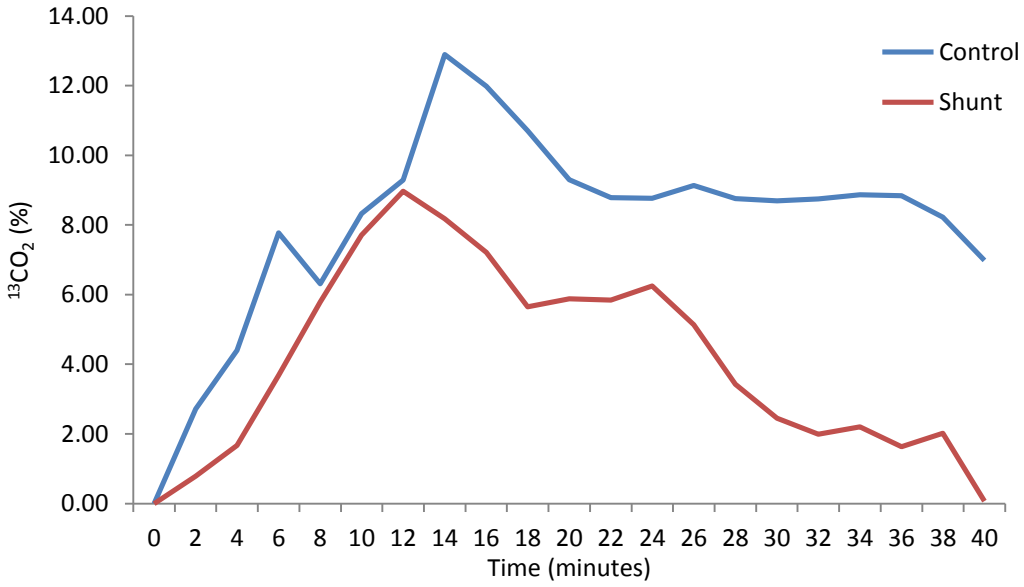

Figure 4.3: Pilot results of $^{13}CO_2$ ratio in the breath of a shunted and non-shunted pig.

4.2.5 Intravenous Anaesthesia

In a follow on study (see *Chapter 5: Portosystemic simulation*), three additional animals had a similar portosystemic shunt inserted. These animals were anaesthetised via intravenous administration only using compounds that are excreted by the renal system. Anaesthesia used was alfaxalone (Alfaxan®, Jurox Pty Ltd, Australia), diazepam (Pamlin injection®, Parnell Laboratories, Australia) and ketamine (Ketamil®, Ilium, Australia). Alfaxalone is a common intravenous and intramuscular anaesthetic for cats and dogs.

Each animal was initially sedated with 7 mL of ketamine injected intramuscularly. This was followed two minutes later by a secondary intramuscular injection of 100 mg (10 mL) alfaxalone (Alfaxan®, Jurox Pty Ltd, Australia). The animal was placed on the surgical table and an additional dose of 10 mL alfaxalone was administered intravenously via an ear vein. The animals were then placed on a respirator and a 16G x 133 mm intravenous catheter (Angiocath™, BD Australia) was inserted into the external jugular vein. A saline drip line was attached and set at 500 mL/hr. To the same intravenous line, alfaxalone was administered at a rate of 50 mL/hr using a syringe pump (P3000 syringe pump, IVAC Medical Systems). It was noted that alfaxalone alone caused the heart rate to rise dangerously above 200 bpm, therefore 30 mg (3 mL) of ketamine and diazepam were administered alternately every 30 minutes to maintain the heart rate around 150 bpm.

4.3 Results

Results from some animals used could not be included in this analysis. Computer technical errors occurred with the LiMON® system for pigs 1, 2 and 3. The LiMON® machine was unstable and therefore did not record for portal vein injections in pig 1 and for the systemic injections in pigs 2 and 3. The LiMON was particularly unstable for pig 1, however results were still recorded. Results from pig 1 were used with caution. There was suspected internal bleeding in pig 4 when the shunt was open as some results were abnormally low, believed to be due to internal bleeding while the shunt is open. This data is still shown, but not included in all the statistical analysis. To clearly identify differences between the control and shunted models and avoiding large variations between each animal, results are shown for each animal instead of their combined mean.

4.3.1 Evans Blue and ^{14}C-Sucrose Clearance

Evans blue in pigs 3 and 5 best show the presence of a shunt with peaks shown early, between 10 to 30 seconds, however opposing results are seen in pigs 4 and 6. As there is large variability, no trends between the animals were seen (Figure 4.4). However, the mean transit time (MTT) can still be determined. The mean area under the curve (AUC) was identical in the shunted pig and the control, being 4707.9 and 4410.3 ($p=0.7$), hence the MTT was also the same in the shunted model ($p=0.6$) (Table 4.2). This data was required to create a model.

Similarly to Evans blue, 14C-sucrose in pigs 3 and 5 best show the presence of a shunt with peaks appearing early between 10 to 30 seconds, with opposing results seen in pigs 2 and 4. Once again, as there is large variability no trends between animals were seen (Figure 4.5) There was a decrease in the mean MTT being 86.7 ± 11.1 seconds in the shunted model and 93.0 ± 15.3 seconds in the control (p=0.6) (Table 4.3).

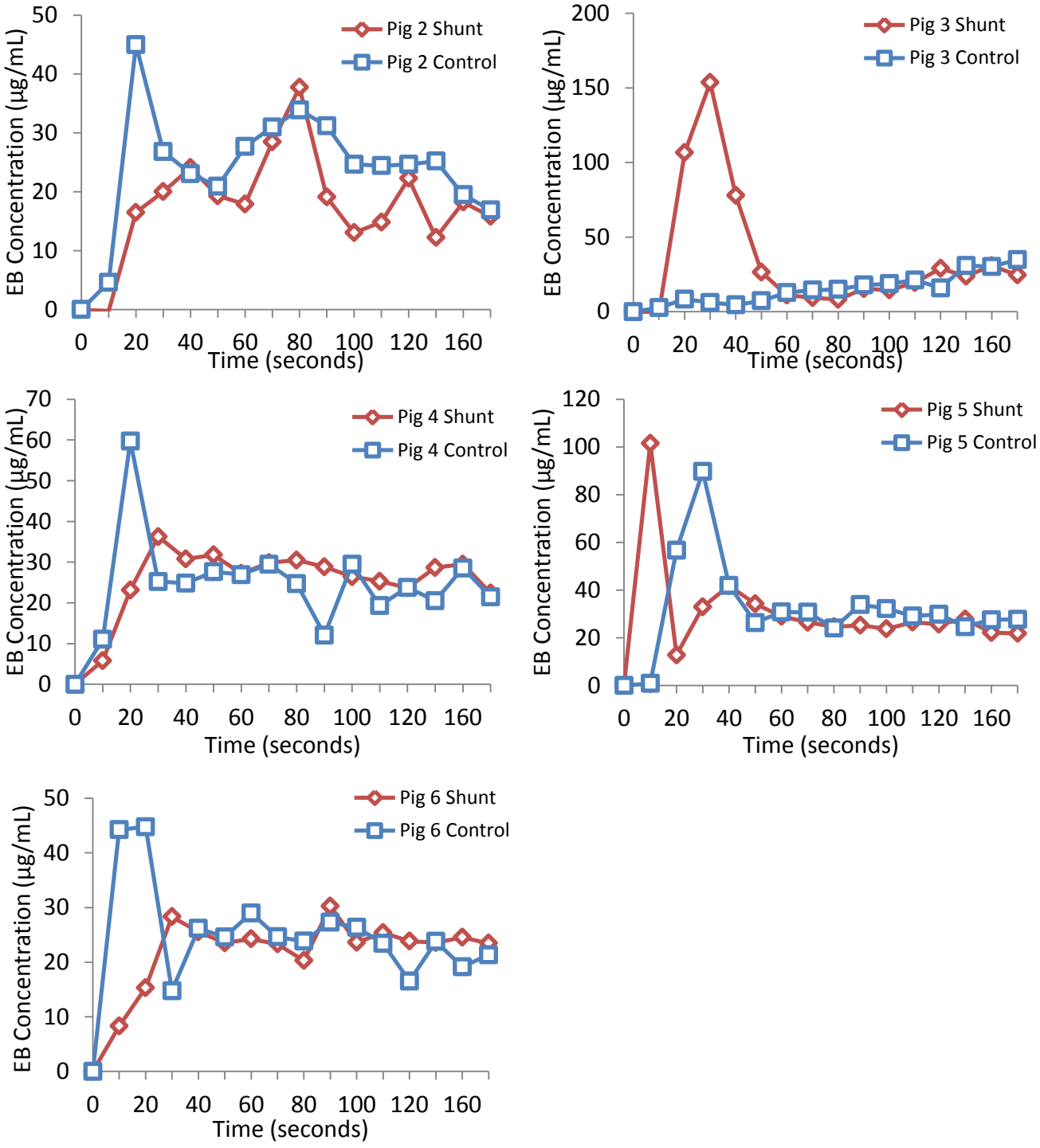

Figure 4.4: Concentration of Evans blue (EB) in each shunted pig and the mean when injected into the portal system. There is an error in pig 4 with regards to concentration as it is thought that there was internal bleeding while the shunt was open, however it is still shown to determine transit time.

Table 4.2: Mean transit time (MTT) with corresponding area under the curve (AUC) from Evans blue dye in the shunted and control models.

	Pig	2	3	4	5	6	Mean ± SD	p value
MTT (s)								
	Shunt	92.6	71.5	94.4	78.3	96.6	86.7 ± 11.1	0.599
	Control	89.3	119.9	88.1	84.2	83.2	93.0 ± 15.3	
AUC								
	Shunt	3209	6190.9	4702.8	5387.1	4034.9	4704.9 ± 1157.6	0.681
	Control	4282.7	4367	3097.4	4459.9	5730	4410.3 ± 933.2	

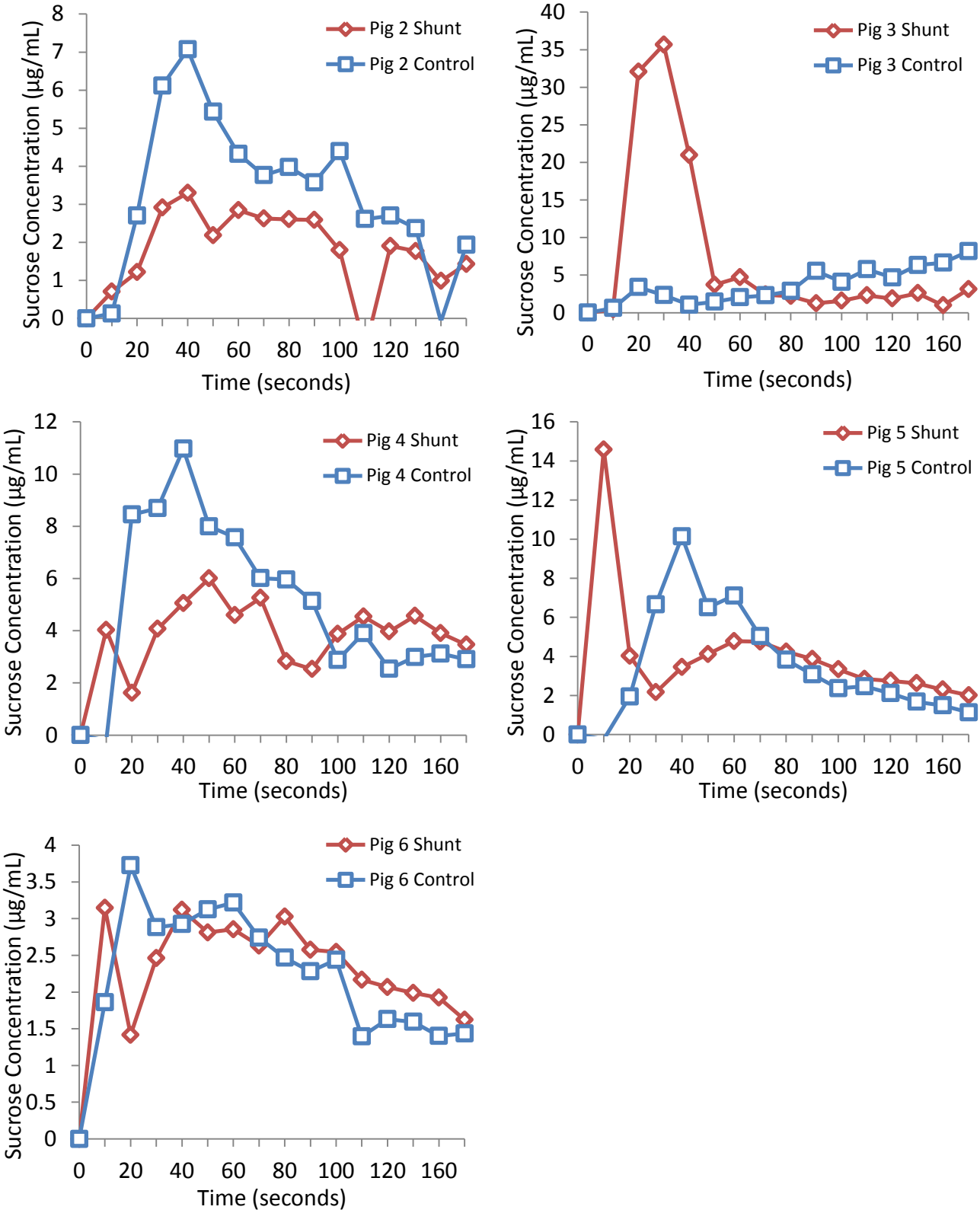

Figure 4.5: Concentration of ^{14}C-Sucrose in each pig when injected into the portal system. There is an error in pig 4 in regards to concentration as it is thought that there was internal bleeding while the shunt was open, however it is still shown to determine transit time.

Table 4.3: Mean transit time (MTT) with corresponding area under the curve (AUC) from ^{14}C-Sucrose in the shunted and control models.

	Pig	2	3	4	5	6	Mean ± SD	p value
MTT (s)								
	Shunt	83.7	48.4	92.5	72.2	86.1	76.6 ± 17.4	0.635
	Control	76	117.4	76.6	73.4	79.2	84.5 ± 18.0	
AUC								
	Shunt	317.6	1202.9	707.5	681.6	413	664.5 ± 344.8	0.759
	Control	546.6	726.3	863	595.7	389.4	624.2 ± 179.9	

4.3.3 Lignocaine and MEGX

No peaks for lignocaine were viewed in any sample therefore it can be concluded that all samples contained an undetectable amount of lignocaine. The standard curve demonstrated that the HPLC method could not detect lignocaine at concentrations lower than 5 μg/mL.

A standard curve for MEGX was prepared in phosphate buffer instead of plasma to determine the recovery of the extraction process [286]. Differences between the buffer and plasma prepared standard curves showed the recovery was 96.3 ± 10.1%. No differences were detected in the AUC between the shunted and control animals ($p=0.09$). Also, no significant differences were identified between the MEGX control and shunted models in AUC or time (Figure 4.6), $p>0.05$.

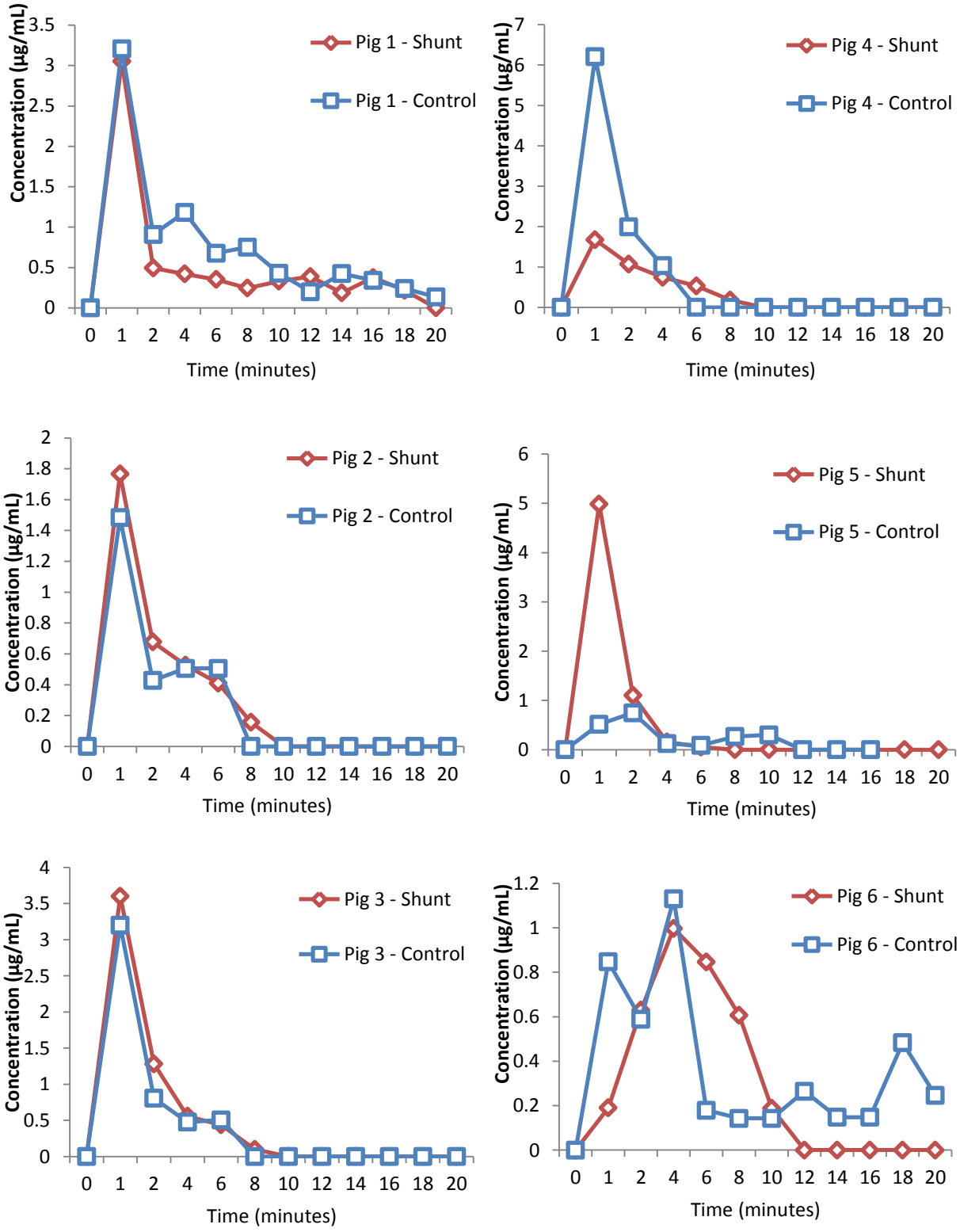

Figure 4.6: Concentration of monoethylglycinexylidide (MEGX) in each pig post injection of Lignocaine into the portal system. There is an error in pig 4 in regards to concentration as it was thought that there was internal bleeding while the shunt was open.

4.3.4 Indocyanine Green and LiMON®

4.3.4.1 ICG Clearance – Portal System Injection Site

There is little noticeable difference in the ICG concentration of the blood samples collected (Figure 4.7). The double peak and lag time cannot be visualised in the plasma samples due to the slow sampling rate causing poor resolution. However, this data was used to determine the relative blood concentration of ICG in the LiMON® data. A conversion factor was created by aligning the peaks and three corresponding time points of the plasma data and LiMON® data to find the ratio (Table 4.4). The ratio was then applied to the LiMON® data to obtain a relative plasma concentration.

There is a notable visual difference in the data from the LiMON® system between the shunt and control, being a bulge, shoulder or even a 'double peak', (Figure 4.8). A double peak is most clearly demonstrated in Pig 3 and 8 while all others presented with a shoulder. This shoulder caused a significant decrease in lag time (threshold of >0.01 μg/mL) with a mean of 33 ± 4.3 seconds in the shunted model and 43.8 ± 5.6 seconds in the control ($p=0.007$)(Table 4.5). The MRT was also shorter in the shunted model, but was not shown to be significant ($p=0.053$) (Table 4.6). A significance may be apparent with a larger sample size

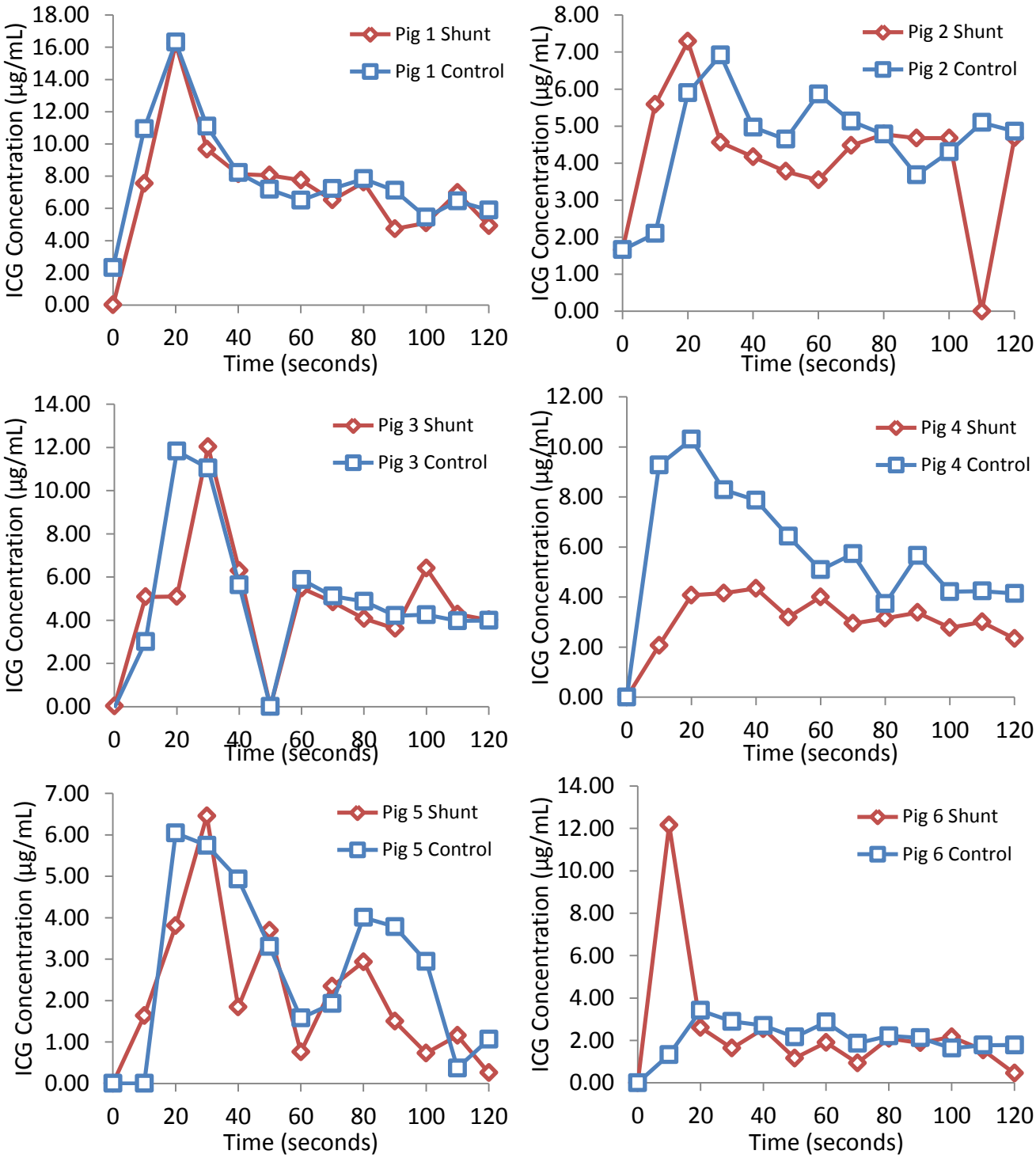

Figure 4.7: Concentration of Indocyanine green dye (ICG) in each pig in the plasma when injected into the portal system. There is an error in pig 4 in regards to concentration as it is thought that there was internal bleeding while the shunt was open, however it is still shown to reference with the LiMON® data.

Table 4.4: LiMON conversion factor to calibrate the LiMON® data into relative concentrations and its correlation coefficient (R^2) when indocyanine green is injected into the portal system.

Pig	Conversion Factor	R^2
2	3.15	0.84
3	4.20	0.89
4	4.30	0.85
5	4.77	0.98
6	5.85	0.98

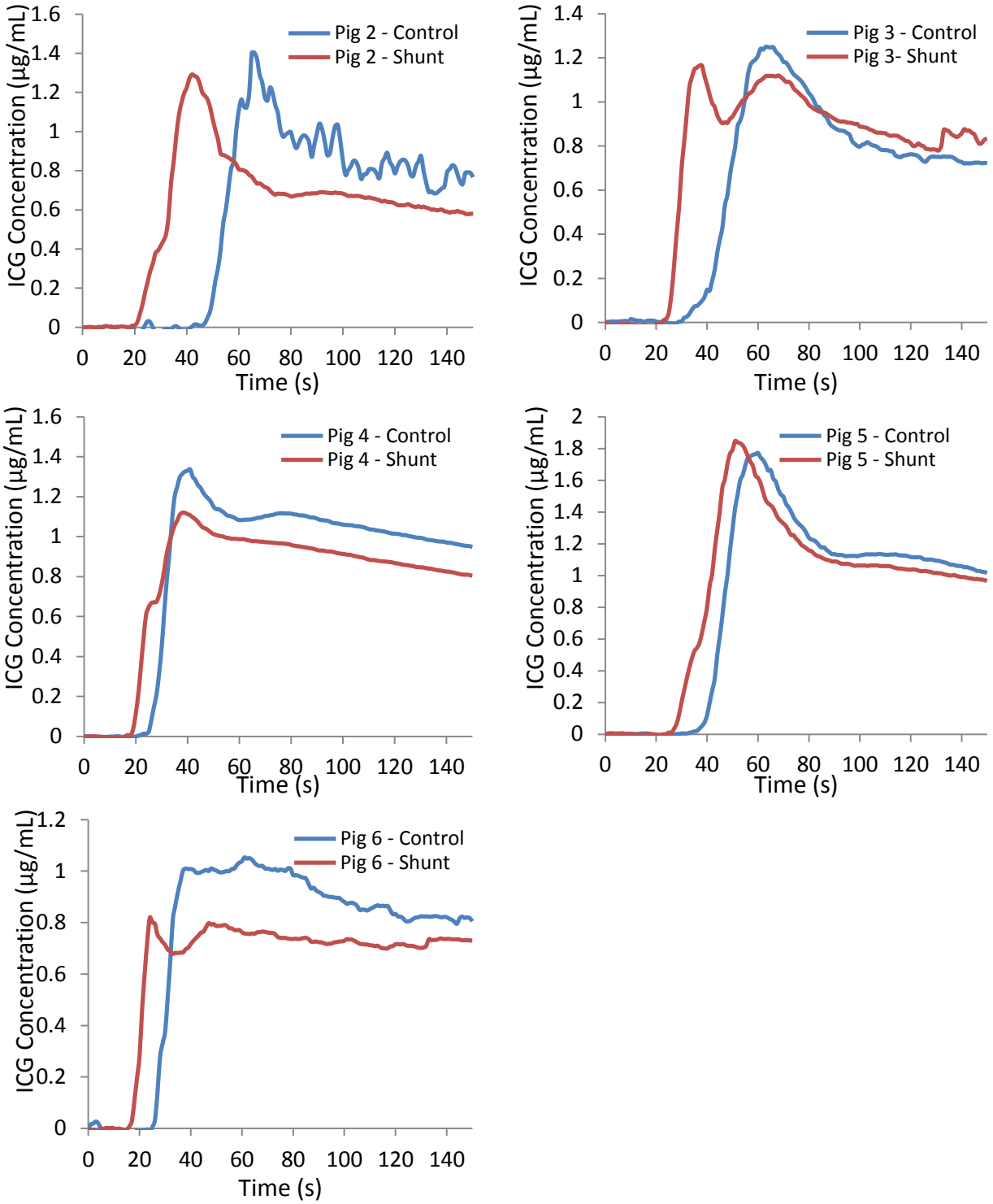

Figure 4.8: Concentration of indocyanine green dye (ICG) in each shunted pig and the mean from the LiMON® system when injected into the portal system. There is a error in pig 4 in regards to concentration, however it is still shown to determine transit times.

Table 4.5: Lag times (threshold > 0.01 μg/L) and time of the first peak from the portal injection using the LiMON® data.

	Pig	2	3	4	5	6	Mean ± SD	p value
Lag time (s)								
	Shunt	20	24	19	25	17	21 ± 3.4	0.034
	Control	43	31	23	34	26	31.4 ± 7.8	
1^{st} Peak time (s)								
	Shunt	33	27	31	38	36	33 ± 4.3	0.023
	Control	48	47	34	45	45	43.8 ± 5.6	

Table 4.6: Mean transit time (MTT) with corresponding area under the curve (AUC) from indocyanine green in the shunted and control models.

	Pig	2	3	4	5	6	Mean ± SD	p value
MRT (s)								
	Shunt	65.4	68	67.2	69.1	67.3	67.4 ± 1.3	0.053
	Control	76.6	72.5	69.4	73.2	68.7	72.1 ± 3.0	
AUC								
	Shunt	107.2	126.3	72.2	63	42.4	82.2 ± 34.0	0.429
	Control	109.0	109.2	164	75.2	38.4	99.2 ± 46.5	

4.3.4.2 ICG Clearance - Systemic Injection Site

Pigs 2 and 3 were excluded from this data set due to technical errors resulting in unrecoverable data.

As previously stated, a conversion factor was created by aligning the peaks and three corresponding time points of the plasma data (Figure 4.9) and LiMON® data (Figure 7.10) to find the ratio (Table 4.7). The ratio was then applied to the LiMON® data to obtain a relative plasma concentration.

The mean peak time in the shunt model was 23.5 ± 2.5 seconds, while the control mean peak time was 25.3 ± 5.6 seconds (p=0.5). The lag time neither showed any significant difference with the mean lag time in the shunt model being 11.5 ± 5.7 seconds and the control being 16.8 ± 5.7 seconds (p=0.4)(Table 4.8). Similarly, the MRT showed no significant difference in either shunt or control (Table 4.9).

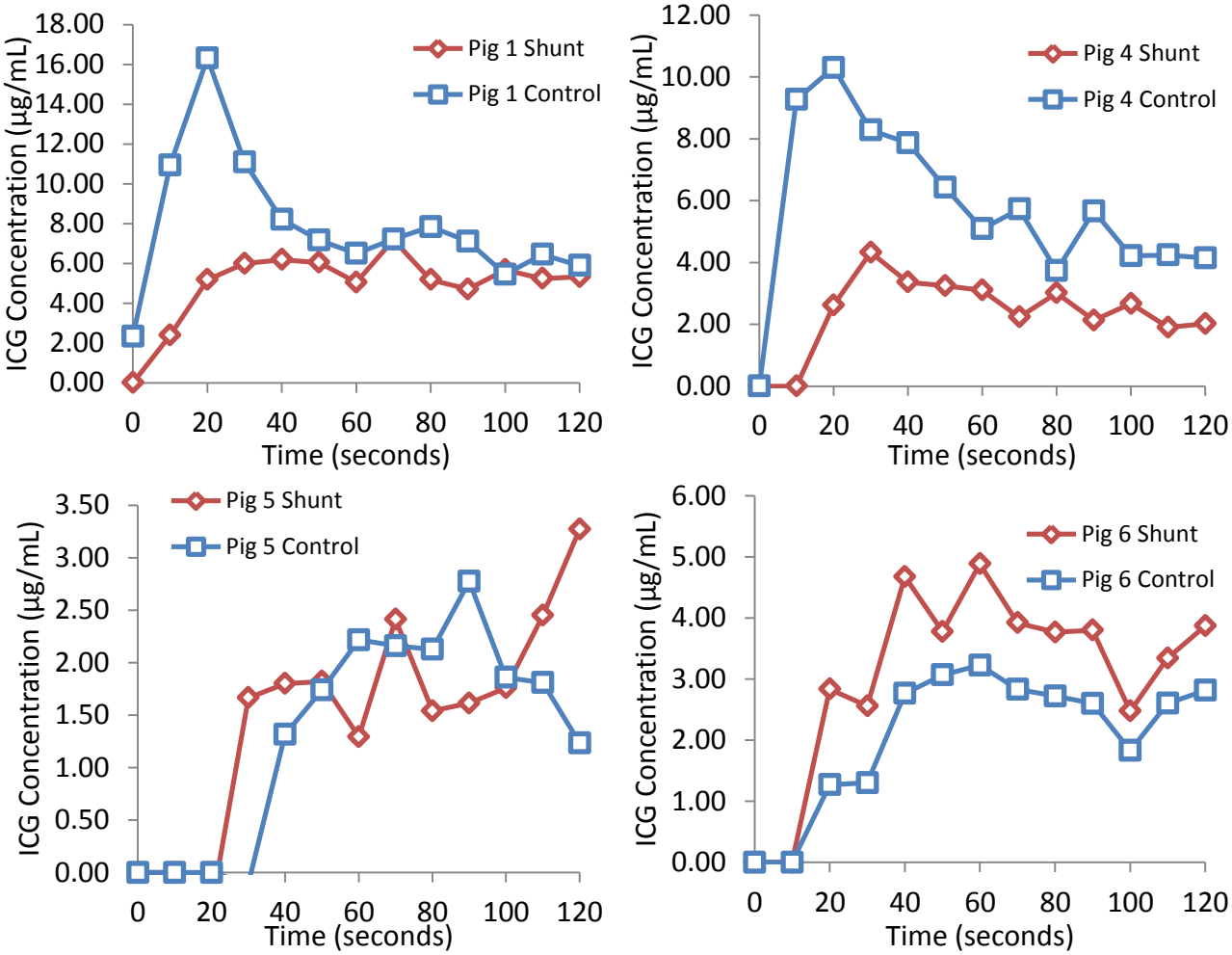

Figure 4.9: Indocyanine green concentration in the plasma as collected from the confluence of the hepatic veins in the inferior vena cava when injected into the systemic venous system (Jugular vein). There is an error in pig 4 in regards to concentration as it is thought that there was internal bleeding while the shunt was open, however it is still shown to reference against the LiMON® data.

Table 4.7: LiMON conversion factor to calibrate the LiMON® data into relative concentrations and its correlation coefficient (R^2) when Indocyanine green is injected systemically.

Pig	Conversion Factor	R^2
1	5.20	0.93
4	5.69	0.95
5	4.68	0.98
6	5.24	0.95

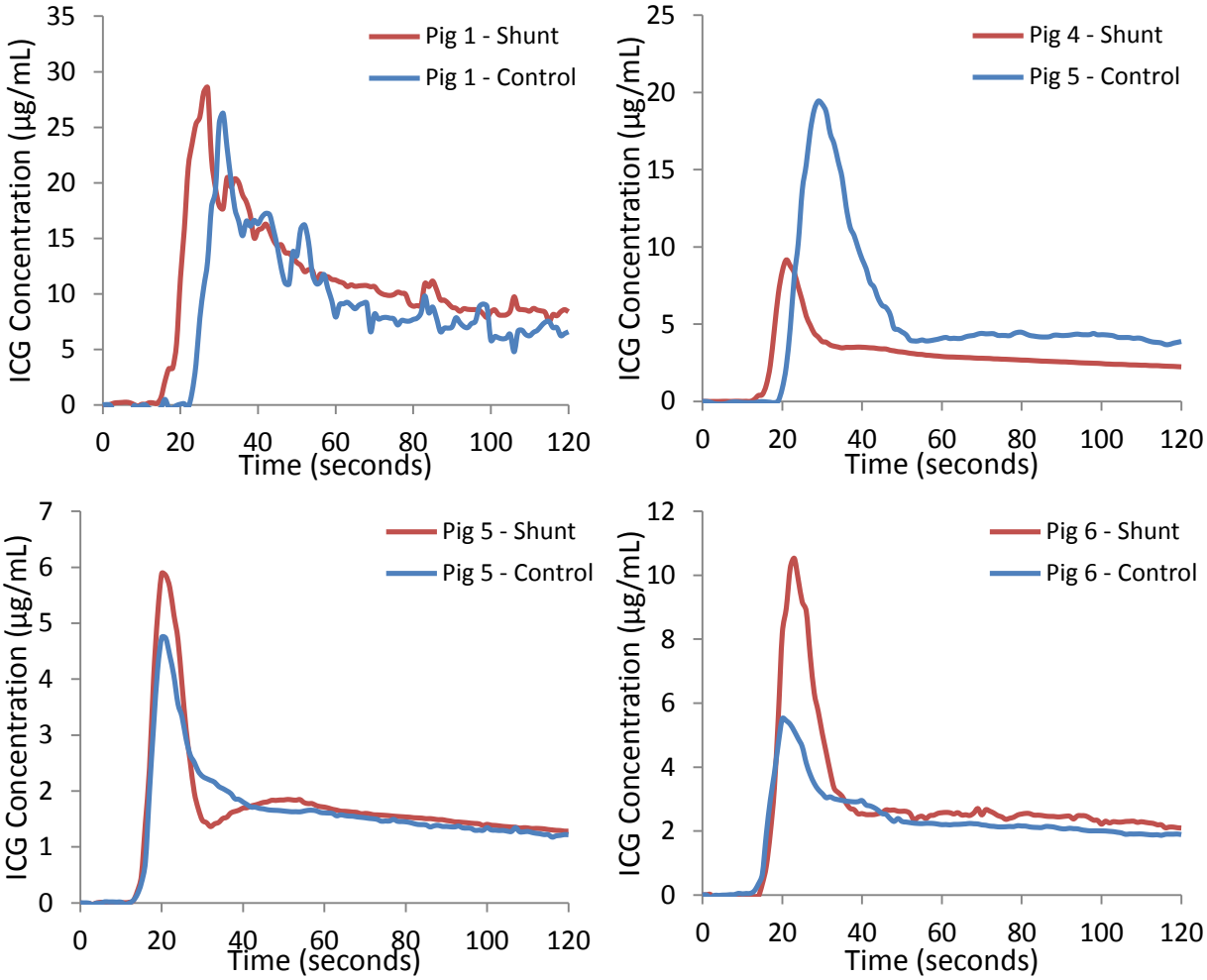

Figure 4.10: Concentration of indocyanine green dye (ICG) in each shunted pig and the mean from the LiMON® system when injected into the systemic venous system (jugular vein). There is an error in pig 4 in regards to concentration as it is thought that there was internal bleeding while the shunt was open, however it is still shown determine transit times.

Table 4.8: Lag times (threshold > 0.01 µg/L) and time of the first peak from the systemic injection using the LiMON® data.

	Pig	1	4	5	6	Mean ± SD	p value
Lag time (s)							
	Shunt	11	13	15	15	13.5 ± 1.9	0.452
	Control	23	20	13	11	16.8 ± 5.7	
1st Peak time (s)							
	Shunt	27	21	23	23	23.5 ± 2.5	0.548
	Control	31	29	20	21	25.3 ± 5.6	

Table 4.9: Liver mean residence time data for indocyanine green dye injected into the systemic system.

	Pig	1	4	5	6	Mean ± SD	p value
MRT (s)							
	Shunt	59.7	59	58.5	57.7	58.7 ± 0.8	0.381
	Control	62.1	57.7	58.7	60.1	56.2 ± 8.0	
AUC							
	Shunt	198.5	60.46	48.42	72.02	94.9 ± 69.8	0.821
	Control	147.7	107.8	39.1	64.9	101.4 ± 48.8	

4.3.5 Methacetin

4.3.5.1 Methacetin Clearance - Portal System Injection Site

There is variance between each pig of the residual methacetin in the plasma, particularly in the time of the peaks (Figures 4.11). The shunted model in pigs 3, 5 and 6 peaked early, while pigs 1, 2 and 4 occurred between 30 - 50 seconds. All peaks from the control were also seen between 30 to 50 seconds. The mean AUC, was similar between the shunt and control being 3308 ± 726 and 3727 ± 813 respectively ($p=0.10$). The area between 0 to 20 seconds is larger in the shunted model than the control, but not significant ($p=0.19$), with 358 ± 478 in the shunted model and 59 ± 57 in the control. This difference may be due to the small sample size and large variance in peak time of each animal.

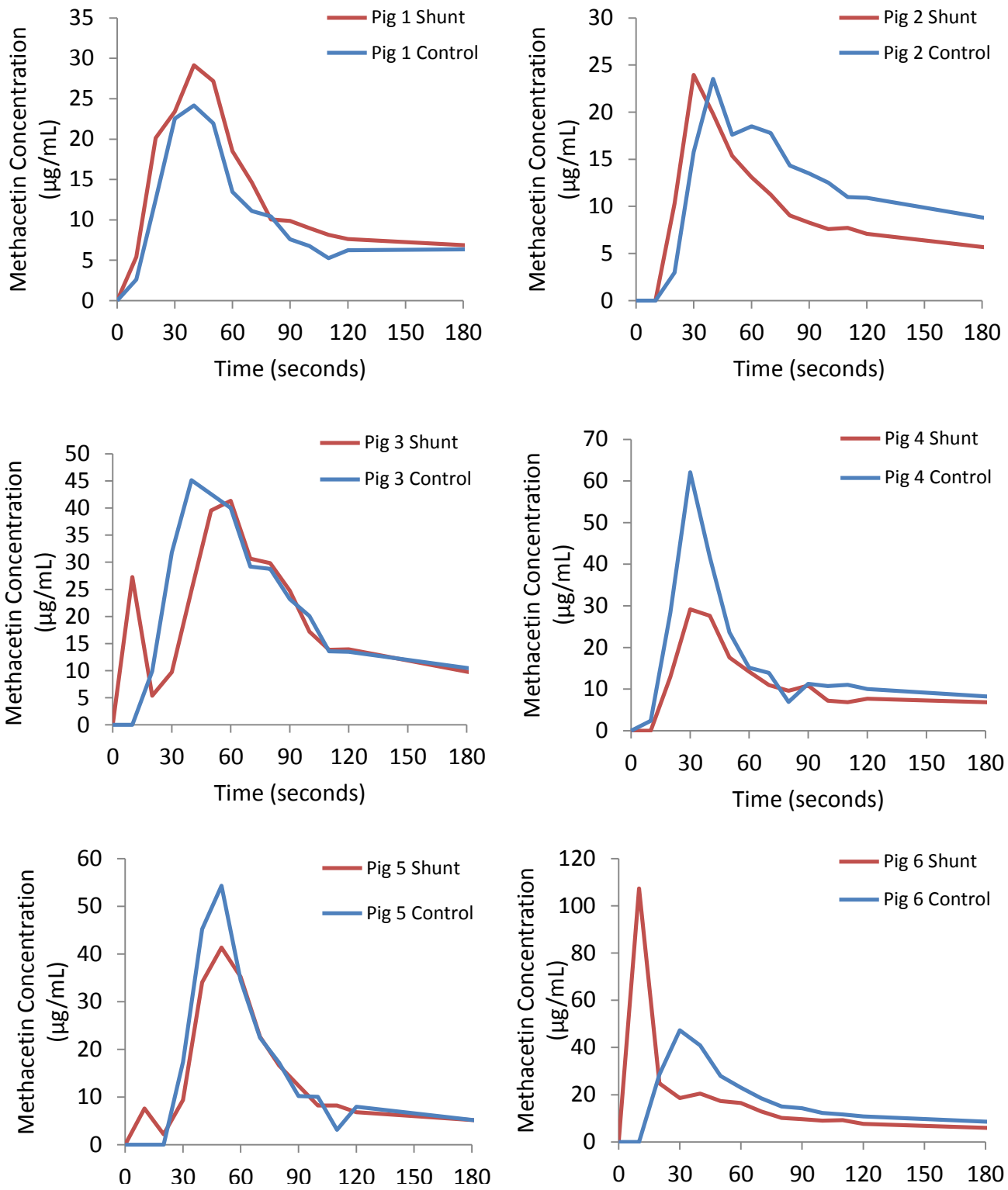

Figure 4.11: Methacetin concentration in the plasma from injecting into the portal system and collected from the confluence of the hepatic veins in the inferior vena cava. There is an error in pig 4 in regards to concentration as it is thought that there was internal bleeding while the shunt was open.

4.3.5.2 Methacetin Clearance - Systemic Injection Site

Due to the rapid uptake of methacetin into the liver, there is very little difference between the shunt and the control (Figures 4.12). Unlike the portal injection, there is no early peak in the shunted model followed by a secondary peak. All peaks appear at similar times. There is also no significant differences between the AUC ($p=0.9$), nor the area between 0 to 20 seconds ($p=0.5$).

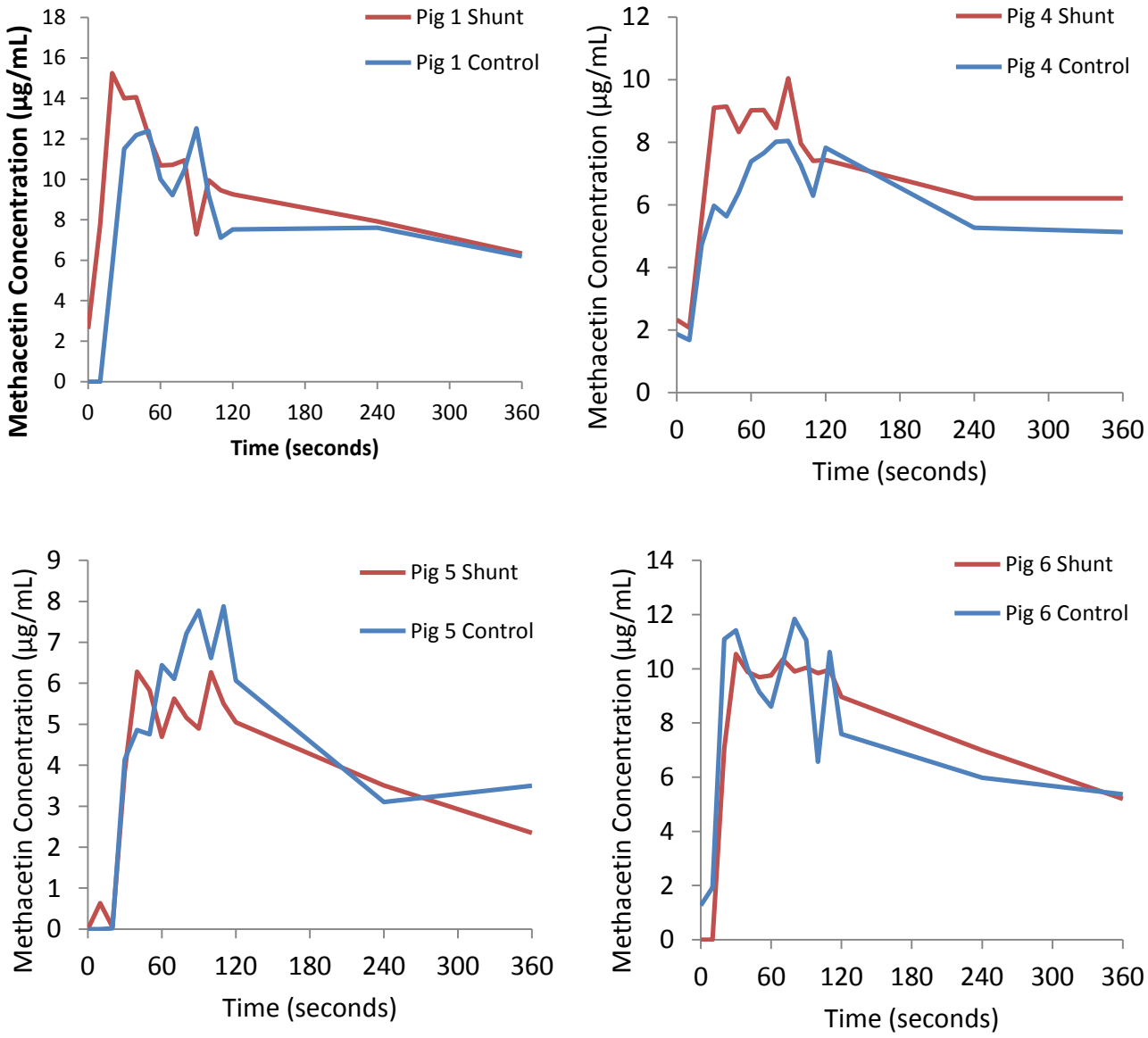

Figure 4.12: Methacetin concentration in the plasma from injecting into the jugular vein and collected from the confluence of the hepatic veins in the inferior vena cava. There is an error in pig 4 in regards to concentration as it is thought that there was internal bleeding while the shunt was open.

4.3.6 Breath Analysis

No significant difference was observed between the shunted and controlled scenarios (p=0.4, Figure 4.13). The accuracy of the breath test is undetermined as each vial contained less than 2% CO_2. The IRMS was calibrated for samples containing between 2% to 10% CO_2. However, the sampling window for $^{13}CO_2$ did not shift throughout the sampling, therefore validating the influence of isoflurane in the previous samples on the results.

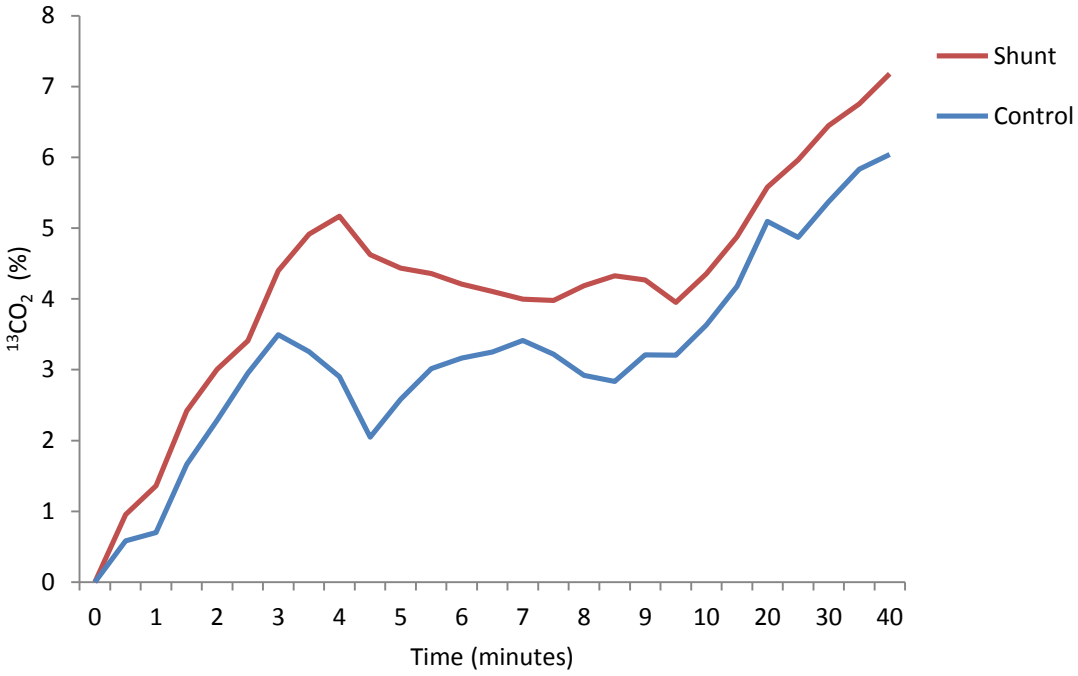

Figure 4.13: Ratio of $^{13}CO_2$ to $^{12}CO_2$ in the breath of a shunted and non-shunted pig. (p=0.4, n=3)

4.4 Discussion

The shunt created in the animal is a two compartment model (Figure 4.14) with presumed different flow rates in each compartment, one being the liver (*qQ*) the other being the shunt (*(1-q)Q*). Due to the sheer size of the shunt, it was hypothesised that the transit times and AUC would be significantly different in the shunted model than the control.

From the compounds and metabolites tested, only ICG was a potential PSS marker. This is mostly due to the direct blood extraction sampling rate. A sampling rate of 1 mL every ten seconds does not provide enough spatial resolution to differentiate transit times between shunt and control. Additionally, catheter distortion aids in the increased variability and inconsistency. Catheter distortion occurs when remanent blood from the previous sample is trapped inside the catheter and can affect the following sample. Due to the sampling time, it was not possible to flush the catheter between sample times. With both a slower sampling rate and catheter distortion, some results may be inaccurate and inconsistent. It was expected that a large difference in transit times and AUC would be viewed from the sheer large size of the shunt. Serial blood sampling is not be a plausible to detect PSSs of different sizes and flow rates. It is unable to detect small differences and therefore not show significant differences. However, ICG with the LiMON® machine overcomes this issue through its non-invasive rapid serial sampling via spectrophotometry.

ICG binds to plasma proteins [287] and ICG extraction would therefore be proportional to the extraction of the facilitating protein [288]. Therefore, the presence of a PSS would reduce the hepatic extraction of ICG. However, a perfused cirrhotic liver model demonstrated that the intrahepatic PSSs only accounted for a small portion of the decreased ICG extraction [289], thus concluding that reduced ICG extraction was due to impaired hepatocytes. PSSs, especially small PSSs were not clearly discernible using multiple indicator dilution technique, unless using large radio labelled microspheres are used [288, 290]. Despite a small difference of reduced ICG extraction from PSSs, transit times are able to discern differences in cirrhotic livers [291] and therefore can detect PSSs.

The LiMON® data showed a minor shoulder or bulge in the peak which was seen in all pigs, but varied greatly in size. This can only be visualised when ICG is administered directly into the portal system. This shoulder in the rise to the peak causes different transit times particularly with ICG flowing through the shunt at a faster rate than the ICG flowing through the liver.

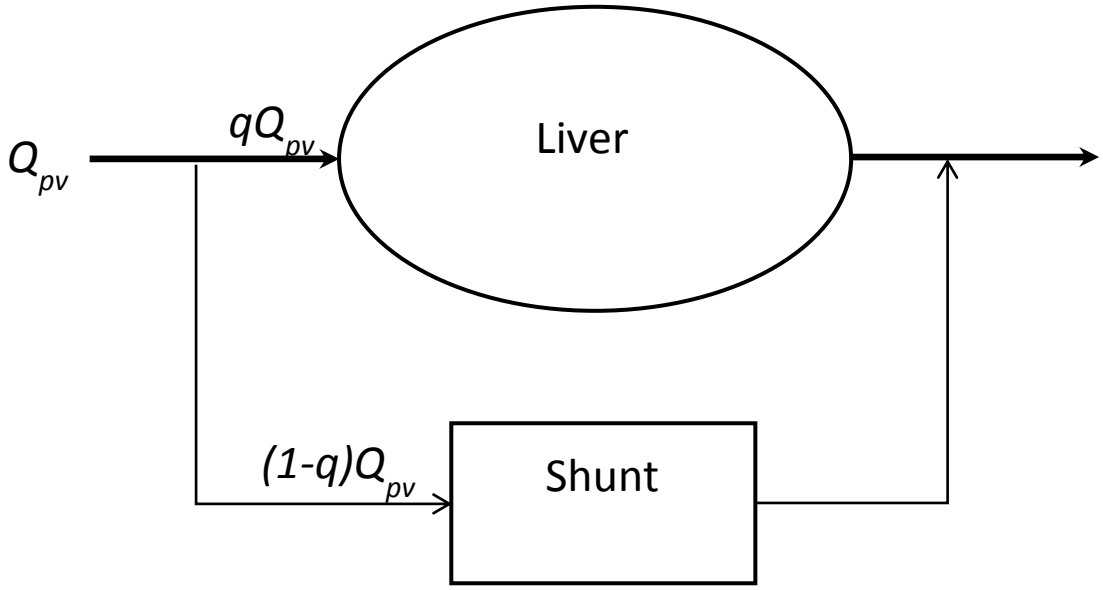

Figure 4.14: Two compartment showing the liver and shunt in parallel with the blood flow of the portal vein (Q_{pv}) being split into the flow through the liver (qQ_{pv}) and the shunt ($(1\text{-}q)Q_{pv}$).

As a comparator, the ICG was injected into the systemic system to determine if this technique could be used at the bedside while the patient is not anaesthetised. Although the ICG would reach the sensor before passing through the liver, the recirculation would show a difference in metabolisation and extraction rates in the shunt and control models. However, due to equipment and technical failures, little data could be recovered. No conclusions can be made due to the low sample size and high variability, but this deserves further attention.

Breath testing may have had the advantage of being able to detect a PSS while the patient is not anesthetised as direct access to the portal system is not essential. However, it was demonstrated that the isoflurane in the breath sample reacted with the gas chromatography column and caused inaccurate results (see *6.2.2 Breath Sampling During Anaesthesia* for a detailed report). There is no evidence in the literature of this issue previously being reported. A study conducted by Kowalczyk *et al.* [292] used a molecular sieve called carbosieve G which was also used within the IRMS column. Carbosieve G was used to adsorb the greenhouse gas tetrafluromethane. No solution has yet been found to remove isoflurane from the samples, and therefore it is recommended that any future breath test studies use an intravenous general anaesthetic instead. The use of alfaxalone, diazepam and ketamine can be suitable for anaesthesia required for short or long periods, however this is an expensive option rather than using inhalational anaesthetics.

Additionally, other continuous intravenous anaesthetics that may be suitable either singularly or in a combination are propofol, midazolam and sufentanil [293-295].

Of note, breath sampling must be timed precisely with the ventilator; however the precise timing is difficult as there are no cues. In pigs 7, 8 and 9 a, many samples only contained a small percentage of CO_2 (<2%). This is most likely attributed to the breath sampling technique. As each breath is exhaled, there is only a small window to collect the breath sample and can be easily missed, with only a small portion of CO_2 enters each vial. It is unknown what percentage of CO_2 was collected until after it had been analysed.

There are two probable reasons for poor lignocaine HPLC detection. Firstly there may be poor lignocaine recovery in plasma sample preparation method or long term storage at -80°C denatured the compound. A previous study showed that lignocaine was more sensitive when samples are stored in sulphuric acid for longer than six months [296]. However, as multiple drugs were being assayed from the same sample, the volume required to use sulphuric acid was also not viable. Solid phase extraction may have increased extraction and yield stronger concentrations. However this requires 1 mL of plasma per sample [281], however as only 500 – 800 µL was collected in each blood sample (equivalent to 1 – 1.2 mL whole blood) and there are other compounds that required analysis from the same sample, this was not sample to appropriately assay for lignocaine.

Although the assay for lignocaine's metabolite MEGX yielded results, the reliability is still questionable as the stability of MEGX in plasma stored at -80°C is unknown. Although MEGX has been described as an accurate liver function test [239, 297-299], no significant difference could be determined in the shunted and control models. This is most likely to be attributed to a slow flowing shunt, high variability between the pigs and low resolution in sampling frequency.

It was not clearly understood why the assay for sorbitol was not successful. Sample preparation for sorbitol takes approximately 30 minutes per sample and a 30 minute HPLC run time [278, 284]. In a clinical setting, with numerous samples this time length would not be appropriate. Samples were run for up to 60 minutes, the pH level was adjusted and mobile phase was changed to find the peak, but without success. As no peak for sorbitol could be seen in a positive standard set, this compound was deemed inappropriate for the detection of PSS.

Evans blue dye and ^{14}C-sucrose were the control compounds as they are not metabolised or excreted by the liver. Although no significant difference between the transit times, they can still be used to determine the transit times through the hepatic sinusoids and shunt, which are also the relative upper and lower limits of the transit times (see *Chapter 5: Determining Portosystemic Shunt Fractions*). Due

to high cost of ^{14}C-sucrose per injection, only Evans blue dye was used in following animal PSS studies.

4.5 Conclusion

Given the large size of the created shunt, the small difference between the two groups is surprising. Due to the rapid sampling rate of LiMON®, it is suggested that ICG should be considered for further studies in PSS detection. However, it is similarly questionable of how sensitive ICG will be as a PSS biomarker, but does demonstrate a reduced lag time in the shunted animal as a result of differentiated transit times.

CHAPTER 5

Determining Portosystemic Shunt Fractions

5.1 Introduction

From the studied compounds, the main element in PSS detection is rapid serial sampling. Although the other compounds studied may have had the potential to demonstrate the presence of a PSS, they are limited to blood sampling times and their corresponding assays. The LiMON® technique has a high appeal for clinical use due to its non-invasive rapid serial sampling.

Noted in the previous chapter, a significant difference in the control and shunted animal was seen when comparing the lag times of ICG. This decreased lag time, also known as arrival time has been viewed in cirrhotic patients with a large degree of shunting when using Doppler ultrasound with a microbubble contrast [291] and radiolabelled red blood cells [300]. The lag time is similar to the definition of MTT and can be used to calculate the flow rate provided the volume of the vessel is known (see *Chapter 5.2 Flow Rate Calculation*). By knowing the respective flow rates in both the portal vein and shunt, the fraction of blood shunted can be determined.

The rapid sampling is ideal for pharmacokinetic modelling as it provides a real-time accurate assessment of the PSS. Despite what initially appears to be either a slow flowing shunt or a low specificity analysis, the LiMON® technique can be used to distinguish each component (liver and PSS) by isolation. In this chapter, LiMON®

technique is explored further by isolating each component of the PSS and Llver to show a theoretical representation of each component.

This chapter aims to review the different techniques for determining shunt fraction based on the data collected from *Chapter 4: Analytical Methods and Results.*

5.2 Flow Rate Calculation

Flow rate (*Q*) can be determined by volume (*V*) divided by *MTT* (Equation 5.1). The lag time can also be used interchangeably with *MTT* (Equation 5.2). Similarly, the MRT can be also used interchangeably with MTT, with *in vivo* models.

$$Q = V/MTT$$

Equation 5.1: Pharmacokinetic question to measure flow (*Q*) by volume (*V*) and the mean transit time (*MTT*).

$$Q = V/Lag\ Time$$

Equation 5.2: Adapted pharmacokinetic question to measure flow (*Q)* by volume (*V*) and the lag time.

5.2.1 Flow Rate Calculation Methods

To show the accuracy of Equation 5.2, a 15 cm length of 8 mm diameter PTFE material that was used to create the shunts in each pig. The PTFE was stretched to its maximum length of 17 cm and attached to a rotary pump (Brand model) using 8mm diameter silicon tubing. The other end of the tube is attached to a fraction collector (BRAND), which is set to collect samples each second. Into the start of the shunt, 5 mg of Evans blue was injected over one second using an 18G safety needle while the pump was turned on and samples were collected until all the dye had visually passed through. Each sample was diluted ten times so it was detectable by the FluroStar Optima®. The dilution was performed by aliquoting 100 µL of each sample into a micro-centrifugation tube and adding 900 µL double distilled water and vortexing for ten seconds. The samples were then prepared and assayed (see *Chapter 4.2.4.7: ^{14}C-sucrose and Evans Blue Analytical Methods*).

Lag time was determined by the time taken for the samples to reach a tenth of the amount injected, 500 µg. This time was then applied to Equation 5.2 using a shunt volume of 8.54 mL.

5.2.2 Flow Rate Calculation Results and Discussion

The dispersion of Evans blue dye can be viewed in Figure 5.1, which also demonstrates the lag times (Table 5.1). The mean difference between the actual flow rate and calculated rate was 11.1 ± 6.2%. However, there is a high correlation

between the lag time and flow rate with R^2 being 0.81 and also a high correlation of 0.99 between the calculated flow rates and the pump flow rate (Figure 5.2). The latter particularly demonstrates the accuracy of using lag time to determine flow rate when the volume is known. However, the limitation of using Equation 5.4 is the specificity of the lag time and the resolution of the sampling rate.

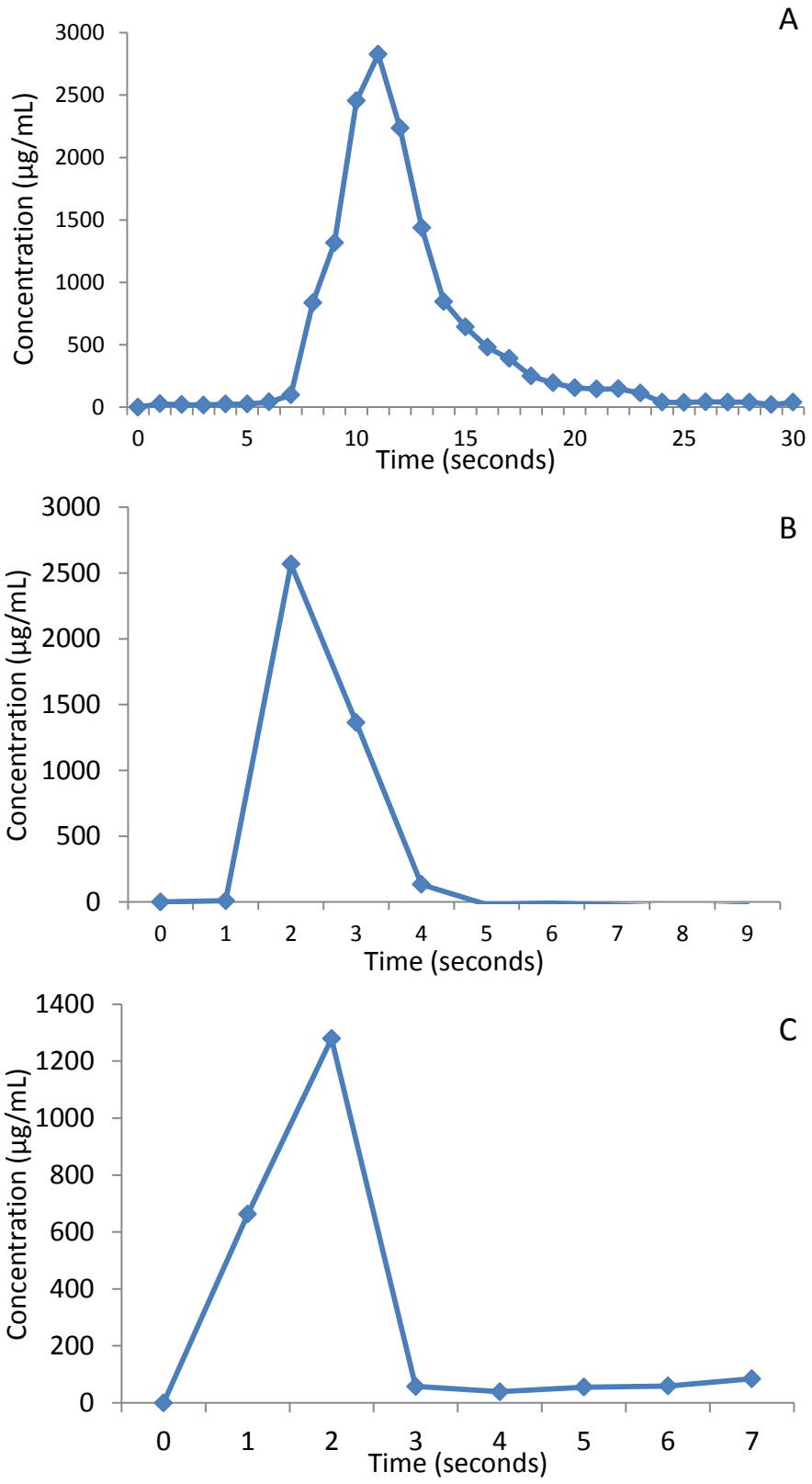

Figure 5.1: Dispersion of Evans blue dye injected through a 17 cm length 8 mm diameter PTFE tubing *ex vivo* with flow rates set at (**A**) 1 mL/s, (**B**) 5 mL/s, and (**C**) 10 mL/s.

Table 5.1: Calculated flow rate of Evans blue in an *ex vivo* model as determined by the lag time and compared to the set pump flow rate.

Pump Q (mL/s)	Lag Time (s)	Calculated Q (mL/s)	Error (%)
1	7.8	1.1	8.72
5	1.4	6.1	18.08
10	0.8	10.7	6.38

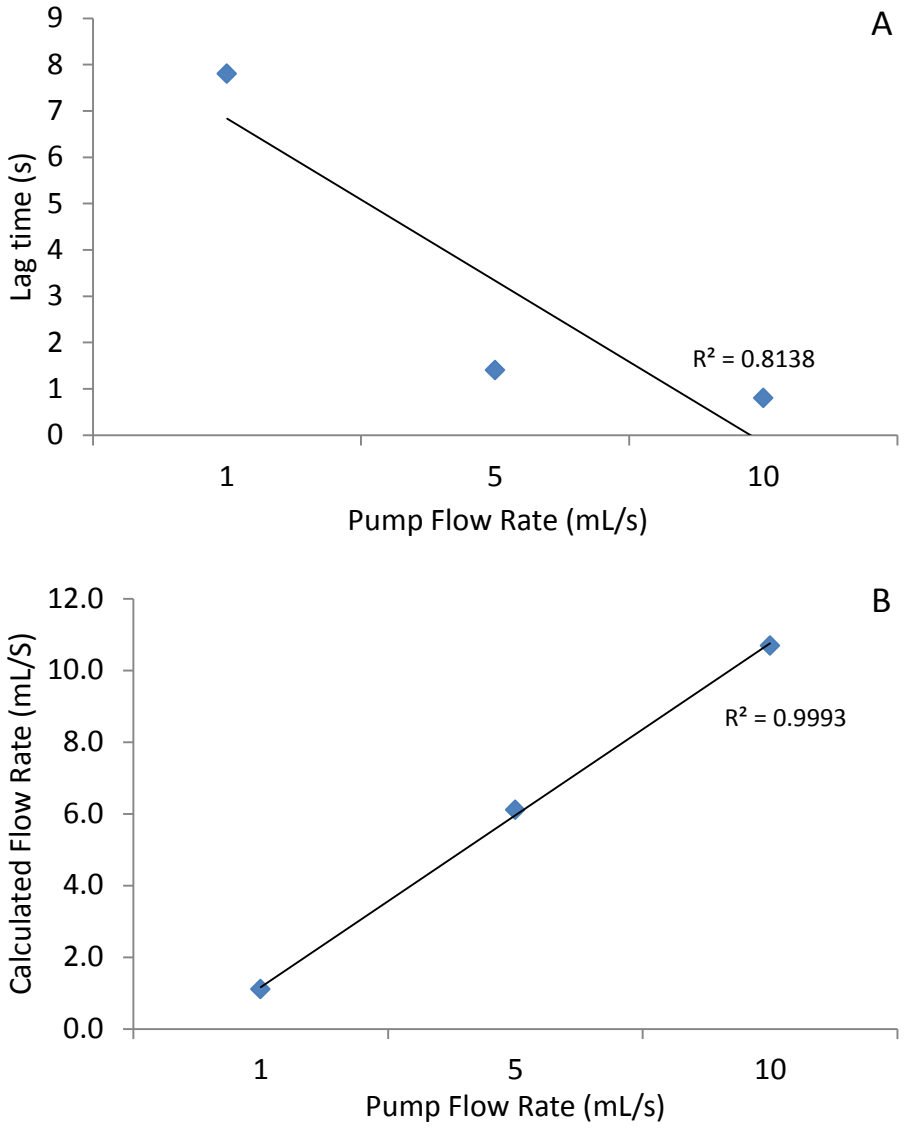

Figure 5.2: Correlation between the set pump flow rate and the (**A**) lag time, and (**B**) the calculated flow rate based on lag time.

5.3 Pharmacokinetic Modelling

The LiMON®, Evans blue and sucrose data was sent to Professor Michael Weiss of Martin Luther University, Germany for modelling using the software ADAPT 5 (Biomedical Simulations Resource, University of Southern California). ADAPT 5 is a freely available computer software programme specifically designed for the purpose of developing computational models within the fields of pharmacokinetics and pharmacodynamics (<http://bmsr.usc.edu/software/adapt/>, last accessed 22/04/2013). Coding to create the model within the ADAPT 5 software can be found in Appendix B.

Model development was adapted as a single pass system from Weiss *et al* [301, 302]. The shunted liver was modelled using an inverse Gaussian density function (f_I *(t)*), based on the first pass transit times (TTD) of ICG (Equation 5.3).

Based the experimental design shown in Figure 5.3, the data was truncated before there was a contribution by recirculation. First, the control data (no shunt) was fitted to a single TTD, (f_L (*t*)). The MTT_L, and relative dispersion (RD_L^2) of the liver could then be calculated. The fraction of blood flow from the shunt (1-*q*) can be determined by the TTD through the shunt (f_S (*t*)). The total function (f_{LS}(*t*)) and ratio of blood bypassing the liver can then be determined by the collaboration of the liver and shunted functions (Equation 5.4).

The parameters of $f_L(t)$ were fixed to those obtained in the control after correcting them for the change in flow, i.e., $MTT_L \rightarrow MTT_L/q$ and $MTT_S \rightarrow MTT_S/q$. The estimated fractions of shunt flow, 1-q ($0 < q < 1$), and R^2 as a measure of goodness of fit are listed in Table 5.2, with an example of the fitted model shown in Figure 5.4. The model, however was not able to be validated as exact flow rates could not to be taken at the time of the procedure. As a comparison the ratio of total volume between the portal vein and the total volume of the shunt are shown (Table 5.2).

$$f_{IG}(t) = \sqrt{\frac{MTT}{2\pi RD^2 t^3}} \exp\left[-\frac{(t - MTT)^2}{2RD^2 MTT\, t} \right]$$

Equation 5.3: Inverse Gaussian Distribution model using the mean transit time (MTT), the point of time (t) and the relative dispersion (RD).

$$f_{LS}(t) = q\, f_L(t) + (1\text{-}q)\, f_S(t)$$

Equation 5.4: Combination of inverse Gaussian distribution models for a two compartment model, with the liver (qf_L) and the shunt ($(1\text{-}q)f_S$).

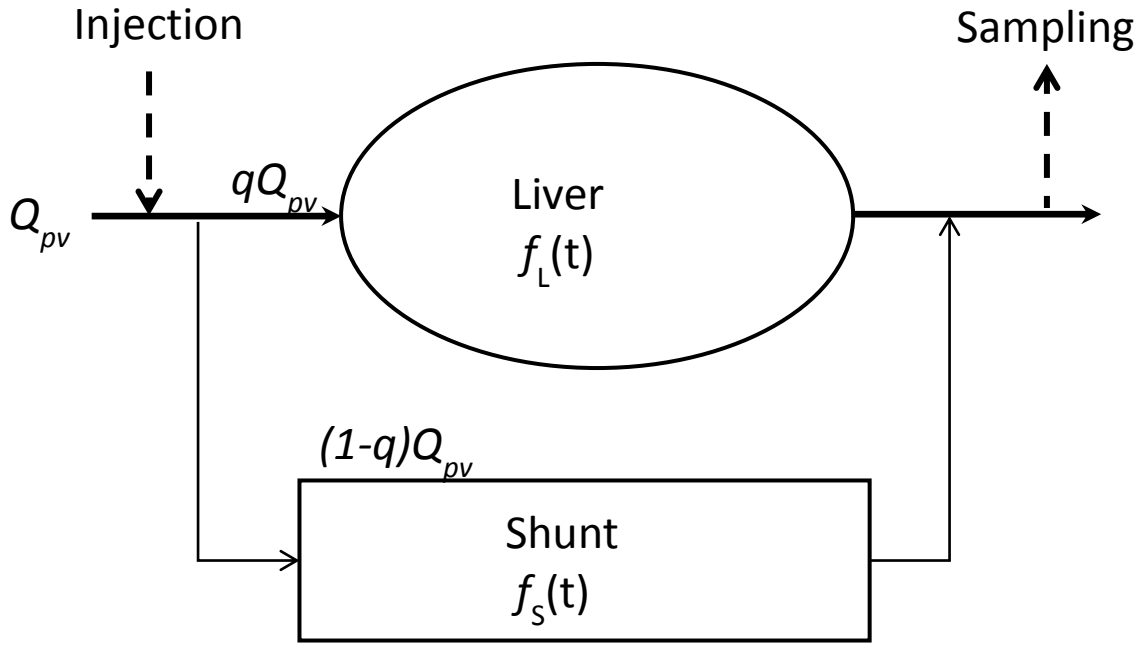

Figure 5.3: Single pass model of indocyanine green (ICG) clearance in the liver with the presence of a portosystemic shunt, when injected into the portal system. The liver and the shunt are in parallel with blood flows *qQ* and *(1-q)Q* respectively (Q_{pv} is portal flow, and $0<q<1$). The liver and body are individually characterised by inverse Gaussian transit time density functions shown as $f_i(t)$.

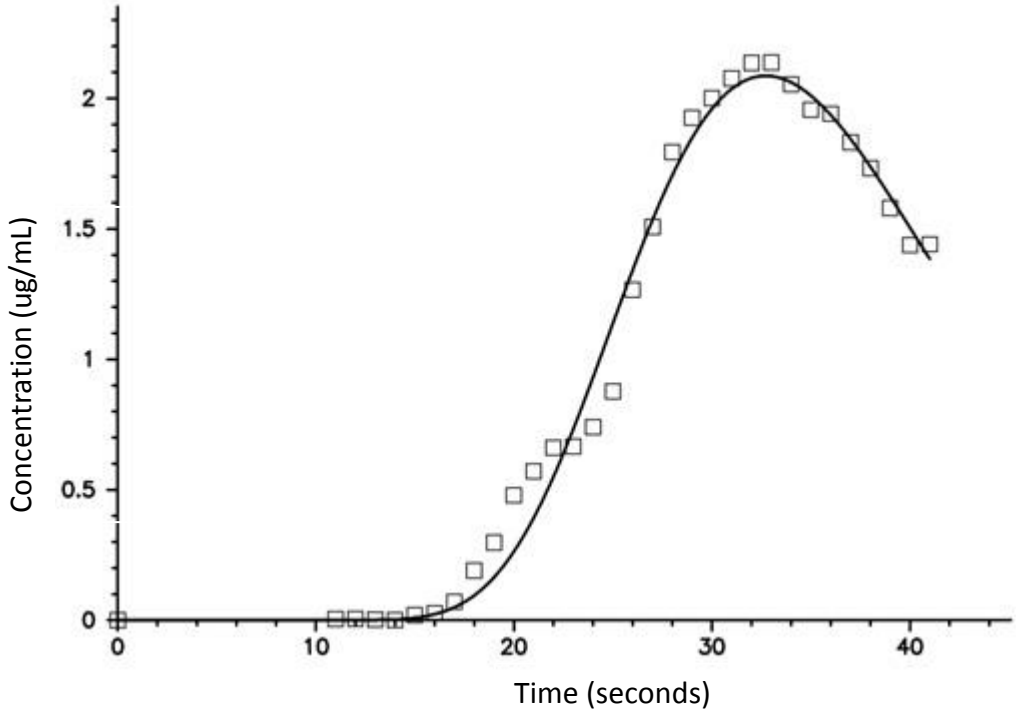

Figure 5.4: Example of a typical fit of $f_{LS}(t)$ to data observed with an open shunt. R^2 = 0.99.

Table 5.2: Estimated fractions of shunt flow (*1-q*) as deemed from the model with its correlation to the fitted data (R^2) the corresponding portal vein (PV) and shunt (PSS) volume ratio.

Pig	Estimated *1-q*	R^2	PV:PSS
2	0.33	0.99	0.39 ± 0.10
3	0.37	0.99	0.42 ± 0.11
4	0.46	0.99	0.42 ± 0.11
5	0.53	0.99	0.43 ± 0.11
6	0.62	0.99	0.55 ± 0.14
Mean ± SD	0.46 ± 0.12	0.99 ± 0.01	0.17 ± 0.67

5.4 Portosystemic Shunt Fractional Calculations and Limits

Additional animal ethic were approved from the University of Adelaide Ethics committee (Approval number: 14917) and SA Pathology Animal Ethics committee (Approval number 91/13) for follow on studies.

5.4.1 Methods

A shunt was inserted into three additional animals as outlined in *Chapter 2 – Development of a portosystemic shunt in a swine model.* The animal's abdomen was cleaned and prepared with a povidone-iodine solution. A 20 cm incision was made through the abdominal wall to locate the liver, IVC and portal vein. A single dose of 80 units/kg of heparin will be administered followed by a continuous flow of heparinised saline (5000 units per litre) at 10 mL/min.

A Gore-tex (Polytetrafluorethylene) tube (8 mm diameter, 13 ± 2 cm length) will be connected between the IVC and portal vein. Flow direction were determined by measuring pressure differences between the portal vein and IVC. Two 5Fr catheters were inserted into the portal vein (later used for drug administration) and the IVC (later used for blood sampling). Both catheters were flushed with saline and connected to a pressure transducer, which was measured via the anaesthesia/respirator machine.

5.4.1.1 Injection sites and Scenarios

In each pig, ICG (0.25 mg/kg) was injected as a bolus in four scenarios via the 5Fr catheter inserted into the portal vein and positioned depending on the scenario (Figure 5.3). This was later followed by an injection of Evans blue dye (1 mg/kg) for each of the scenarios.

The first scenario (D1) was a control with ICG injected into portal vein with the shunt clamped. This was to show normal function of the pig. The second scenario (D2) is a secondary control where the shunt was opened and ICG was injected above the shunt. This isolated the liver to show function with a decreased portal flow rate. With the third scenario (D3), ICG was injected directly into the start of the shunt to show the dynamics of the shunt alone. The last scenario (D4), ICG was injected below the shunt to capture both the functions of the shunt and the liver at the same time. An additional dose of ICG was injected into the IVC to determine the transit time between the confluence of the hepatic veins to the IVC and the LiMON® sensor on the bottom lip.

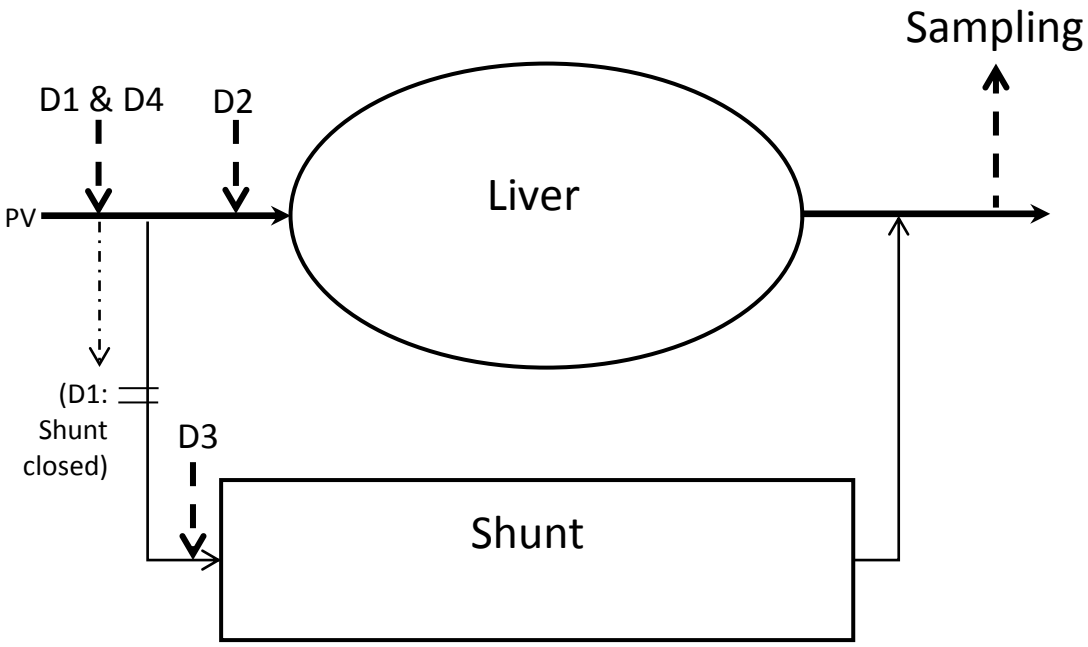

Figure 5.5: Schematic of injection plan. D1. Control 1: Into portal vein (PV) with shunt clamped. D2. Control 2: Into portal vein, above shunt (open) to capture liver function only. D3. Directly into the shunt. D4. Into portal vein below shunt, to capture both shunt and liver.

5.4.2 Sampling

As previously mentioned in Chapter *4.2.3 Sample collection*, ICG data was collected via the LiMON® spectrometer attached to the bottom lip. At the same time, blood samples were collected every 30 seconds for two minutes then every two minutes thereafter until 10 minutes reached for LiMON® calibration against ICG concentration in the plasma.

Blood samples for Evans blue dye were collected from the IVC every five seconds for two minutes, then every 30 seconds until 10 minutes had elapsed. Due to the rapid serial sampling, manual syringe drawing was not plausible. Instead, a blood transfer device was connected to the IVC central line to allow blood withdrawal into 8 mL Vacuette® evacuated blood specimen tubes (Greiner Bio-one, Australia). Each tube was held down for two seconds, which collected approximately 1 mL of whole blood. These samples were then centrifuged at 1900 x g for 15 minutes. The supernatant was then placed in 1.5 mL micro-centrifugation tubes and stored at -80°C.

5.5 Results

Three animals (pigs 7, 8 and 9) had a shunt inserted with a medium length of 5.3 ± 2.0cm and a shunt volume of 2.68 ± 1.02 mL (Figure 5.6, Table 5.3). The injection

sites D1 and D4 are the same as the control and shunted scenarios in pigs 1 to 6, which have been included in the tables for comparison.

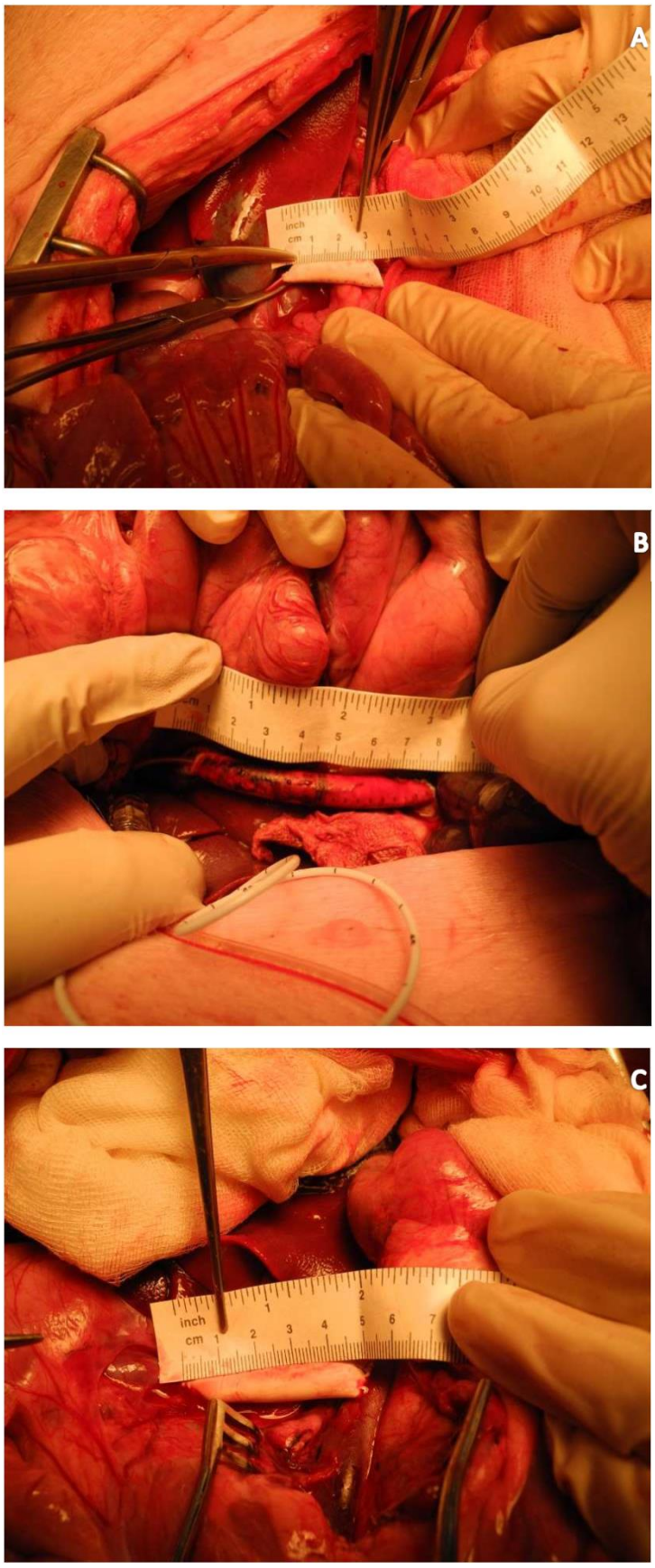

Figure 5.6: Portosystemic shunt created in (**A**) pig 7, (**B**) pig 8, and (**C**) pig 9 using 8 mm diameter PTFE.

Table 5.3: Length of each anastomosis that was inserted into each pig with portal vein (PV) volume and the shunt (PSS) volume ratio. A range is given as the portal vein length was assumed of 6.5 ± 2.1 cm

Pig	Length (cm)	Volume (mL)	PV:PSS
7	3.5	1.76	0.19 ± 0.06
8	7.5	3.77	0.40 ± 0.13
9	5	2.51	0.28 ± 0.09
Mean ± SD	5.33 ± 2.02	2.68 ± 1.02	0.29 ± 0.11

5.5.1 LiMON® Analysis

Only two of the scenarios D3 and D4 demonstrated an early peak (Figure 5.7) at 26 ± 1.5 seconds and 36 ± 8.7 seconds. D4 has a smaller peak due to a portion of the ICG flowing through the liver. These peak times are comparatively shorter than those observed in scenarios D1 and D2, being 41 ± 4.0 and 44 ± 6.1 seconds respectively, although not significantly due to small sample size. Additionally, the rise to the peaks in scenarios D3 and D4 are steeper than D1 and D2.

The transit time of ICG between the confluences of the hepatic veins to the LiMON® sensor on the bottom lip was 16.7 ± 2.1 seconds. This time was deducted from the other lag times (Table 5.4) to find the transit time of the different scenarios (Figure 5.5) to the confluence of the hepatic veins. There is a mean difference of 1.3 ± 9.5 seconds between both controls D1 and D2, indicating a slightly decreased flow rate of the portal vein into the liver in the presence of a shunt. There is also a mean decrease of 10.1 ± 11.7 seconds between the liver only control (D2) and the combination of shunt and liver (D4). Despite a clear difference between the lag times, there is no significant difference ($p>0.05$) due to large variability and small sample size. However, a significant difference was depicted between the lag times of the shunted model (D4) and the normal control (D1) with a mean difference of 8.8 ± 2.2 seconds ($n=8$, $p=0.01$. An emulated mean maximum lag time difference of 14.4 ± 11.8 seconds was observed between the shunt (D3) and the corresponding control (D2).

As the system is *in vivo* and only a portion of blood is collected, blood flow descripted in Table 5.5 is not true blood flow rate, but a relative flow rate of the portal vein and shunt. No significant differences were found between each scenario, however this is mostly due to a small sample size. These flow rates are then used to determine the actual shunted fraction (D4/D2) 0.46 ± 0.28, the relative shunted fraction compared to a normal liver (D4/D1) 1.62 ± 2.28, the maximum possible shunted fraction (D2/D3) 1.35 ± 1.11, and the difference between portal vein flow rates in a normal liver and one with a PSS (D2/D1) 0.86 ± 0.30 (Table 5.6).

The MRT (Table 5.7) is comparatively similar to lag time, and both can be used to calculate flow rates (Table 5.8), however the lag time and MRT cannot be compared side by side. The shunted fractions based on the MRT (Table 5.9), equally show a similar shunt fraction of 0.32 ± 0.28 to that of fraction based on lag time ($p>0.05$). This is similar with the relative shunted fraction and maximum shunted fraction being 0.48 ± 0.27 and 8.56 ± 3.2 ($p>0.05$).

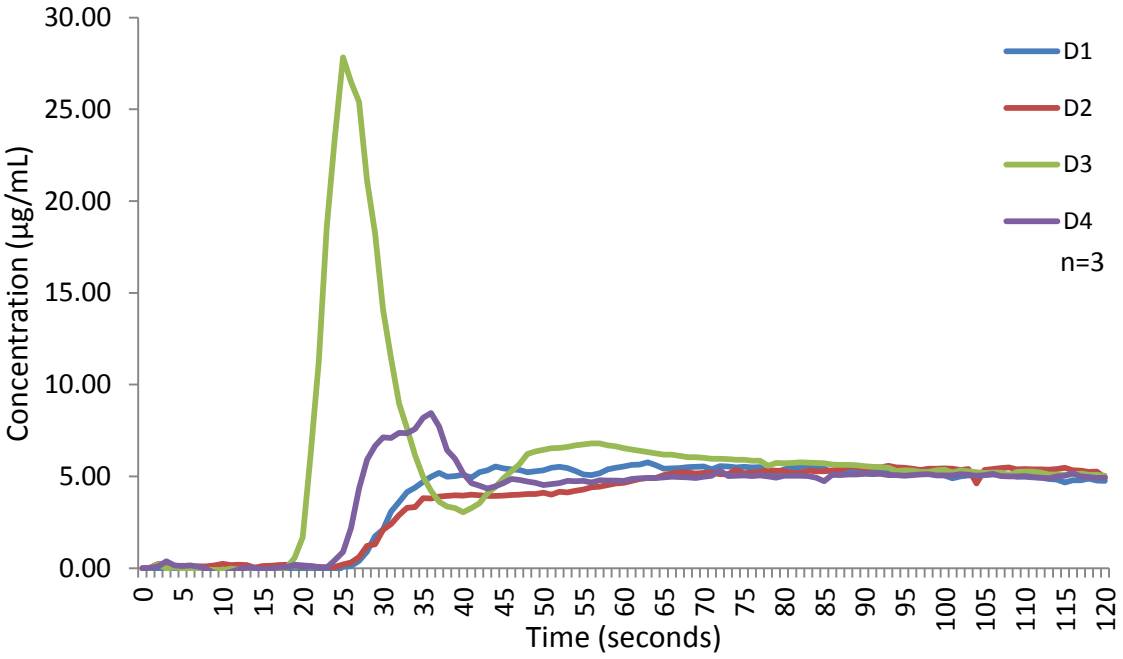

Figure 5.7: Mean concentration of indocyanine green dye of pigs 7, 8 and 9 in each scenario as depicted from the LiMON® system. D1. Control 1: Into portal vein with shunt clamped. D2. Control 2: Into portal vein, above shunt (open) to capture liver function only. D3. Directly into the shunt. D4. Into portal vein below shunt, to capture both shunt and liver.

Table 5.4: Lag times (threshold > 0.01 μg/L) for different injected scenarios using the LiMON® data for all pigs.

	Injection Scenario				
Pig	**D1**	**D2**	**D3**	**D4**	**Lag Correction**
2	18	-	-	5	-15
3	13	-	-	10	-14
4	18	-	-	6	-13
5	24	-	-	11	-14
6	21	-	-	2	-15
7	20	35	6	8	-16
8	10	12	3	13	-15
9	7	6	1	6	-19
Mean ± SD	16.4* ± 5.8	17.7 ± 15.3	3.3 ± 2.5	7.6* ± 3.6	-16.7 ± 1.8

*p=0.01. Injected Scenarios - D1. Control 1: Into portal vein with shunt clamped. D2. Control 2: Into portal vein, above shunt (open) to capture liver function only. D3. Directly into the shunt. D4. Into portal vein below shunt, to capture both shunt and liver.

Table 5.5: Relative flow rate *Q* (mL/s) derived from lag time for different injected scenarios using the LiMON® data in all pigs.

	Injection Scenario			
Pig	**D1**	**D2**	**D3**	**D4**
2	0.56	-	-	0.85
3	0.77	-	-	0.43
4	0.56	-	-	0.84
5	0.42	-	-	0.50
6	0.48	-	-	3.39
7	0.50	0.29	0.29	0.22
8	1.00	0.83	1.26	0.29
9	1.43	1.67	2.51	0.42
Mean ± SD	0.71 ± 0.35	0.93 ± 0.69	1.35 ± 1.11	0.87 ± 1.05

$p>0.05$ for all comparisons. Injected Scenarios - D1. Control 1: Into portal vein with shunt clamped. D2. Control 2: Into portal vein, above shunt (open) to capture liver function only. D3. Directly into the shunt. D4. Into portal vein below shunt, to capture both shunt and liver.

Table 5.6: Shunted ratios, *1-q* derived from lag time for different injected scenarios using the LiMON® data in all pigs.

Pig	***Actual 1-q*** **(D4/D2)**	**Relative *1-q*** **(D4/D1)**	**Max *1-q*** **(D2/D3)**	**Difference in *q*** **(D2/D1)**
2	-	1.54	-	-
3	-	0.56	-	-
4	-	1.51	-	-
5	-	1.21	-	-
6	-	7.12	-	-
7	0.77	0.44	1.03	0.57
8	0.35	0.29	1.51	0.83
9	0.25	0.29	1.51	1.17
Mean ± SD	0.46 ± 0.28	1.62 ± 2.28	1.35 ± 0.28	0.86 ± 0.30

$p>0.05$ for all comparisons. Injected Scenarios - D1. Control 1: Into portal vein with shunt clamped. D2. Control 2: Into portal vein, above shunt (open) to capture liver function only. D3. Directly into the shunt. D4. Into portal vein below shunt, to capture both shunt and liver.

Table 5.7: Mean residence time (seconds) for each different injected scenarios using the LiMON® data in all pigs.

	Injection Scenario			
Pig	**D1**	**D2**	**D3**	**D4**
2	76.6	-	-	65.4
3	72.5	-	-	68.0
4	69.4	-	-	67.2
5	73.2	-	-	69.1
6	68.7	-	-	67.3
7	179.9	299.2	25.3	32.1
8	158.2	137.0	25.3	87.8
9	67.0	215.2	25.4	47.7
Mean ± SD	135.0 ± 59.9	217.1 ± 81.1	25.6 ± 0.05	55.9 ± 28.8

$p>0.05$ for all comparisons. Injected Scenarios - D1. Control 1: Into portal vein with shunt clamped. D2. Control 2: Into portal vein, above shunt (open) to capture liver function only. D3. Directly into the shunt. D4. Into portal vein below shunt, to capture both shunt and liver.

Table 5.8: Relative flow rates, Q (mL/s) derived from mean residence time for each different injected scenarios using the LiMON® data in all pigs.

	Injected Scenario			
Pig	**D1**	**D2**	**D3**	**D4**
2	0.131	-	-	0.065
3	0.138	-	-	0.063
4	0.144	-	-	0.075
5	0.137	-	-	0.080
6	0.146	-	-	0.101
7	0.056	0.033	0.069	0.055
8	0.063	0.073	0.149	0.043
9	0.149	0.046	0.099	0.053
Mean ± SD	0.09 ± 0.05	0.05 ± 0.02	0.11 ± 0.04	0.05 ± 0.01

$p>0.05$ for all comparisons. Injected Scenarios - D1. Control 1: Into portal vein with shunt clamped. D2. Control 2: Into portal vein, above shunt (open) to capture liver function only. D3. Directly into the shunt. D4. Into portal vein below shunt, to capture both shunt and liver.

Table 5.9: Actual, relative and maximum shunted fractions 1-q derived from mean residence time for each different injected scenarios using the LiMON® data in all pigs.

Pig	*Actual 1-q* (D4/D2)	Relative *1-q* (D4/D1)	Max *1-q* (D2/D3)
2	-	0.85	-
3	-	0.94	-
4	-	0.97	-
5	-	0.94	-
6	-	0.98	-
7	0.11	0.18	11.81
8	0.64	0.56	5.41
9	0.22	0.71	8.47
Mean ± SD	0.32 ± 0.28	0.48 ± 0.27	8.56 ± 3.2

$p>0.05$ for all comparisons. Injected Scenarios - D1. Control 1: Into portal vein with shunt clamped. D2. Control 2: Into portal vein, above shunt (open) to capture liver function only. D3. Directly into the shunt. D4. Into portal vein below shunt, to capture both shunt and liver.

5.5.2 Evans Blue

Serial sampling and an erratic heart rate produced large catheter distortion. For this reason, a moving average twice was applied twice to the data to remove the distortion (Figure 5.11). Differentiation between lag times is difficult with a sampling rate of less than once every second, therefore the MTT is used. Similarly, due to the catheter distortion, peak times are indistinguishable from each other.

There was no significant difference with the MTT in any of the scenarios (Table 5.10). However, there were significant differences in the corresponding calculated flow rates between D1 and D4, D2 and D4, and D2 and D3, $p<0.01$, $p=0.04$ and $p=0.02$ respectively (Table 5.11). As previously mentioned, the blood flow descripted in Table 5.11 is not a true blood flow rate, but a relative flow of the portal vein and shunt. These rates can be used to determine the actual shunted fraction (D4/D2), the relative shunted fraction compared to a normal liver (D4/D1), the maximum possible shunted fraction (D2/D3) and the difference between portal vein flow rates in a normal liver and one with a PSS (D2/D1) (Table 5.12). The actual flow rate and the relative shunted fractions are very similar being 0.34 ± 0.17 and 0.32 ± 0.16 respectively ($p=0.1$). The maximum theoretical shunted fraction cannot be above 1.00 and therefore, as is seen in D2/D3, any values above 1.00 can be viewed as being 100%.

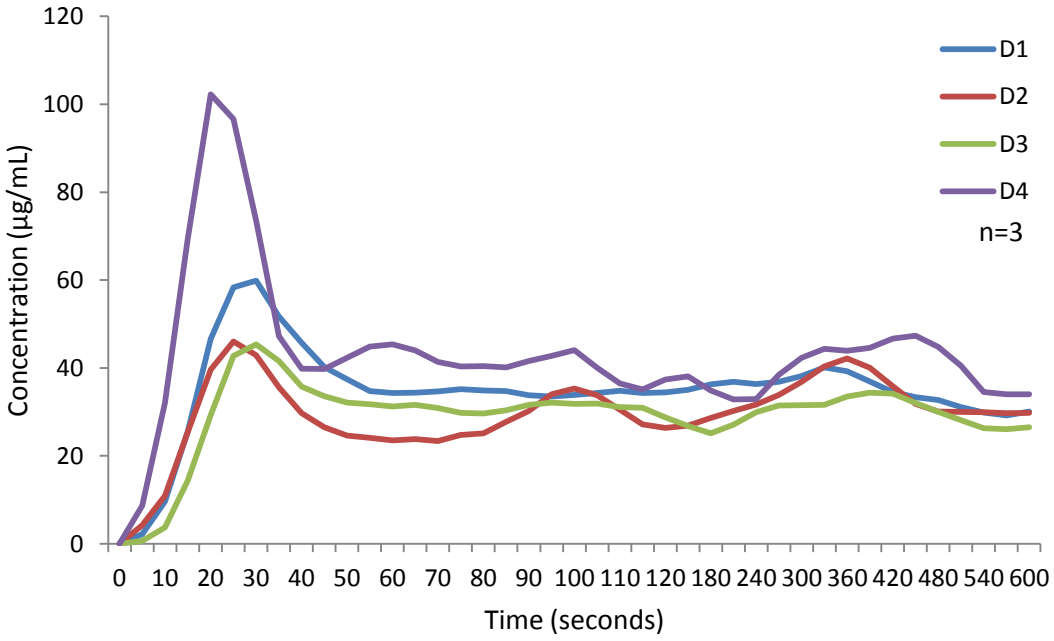

Figure 5.8: Relative concentration of Evans Blue in Pig 7, 8 and 9 of each of the scenarios. D1. Control 1: Into portal vein with shunt clamped. D2. Control 2: Into portal vein, above shunt (open) to capture liver function only. D3. Directly into the shunt. D4. Into portal vein below shunt, to capture both shunt and liver.

Table 5.10: Mean transit time (seconds) of Evans blue for each injected scenario in all pigs.

	Injected Scenario			
Pig	**D1**	**D2**	**D3**	**D4**
2	89.3	-	-	92.6
3	119	-	-	71.5
4	88.1	-	-	94.4
5	84.2	-	-	78.3
6	83.2	-	-	96.6
7	103.6	111.7	93.3	84.3
8	87.8	92.8	93.6	64.7
9	74.7	75.4	78.3	78.2
Mean ± SD	91.2* ± 14.6	93.3**^ ± 18.2	88.4** ± 8.7	82.6*^ ± 10.0

*p=0.01, **p=0.02, ^p=0.04. Injected Scenarios - D1. Control 1: Into portal vein with shunt clamped. D2. Control 2: Into portal vein, above shunt (open) to capture liver function only. D3. Directly into the shunt. D4. Into portal vein below shunt, to capture both shunt and liver.

Table 5.11: Relative flow rates (mL/s) derived from Evans blue mean transit time for each injected scenario in all pigs.

	Injection Scenario			
Pig	**D1**	**D2**	**D3**	**D4**
2	0.113	-	-	0.046
3	0.084	-	-	0.060
4	0.114	-	-	0.053
5	0.119	-	-	0.071
6	0.121	-	-	0.070
7	0.097	0.090	0.019	0.021
8	0.114	0.108	0.040	0.058
9	0.135	0.133	0.032	0.032
Mean ± SD	0.112 ± 0.02	0.110 ± 0.02	0.030 ± 0.01	0.051 ± 0.02

$p>0.05$ for all comparisons. Injected Scenarios - D1. Control 1: Into portal vein with shunt clamped. D2. Control 2: Into portal vein, above shunt (open) to capture liver function only. D3. Directly into the shunt. D4. Into portal vein below shunt, to capture both shunt and liver.

Table 5.12: Actual, relative and maximum shunted fractions (*1-q*) derived from Evans blue mean transit time for each injected scenario in all pigs.

Pig	***Actual 1-q*** **(D4/D2)**	**Relative *1-q*** **(D4/D1)**	**Max *1-q*** **(D2/D3)**
2	-	0.41	-
3	-	0.71	-
4	-	0.47	-
5	-	0.59	-
6	-	0.58	-
7	0.23	0.22	4.77
8	0.54	0.51	2.69
9	0.24	0.24	4.16
Mean ± SD	0.34 ± 0.17	0.32 ± 0.16	3.87 ± 1.07

p>0.05 for all comparisons. Injected Scenarios - D1. Control 1: Into portal vein with shunt clamped. D2. Control 2: Into portal vein, above shunt (open) to capture liver function only. D3. Directly into the shunt. D4. Into portal vein below shunt, to capture both shunt and liver.

5.6 Discussion

The transit times of markers are a key feature that can distinguish hepatic hemodynamic changes in patients with and without shunting. As shown in patients with cirrhosis, there is a significantly shorter transit time compared to patients with healthy livers [291, 300]. However, these studies do not go on to determine the shunted fraction of blood bypassing the liver sinusoids using the transit times. The flow rates calculated from the transit times are not absolute flow rates, but instead a relative flow rate of the portal vein and shunt. This is because only a portion of blood was collected and sampled. In order to calculate actual flow rates, all of the blood must be collected at serial time points and therefore not feasible.

This study demonstrated shunted fractions by means of using lag time, MRT, MTT and a transit time model, with a portal vein and shunt volume ratio as a comparison (Table 5.13). Unfortunately, the shunted fractions as determined by the model were not available for pigs 8 and 9 due to technical difficulties. The shunted fractions were similar for each method, demonstrating consistency using transit times ($p=0.13$). Although the shunted fraction for the lag time had a large variability, the other methods of shunt fraction determination are similar showing consistent reliability in this method. However, further accuracy measures are required.

Table 5.13: D4/D1 Shunted fractions (*1-q*) based on indocyanine green dye lag time and mean residence time (MRT), mean transit time (MTT) of Evans blue, and the pharmacokinetic model. Included is the portal vein (PV) and Shunt (PSS) ratio as a comparison. Model data for pigs 8 and 9 could not be included due to technical difficulties.

Pig	PSS:PV	Lag time	MRT	MTT	Model
2	0.39	1.54	0.85	0.41	0.33
3	0.42	0.56	0.94	0.71	0.37
4	0.42	1.51	0.97	0.47	0.46
5	0.43	1.21	0.94	0.59	0.53
6	0.55	7.12	0.98	0.58	0.62
7	0.19	0.44	0.18	0.22	0.52
8	0.40	0.29	0.56	0.51	-
9	0.28	0.29	0.71	0.24	-
Mean ± SD	0.39 ± 0.11	1.62 ± 2.28	0.48 ± 0.27	0.32 ± 0.16	0.46 ± 0.12

p>0.05 for all comparisons. Injected Scenarios - D1. Control 1: Into portal vein with shunt clamped. D4. Into portal vein below shunt, to capture both shunt and liver.

The pharmacokinetic model was developed by Professor Michael Weiss of Martin Luther University, Germany. This model was based on his previous work [303] and can determine the fraction of shunted blood using the Adapt 5 software. The fraction shunted as predicted from the model lies near what is estimated. The model depicts the ratio of blood bypassing the liver at any given moment. However, as the exact flow rate could not be determined within the shunt itself, therefore the fraction shunted could not be calculated, further validation is required. The similarities compared to the other methods do demonstrate a consistent level of accuracy.

This pharmacokinetic model was based on previous work [301, 302] using the inverse Gaussian distribution as TTD for ICG, showing the estimated fraction of shunted blood bypassing the liver. This density function particularly shows first pass time distribution [301] and has been used previously in tracer kinetics [304-306], modelling sorbitol disposition [307] and ICG [301, 302]. The model is simplified to the parameters of two compartments being the liver and shunt, which demonstrate the distribution kinetics of blood flow without recirculation. However, the model was not able to be validated as exact flow rates were not able to be taken at the time of the procedure. Instead, the estimated shunted fraction was compared to the ratio of total volume between the portal vein and the total volume of the shunt [118] along with the other shunted fractions based on the lag time, MRT and MTT.

Calculation of the transit times and consequently shunted fraction maybe limited to patients without liver metastases. Previous studies using ultrasound to determine transit times reported a shortening in the transit time in the control patients who had liver metastases [291, 308]. This shift is similar to patients with known PSS caused from cirrhosis.

5.7 Conclusion

The model and transit times depict a reliable way of determining shunted fractions. By isolating the components of the liver and shunt, the maximum and minimum transit times can be demonstrated relating to the injected compound. Further studies are required to show accuracy, specificity and limitations of detectable limits.

CHAPTER 6

General Discussion

6.1 Portosystemic Shunt Detection Technique

A conclusive technique for PSS detection still requires further investivation. This study creates the foundation and a starting point for future studies in PSS detection. From all compounds reviewed, ICG was the only compound able to provide a basis for the PSS prognostic and quantifying model due to the ability for real time rapid sampling via the LiMON® system. It has been demonstrated that a combination of liquid chromatography and mass spectrometer provides a far more sensitive ICG detection assay than spectrophotometric methods [309], such as the LiMON®. Unlike the LiMON® this method is not able to be performed at the bedside, not suited for rapid sampling and therefore not practical for clinical use.

The LiMON® system is ideal for PSS detection as it is minimally invasive, time efficient (<15 minutes) and cost effective (AU$80 per injection). Due to the LiMON® rapid sampling rate, accurate transit times can be calculated. The PSS provides a lower resistance, and therefore faster passageway than the liver, therefore reducing transit times. However, a limiting factor in determining transit times is that ICG must be administered directly into the portal system. If, ICG is administered into the systemic system, the dye may reach the LiMON® sensor before passing through the liver and no transit time differentiation can be defined.

The two compartmental pharmacokinetic modelling approach is a necessary step in not only understanding the properties of a PSS, but also in developing methods for detection. Upon further validation, the model will provide ways to determine the sensitivity and accuracy of different PSS detection techniques without the need for animals. Similarly, it provides clear characterisation of a PSS. In its current state, the model was able to provide predictive shunted fractions due to transit times for a large PSS.

The other transit times including lag time, MRT and MTT, were also able to provide a relative shunted fraction. However, to be able to determine the relative flow rate, the volume of the shunt is required. In a clinical setting, shunt volume would not be known without initial diagnostics of ultrasound, CT or MRI. Therefore, this current method would only be able to suggest the presence of a PSS from the reduced transit time, and no characterisation of the PSS could occur until it has been imaged. With further development of the model, and combined with the current test, characterisation of the PSS may be able to be provided without the need for radiological imaging.

6.2 Limitations and Complications

A limitation with using pigs in this model is that they are known to be susceptible to anaesthetics and possibly be accidently euthanised. Although no animals prematurely died, it is possible that independent breathing may occur against the

respirator. This can cause possible suffocation if the pig is breathing in reverse phase to the ventilator, and also affect the venous blood flow by increasing the pressure and heart rate. Abnormal venous return can consequently cause erratic flow rates through the shunt.

Another limitation with the use of the LiMON® machine was it became unstable at heart rates above 180 bpm and also rapid changes in heart rate, therefore unable to record data. The heart rate had to be maintained less than 180 bpm, preferably around 120-150 bpm in order to able to record data and avoid distortion.

6.2.1 Measuring Shunt Flow

As a consequence of being unable to measure flow via Doppler Ultrasound, pressures of the portal vein and IVC were measured and using Bernoulli's principle, it can be concluded that flow is from portal vein to IVC. The swine venous system is very fragile and obtaining pressures at direct opposing ends of the shunt is not practical without due care. The risk of tearing is reduced when the portal and IVC pressures are measured away from the shunt. Measuring pressure difference will only show flow direction. Without other equipment available to measure vascular flow or shunt flow, the total volume ratio between the portal vein and the shunt is an alternative method to estimate the fraction of blood shunted.

Doppler ultrasound was unable to determine flow velocity through the PTFE or surrounding blood vessels. The transducer available had a lower special resolution and was subsequently not designed to be positioned directly above blood vessels or grafts. There were several reason why flow velocity could not be obtained. The PTFE compound is hydrophobic and through a process of heating, stretching and extruding, a microporous structure can be formed (Figure 6.1). This forms 'air pockets', where ultrasound is poorly transmitted between two mediums of different density. The impedance mismatch causes high scattering and any ultrasound echo is lost [310]. A smaller transducer with a focused sensor may yield high special resolution and may have been able to image flow within the shunt.

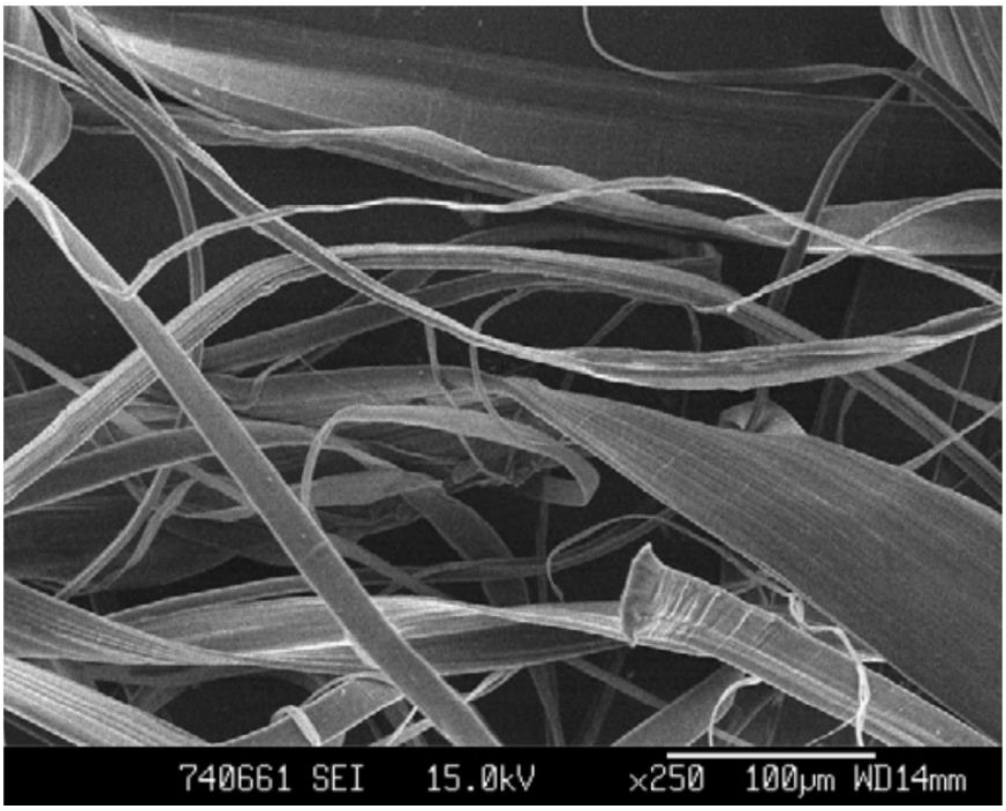

Figure 6.1: Scanning electron micrograph of the microporous PTFE structure (image from Zhang *et al.* [311])

6.2.2 Breath Sampling During Anaesthesia

Breath testing with stable isotopes is becoming more widely used to test metabolic processes. Particularly, [^{13}C] labelled compounds are increasingly being used in a number of large animal experiment models for the use in breath testing [312-314]. Although, breath sampling has not yet been used while an animal or patient is under general anaesthesia due to sampling difficulty. Hence, this is not widely used in a clinical setting. Lack of clinical breath testing maybe due to limited understanding of the metabolic process, the efficacy of metabolism does not necessarily match to data readings and some machinery may not be sensitive enough to determine small changes [274]. However, future studies involving surgery may require use of breath testing while the animal or patient is under general anaesthesia.

[^{13}C] Breath testing has been used for a range of tests including detection of *Helicobacter pylori* [265-267], lung cancer detection [268-270], gastric emptying [271] and liver function [232, 272]. In particular ^{13}C-methacetin has been used to predict liver failure post hepatectomy [264] and graft failure [273]. For this study ^{13}C-methacetin is used as it is exclusively taken up and metabolised by the liver, and its metabolite $^{13}CO_2$ can non-invasively be collected in 12 mL vials and assayed isotope-mass spectrometer (IRMS).

^{13}C-methacetin has been used as a liver function assessment by measuring the

ratio and decay of $^{13}CO_2$ in the breath. Methacetin is passively taken up into the hepatocyte and entirely metabolised by cytochrome 1A2 (CYP1A2) [245], which has been directly linked to assessing the function of the liver. CYP1A2 metabolises methacetin into acetaminophen (paracetamol) and CO_2 [232]. The $^{13}CO_2$ breathed out, measured in liver function tests, may not match the amount of ^{13}C-methacetin injected, which could be due to either the diffusion process in the blood [246] or from the presence of a PSS, allowing methacetin to directly bypass the hepatocytes. As methacetin is exclusively metabolized in the liver and has a high extraction fraction, methacetin may be used to measure a PSS by finding the ratio of methacetin and its metabolite in blood samples. PSSs may also be identified by measuring the rate of $^{13}CO_2$ decay in the breath.

Volatile organic compounds (VOCs) are commonly used as a used for general anaesthesia in both human and animal surgical procedures. Current inhalational general anaesthetic compounds used include isoflurane, desflurane and sevoflurane which can also be combined with nitrous oxide (N_2O). However, isoflurane is used more routinely for animal surgery. To date, the only known issues with ^{13}C isotope breath analysis and volatile organic compound (VOCs) is with N_2O. N_2O has a mass overlap with CO_2 when using isotope ratio mass spectrometry (IRMS), thus causing large variability and drift of the analysis window [315, 316]. During an animal study of liver function analysis, ^{13}C-methacetin was intravenously administered into six female pigs. During the breath sample analysis, it was noted that the $^{13}CO_2$ peak time gradually decreased and escaped the

analysis window. As N_2O was not being used in this study, it was unknown what was causing the peak shift in the IRMS.

6.2.2.1 Breath Analysis

Breath samples were analysed from a trial pig showing typical $^{13}CO_2/^{12}CO_2$ ratios. Due to technical errors and machine failure, all further breath samples that were assayed showed inconsistencies and inaccuracies. The quality control (QC) reference gas of 5 ± 0.5% was tracked throughout which showed a decrease in $^{13}CO_2/^{12}CO_2$ ratio and thus a drift in the peak (Figure 6.2). Raw data from the samples was digitally re-run and the analysis window time lag was systematically decreased for each sample set until the QC was near linear and consistent within each set (Figure 6.3). The analysis window has a normal lag time of approximately 80 seconds. Each sample set was rerun with the analysis window lag time shortened in five second increments, until all QC ratios were consistent.

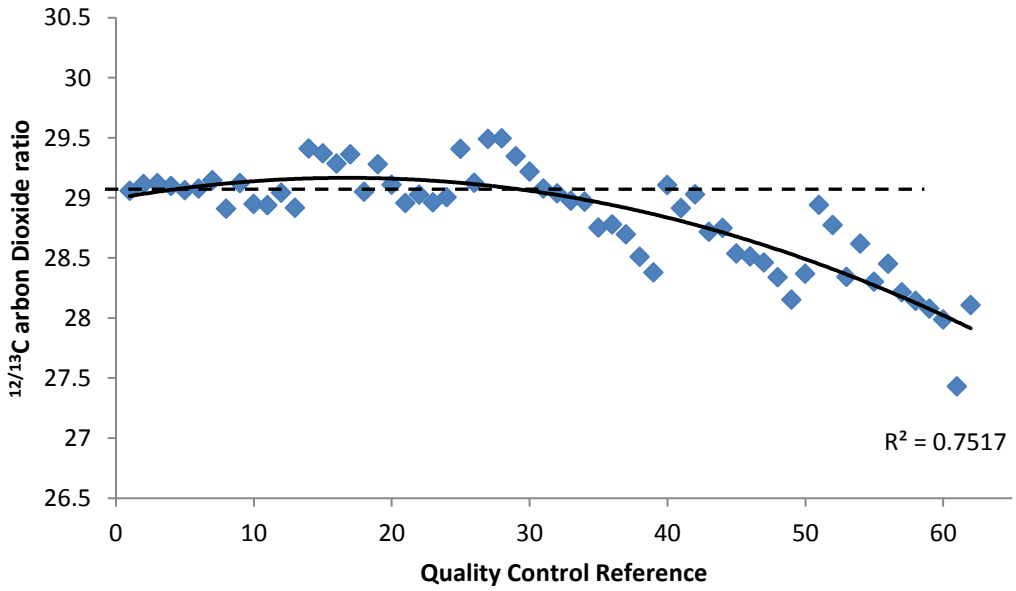

Figure 6.2: Series of quality control references throughout sampling for $^{13}CO_2$ in the presence of isoflurane. Each quality control should maintain similar ratio of 29.1 ± 0.2 (dashed line), however a drift occurs (solid line) as more isoflurane contaminated samples are analysed. The black dash line shows the standard deviation of the drift.

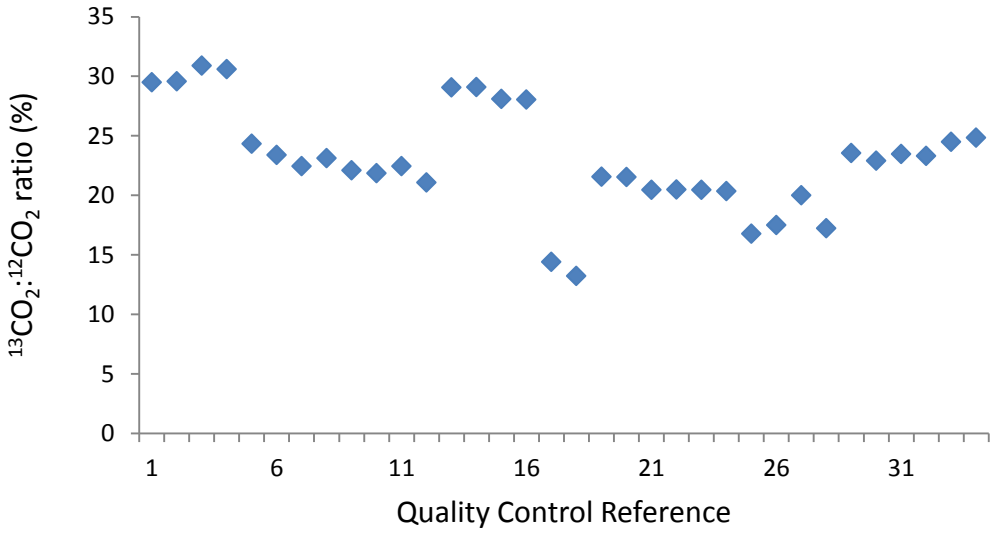

Figure 6.3: Series of quality control references throughout sampling for $^{13}CO_2$ in the presence of isoflurane. Digital raw sample data was rerun in sample sets with the analysis window being changed to correct for the drift, so each quality control should maintained similar within each set.

6.2.2.2 Isoflurane Contamination

Breath testing while patients or animals are anaesthetised will become a necessity for future research. Breath collection for large animals is difficult as they are currently not sedated. For example, a pig must be restrained and breath samples taken using a modified mask [312]. This is not only dangerous for the technician taking the breath samples, but can also be harmful and stressful for the animal. However, here we describe a previously unreported issue with inhalational anaesthetics affecting the IRMS separating column. This issue using isoflurane in the presence of breath sampling is different to the previous known issue of N_2O contaminating breath samples. In this case, the mass overlap of N_2O and CO_2 caused non-linearity and consequently skewed results [315].

It is thought that the isoflurane used to anaesthetise the pigs contaminated the breath samples. The IRMS column is used to separate gas compounds according to molecular size. The column contains a molecular sieve called Carbosieve G that allows small gas compounds such as CO_2 to pass through with resistance. However, the presence of isoflurane gradually coats Carbosieve G and consequently reduces the resistance. This therefore, decreases the retention time of $^{13}CO_2$. A previous study used Carbosieve G to adsorb the greenhouse gas tetrafluromethane (CF_4) [292]. Here, Carbosieve G was shown to adsorb a large amount (1.7 mol/kg) of CF_4 before saturation. The smaller sized pores within the Carbosieve G increase the adsorption potential [292]. Isoflurane's chemical structure contains a trifluroethane

group, similar to the active fluorine group in CF_4 and causing it to adsorb to Carbosieve G.

The QC is a known concentration of 5 ± 0.5% $^{13}CO_2$ which is used to determine the linearity and accuracy of the results and were run repeatedly throughout the other breath samples. When the peak of $^{13}CO_2$ drifts out of the analysis window, the concentration of $^{13}CO_2$ reduces. The IRMS separating column was affected by gradual and continued presence of isoflurane, which caused the peak time to steadily reduce and consequently was not analysed within the elected time window. The analysis window can be shifted according to the drift of the peak; however this will increase the error margin. This correction is not ideal as the analysis window would be needed to be shifted after every five to ten samples and would be different for every machine. Several solutions were researched including using a silica zeolite filter, however this also removes CO_2 from the breath [285], and also heating the column to desorb the isoflurane from the Carbosieve G was attempted. However, no attempts have been successful and hence, no solution has yet been found. Other analytical techniques may include non-dispersive infrared spectroscopy (NDIRS), which has been used to detect $^{13}CO_2$ as an alternative to IRMS [317]. NDIRS does not use a filter or separating column, however, mechanical ventilation can cause a bias in $^{13}CO_2$ and $^{12}CO_2$ measurements due to additional O_2 [317].

As inhalational general anaesthesia compounds desflurane and sevoflurane also have an active tetrafluroethane group, they may cause similar issues for gas chromatography. It is advisable that if breath testing is required in research or in patients under general anaesthesia, any gas analytical techniques that require a gas chromatography column for separation should not be used. It is recommended that any future breath sampling studies that require sedation use intravenous general anaesthetics.

During the breath sample analysis, it was noted that the $^{13}CO_2$ peak time decreased and missed the analysis window. It is possible that the VOC used for general anaesthesia cross-contaminated the breath samples. There are a wide range of VOCs used for general anaesthesia, while there are only four VOCs that are currently used being isoflurane, desflurane, nitrous oxide and sevoflurane. To date, there have been no known issues with ^{13}C isotope breath analysis and VOCs cross contamination, except for nitrous oxide. Nitrous oxide has a similar mass as $^{13}CO_2$ (molecular mass 44 g/mol), showing simultaneous peaks, thus causing large variability and drift of the analysis window [315].

Pigs 7, 8 and 9 were anaesthetised via intravenous administration of alfaxalone without the use of isoflurane. During the breath sample analysis, the quality QC reference gas was tracked throughout and did not show a decrease in the QC,

therefore peak did not drift out of the analysis window (Figure 6.4). This validates that isoflurane is a problematic constitute during breath sampling analysis.

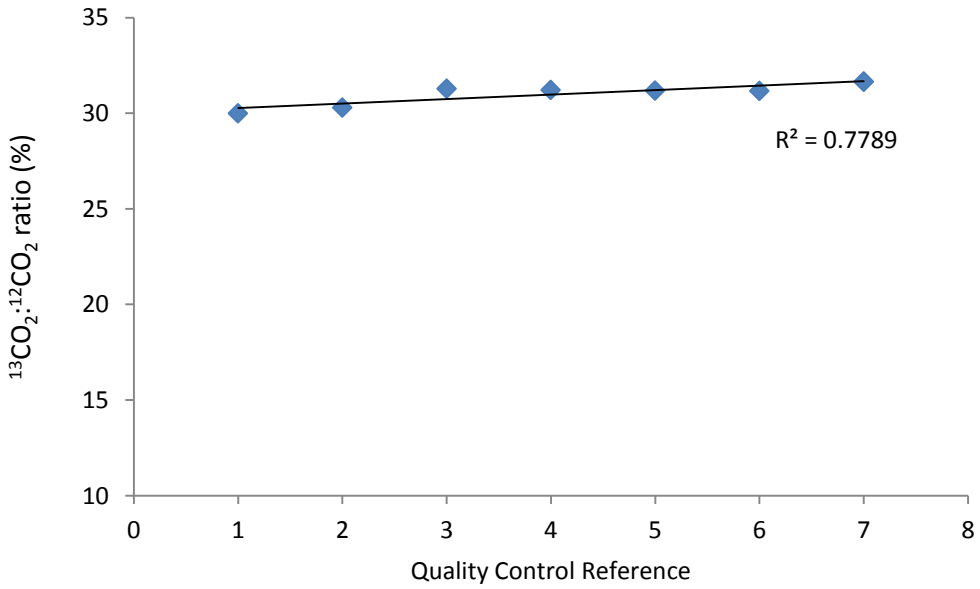

Figure 6.4: Series of quality control references samples that were not used in the presence of isoflurane. Each quality control maintained similar ratio of 31.1 ± 0.6%.

Breath testing may have had the advantage of being able to detect a PSS while the patient is not anesthetised or if direct access to the portal system is not required. However, it was thought that the isoflurane in the breath sample reacted with the gas chromatography column and caused inaccurate results. There is no current literature that has reported of this issue. There is a known issue that nitrogen oxide can cause inaccurate results in breath tests as this has the same mass as $^{13}CO_2$ [315], although nitrogen oxide was not used to anesthetise the animals.

The QC is a known concentration of 5 ± 0.5% $^{13}CO_2$. When the peak of $^{13}CO_2$ drifts out of the analysis window, the concentration of $^{13}CO_2$ reduces. The analysis window can be shifted according to the drift of the peak; however this can increase the error margin. This correction is not ideal as the analysis window would need to be shifted after every five to ten samples and would be different for every machine. Several solutions were researched including using a silica zeolite filter, however this also removes CO_2 from the breath [285], and also heating the column to 'unblock' the column was attempted. No solution has yet been found and it is recommended that any future breath test studies use an intravenous general anaesthetic instead.

6.2.2.3 Sampling Accuracy

Upon further analysis of pigs 7, 8 and 9, it was noted that the total volume of CO_2 in each sample was less than 2% is the majority of the samples (Figure 6.5). Each pig was ventilated with 100% oxygen, therefore the only CO_2 must be from exhaled

breath. The IRMS machine that assays each sample is calibrated for samples containing between 2% to 10%, therefore the accuracy of the results is questionable. It is most likely that this is due to sample timing. Samples need to be collected in time with the respirator as the pig is exhaling. The sampling window is small, and can easily be missed; filling the container with mostly inhaled pure oxygen, rather than the exhaled CO_2.

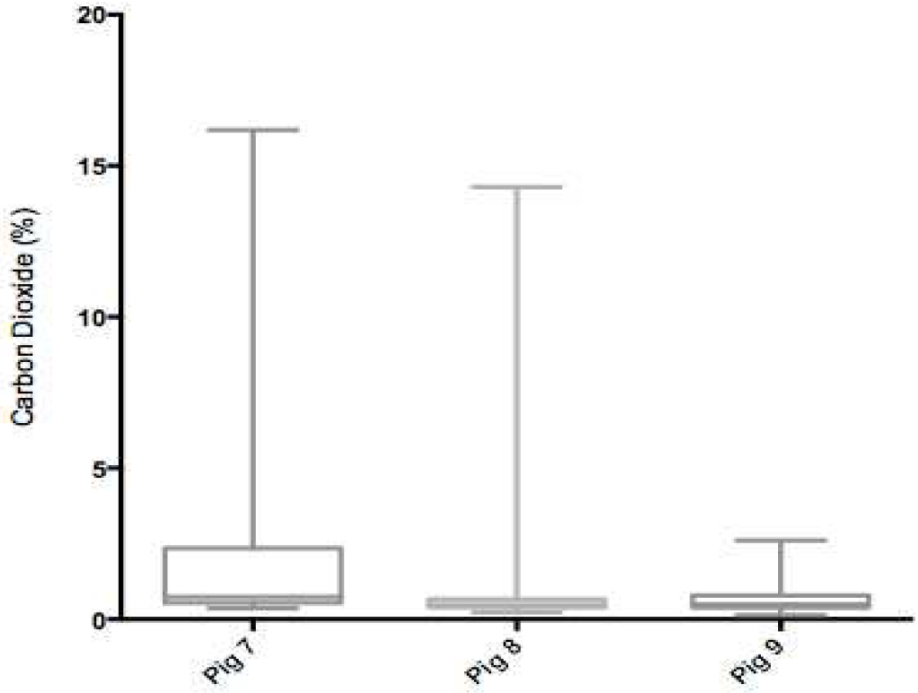

Figure 6.5: Ratio of total CO_2 contained within the breath samples of pigs 7, 8 and 9.

6.4 Significance

The incidence of PSSs occurring in patients without liver cirrhosis is still relatively unknown as few, if any, symptoms, such as encephalopathy are seen [157, 318]. However, the incidence of secondary lung metastases without liver metastases is estimated to be between 1.7% to 7.2% [94]. This distribution of metastases beyond the confines the liver in patients with colorectal cancer raises questions about mechanism. Theoretically, most CTC should be trapped by the liver. Although most patients do present with liver metastases first, if a patient has a PSS, it may allow these CTC to directly bypass the liver, whereby greatly increasing the risk of secondary cancer in the lung before (or at synchronous timing) liver metastases are present. This hypothesis was originally acclaimed by Lore *et al.* [106] and later re-emphasised by Saitoh *et al.* [107], which still remains unanswered. This may be due to the lack of focus toward PSS detection. Currently, there is no literature, which directly correlates a natural PSS and metastatic distribution. However in support of Lore's *et al.* [106] hypothesis, two patients with gastrointestinal cancer were later diagnosed with secondary pulmonary nodules, which was attributed to a direct cause of an artificial PSS (TIPS) [108].

It should be noted that PSSs may not be the sole influence on secondary metastases in the lung. CTC may still pass through the liver provided they are not detected by the hepatic immune system, avoiding Kupffer cells [109]. However, only a small portion is able to move through the liver in this way. A PSS greatly increases the

concentration of CTC to the lung. Therefore, potentially increasing the risk of secondary metastases.

6.5 Clinical Implications

Even though radiological methods have incidentally demonstrated the presence of PSS successfully, the practical implications do not make it a viable option to be performed routinely. The LiMON® system is simple and quick procedure, which may provide a real time assessment. The LiMON® test would be aimed at colorectal cancer patients undergoing a colonic resection as veins confound to the portal system are accessible.

Lore *et al.* [106] hypothesis of metastases distribution in the presence of a PSS may account for some of the 15 -20% of all colorectal cancer patients with healthy livers [93], or the 1.7 -7.2% with isolated lung metastases [94]. However, the lack of an effective clinical test for PSS detection may be the reason for the lack of evidence to support this hypothesis and also a lack of understanding in the implications of a PSS in a patient without cirrhosis.

6.5.1 Cancer Catagorisation and Risk Factors

Cancer therapy or management can change dramatically depending on the staging of the cancer. The current standard for cancer staging is the tumour, node and

metastases (TNM) staging system. ‘T(0-4)’ describes the depth and extent of the primary tumour, with N(0-2) describing the degree of lymph node involvement and ‘M(0-1)’ describing the presence of secondary metastases [319, 320].

Typical treatment for colorectal carcinomas categorised with T0-3, N0, M0 would be surgical resection without adjuvant chemotherapy [321]. Adjuvant chemotherapy treatment for patients staged with T3, N0 and M0 colorectal cancer may be seen as controversial without high-risk pathological features [322]. A PSS can be categorised as a pernicious high-risk pathological feature. Therefore adjuvant chemotherapy may be deemed necessary for colorectal cancer staged as T1-3, N0 and M0. A PSS may even be a reason to increase the cycles of chemotherapy for more aggressive treatment in patients categorised into a higher stage colorectal cancer.

6.6 Future Considerations

Several different directions can be taken to further develop a PSS detection technique. The first direction includes finding other administration sites for ICG that will provide similar results. Administration into the portal system can be difficult as access to the portal vein or even mesenteric vein may require dissection. Another site may include the bowel wall where the ICG can be absorbed by the capillary bed. Additional injection sites would reduce the limitation of patients undergoing a laparotomy.

Further study is needed to envelop this method and pharmacokinetic model. This would include modelling different sized shunts and determining the accuracy and sensitivity of the model. Addionally, this model could be applied to liver cirrhotic patients to determine the severity of cirrhosis.

Breath testing could provide an innotive method for PSS detection, however careful consideration needs to be focused on the sampling method. However, breath sampling may not be practical in a clinical setting due to the need for intravenous anasthesia.

Once a technique has been fully developed and is ready for clinical application, patients with known secondary colon lung metastases can be checked for PSSs. Additionally, the clinical test could be applied to routine testing during the initial colonic resection to define the risk profile of the patient.

6.7 Conclusions

This study is the first stage toward PSS detection. Despite the assumed rarity of PSSs occurring in patients with healthy livers, there is still an incidence of 1.7 - 7.2% of colorectal cancer patients with lung metastases in the absence of any liver metastases with an unknown reason for distribution. It is believed that a PSS may be an influencing factor toward metastatic distribution; however PSS detection has

mostly been incidental (Chapter 1). This thesis aimed to create a technique to identify PSS in a healthy liver. The first step was to mimic a PSS within a pig. Arterial vascular anastomoses have been commonly used in patients; however venous anastomoses are not as common and have not been performed in pigs in the last 50 years. Therefore, a protocol for a working shunt in a pig needed to be established before experimentation could occur (Chapter 2). Most previous PSS have been detected incidentally by radiological methods, which are not specific enough for high accurate PSS detection. Therefore, a range of dynamic biomarkers that are exclusively metabolised by the liver were chosen, which could have a higher accuracy and reliability than radiological methods (Chapter 3). Of the compounds chosen, ICG maintained the best PSS detection ability. The key feature was the ability to detect ICG non-invasively and rapidly (Chapter 4). Further exploring the unique abilities of ICG and its detection method using a LiMON® machine, accurate transit times can be identified and used to calculate the relative flow rates and therefore the fraction of blood bypassing the liver (Chapter 5). Although this study has not yet provided a concise method for PSS detection to be used immediately in a clinical setting, it does provide a large foundation for further exploration into a quantitative technique.

CHAPTER 7

References

1. Hales MR, Allan JS, Hall EM. Injection-corrosion studies of normal and cirrhotic livers. The American Journal of Pathology. 1959;35:909-41
2. Stringer MD. The clinical anatomy of congenital portosystemic venous shunts. Clinical Anatomy. 2008;21(2):147-57
3. Abernethy J, Banks J. Account of two instances of uncommon formation, in the viscera of the human body. Philosophical Transactions of the Royal Society of London. 1793;83:59-66
4. Bellah RD, Hayek J, Teele RL. Anomalous portal venous connection to the suprahepatic vena cava: sonographic demonstration. Pediatric Radiology. 1989;20(1-2):115-7
5. Morgan G, Superina R. Congenital absence of the portal vein: two cases and a proposed classification system for portasystemic vascular anomalies. Journal of Pediatric Surgery. 1994;29(9):1239-41
6. Murray CP, Yoo SJ, Babyn PS. Congenital extrahepatic portosystemic shunts. Pediatric Radiology. 2003;33(9):614-20
7. Doehner GA, Ruzicka FF, Jr., Rousselot LM, Hoffman G. The portal venous system: on its pathological roentgen anatomy. Radiology. 1956;66(2):206-17
8. Mori H, Hayashi K, Fukuda T, Matsunaga N, Futagawa S, Nagasaki M, Mutsukura M. Intrahepatic portosystemic venous shunt: Occurrence in patients with and without liver cirrhosis. American Journal of Roentgenology. 1987;149(4):711-4
9. Park JH, Cha SH, Han JK, Han MC. Intrahepatic portosystemic venous shunt. American Journal of Roentgenology. 1990;155(3):527-8
10. Couinaud C. Bases anatomiques des hépatectomies gauche et droite réglées. Journal de Chirurgie. 1954;70:933-66
11. Couinaud C. Le fouie: études anatomiques et chirurgicales. Masson. 1957:74-5

12. Guerin F, Blanc T, Gauthier F, Abella SF, Branchereau S. Congenital portosystemic vascular malformations. Seminars in Pediatric Surgery. 2012;21(3):233-44

13. Joyce AD, Howard ER. Rare congenital anomaly of the portal vein. British Journal of Surgery. 1988;75(10):1038-9

14. Grazioli L, Alberti D, Olivetti L, Rigamonti W, Codazzi F, Matricardi L, Fugazzola C, Chiesa A. Congenital absence of portal vein with nodular regenerative hyperplasia of the liver. European Radiology. 2000;10(5):820-5

15. Altavilla G, Cusatelli P. Ultrastructural analysis of the liver with portal vein agenesis: A case report. Ultrastructural Pathology. 1998;22(6):477-83

16. Kinjo T, Aoki H, Sunagawa H, Kinjo S, Muto Y. Congenital absence of the portal vein associated with focal nodular hyperplasia of the liver and congenital choledochal cyst: A case report. Journal of Pediatric Surgery. 2001;36(4):622-5

17. Kim SZ, Marz PL, Laor T, Teitelbaum J, Jonas MM, Levy HL. Elevated galactose in newborn screening due to congenital absence of the portal vein European Journal of Pediatrics. 1998;157(7):608-9

18. Shinkai M, Ohhama Y, Nishi T, Yamamoto H, Fujita S, Take H, Adachi M, Tachibana K, Aida N, Kato K, Tanaka Y, Takemiya S. Congenital absence of the portal vein and role of liver transplantation in children. Journal of Pediatric Surgery. 2001;36(7):1026-31

19. Bonington SC, Hodgson DI, Mehta S, Lynch N, Chalmers N. A congenital venous anomaly, with a portal-systemic shunt into a previously undescribed intra-thoracic vein. Clinical Radiology. 2002;57(7):658-60

20. Arana E, Martí-Bonmatí L, Martínez V, Hoyos M, Montes H. Portal vein absence and nodular regenerative hyperplasia of the liver with giant inferior mesenteric vein. Abdominal Imaging. 1997;22(5):506-8

21. Goo HW. Extrahepatic portosystemic shunt in congenital absence of the portal vein depicted by time-resolved contrast-enhanced MR angiography. Pediatric Radiology. 2007;37(7):706-9

22. Mboyo A, Lemouel A, Sohm O, Gondy S, Destuynder O, De Billy B, Schirrer J, Aubert D. Congenital extra-hepatic portocaval shunt. Concerning a case of antenatal diagnosis. European Journal of Pediatric Surgery. 1995;5(4):243-5

23. Howard ER, Davenport M. Congenital extrahepatic portocaval shunts - The Abernethy malformation. Journal of Pediatric Surgery. 1997;32(3):494-7

24. Kanamori Y, Hashizume K, Kitano Y, Sugiyama M, Motoi T, Tange T. Congenital extrahepatic portocaval shunt (Abernethy type 2), huge liver mass, and patent ductus arteriosus--a case report of its rare clinical presentation in a young girl. Journal of Pediatric Surgery. 2003;38(4):E15

25. Ikeda S, Sera Y, Ohshiro H, Uchino S, Uchino T, Endo F. Surgical indications for patients with hyperammonemia. Journal of Pediatric Surgery. 1999;34(6):1012-5

26. Tercier S, Delarue A, Rouault F, Roman C, Bréaud J, Petit P. Congenital portocaval fistula associated with hepatopulmonary syndrome: Ligation vs liver transplantation. Journal of Pediatric Surgery. 2006;41(2):E1-E3

27. Takayama Y, Moriura S, Nagata J, Akutagawa A, Hirano A, Ishiguro S, Matsumoto T, Sato T. Embolization of the left portal vein to inferior vena cava shunts for chronic recurrent hepatic encephalopathy via the mesenteric vein. Journal of Gastroenterology and Hepatology. 2001;16(12):1425-8

28. Akita H, Suzuki H, Ito K, Kinoshita S, Sato N, Takikawa H, Sugiyama Y. Characterization of bile acid transport mediated by multidrug resistance associated protein 2 and bile salt export pump. Biochimica et Biophysica Acta - Biomembranes. 2001;1511(1):7-16

29. Akahoshi T, Nishizaki T, Wakasugi K, Mastuzaka T, Kume K, Yamamoto I, Sugimachi K. Portal-systemic encephalopathy due to a congenital extrahepatic portosystemic shunt: three cases and literature review. Hepato-Gastroenterology. 2000;47(34):1113-6

30. Tarantino G, Citro V, Esposito P, Giaquinto S, de Leone A, Milan G, Tripodi FS, Cirillo M, Lobello R. Blood ammonia levels in liver cirrhosis: a clue for the presence of portosystemic collateral veins. Biomed Central Gastroenterology. 2009;9:21

31. Sakura N, Mizoguchi N, Eguchi T, Ono H, Mawatari H, Naitou K, Ito K. Elevated plasma bile acids in hypergalactosaemic neonates: a diagnostic clue to portosystemic shunts. European Journal of Pediatrics. 1997;156(9):716-8

32. Kono T, Hiki T, Kuwashima S, Hashimoto T, Kaji Y. Hypergalactosemia in early infancy: diagnostic strategy with an emphasis on imaging. Pediatrics International. 2009;51(2):276-82

33. Nishimura Y, Tajima G, Dwi Bahagia A, Sakamoto A, Ono H, Sakura N, Naito K, Hamakawa M, Yoshii C, Kubota M, Kobayashi K, Saheki T. Differential diagnosis of neonatal mild hypergalactosaemia detected by mass screening: clinical significance of portal vein imaging. Journal of Inherited Metabolic Disease. 2004;27(1):11-8

34. Marois D, Van Heerden JA, Carpenter HA, Sheedy Ii PF. Congenital absence of the portal vein. Mayo Clinic Proceedings. 1979;54(1):55-9

35. Laverdiere JT, Laor T, Benacerraf B. Congenital absence of the portal vein: Case report and MR demonstration. Pediatric Radiology. 1995;25(1):52-3

36. Yonemitsu H, Mori H, Kimura T, Kagawa K, Tsuda T, Yamada Y, Kiyosue H, Matsumoto S. Congenital extrahepatic portocaval shunt associated with hepatic hyperplastic nodules in a patient with Dubin-Johnson syndrome. Abdominal Imaging. 2000;25(6):572-5

37. Massin M, Verloes A, Jamblin P. Cardiac anomalies associated with congenital absence of the portal vein. Cardiology in the Young. 1999;9(5):522-5

38. Kitagawa S, Gleason WA, Jr., Northrup H, Middlebrook MR, Ueberschar E. Symptomatic hyperammonemia caused by a congenital portosystemic shunt. Journal of Pediatrics. 1992;121(6):917-9

39. Mizoguchi N, Sakura N, Ono H, Naito K, Hamakawa M. Congenital porto-left renal venous shunt as a cause of galactosaemia. Journal of Inherited Metabolic Disease. 2001;24(1):72-8

40. Woodle ES, Thislethwaite JR, Emond JC, Whitington PF, Vogelbach P, Yousefzadeh DK, Broelsch CE. Successful hepatic transplantation in congenital absence of recipient portal vein. Surgery. 1990;107(4):475-9

41. Nakasaki H, Tanaka Y, Ohta M, Kanemoto T, Mitomi T, Iwata Y, Ozawa A. Congenital absence of the portal vein. Annals of Surgery. 1989;210(2):190-3

42. Ikeda H, Aotsuka H, Nakajima H, Sawada M. Portosystemic shunt with polysplenia and hypoplastic left heart syndrome. Pediatric Cardiology. 2005;26(4):446-8

43. Olling S, Olsson R. Congenital absence of portal venous system in a 50 year old woman. Acta Medica Scandinavica. 1974;196(4):343-5

44. Morse SS, Taylor KJW, Strauss EB. Congenital absence of the portal vein in oculoauriculovertebral dysplasia (Goldenhar syndrome). Pediatric Radiology. 1986;16(5):437-9

45. Guariso G, Fiorio S, Altavilla G, Gamba PG, Toffolutti T, Chiesura-Corona M, Tedeschi U, Zancan L. Congenital absence of the portal vein associated with focal nodular hyperplasia of the liver and cystic dysplasia of the kidney. European Journal of Pediatrics. 1998;157(4):287-90

46. Wakamoto H, Manabe K, Kobayashi H, Hayashi M. Subclinical portal-systemic encephalopathy in a child with congenital absence of the portal vein. Brain and Development. 1999;21(6):425-8

47. Motoori S, Shinozaki M, Goto N, Kondo F. Case report: Congenital absence of the portal vein associated with nodular hyperplasia in the liver. Journal of Gastroenterology and Hepatology. 1997;12(9-10):639-43

48. Matsuoka Y, Ohtomo K, Okubo T, Nishikawa J, Mine T, Ohno S. Congenital absence of the portal vein. Gastrointestinal Radiology. 1992;17(1):31-3

49. Shah R, Ford EG, Woolley MM. Congenital portocaval shunt. Pediatric Surgery International. 1992;7(3):216-7

50. Usuki N, Miyamoto T. A case of congenital absence of the intrahepatic portal vein diagnosed by MR angiography. Journal of Computer Assisted Tomography. 1998;22(5):728-9

51. Ohwada S, Hamada Y, Morishita Y, Tanahashi Y, Takeyoshi I, Kawashima Y, Nakamura S, Iino Y, Miyamoto Y, Hirato J. Hepatic encephalopathy due to congenital splenorenal shunts: report of a case. Surgery Today. 1994;24(2):145-9

52. Tanano H, Hasegawa T, Kawahara H, Sasaki T, Okada A. Biliary atresia associated with congenital structural anomalies. Journal of Pediatric Surgery. 1999;34(11):1687-90

53. Ji EK, Yoo SJ, Kim JH, Cho KS. Congenital splenorenal venous shunt detected by prenatal ultrasonography. Journal of Ultrasound in Medicine. 1999;18(6):437-9

54. Gitzelmann R, Forster I, Willi UV. Hypergalactosaemia in a newborn: Self-limiting intrahepatic portosystemic venous shunt. European Journal of Pediatrics. 1997;156(9):719-22

55. Uchino T, Matsuda I, Endo F. The long-term prognosis of congenital portosystemic venous shunt. Journal of Pediatrics. 1999;135(2 I):254-6

56. Barton Iii JW, Keller MS. Liver transplantation for hepatoblastoma in a child with congenital absence of the portal vein. Pediatric Radiology. 1989;20(1-2):113-4

57. Pohl A, Jung A, Vielhaber H, Pfluger T, Schramm T, Lang T, Kellnar S, Schöber JG. Congenital atresia of the portal vein and extrahepatic portocaval shunt associated with benign neonatal hemangiomatosis, congenital adrenal hyperplasia, and atrial septal defect. Journal of Pediatric Surgery. 2003;38(4):633-4

58. Valls E, Ceres L, Urbaneja A, Muñoz R, Alonso I. Color doppler sonography in the diagnosis of neonatal intrahepatic portosystemic shunts. Journal of Clinical Ultrasound. 2000;28(1):42-6

59. Yamagami T, Nakamura T, Tokiwa K, Ohno K, Itoh H, Maeda T. Intrahepatic portosystemic venous shunt associated with biliary atresia: Case report. Pediatric Radiology. 2000;30(7):489-91

60. Komaba Y, Nomoto T, Hiraide T, Kitamura S, Terashi A. Persistent primitive hypoglossal artery complicated by atrial septal defect and congenital intrahepatic shunts. Internal Medicine. 1998;37(1):60-4

61. Ono H, Mawatari H, Mizoguchi N, Eguchi T, Sakura N. Clinical features and outcome of eight infants with intrahepatic porto- venous shunts detected in neonatal screening for galactosaemia. Acta Paediatrica, International Journal of Paediatrics. 1998;87(6):631-4

62. Mori K, Dohi T, Yamamoto H, Kamada M. An enormous shunt between the portal and hepatic veins associated with multiple coronary artery fistulas. Pediatric Radiology. 1990;21(1):66-8

63. Kalifa G, Brunelle F, Chaumont P. Congenital porto-caval fistula. Fistule Porto-Cave Congenitale. 1978;21(2-3):183-6

64. Gallego C, Miralles M, Marín C, Muyor P, González G, García-Hidalgo E. Congenital hepatic shunts. Radiographics. 2004;24(3):755-72

65. Starzl TE, Francavilla A, Halgrimson CG, Francavilla FR, Porter KA, Brown TH, Putnam CW. The origin, hormonal nature, and action of hepatotrophic substances in portal venous blood. Surgery Gynecology and Obstetrics. 1973;137(2):179-99

66. Chiu B, Melin-Aldana H, Pillai S, Chu F, Superina RA. Factor VII transcription correlates with hepatocyte proliferation and hepatocyte growth factor expression in a rodent extrahepatic portal vein obstruction model. Journal of the American College of Surgeons. 2007;205(2):277-83

67. Gandhi CR, Murase N, Subbotin VM, Uemura T, Nalesnik M, Demetris AJ, Fung JJ, Starzl TE. Portacaval shunt causes apoptosis and liver atrophy in rats despite increases in endogenous levels of major hepatic growth factors. Journal of Hepatology. 2002;37(3):340-8

68. Superina R, Bambini DA, Lokar J, Rigsby C, Whitington PF. Correction of extrahepatic portal vein thrombosis by the mesenteric to left portal vein bypass. Annals of Surgery. 2006;243(4):515-21

69. Vonnahme FJ, Dubuisson L, Kubale R. Ultrastructural characteristics of hyperplastic alterations in the liver of congenital portacaval-shunt rats. British Journal of Experimental Pathology. 1984;65(5):585-96

70. Bioulac-Sage P, Saric J, Boussarie L, Balabaud C. Congenital portacaval shunt in rats: Liver adaptation to lack of portal vein - A light and electron microscopic study. Hepatology. 1985;5(6):1183-9

71. Satoh M, Yokoya S, Hachiya Y, Hachiya M, Fujisawa T, Hoshino K, Saji T. Two hyperandrogenic adolescent girls with congenital portosystemic shunt. European Journal of Pediatrics. 2001;160(5):307-11

72. Kamata S, Kitayama Y, Usui N, Kuroda S, Nose K, Sawai T, Okada A. Patent ductus venosus with a hypoplastic intrahepatic portal system presenting intrapulmonary

shunt: a case treated with banding of the ductus venosus. Journal of Pediatric Surgery. 2000;35(4):655-7

73. Uchino T, Endo F, Ikeda S, Shiraki K, Sera Y, Matsuda I. Three brothers with progressive hepatic dysfunction and severe hepatic steatosis due to a patent ductus venosus. Gastroenterology. 1996;110(6):1964-8

74. Hori T, Yonekawa Y, Okamoto S, Ogawa K, Ogura Y, Oike F, Takada Y, Egawa H, Nguyen JH, Uemoto S. Pediatric orthotopic living-donor liver transplantation cures pulmonary hypertension caused by Abernethy malformation type Ib. Pediatric Transplantation. 2011;15(3):e47-52

75. Yoshidome H, Edwards MJ. An embryological perspective on congenital portacaval shunt: a rare anomaly in a patient with hepatocellular carcinoma. American Journal of Gastroenterology. 1999;94(9):2537-9

76. Santamaría G, Pruna X, Serres X, Inaraja L, Zuasnabar A, Castellote A. Congenital intrahepatic portosystemic venous shunt: Sonographic and magnetic resonance imaging. European Radiology. 1996;6(1):76-8

77. Caiulo VA, Presta G, Latini G, Mattioli G, Jasonni V. Diagnosis and follow-up of congenital intrahepatic portosystemic venous shunt by ultrasounds [2]. Acta Paediatrica, International Journal of Paediatrics. 2001;90(10):1209-10

78. Meyer WW, Lind J. The ductus venosus and the mechanism of its closure. Archives of Disease in Childhood. 1966;41(220):597-605

79. Loberant N, Barak M, Gaitini D, Herskovits M, Ben-Elisha M, Roguin N. Closure of the ductus venosus in neonates: Findings on real-time gray- scale, color-flow Doppler, and duplex Doppler sonography. American Journal of Roentgenology. 1992;159(5):1083-5

80. Fugelseth D, Lindemann R, Liestøl K, Kiserud T, Langslet A. Ultrasonographic study of ductus venosus in healthy neonates. Archives of Disease in Childhood: Fetal and Neonatal Edition. 1997;77(2):F131-F4

81. Yoshimoto Y, Shimizu R, Saeki T, Harada T, Sugio Y, Nomura S, Tanaka H. Patent ductus venosus in children: a case report and review of the literature. Journal of Pediatric Surgery. 2004;39(1):E1-5

82. Jacob S, Farr G, De Vun D, Takiff H, Mason A. Hepatic manifestations of familial patent ductus venosus in adults. Gut. 1999;45(3):442-5

83. Matsubara T, Sumazaki R, Saitoh H, Imai H, Nakayama J, Takita H. Patent ductus venosus associated with tumor-like lesions of the liver in a young girl. Journal of Pediatric Gastroenterology and Nutrition. 1996;22(1):107-11

84. Moncure AC, Waltman AC, Vandersalm TJ. Gastrointestinal hemorrhage from adhesion related mesenteric varices. Annals of Surgery. 1976;183(1):24-9

85. Wall BF, Hart D. Revised radiation doses for typical X-ray examinations: Report on a recent review of doses to patients from medical X-ray examinations in the UK by NRPB. British Journal of Radiology. 1997;70(MAY):437-9

86. Afzal S, Nair A, Grainger J, Latif S, Rehman AU. Spontaneous thrombosis of congenital extrahepatic portosystemic shunt (abernethy malformation) simulating inguinal hernia incarceration. Vascular and Endovascular Surgery. 2010;44(6):508-10

87. Rizzatto G. Ultrasound transducers. European Journal of Radiology. 1998;27 Suppl 2:S188-95

88. Lisovsky M, Konstas AA, Misdraji J. Congenital extrahepatic portosystemic shunts (abernethy malformation): A histopathologic evaluation. American Journal of Surgical Pathology. 2011;35(9):1381-90

89. Charre L, Roggen F, Lemaire J, Mathijs J, Goffette P, Danse E, Lerut J. Hematochezia and congenital extrahepatic portocaval shunt with absent portal vein: Successful treatment by liver transplantation Transplantation. 2004;78(9):1404-6

90. Florio F, Nardella M, Balzano S, Giacobbe A, Perri F. Congenital intrahepatic portosystemic shunt. Cardiovascular and Interventional Radiology. 1998;21(5):421-4

91. Pantel K, Brakenhoff RH. Dissecting the metastatic cascade. Nature Reviews Cancer. 2004;4(6):448-56

92. Wolfrum F, Vogel I, Fandrich F, Kalthoff H. Detection and clinical implications of minimal residual disease in gastro-intestinal cancer. Langenbecks Archives of Surgery. 2005;390(5):430-41

93. Ghetie C, Davies M, Cornfeld D, Suh N, Saif MW. Expectoration of a lung metastasis in a patient with colorectal carcinoma. Clinical Colorectal Cancer. 2008;7(4):283-6

94. Tan KK, Lopes Gde L, Jr., Sim R. How uncommon are isolated lung metastases in colorectal cancer? A review from database of 754 patients over 4 years. Journal of Gastrointestinal Surgery. 2009;13(4):642-8

95. Netter F. Portal vein tributaries: portacaval anastomoses. In: Colacino S, editor. Atlas of Human Anatomy. Basle, Switzerland: CIBA-GEIGY Limited; 1989.

96. Gupta GP, Massague J. Cancer metastasis: building a framework. Cell. 2006;127(4):679-95

97. Steinert G, Scholch S, Koch M, Weitz J. Biology and significance of circulating and disseminated tumour cells in colorectal cancer. Langenbecks Archives of Surgery. 2012;397(4):535-42

98. Yu M, Stott S, Toner M, Maheswaran S, Haber DA. Circulating tumor cells: approaches to isolation and characterization. Journal of Cell Biology. 2011;192(3):373-82

99. Miller MC, Doyle GV, Terstappen LW. Significance of circulating tumor cells detected by the cell search system in patients with metastatic breast colorectal and prostate Cancer. Journal of Oncology. 2010;2010:617421

100. Chambers AF, Groom AC, MacDonald IC. Dissemination and growth of cancer cells in metastatic sites. Nature Reviews Cancer. 2002;2(8):563-72

101. Hanahan D, Weinberg RA. The hallmarks of cancer. Cell. 2000;100(1):57-70

102. Chaffer CL, Weinberg RA. A perspective on cancer cell metastasis. Science. 2011;331(6024):1559-64

103. Fidler IJ. The pathogenesis of cancer metastasis: the 'seed and soil' hypothesis revisited. Nature Reviews Cancer. 2003;3(6):453-8

104. Joyce JA, Pollard JW. Microenvironmental regulation of metastasis. Nature Reviews Cancer. 2009;9(4):239-52

105. Zhe X, Cher ML, Bonfil RD. Circulating tumor cells: finding the needle in the haystack. American Journal of Cancer Research. 2011;1(6):740-51

106. Lore JM, Jr., Madden JL, Gerold FP. Pre-existing portacaval shunts: a hypothesis for the bizarre metastases of some carcinomas. Cancer. 1958;11(1):24-7

107. Saitoh H, Yoshida KI, Uchijima Y, Kobayashi N, Suwata J, Nakame Y. Possible metastatic routes via portacaval shunts in renal adenocarcinoma with liver metastasis. Urology. 1991;37(6):598-601

108. Wallace MJ, Madoff DC, Ahrar K, Warneke CL. Transjugular intrahepatic portosystemic shunts: Experience in the oncology setting. Cancer. 2004;101(2):337-45

109. Bayon LG, Izquierdo MA, Sirovich I, van Rooijen N, Beelen RH, Meijer S. Role of Kupffer cells in arresting circulating tumor cells and controlling metastatic growth in the liver. Hepatology. 1996;23(5):1224-31

110. Pearson HJ, Anderson J, Chamberlain J, Bell PR. The effect of Kupffer cell stimulation or depression on the development of liver metastases in the rat. Cancer Immunology, Immunotherapy. 1986;23(3):214-6

111. Ryden S, Bergqvist L, Hafstrom L, Hultberg B, Stenram U, Strand SE. Influence of a reticuloendothelial-suppressing agent on liver tumor growth in the rat. Journal of Surgical Oncology. 1984;26(4):245-51

112. Geng Y, Marshall JR, King MR. Glycomechanics of the metastatic cascade: tumor cell-endothelial cell interactions in the circulation. Annals of Biomedical Engineering. 2012;40(4):790-805

113. Li J, King MR. Adhesion receptors as therapeutic targets for circulating tumor cells. Frontiers in Oncology. 2012;2:79

114. Kansas GS. Selectins and their ligands: current concepts and controversies. Blood. 1996;88(9):3259-87

115. Varki A. Selectin ligands: will the real ones please stand up? Journal of Clinical Investigation. 1997;100(11 Suppl):S31-5

116. Kohler S, Ullrich S, Richter U, Schumacher U. E-/P-selectins and colon carcinoma metastasis: first in vivo evidence for their crucial role in a clinically relevant model of spontaneous metastasis formation in the lung. British Journal of Cancer. 2010;102(3):602-9

117. Nishie A, Yoshimitsu K, Honda H, Kaneko K, Kuroiwa T, Fukuya T, Irie H, Ninomiya T, Yoshimitsu T, Hirakata H, Okuda S, Masuda K. Treatment of hepatic encephalopathy by retrograde transcaval coil embolization of an ileal vein-to-right gonadal vein portosystemic shunt. Cardiovascular and Interventional Radiology. 1997;20(3):222-4

118. Kudo M, Tomita S, Tochio H, Minowa K, Todo A. Intrahepatic portosystemic venous shunt: Diagnosis by color Doppler imaging. American Journal of Gastroenterology. 1993;88(5):723-9

119. Bodner G, Gluck A, Springer P, Konig P, Perkmann R. Aneurysmal portosystemic venous shunt: A case report. Ultraschall in der Medizin. 1999;20(5):215-7

120. Fanelli F, Marcelli G, Bezzi M, Salvatori FM, Rossi M, Rossi P, Passariello R. Intrahepatic aneurysmal portohepatic venous shunt: Embolization with a tissue adhesive solution. Journal of Endovascular Therapy. 2003;10(1):147-53

121. Komori A, Kataoka C, Okamura S, Tanoue K, Hashizume M, Ichiki Y, Takasaki T, Shigematsu H, Hayashida K, Ishibashi H. Aneurysmal intraheptic portosystemic venous shunt associated with idiopathic portal hypertension: A lesion evaluated by a 3D image reconstructed from power doppler flow imaging. Journal of Medical Ultrasonics. 2000;27(2):131-7

122. Gheorghiu D, Leibowits O, Bloom RA. Asymptomatic aneurysmal intrahepatic porto-hepatic venous shunt - Diagnosis by ultrasound. Clinical Radiology. 1994;49(1):64-5

123. Cacciapaglia F, Vadacca M, Coppolino G, Buzzulini F, Rigon A, Zennaro D, Zardi E, Afeltra A. Spontaneous splenorenal shunt in a patient with antiphospholipid syndrome: The first case reported. Lupus. 2007;16(1):56-8

124. Matsuo M, Kanematsu M, Kato H, Kondo H, Sugisaki K, Hoshi H. Osler-Weber-Rendu disease: Visualizing portovenous shunting with three-dimensional sonography. American Journal of Roentgenology. 2001;176(4):919-20

125. Oktenli C, Gul D, Deveci MS, Saglam M, Upadhyaya M, Thompson P, Consoli C, Kocar IH, Pilarski R, Zhou XP, Eng C. Unusual features in a patient with neurofibromatosis type 1: Multiple subcutaneous lipomas, a juvenile polyp in

ascending colon, congenital intrahepatic portosystemic venous shunt, horseshoe kidney. American Journal of Medical Genetics. 2004;127(3):298-301

126. Lin ZY, Chen SC, Hsieh MY, Wang CW, Chuang WL, Wang LY. Incidence and clinical significance of spontaneous intrahepatic portosystemic venous shunts detected by sonography in adults without potential cause. Journal of Clinical Ultrasound. 2006;34(1):22-6

127. Di Candio G, Campatelli A, Mosca F, Santi V, Casanova P, Bolondi L. Ultrasound detection of unusual spontaneous portosystemic shunts associated with uncomplicated portal hypertension. Journal of Ultrasound in Medicine. 1985;4(6):297-305

128. Leyendecker JR, Grayson DE, Good R. Transient postpartum portosystemic shunting revealed by MR venography. AJR American Journal of Roentgenology. 2002;178(5):1152-4

129. Konno K, Ishida H, Uno A, Ohnami Y, Masamune O. Large extrahepatic portosystemic shunt without portal hypertension. Abdominal Imaging. 1997;22(1):79-81

130. Horiguchi Y, Kitano T, Takagawa H, Imai H, Itoh M, Miyakawa S, Nakamura Y, Miura K, Itoh K. A large inferior mesenteric-caval shunt via the internal iliac vein. Gastroenterologia Japonica. 1988;23(6):684-7

131. Kerlan RK, Jr., Sollenberger RD, Palubinskas AJ, Raskin NH, Callen PW, Ehrenfeld WK. Portal-systemic encephalopathy due to a congenital portocaval shunt. AJR American Journal of Roentgenology. 1982;139(5):1013-5

132. Horiguchi Y, Kitano T, Imai H, Ohsuki M, Yamauchi M, Itoh M. Intrahepatic portal-systemic shunt: its etiology and diagnosis. Gastroenterologia Japonica. 1987;22(4):496-502

133. Oguz B, Akata D, Balkanci F, Akhan O. Intrahepatic portosystemic venous shunt: Diagnosis by colour/power Doppler imaging and three-dimensional ultrasound. British Journal of Radiology. 2003;76(907):487-90

134. Shapiro RS, Winsberg F, Stancato-Pasik A, Sterling KM. Color Doppler sonography of vascular malformations of the liver. Journal of Ultrasound in Medicine. 1993;12(6):343-8

135. Wittich G, Jantsch H, Tscholakoff D. Congenital portosystemic shunt diagnosed by combined real-time and Doppler sonography. Journal of Ultrasound in Medicine. 1985;4(6):315-8

136. Chagnon SF, Vallee CA, Barge J, Chevalier LJ, Le Gal J, Blery MV. Aneurysmal portahepatic venous fistula: report of two cases. Radiology. 1986;159(3):693-5

137. Thakur SK, Dalai SS. Balloon retrograde transvenous occlusion of fundic varix. Indian Journal of Gastroenterology. 2010;29(2):88-9

138. Matsumoto S, Mori H, Yamada Y, Hayashida T, Hori Y, Kiyosue H. Intrahepatic porto-hepatic venous shunts in Rendu-Osler-Weber disease: Imaging demonstration. European Radiology. 2004;14(4):592-6

139. Filik L, Boyacioglu S. Asymptomatic aneurysmal portosystemic venous shunt: a case report and review of the literature. Acta Medica (Hradec Králové) / Universitas Carolina, Facultas Medica Hradec Králové. 2006;49(4):241-4

140. Crespin J, Nemcek A, Rehkemper G, Blei AT. Intrahepatic portal-hepatic venous anastomosis: A portal-systemic shunt with neurological repercussions. American Journal of Gastroenterology. 2000;95(6):1568-71

141. Machida H, Ueno E, Isobe Y, Nishimaki H, Fujimura M, Tomimatsu M, Endo H. Stent-graft to treat intrahepatic portosystemic venous shunt causing encephalopathy. Hepato-Gastroenterology. 2008;55(81):237-40

142. Lin YT, Chang CH, Chen WC. Asymptomatic congenital splenorenal shunt in a noncirrhotic patient with a left adrenal aldosterone-producing adenoma. Kaohsiung Journal of Medical Sciences. 2009;25(12):669-74

143. Konstas AA, Digumarthy SR, Avery LL, Wallace KL, Lisovsky M, Misdraji J, Hahn PF. Congenital portosystemic shunts: Imaging findings and clinical presentations in 11 patients. European Journal of Radiology. 2011;80(2):175-81

144. Kuramitsu T, Komatsu M, Matsudaira N, Naganuma T, Niizawa M, Zeniya A, Yoshida T, Toyoshima I, Chiba M, Masamune O. Portal-systemic encephalopathy from a spontaneous gastrorenal shunt diagnosed by three-dimensional computed tomography and treated effectively by percutaneous vascular embolization. Liver. 1998;18(3):208-12

145. Ortiz M, Cordoba J, Alonso J, Rovira A, Quiroga S, Jacas C, Esteban R, Guardia J. Oral glutamine challenge and magnetic resonance spectroscopy in three patients with congenital portosystemic shunts. Journal of Hepatology. 2004;40(3):552-7

146. Sawyer B, Dow C, Frank J, Lau E. Congenital portocaval shunt-associated liver lesions in a patient with cancer. Australia and New Zealand Journal of Surgery. 2008;78(7):613-4

147. Ishii Y, Inagaki Y, Hirai K, Aoki T. Hepatic encephalopathy caused by congenital extrahepatic portosystemic venous shunt. Journal of Hepato-Biliary-Pancreatic Surgery. 2000;7(5):524-8

148. Imamura H, Momose T, Kitabayashi H, Takahashi W, Yazaki Y, Takenaka H, Isobe M, Sekiguchi M, Kubo K. Pulmonary hypertension as a result of asymptomatic portosystemic shunt. Japanese Circulation Journal. 2000;64(6):471-3

149. Senocak E, Oguz B, Edguer T, Cila A. Congenital intrahepatic portosystemic shunt with variant inferior right hepatic vein. Diagnostic and Interventional Radiology. 2008;14(2):97-9

150. Soyer P, Bluemke DA, Sitzmann JV, Hruban RH, Fishman EK. Hepatocellular carcinoma: findings on spiral CT during arterial portography. Abdominal Imaging. 1995;20(6):541-6

151. Hekimoglu K, Ustundag Y. Cavernous hemangioma with arterioportal and portosystemic shunts: precise diagnosis with dynamic multidetector computed tomography imaging. Abdominal Imaging. 2010;35(3):328-31

152. Eren S, Karaman A, Okur A. The superior vena cava syndrome caused by malignant disease. Imaging with multi-detector row CT. European Journal of Radiology. 2006;59(1):93-103

153. Park SW, Kang HS, Kim YJ, Lee MW, Roh HG. Successful occlusion of spontaneous portosystemic shunts leading to encephalopathy in a non-cirrhotic patient by using the Amplatzer vascular plug. Acta Radiologica. 2007;48(10):1077-81

154. Kimura N, Kumamoto T, Hanaoka T, Nakamura K, Hazama Y, Arakawa R. Portal-systemic shunt encephalopathy presenting with diffuse cerebral white matter lesion: an autopsy case. Neuropathology. 2008;28(6):627-32

155. Ito K, Takada T, Amano H, Toyota N, Yasuda H, Yoshida M, Takada Y, Takeshita K, Koutake H, Takada K, Furuya S. Localization of islet-cell hyperplasia: value of pre- and intraoperative arterial stimulation and venous sampling. Journal of Hepato-Biliary-Pancreatic Surgery. 2004;11(3):203-6

156. Handra-Luca A, Paradis V, Vilgrain V, Dubois S, Durand F, Belghiti J, Valla D, Degott C. Multiple mixed adenoma-focal nodular hyperplasia of the liver associated with spontaneous intrahepatic porto-systemic shunt: a new type of vascular malformation associated with the multiple focal nodular hyperplasia syndrome? Histopathology. 2006;48(3):309-11

157. Raskin NH, Bredesen D, Ehrenfeld WK, Kerlan RK. Periodic confusion caused by congenital extrahepatic portacaval shunt. Neurology. 1984;34(5):666-9

158. Tanaka O, Ishihara K, Oyamada H, Harusato A, Yamaguchi T, Ozawa M, Nakano K, Yamagami T, Nishimura T. Successful portal-systemic shunt occlusion with balloon-occluded retrograde transvenous obliteration for portosystemic encephalopathy without liver cirrhosis. Journal of Vascular and Interventional Radiology. 2006;17(12):1951-5

159. Serrien B, Rigauts H, Marchal G, Lambrechts P. Congenital intrahepatic porto-systemic shunt. Journal Belge de Radiologie. 1992;75(6):492-4

160. Seyama Y, Sano K, Tang W, Kokudo N, Sakamoto Y, Imamura H, Makuuchi M. Simultaneous resection of liver cell adenomas and an intrahepatic portosystemic venous shunt with elevation of serum PIVKA-II level. Journal of Gastroenterology. 2006;41(9):909-12

161. Brandenburg VM, Krueger S, Haage P, Mertens P, Riehl J. Heterotaxy syndrome with severe pulmonary hypertension in an adult. Southern Medical Journal. 2002;95(5):536-8

162. Momoo T, Johkura K, Kuroiwa Y. Spike-wave stupor in a patient with metabolic disorder. Journal of lcinical Neuroscience. 2006;13(2):301-3

163. Nagino M, Hayakawa N, Kitagawa S, Katoh M, Komatsu S, Nimura Y, Shionoya S. Interventional embolization with fibrin glue for a large inferior mesenteric-caval shunt. Surgery. 1992;111(5):580-4

164. Shimono J, Tsuji H, Azuma K, Hashiguchi M, Fujishima M. Recurring encephalopathy abolished by gastrorenal shunt ligation in a diabetic hemodialysis patient. American Journal of Gastroenterology. 1998;93(2):270-2

165. Ohno T, Muneuchi J, Ihara K, Yuge T, Kanaya Y, Yamaki S, Hara T. Pulmonary hypertension in patients with congenital portosystemic venous shunt: A previously unrecognized association. Pediatrics. 2008;121(4):e892-e9

166. Takada K, Homma H, Takahashi M, Mezawa S, Miyanishi K, Sumiyoshi T, Doi T, Kukitsu T, Kato J, Niitsu Y. A case of successful management of portosystemic shunt with autosomal dominant polycystic kidney disease by balloon-occluded retrograde transvenous obliteration and partial splenic embolization. European Journal of Gastroenterology and Hepatology. 2001;13(1):75-8

167. Yamagami T, Arai Y, Takeuchi Y, Nakamura T, Inaba Y, Matsueda K, Nishimura T. Increased hepatic arterial blood flow after decreased portal supply to the liver parenchyma owing to intrahepatic portosystemic venous shunt: Angiographic demonstration using helical CT. British Journal of Radiology. 2000;73(874):1042-5

168. Yoshimitsu K, Andou H, Kudo S, Matsuo Y, Matsumoto S, Nakao T, Shimoda Y. Multiple intrahepatic portosystemic venous shunts: treatment by portal vein embolization. Cardiovascular and Interventional Radiology. 1993;16(1):49-51

169. Yoshikawa K, Matsumoto M, Hamanaka M, Nakagawa M. A case of manganese induced parkinsonism in hereditary haemorrhagic telangiectasia. Journal of Neurology, Neurosurgery and Psychiatry. 2003;74(9):1312-4

170. Ito T, Ikeda N, Watanabe A, Sue K, Kakio T, Mimura H, Tsuji T. Obliteration of portal systemic shunts as therapy for hepatic encephalopathy in patients with non-cirrhotic portal hypertension. Gastroenterologia Japonica. 1992;27(6):759-64

171. Suga K, Ishikawa Y, Matsunaga N, Tanaka N, Suda H, Handa T. Liver involvement in hereditary haemorrhagic telangiectasia: assessment with 99Tcm-phytate radionuclide angiography and 123I-IMP transrectal portal scintigraphy. British Journal of Radiology. 2000;73(874):1115-9

172. Nishida T, Okuda A. Case report: Diagnosis of cavo-portal shunt in inferior vena cava obstruction: Comparison between venography and dynamic scintigraphy. Clinical Radiology. 1991;43(4):274-5

173. Chu LS, Chang CP, Liu RS, Wynchank S, Sheu MH, Chiang JH, Yeh SH. The 'Fisherman's Waders' sign in a bone scan of inferior vena cava thrombosis associated with nephrotic syndrome. Annals of Nuclear Medicine. 1995;9(4):237-41

174. Ceylan Gunay E, Erdogan A. Incidentally diagnosed portosystemic shunt on 99mTc red blood cell gastrointestinal bleeding scintigraphy. Revista Espanola de Medicina Nuclear. 2011;30(5):329-30

175. Matsuura T, Morimoto Y, Nose K, Hara Y, Akiyama T, Kurita T. Venous abnormalities incidentally accompanied by renal tumors. Urologia Internationalis. 2004;73(2):163-8

176. Tanaka A, Morimoto T, Yamamori T, Moriyasu F, Yamaoka Y. Atypical liver hemangioma with shunt: long-term follow-up. Journal of Hepato-Biliary-Pancreatic Surgery. 2002;9(6):750-4

177. Ali S, Stolpen AH, Schmidt WN. Portosystemic encephalopathy due to mesoiliac shunt in a patient without cirrhosis. Journal of Clinical Gastroenterology. 2010;44(5):381-3

178. Kanda T, Nogawa S, Muramatsu K, Koto A, Fukuuchi Y. Portal systemic encephalopathy presenting with dressing and constructional apraxia. Internal Medicine. 2000;39(5):419-23

179. Jeng LBB, Chen MF. Intrahepatic portohepatic venous shunt: A case report of successful surgical resection. Archives of Surgery. 1993;128(3):349-52

180. Sato T, Asanuma Y, Ishida H, Hashimoto M, Tanaka J, Andoh H, Yasui O, Kurokawa T, Komatsuda T, Konno K, Heianna J, Koyama K. A case of extrahepatic portosystemic shunt without portal hypertension treated by laparoscopically assisted embolization. Surgery. 1999;126(5):984-6

181. Yamaguchi Y, Okai T, Watanabe H, Motoo Y, Mai M, Matsui O, Nakanuma Y, Sawabu N. Myxedema accompanied by huge portal-systemic shunt without portal hypertension. Internal Medicine. 2001;40(12):1200-4

182. De Gaetano AM, Rinaldi P, Barbaro B, Mirk P, Di Stasi C, Gui B, Maresca G, Bonomo L. Intrahepatic portosystemic venous shunts: Color Doppler sonography. Abdominal Imaging. 2007;32(4):463-9

183. Barchetti F, Pellegrino L, Al-Ansari N, De Marco V, Scarpato P, Ialongo P. Congenital absence of the portal vein in a middle-aged man. Surgical and Radiologic Anatomy. 2011;33(4):369-72

184. Yokota T, Tsuchiya K, Umetani K, Furukawa T, Tsukagoshi H. Choreoathetoid movements associated with a spleno-renal shunt. Journal of Neurology. 1988;235(8):487-8

185. Kumar A, Kumar J, Aggarwal R, Srivastava S. Abernethy malformation with portal vein aneurysm. Diagnostic and Interventional Radiology. 2008;14(3):143-6

186. Teshima H, Hayashida N, Akashi H, Aoyagi S. Surgical treatment of a descending aortic aneurysm in a patient with noncirrhotic portal hypertension and a portal systemic shunt. Circ J. 2002;66(12):1176-7

187. Matsumoto S, Mori H, Yoshioka K, Kiyosue H, Komatsu E. Effects of portal-systemic shunt embolization on the basal ganglia: MRI. Neuroradiology. 1997;39(5):326-8

188. Collard B, Maleux G, Heye S, Cool M, Bielen D, George C, Roskams T, Van Steenbergen W. Value of carbon dioxide wedged venography and transvenous liver biopsy in the definitive diagnosis of Abernethy malformation. Abdominal Imaging. 2006;31(3):315-9

189. Chandler TM, Heran MK, Chang SD, Parvez A, Harris AC. Multiple focal nodular hyperplasia lesions of the liver associated with congenital absence of the portal vein. Magnetic Resonance Imaging. 2011;29(6):881-6

190. Hanatate F, Matsuoka H, Mizuno Y, Kitamura T. Porto-hepatic venous shunt via portal vein aneurysm with splenomegaly. Journal of Gastroenterology. 1995;30(6):786-9

191. Villeneuve PJ, Sundaresan RS. Surgical management of colorectal lung metastasis. Clinics in Colon and Rectal Surgery. 2009;22(4):233-41

192. Liu Y, Ren W, Liu C, Huang K, Feng Y, Wang X, Tong Y. Contrast-enhanced ultrasonography of the rabbit VX2 tumor model: Analysis of vascular pathology. Oncology Letters. 2012;4(4):685-90

193. Sati P, George IC, Shea CD, Gaitan MI, Reich DS. FLAIR*: a combined MR contrast technique for visualizing white matter lesions and parenchymal veins. Radiology. 2012;265(3):926-32

194. Duddalwar VA. Multislice CT angiography: a practical guide to CT angiography in vascular imaging and intervention. British Journal of Radiology. 2004;77 Spec No 1:S27-38

195. Degos B, Daelman L, Huberfeld G, Meppiel E, Rabier D, Galanaud D, Magis AS, Lyon-Caen O, Samuel D, Sedel F. Portosystemic shunts: an underdiagnosed but treatable cause of neurological and psychiatric disorders. Journal of the Neurological Sciences. 2012;321(1-2):58-64

196. Hufnagel CA. Permanent intubation of the thoracic aorta. Archives of Surgery. 1947;54(4):382-9

197. Xue L, Greisler H. Prosthetic Graphs. In: Rutherford R, editor. Vascular Surgery. 1. 6th ed. Philadelphia: Elsevier Saunders; 2005. p. 723-40.

198. Landry GJ, Moneta GL, Taylor LM, Jr., Porter JM. Axillobifemoral bypass. Annals of Vascular Surgery. 2000;14(3):296-305

199. Berce M, Sayers RD, Miller JH. Femorofemoral crossover grafts for claudication: a safe and reliable procedure. European Journal of Vascular and Endovascular Surgery. 1996;12(4):437-41

200. Christenson JT, Broome A, Norgren L, Eklof B. The late results after axillo-femoral bypass grafts in patients with leg ischaemia. Journal of Cardiovascular Surgery. 1986;27(2):131-5

201. Sarfeh IJ, Rypins EB, Mason GR. A systematic appraisal of portacaval H-graft diameters. Clinical and hemodynamic perspectives. Annals of Surgery. 1986;204(4):356-63

202. Collins JC, Ong MJ, Rypins EB, Sarfeh IJ. Partial portacaval shunt for variceal hemorrhage: longitudinal analysis of effectiveness. Archives of Surgery. 1998;133(6):590-2; discussion 2-4

203. Kawamata H, Kumazaki T, Kanazawa H, Takahashi S, Tajima H, Hayashi H. Transjugular intrahepatic portosystemic shunt in a patient with cavernomatous portal vein occlusion. Cardiovascular and Interventional Radiology. 2000;23(2):145-9

204. Shi HJ, Cao AH, Chen J, Deng G, Teng GJ. Transjugular intrahepatic portosystemic shunt with an autologous endothelial progenitor cell seeded stent: A porcine model. Academic Radiology. 2010;17(3):358-67

205. Hirasaki KK, Watts JA, Suhocki PV. Wireless surveillance for transjugular intrahepatic portosystemic shunts (TIPS): A feasibility study. Academic Radiology. 2010;17(4):418-20

206. Dupont J, Lumb WV, Nelson AW, Seegmiller JP, Hotchkiss D, Chase HP. Portacaval shunt as treatment for hypercholesterolemia. Metabolic and morphological effects in a swine model. Atherosclerosis. 1985;58(1-3):205-22

207. Chase HP, Morris T. Cholesterol metabolism following portacaval shunt in the pig. Atherosclerosis. 1976;24(1-2):141-8

208. NHMRC. Australian code of practice for the care and use of animals for scientific purposes. 7th ed. Australia: National Health and Medical Research Council; 2004.

209. Rutherford R. Basic Vascular Surgical Techniques. In: Rutherford R, editor. Vascular Surgery. 1. 6th ed. Philadelphia, Pennsylvania: Elsevier Saunders; 2005. p. 661-71.

210. Washizu M, Torisu S, Kondo Y, Shimizu N, Washizu T, Takemura N, Kinoshita G. A simple calculation for obtaining shunt fractions of portosystemic shunts. Journal of Veterinary Medical Science. 2004;66(4):449-51

211. Ross MH, Pawlina W. Disgestive System III: Liver, Gallbladder, and Pancreas. Histology: A Text and Atlas. 5th ed. Baltimore, USA: Lippincott Williams & Wilkins; 2006. p. 576-91.

212. Roberts MS, Magnusson BM, Burczynski FJ, Weiss M. Enterohepatic circulation: Physiological, pharmacokinetic and clinical implications. Clinical Pharmacokinetics. 2002;41(10):751-90

213. Ishikawa T. The ATP-dependent glutathione S-conjugate export pump. Trends in Biochemical Sciences. 1992;17(11):463-8

214. Nakata K, Tanaka Y, Nakano T, Adachi T, Tanaka H, Kaminuma T, Ishikawa T. Nuclear receptor-mediated transcriptional regulation in Phase I, II, and III xenobiotic metabolizing systems. Drug Metabolism and Pharmacokinetics. 2006;21(6):437-57

215. Eloranta JJ, Meier PJ, Kullak-Ublick GA. Coordinate transcriptional regulation of transport and metabolism. Methods in Enzymology2005. p. 511-30.

216. Li P, Wang GJ, Robertson TA, Roberts MS. Liver transporters in hepatic drug disposition: An update. Current Drug Metabolism. 2009;10(5):482-98

217. Lecureur V, Courtois A, Payen L, Verhnet L, Guillouzo A, Fardel O. Expression and regulation of hepatic drug and bile acid transporters. Toxicology. 2000;153(1-3):203-19

218. Jaffe V, Alexander B, Mathie RT. Intrahepatic portal occlusion by microspheres: New model of portal hypertension in the rat. Gut. 1994;35(6):815-8

219. Li X, Benjamin IS, Alexander B. The relationship between intrahepatic portal systemic shunts and microsphere induced portal hypertension in the rat liver. Gut. 1998;42(2):276-82

220. Li X, Benjamin IS, Naftalin R, Alexander B. Location and function of intrahepatic shunts in anaesthetised rats. Gut. 2003;52(9):1339-46

221. Alexander B, Cottam H, Naftalin R. Hepatic arterial perfusion regulates portal venous flow between hepatic sinusoids and intrahepatic shunts in the normal rat liver in vitro. Pflugers Archiv European Journal of Physiology. 2001;443(2):257-64

222. Alexander B, Rogers C, Naftalin R. Hepatic arterial perfusion decreases intrahepatic shunting and maintains glucose uptake in the rat liver. European Journal of Physiology. 2002;444(1-2):291-8

223. Chojkier M, Groszmann RJ. Measurement of portal-systemic shunting in the rat by using gamma-labeled microspheres. The American Journal of Physiology. 1981;240(5)

224. Groszmann RJ, Vorobioff J, Riley E. Splanchnic hemodynamics in portal-hypertensive rats: measurement with gamma-labeled microspheres. The American Journal of Physiology. 1982;242(2)

225. Molino G, Bar F, Battista S, Torchio M, Niro AG, Garello E, Avagnina P, Fava C, Grosso M, Spalluto F. Arterial-venous shunting in liver cirrhosis. Digestive Diseases and Sciences. 1998;43(1):51-5

226. Ott P, Clemmesen O, Keiding S. Interpretation of simultaneous measurements of hepatic extraction fractions of indocyanine green and sorbitol: Evidence of hepatic shunts and capillarization? Digestive Diseases and Sciences. 2000;45(2):359-65

227. Clemmesen JO, Gerbes AL, Gülberg V, Hansen BA, Larsen FS, Skak C, Tygstrup N, Ott P. Hepatic blood flow and splanchnic oxygen consumption in patients with liver failure. Effect of high-volume plasmapheresis. Hepatology. 1999;29(2):347-55

228. AMH. Australian Medicines Handbook. Adelaide, Australia: Australian Medicines Handbook; 2007.

229. Oellerich M, Armstrong VW. The MEGX test: a tool for the real-time assessment of hepatic function. Therapeutic Drug Monitoring. 2001;23(2):81-92

230. Gerlach JC, Brayfield C, Puhl G, Borneman R, Muller C, Schmelzer E, Zeilinger K. Lidocaine/monoethylglycinexylidide test, galactose elimination test, and sorbitol elimination test for metabolic assessment of liver cell bioreactors. Artificial Organs. 2010;34(6):462-72

231. Suzuki S, Ishii Y, Asai S, Kohno T, Mazaki T, Takahashi Y, Iwai S, Ishikawa K. [1-(13)C] breath test of galactose and fructose for quantitative liver function. Journal of Surgical Research. 2001;96(1):90-5

232. Stockmann M, Lock JF, Riecke B, Heyne K, Martus P, Fricke M, Lehmann S, Niehues SM, Schwabe M, Lemke AJ, Neuhaus P. Prediction of postoperative outcome after hepatectomy with a new bedside test for maximal liver function capacity. Annals of Surgery. 2009;250(1):119-25

233. Hung DY, Siebert GA, Chang P, Roberts MS. Hepatic pharmacokinetics of taurocholate in the normal and cholestatic rat liver. British Journal of Pharmacology. 2005;145(1):57-65

234. PSA. Australian Pharmaceutical Formulary and Handbook. 21st ed. Deakin West, ACT: Pharmaceutical Society of Australia; 2009.

235. de Liguori Carino N, O'Reilly DA, Dajani K, Ghaneh P, Poston GJ, Wu AV. Perioperative use of the LiMON method of indocyanine green elimination measurement for the prediction and early detection of post-hepatectomy liver failure. European Journal of Surgical Oncology. 2009;35(9):957-62

236. Roberts MS, Fraser S, Wagner A, McLeod L. Residence time distributions of solutes in the perfused rat liver using a dispersion model of hepatic elimination: 2. Effect of pharmacological agents, retrograde perfusions, and enzyme inhibition on evans blue, sucrose, water, and taurocholate. Journal of Pharmacokinetics and Biopharmaceutics. 1990;18(3):235-58

237. Bass L. Saturation kinetics in hepatic drug removal: A statistical approach to functional heterogeneity. American Journal of Physiology - Gastrointestinal and Liver Physiology. 1983;7(6)

238. Oellerich M, Burdelski M, Ringe B, Lamesch P, Gubernatis G, Bunzendahl H, Pichlmayr R, Herrmann H. Lignocaine metabolite formation as a measure of pre-transplant liver function. Lancet. 1989;1(8639):640-2

239. Conti F, Dousset B, Cherruau B, Guérin C, Soubrane O, Houssin D, Calmus Y. Use of lidocaine metabolism to test liver function during the long-term follow-up of liver transplant recipients. Clinical Transplantation. 2004;18(3):235-41

240. Tanaka E, Inomata S, Yasuhara H. The clinical importance of conventional and quantitative liver function tests in liver transplantation. Journal of Clinical Pharmacy and Therapeutics. 2000;25(6):411-9

241. Sakka SG. Assessing liver function. Current Opinion in Critical Care. 2007;13(2):207-14

242. Adcock LH, Gray CH. The metabolism of sorbitol in the human subject. The Biochemical Journal. 1957;65(3):554-60

243. Barstow L, Small RE. Liver function assessment by drug metabolism. Pharmacotherapy. 1990;10(4):280-8

244. Crocenzi FA, Mottino AD, Roma MG. Regulation of synthesis and trafficking of canalicular transporters and its alteration in acquired hepatocellular cholestasis. Experimental therapeutic strategies for its prevention. Current Medicinal Chemistry. 2004;11(4):501-24

245. Guengerich FP, Krauser JA, Johnson WW. Rate-limiting steps in oxidations catalyzed by rabbit cytochrome P450 1A2. Biochemistry. 2004;43(33):10775-88

246. Crandall ED, Bidani A. Effects of red blood cell HCO3Cl exchange kinetics on lung CO2 transfer: Theory. Journal of Applied Physiology Respiratory Environmental and Exercise Physiology. 1981;50(2):265-71

247. Chijiiwa K, Watanabe M, Nakano K, Noshiro H, Tanaka M. Biliary indocyanine green excretion as a predictor of hepatic adenosine triphosphate levels in patients with obstructive jaundice. American Journal of Surgery. 2000;179(2):161-6

248. Hashimoto M, Watanabe G. Hepatic parenchymal cell volume and the indocyanine green tolerance test. Journal of Surgical Research. 2000;92(2):222-7

249. Faybik P, Hetz H. Plasma Disappearance Rate of Indocyanine Green in Liver Dysfunction. Transplantation Proceedings. 2006;38(3):801-2

250. Mullin EJ, Metcalfe MS, Maddern GJ. How much liver resection is too much? American Journal of Surgery. 2005;190(1):87-97

251. Lau H, Man K, Fan ST, Yu WC, Lo CM, Wong J. Evaluation of preoperative hepatic function in patients with hepatocellular carcinoma undergoing hepatectomy. British Journal of Surgery. 1997;84(9):1255-9

252. Sugimoto H, Okochi O, Hirota M, Kanazumi N, Nomoto S, Inoue S, Takeda S, Nakao A. Early detection of liver failure after hepatectomy by indocyanine green

elimination rate measured by pulse dye-densitometry. Journal of Hepato-Biliary-Pancreatic Surgery. 2006;13(6):543-8

253. Aoki T, Yasuda D, Shimizu Y, Odaira M, Niiya T, Kusano T, Mitamura K, Hayashi K, Murai N, Koizumi T, Kato H, Enami Y, Miwa M, Kusano M. Image-guided liver mapping using fluorescence navigation system with indocyanine green for anatomical hepatic resection. World Journal of Surgery. 2008;32(8):1763-7

254. Okochi O, Kaneko T, Sugimoto H, Inoue S, Takeda S, Nakao A. ICG pulse spectrophotometry for perioperative liver function in hepatectomy. Journal of Surgical Research. 2002;103(1):109-13

255. Skak C, Keiding S. Methodological problems in the use of indocyanine green to estimate hepatic blood flow and ICG clearance in man. Liver. 1987;7(3):155-62

256. Sakka SG, Reinhart K, Meier-Hellmann A. Comparison of invasive and noninvasive measurements of indocyanine green plasma disappearance rate in critically ill patients with mechanical ventilation and stable hemodynamics. Intensive Care Medicine. 2000;26(10):1553-6

257. Iijima T, Aoyagi T, Iwao Y, Masuda J, Fuse M, Kobayashi N, Sankawa H. Cardiac output and circulating blood volume analysis by pulse dye-densitometry. Journal of Clinical Monitoring. 1997;13(2):81-9

258. Hsieh CB, Chen CJ, Chen TW, Yu JC, Shen KL, Chang TM, Liu YC. Accuracy of indocyanine green pulse spectrophotometry clearance test for liver function prediction in transplanted patients. World Journal of Gastroenterology. 2004;10(16):2394-6

259. Imai T, Takahashi K, Goto F, Morishita Y. Measurement of blood concentration of indocyanine green by pulse dye densitometry--comparison with the conventional spectrophotometric method. Journal of Clinical Monitoring and Computing. 1998;14(7-8):477-84

260. Leevy CM, Smith F, Longueville J, Paumgartner G, Howard MM. Indocyanine green clearance as a test for hepatic function. Evaluation by dichromatic ear densitometry. Journal of the American Medical Association. 1967;200(3):236-40

261. Purcell R, Kruger P, Jones M. Indocyanine green elimination: a comparison of the LiMON and serial blood sampling methods. Australia and New Zealand Journal of Surgery. 2006;76(1-2):75-7

262. Nanashima A, Sumida Y, Morino S, Yamaguchi H, Tanaka K, Shibasaki S, Ide N, Sawai T, Yasutake T, Nakagoe T, Nagayasu T. The Japanese integrated staging score using liver damage grade for hepatocellular carcinoma in patients after hepatectomy. European Journal of Surgical Oncology. 2004;30(7):765-70

263. Wakabayashi H, Ishimura K, Izuishi K, Karasawa Y, Maeta H. Evaluation of liver function for hepatic resection for hepatocellular carcinoma in the liver with damaged parenchyma. Journal of Surgical Research. 2004;116(2):248-52

264. Stockmann M, Lock JF, Malinowski M, Niehues SM, Seehofer D, Neuhaus P. The LiMAx test: a new liver function test for predicting postoperative outcome in liver surgery. HPB (Oxford). 2010;12(2):139-46

265. Klein PD. ^{13}C breath tests: visions and realities. Journal of Nutrition. 2001;131(5):1637S-42S

266. Braden B, Lembcke B, Kuker W, Caspary WF. 13C-breath tests: Current state of the art and future directions. Digestive and Liver Disease. 2007;39(9):795-805

267. Cutler AF, Havstad S, Ma CK, Blaser MJ, Perez-Perez GI, Schubert TT. Accuracy of invasive and noninvasive tests to diagnose Helicobacter pylori infection. Gastroenterology. 1995;109(1):136-41

268. Bajtarevic A, Ager C, Pienz M, Klieber M, Schwarz K, Ligor M, Ligor T, Filipiak W, Denz H, Fiegl M, Hilbe W, Weiss W, Lukas P, Jamnig H, Hackl M, Haidenberger A,

Buszewski B, Miekisch W, Schubert J, Amann A. Noninvasive detection of lung cancer by analysis of exhaled breath. Biomed Central Cancer. 2009;9:348

269. Phillips M, Cataneo RN, Cummin AR, Gagliardi AJ, Gleeson K, Greenberg J, Maxfield RA, Rom WN. Detection of lung cancer with volatile markers in the breath. Chest. 2003;123(6):2115-23

270. McCulloch M, Jezierski T, Broffman M, Hubbard A, Turner K, Janecki T. Diagnostic accuracy of canine scent detection in early- and late-stage lung and breast cancers. Integrative Cancer Therapies. 2006;5(1):30-9

271. Uchida M, Yoshida-Iwasawa K. Simultaneous measurement of gastric emptying and gastrocecal transit times in conscious rats using a breath test after ingestion of [1-13C] acetic acid and lactose-[13C] ureide. Journal of Smooth Muscle Research. 2012;48(4):105-14

272. Miura Y, Washizawa N, Urita Y, Imai T, Kaneko H. Evaluation of remnant liver function using 13C-breath tests in a rat model of 70% partial hepatectomy. Hepato-Gastroenterology. 2012;59(114):311-6

273. Stockmann M, Lock JF, Malinowski M, Seehofer D, Puhl G, Pratschke J, Neuhaus P. How to define initial poor graft function after liver transplantation? - a new functional definition by the LiMAx test. Transplant International. 2010;23(10):1023-32

274. Rubin T, von Haimberger T, Helmke A, Heyne K. Quantitative determination of metabolization dynamics by a real-time 13CO2 breath test. J Breath Res. 2011;5(2):027102

275. Sobanko JF, Miller CJ, Alster TS. Topical anesthetics for dermatologic procedures: a review. Dermatologic Surgery. 2012;38(5):709-21

276. Bruchim Y, Itay S, Shira BH, Kelmer E, Sigal Y, Itamar A, Gilad S. Evaluation of lidocaine treatment on frequency of cardiac arrhythmias, acute kidney injury, and

hospitalization time in dogs with gastric dilatation volvulus. Journal of Veterinary Emergency and Critical Care (San Antonio). 2012;22(4):419-27

277. Teo G, Suzuki Y, Uratsu SL, Lampinen B, Ormonde N, Hu WK, DeJong TM, Dandekar AM. Silencing leaf sorbitol synthesis alters long-distance partitioning and apple fruit quality. Proceedings of the National Academy of Sciences of the United States of America. 2006;103(49):18842-7

278. Kwang-Hyok S, Ui-Nam P, Sarkar C, Bhadra R. A sensitive assay of red blood cell sorbitol level by high performance liquid chromatography: potential for diagnostic evaluation of diabetes. Clinica Chimica Acta. 2005;354(1-2):41-7

279. Zhang S, Mada SR, Torch M, Goyal RK, Venkataramanan R. Development and validation of a high-performance liquid chromatographic assay for the determination of fluconazole in human whole blood using solid phase extraction. Therapeutic Drug Monitoring. 2008;30(3):314-9

280. Soons PA, Kroon JM, Breimer DD. Effects of single-dose and short-term oral nifedipine on indocyanine green clearance as assessed by spectrophotometry and high performance liquid chromatography. Journal of Clinical Pharmacology. 1990;30(8):693-8

281. Chen Y, Potter JM, Ravenscroft PJ. A quick, sensitive high-performance liquid chromatography assay for monoethylglycinexylidide and lignocaine in serum/plasma using solid-phase extraction. Therapeutic Drug Monitoring. 1992;14(4):317-21

282. Abraham I, Fawcett JP, Kennedy J, Kumar A, Ledger R. Simultaneous analysis of lignocaine and bupivacaine enantiomers in plasma by high-performance liquid chromatography. J Chromatogr B Biomed Sci Appl. 1997;703(1-2):203-8

283. Wisnicki JL, Tong WP, Ludlum DB. Analysis of lidocaine and its dealkylated metabolites by high-pressure liquid chromatography. Clinica Chimica Acta. 1979;93(2):279-82

284. Richmond ML, Brandao SC, Gray JI, Markakis P, Stine CM. Analysis of simple sugars and sorbitol in fruit by high-performance liquid chromatography. Journal of Agricultural and Food Chemistry. 1981;29(1):4-7

285. Doyle DJ, Byrick R, Filipovic D, Cashin F. Silica zeolite scavenging of exhaled isoflurane: a preliminary report. Canadian Journal of Anaesthesia. 2002;49(8):799-804

286. Shabir GA. Validation of high-performance liquid chromatography methods for pharmaceutical analysis. Understanding the differences and similarities between validation requirements of the US Food and Drug Administration, the US Pharmacopeia and the International Conference on Harmonization. Journal of Chromatography A. 2003;987(1-2):57-66

287. Baker KJ. Binding of sulfobromophthalein (BSP) sodium and indocyanine green (ICG) by plasma alpha-1 lipoproteins. Proceedings of the Society for Experimental Biology and Medicine. 1966;122(4):957-63

288. Huet PM, Goresky CA, Villeneuve JP, Marleau D, Lough JO. Assessment of liver microcirculation in human cirrhosis. Journal of Clinical Investigation. 1982;70(6):1234-44

289. Villeneuve JP, Huet PM, Gariepy L, Fenyves D, Willems B, Cote J, Lapointe R, Marleau D. Isolated perfused cirrhotic human liver obtained from liver transplant patients: a feasibility study. Hepatology. 1990;12(2):257-63

290. Varin F, Huet PM. Hepatic microcirculation in the perfused cirrhotic rat liver. Journal of Clinical Investigation. 1985;76(5):1904-12

291. Albrecht T, Blomley MJ, Cosgrove DO, Taylor-Robinson SD, Jayaram V, Eckersley R, Urbank A, Butler-Barnes J, Patel N. Transit-time studies with levovist in patients with and without hepatic cirrhosis: a promising new diagnostic tool. European Radiology. 1999;9 Suppl 3:S377-81

292. Kowalczyk P, Holyst R. Efficient adsorption of super greenhouse gas (tetrafluoromethane) in carbon nanotubes. Environ Sci Technol. 2008;42(8):2931-6

293. Gaviria E, Restrepo J, Marin J, Arango G, Aramburo D, Franco F, Tintinago L. Evaluation of propofol as an anesthetic in swine tracheal transplant surgery. Revista Colombiana de Ciencias Pecuarias. 2007;20:447-54

294. Hedenqvist P, Edner A, Fahlman A, Jensen-Waern M. Continuous intravenous anaesthesia with sufentanil and midazolam in medetomidine premedicated New Zealand white rabbits. Biomed Central Veterinary Research. 2013;9:21

295. Mistraletti G, Mantovani ES, Cadringher P, Cerri B, Corbella D, Umbrello M, Anania S, Andrighi E, Barello S, Di Carlo A, Martinetti F, Formenti P, Spanu P, Iapichino G. Enteral vs. intravenous ICU sedation management: study protocol for a randomized controlled trial. Trials. 2013;14(1):92

296. Adams HA, Pawlik D, Bauer H, Mautgreve W. Stability of local anesthetics in heparinized blood, plasma and sulfuric acid. Acta Anaesthesiologica Scandinavica. 1998;42(7):783-5

297. Schroter J, Wandel C, Bohrer H, Schmidt H, Bottiger BW, Martin E. Lignocaine metabolite formation: an indicator for liver dysfunction and predictor of survival in surgical intensive care patients. Anaesthesia. 1995;50(10):850-4

298. Maynard ND, Bihari DJ, Dalton RN, Beale R, Smithies MN, Mason RC. Liver function and splanchnic ischemia in critically ill patients. Chest. 1997;111(1):180-7

299. Addario L, Scaglione G, Tritto G, Di Costanzo GG, De Luca M, Lampasi F, Galeota Lanza A, Picciotto FP, Tartaglione MT, Utech W, Macr M, Giannelli E, Ascione A.

Prognostic value of quantitative liver function tests in viral cirrhosis: a prospective study. European Journal of Gastroenterology and Hepatology. 2006;18(7):713-20

300. Syrota A, Vinot JM, Paraf A, Roucayrol JC. Scintillation splenoportography: hemodynamic and morphological study of the portal circulation. Gastroenterology. 1976;71(4):652-9

301. Weiss M, Krejcie TC, Avram MJ. Transit time dispersion in pulmonary and systemic circulation: effects of cardiac output and solute diffusivity. Am J Physiol Heart Circ Physiol. 2006;291(2):H861-70

302. Weiss M, Krejcie TC, Avram MJ. A physiologically based model of hepatic ICG clearance: interplay between sinusoidal uptake and biliary excretion. European Journal of Pharmaceutical Sciences. 2011;44(3):359-65

303. Weiss M. On the degree of solute mixing in liver models of drug elimination. Journal of Pharmacokinetics and Biopharmaceutics. 1997;25(3):363-75

304. Homer LD, Small A. A unified theory for estimation of cardiac output, volumes of distribution and renal clearance from indicator dilution curves. Journal of Theoretical Biology. 1977;64(3):535-50

305. Millard RK. Indicator-dilution dispersion models and cardiac output computing methods. American Journal of Physiology. 1997;272(4 Pt 2):H2004-12

306. Weiss M. A note on the role of generalized inverse Gaussian distributions of circulatory transit times in pharmacokinetics. Journal of Mathematical Biology. 1984;20(1):95-102

307. Weiss M, Hubner GH, Hubner IG, Teichmann W. Effects of cardiac output on disposition kinetics of sorbitol: recirculatory modelling. British Journal of Clinical Pharmacology. 1996;41(4):261-8

308. Blomley MJ, Albrecht T, Cosgrove DO, Jayaram V, Eckersley RJ, Patel N, Taylor-Robinson S, Bauer A, Schlief R. Liver vascular transit time analyzed with dynamic

hepatic venography with bolus injections of an US contrast agent: early experience in seven patients with metastases. Radiology. 1998;209(3):862-6

309. Chen CY, Fancher RM, Ruan Q, Marathe P, Rodrigues AD, Yang Z. A liquid chromatography tandem mass spectrometry method for the quantification of indocyanine green in dog plasma and bile. Journal of Pharmaceutical and Biomedical Analysis. 2008;47(2):351-9

310. Sun Y, Kruse DE, Dayton PA, Ferrara KW. High-frequency dynamics of ultrasound contrast agents. IEEE Trans Ultrason Ferroelectr Freq Control. 2005;52(11):1981-91

311. Zhang Q, Zhang S, Chen S, Li P, Qin T, Yuan S. Preparation and characterization of a strong basic anion exchanger by radiation-induced grafting of styrene onto poly(tetrafluoroethylene) fiber. Journal of Colloid and Interface Science. 2008;322(2):421-8

312. Terry R, van Wettere WH, Whittaker AL, Herde PJ, Howarth GS. Using the noninvasive (13)C-sucrose breath test to measure intestinal sucrase activity in swine. Comparative Medicine. 2012;62(6):504-7

313. Bauchart-Thevret C, Stoll B, Benight NM, Olutoye O, Lazar D, Burrin DG. Supplementing monosodium glutamate to partial enteral nutrition slows gastric emptying in preterm pigs. Journal of Nutrition. 2013;143(5):563-70

314. Danicke S, Diers S. Effects of ergot alkaloids in feed on performance and liver function of piglets as evaluated by the (1)(3)C-methacetin breath test. Archives of Animal Nutrition. 2013;67(1):15-36

315. Sirignano C, Neubert RE, Meijer HA. N_2O influence on isotopic measurements of atmospheric CO_2. Rapid Communications in Mass Spectrometry. 2004;18(16):1839-46

316. Assonov SS, Brenninkmeijer CA. On the N_2O correction used for mass spectrometric analysis of atmospheric CO_2. Rapid Communications in Mass Spectrometry. 2006;20(11):1809-19

317. Vogt JA, Radermacher P, Georgieff M. $^{13}CO_2$ breath tests, a tool to assess intestinal and liver function in the ICU? Current Opinion in Critical Care. 2010;16(2):169-75

318. Barsky MF, Rankin RN, Wall WJ, Ghent CN, Garcia B. Patent ductus venosus: Problems in assessment and management. Canadian Journal of Surgery. 1989;32(4):271-5

319. Mulla M, Deb R, Singh R. MRI in T staging of rectal cancer: How effective is it? Indian Journal of Radiology Imaging. 2010;20(2):118-21

320. UICC IUAC. TNM Classification of Malignant Tumors. Hoboken, NJ: Wiley-Blackwell; 2009.

321. Labianca R, Nordlinger B, Beretta GD, Mosconi S, Mandala M, Cervantes A, Arnold D, Group EGW. Early colon cancer: ESMO clinical practice guidelines for diagnosis, treatment and follow-up. Annals of Oncology. 2013;24 Suppl 6:vi64-vi72

322. Dotan E, Cohen SJ. Challenges in the management of stage II colon cancer. Seminars in Oncology. 2011;38(4):511-20

CHAPTER 8

Appendices

Appendix A – List of Drugs Searched as a PSS Marker (n= 110)

A.1: Drugs with half-life >2hrs. n=72

Acyclovir	Diazepam	Nicardipine	Sumatriptan
Aldosterone	Digoxin	Nicotine	Tacrine
Allopurinol	Diltiazem	Nifedipine	Tacrolimus
Alprenolol	Disopyramide	Nimodipine	Terbutaline
Aminodarone	Ethinyl estradiol	Nortriptyline	Terfenadine
Amiodarone	Felodipine	Paracetamol	Theophylline
Amitriptyline	Fentanyl	Penicillin	Thiopental
Atorvastatin	Fluvastatin	Phenytoin	Tolbutamide
Bromocriptine	Gentamicin	Pitavastatin	Triazolam
Buprenorphine	Ibuprofen	Pravastatin	Venlafaxine
Buspirone	Imipramine	Proafenone	Verapamil
Carbamazepine	Isoproterenol	Procainamide	Warfarin
Cerivastatin	Labetalol	Propanolol	
Chloropromazine	Nefazodone	Spironolactone	
Chloroquine	Losartan	Quinacrine	

Choline	Lovastatin	Quinidine
Clomethiazole	Metformin	Ranitidine
Codeine	Metoprolol	Rosuvastatin
Cyclosporine	Midazolam	Saquinavir
Desipramine	Morphine	Simvastatin

A.2: Drugs with low hepatic extraction fraction. n= 8

Aminopyrine	Oxaliplatin
Cephalexin	Para-aminobenzoic acid
Cimetidine	Pentoxifylline
Indocyanine green	Tetra-ethylammonium

A.3: Drugs excluded due to similar hepatic uptake pathway or naturally found in plasma. (n= 8)

^{15}N-noradrenaline	Glyceryl trinitrate
Adrenaline	Hyaluronate
Ergotamine	Phenacetin
Galactose	
Technetium-99m-diethylenetriamine-pentaacetic acid-galactosyl-human serum albumin	

A.4: Drugs excluded due to possible reaction with other common medications (n=16)

6-Mercaptopurine	Glycine	P
Amoxycillin	Heparin	Paracetamol
Aspirin	Mevastatin	Propofol
Captopril	Naloxone	Salicylamide
Diclofenac	Oleate	
Erythromycin	Omeprazole	

Appendix B – Coding to Create the Pharmacokinetic Model for the ADAPT 5

FORTRAN for ADAPT5

```
      PSym(1) = 'MT1'
      PSym(2) = 'RD1^2'
      PSym(3) = 'MT2'
      PSym(4) = 'RD2^2'
      PSym(5) = 'q'
      PSym(6) = 'A'
      PSym(7) = 'del'
Enter Output Equations Below   [e.g.  Y(1) = X(1)/P(2) ]        C
C----c------------------------------------------------------------------C
       Integer DelayPar
      Real*8  MAT, CVA2, F,MT, CV2,q
      MAT=P(1)
      CVA2=P(2)
      F=P(6)
      MT=P(3)
      CV2=P(4)
q=P(5)
      if(t .eq. 0.0) then
       Y(1) = 0.0
      else
      DelayPar = 7   ! Specify the parameter number for the delay
       Call SHIFT(P(DelayPar),T)
Y(1) = F*(q*dsqrt((MAT/q)/(2*3.14159*CVA2*t**3))*
dexp(-(t-MAT/q)**2/(2.0D0*CVA2*(MAT/q)*t))
    +(1-q)*dsqrt((MT/(1-q))/(2*3.14159*CV2*t**3))*
dexp(-(t-MT/(1-q))**2/(2.0D0*CV2*(MT/(1-q))*t)))
       endif
```

Appendix C – Surgical Research Society 48th Annual Scientific Meeting 2011 Abstract and Presentation

A Possible New Method for Detecting and Measuring Portosystemic Shunts

Matthews T.[1], Trochsler M.[1], Li P[2], Robertson T.[2], Roberts M.[2], Maddern G.[1]

Introduction:
Portosystemic shunts (PSS) are vessels that allow blood to bypass the liver without being filtered. Congenital and naturally acquired PSS are rare, but have been incidentally found in several cases. It is postulated that these shunts may allow metastases to bypass the liver, causing secondary peripheral tumours. There is no current clinical test to detect and measure PSS.

Methods:
A proposed method is to intravenously inject a range of compounds with a short half life (<2hours) and a high first pass clearance into the portal venous system, and measure the blood concentration once these drugs have passed through the liver. Theoretically, a normal functioning liver will only allow a minute concentration (drug dependent) of the drug to pass though.

Another approach may be by using the LiMON® system (PULSION®, Germany), which measures indocyanine green plasma disappearance rate (ICG-PDR). Normally, ICG-PDR will peak once a 15 minute interval, however, if a shunt is present, ICG will peak early and again later. The early peak may indicate a PSS, while the secondary peak is the ICG that has passed through the liver.

The third plausible method is ^{13}C-methacetin liver function breath test. ^{13}C- metabolises into paracetamol and $^{13}CO_2$, which is measured in the breath. In a normal liver, ^{13}C-methacetin will decay steadily over 1 hour, if a shunt is present, the decay rate may be significantly slower.

Conclusions:
This pilot study aims to develop a technique that can determine and measure the presence of a PSS.

Institution & Contact Details:
1. Discipline of Surgery (TQEH), University of Adelaide.
2. School of Pharmacy and Medical Sciences, Basil Hetzel Institute, University of South Australia.

Ph: 82227045
todd.matthews@adelaide.edu.au

A New Method for Detecting and Measuring Portosystemic Shunts

Matthews T*, Trochsler M*, Li P^, Robertson T^, Roberts M^, Hamilton M*, Maddern G*.
Discipline of Surgery, The Queen Elizabeth Hospital, University of Adelaide. ^School of Pharmacy and Medical Sciences, Basil Hetzel Institute, University of South Australia.

ABSTRACT

Portosystemic shunts (PSS) are vessels that allow blood to bypass the liver without being filtered. Although congenital and naturally acquired PSS are rare in non-cirrhotic patients, they have been incidentally seen in several cases. It is postulated that these shunts may allow metastases to bypass the liver, causing secondary peripheral tumours. There is no current clinical test to detect and measure PSS. A proposed method is to intravenously inject a range of compounds with a short half life (<2hours) and a high first pass clearance into the portal venous system, and measure the blood concentration once these drugs have passed through the liver. Theoretically, a normal functioning liver will only allow a minute concentration (drug dependent) of the drug to pass though. Another approach may be by using the LiMON® system (PULSION®, Germany), which measures indocyanine green plasma disappearance rate (ICG-PDR). Normally, ICG-PDR will peak once over a 15 minute interval, however, if a shunt is present, ICG will peak early and again later. The early peak may indicate a PSS, while the secondary peak is the ICG that has passed through the liver. The third plausible method is a ^{13}C-methacetin liver function breath test. ^{13}C-methacetin metabolises into paracetamol and $^{13}CO_2$, the latter of which is measured in the breath. In a normal liver, ^{13}C-methacetin decays steadily over 1 hour. If the decay rate was significantly slower, it could indicate that a PSS is present. This pilot study aims to develop a technique that can determine and measure the presence of a PSS.

BACKGROUND

Portosystemic shunts (PSS) are natural shunts that redirects blood around the liver without being filtered. These shunts have been catagorised into extrahepatic, Abernethy Types I and II, and intrahepatic, types I to IV [1] Although PSS are rare in non-cirrhotic liver patients, they have been seen in a small number of cases, initially by Bellah et al. [2] and Mori et al. [3]. There is still an unknown question as to how a patient with cancer i.e. colorectal cancer, may develop sole metastases outside of the liver e.g. in the lung. Theoretically, these metastases should be trapped by the liver. However, if a patient has a PSS, it may allow these metastases to directly bypass the liver. Currently, there is no literature, which directly correlates metastases found in lungs, brain or extremities to PSS, nor any for directly measuring PSS using pharmacological agents.

Types of Portosystemic Shunts:

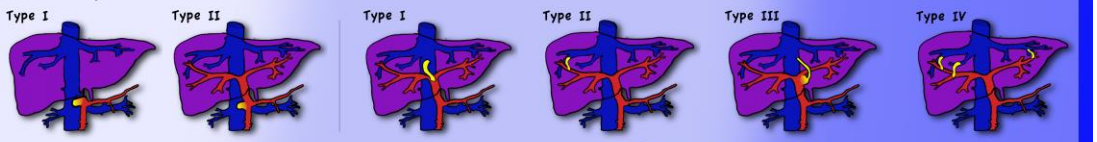

Extrahepatic: Abernethy Type I & II

Abernethy Type I: All blood from the portal vein is diverted into the inferior vena cava. The intrahepatic portal vein is absent.
Abernethy Type II: A portion of the blood from the portal vein is diverted into the inferior vena cava.

Intrahepatic: Park Types I-IV

Park Type I: A single, constant diameter shunt from intrahepatic portal vein to inferior vena cava.
Park Type I: A single or multiple shunts found between portal system and hepatic veins in one segment.
Park Type III: A shunt has formed through a portal vein aneurysm.
Park Type IV: Multiple shunts in both lobes between peripheral portal and hepatic veins.

AIMS

1: To develop a technique that can determine if there are portosystemic shunts in healthy or diseased livers.
2: To develop a technique that can measure the volume of blood that bypasses the liver through a portosystemic shunt.

METHODS

A pilot study will first be trialled on 8 female pigs. A pigs liver is functionally similar to a human liver.

A 4 french catheter will be inserted into the inferior vena cava and guided up to the confluence with the hepatic veins. Highly extracted compounds with a short half-life (table 1) will be injected into the portal vein. Each of these drugs also has a different uptake transporter to avoid saturation of a single uptake pathway. Samples will be taken constantly over a 30 minute period*. At the same time, the indocyanine green plasma disappearance rate is measured via a non-invasive spectrometer and breath samples will be collected every 2 minutes to measure for $^{13}CO_2$.

*sample times are subject to change depending on the pharmacokinetics of each compound.

Blood Collection Catheter:
Small blood samples will be taken every second for 30 seconds then every minute for 10 minutes followed by every 2 minutes untill 30 minutes has elapsed*.

LiMON® System

The LiMON® measures the indocyanine green plasma dissapearance rate via a non-invasive spectrometer.

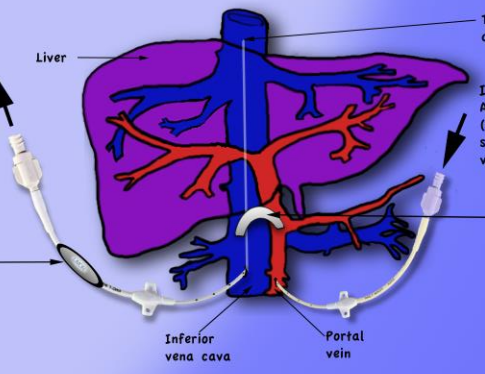

University of South Australia

SIGNIFICANCE

This study may aid in better understand of portosystemic shunts and may also provide reasoning for metastases distribution. No other studies use the same methodology, which if found successful may be able to be used in a clincial setting for diagnostics.

Table 1

Drug name	Uptake Transporter	Half Life	Extraction
Lignocaine	Passive	1.5hrs	99%
Sorbitol	GLUT4	~30mins	96%
Ethanol	Passive	-	*15mL/100mL/hr
Fructose	GLUT2/5	20mins	99%
13C-Methacetin	Passive	1hr	99%
3H-Taurocholate	NTCP, OATP, OAT2, OST	~30mins	90%
Indocyanine Green	OAT7	3mins	66%

*clearance rate

REFERENCES

[1] Konstas AA, Digumarthy SR, Avery LL, Wallace KL, Lisovsky M, Misdraji J, Hahn PF. Congenital portosystemic shunts: Imaging findings and clinical presentations in 11 patients. European Journal of Radiology. 2010.
[2] Bellah RD, Hayek J, Littlewood Teele R. Anomalous portal venous connection to the suprahepatic vena cava: Sonographic demonstration. Pediatric Radiology. 1989;20: 115-7.
[3] Mori H, Hayashi K, Fukuda T, Matsunaga N, Futagawa S, Nagasaki M, Matsukura M. Intrahepatic portosystemic venous shunt: Occurrence in patients with and without liver cirrhosis. American Journal of Roentgenology. 1987;149: 711-9.

THE UNIVERSITY of ADELAIDE

Appendix D – Surgical Research Society 48th Annual Scientific Meeting 2011 Abstract

A Possible New Method for Detecting and Measuring Portosystemic Shunts

Matthews T.[1], Trochsler M.[1], Li P[2], Robertson T.[2], Roberts M.[2], Maddern G.[1]

Introduction:
Portosystemic shunts (PSS) are vessels that allow blood to bypass the liver without being filtered. Congenital and naturally acquired PSS are rare, but have been incidentally found in several cases. It is postulated that these shunts may allow metastases to bypass the liver, causing secondary peripheral tumours. There is no current clinical test to detect and measure PSS.

Methods:
A proposed method is to intravenously inject a range of compounds with a short half life (<2hours) and a high first pass clearance into the portal venous system, and measure the blood concentration once these drugs have passed through the liver. Theoretically, a normal functioning liver will only allow a minute concentration (drug dependent) of the drug to pass though.

Another approach may be by using the LiMON® system (PULSION®, Germany), which measures indocyanine green plasma disappearance rate (ICG-PDR). Normally, ICG-PDR will peak once a 15 minute interval, however, if a shunt is present, ICG will peak early and again later. The early peak may indicate a PSS, while the secondary peak is the ICG that has passed through the liver.

The third plausible method is ^{13}C-methacetin liver function breath test. ^{13}C- metabolises into paracetamol and $^{13}CO_2$, which is measured in the breath. In a normal liver, ^{13}C-methacetin will decay steadily over 1 hour, if a shunt is present, the decay rate may be significantly slower.

Conclusions:
This pilot study aims to develop a technique that can determine and measure the presence of a PSS.

Institution & Contact Details:
1. Discipline of Surgery (TQEH), University of Adelaide.
2. School of Pharmacy and Medical Sciences, Basil Hetzel Institute, University of South Australia.

Ph: 82227045
todd.matthews@adelaide.edu.au

Appendix E – The Queen Elizabeth Hospital Research Day 2011 Abstract and Presentation

Abstract 19

Title:
CLINICAL ANALYSIS OF LIVER FUNCTION: CAN PORTOSYSTEMIC SHUNTS BE MEASURED?

Authors:
Matthews T*, Li P^, Hamilton M*, Trochsler M*, Roberts M^, Maddern G*.

Departments(s):
*Discipline of Surgery, School of Medicine, The University of Adelaide and Basil Hetzel Institute for Medical Research, The Queen Elizabeth Hospital.
^Therapeutics Research Centre, School of Pharmacy and Medical Sciences, Division of Health Sciences, University of South Australia and Basil Hetzel Institute for Medical Research.

Abstract
Portosystemic shunts (PSS) are vessels that allow blood to bypass the liver without being filtered. Although commonly seen in cirrhotic livers, congenital and naturally acquired PSS are rare, but have been found incidentally in several cases. PSS can complicate patient treatment by not allowing medication to metabolise at it's normal rate. This would explain why certain drugs are more effective in some patients, while being less effective in others. It is also thought that PSS have the potential to further spread cancer cells beyond the liver.

As there are currently no clinical tests to detect and quantify PSS, this study aims to develop a new technique which can measure and quantify PSS. A proposed technique is to inject a range of compounds, including Indocyanine green dye, 13C-methacetin, 3H-taurocholate, Evans Blue dye, sorbitol and fructose, directly into the portal venous system using a pig model. These compounds have a short half life of less than 2 hours and a high first pass clearance (except for indocyanine green). After the compounds are administered, the concentration of each compound is measured once they have passed through the liver.

To test this technique, an artificial PSS has been created in a pig with selected compounds injected into the portal vein. Pilot study results have indicated that , Evans Blue dye, indocyanine green dye, 13C-methacetin, and 13C-methacetin's metabolite, 13CO2, can demonstrate a PSS. Further study is required to validate if the other compounds, including 3H-taurocholate and sorbitol, are a useful PSS indicator.

Lay Description
Portosystemic shunts are abnormal vessels that allow blood to bypass the liver prior to being filtered. These shunts may allow small cancer cells to bypass the liver, becoming lodged in the lungs. Portosystemic shunts may also explain why certain drugs are more effective in some patients, while being less effective in others.
This study looks at developing a technique to find these abnormal liver shunts. A proposed method is to inject inoccuous drugs, which are quickly metabolised by the liver and to measure the rate at which the drug is metabolised. If the drug is slowly metabolised, it could indicate the presence of a shunt.

CLINICAL ANALYSIS OF LIVER FUNCTION: Can Portosystemic Shunts be Measured?

Matthews T*, Li P^, Hamilton M*, Trochsler M*, Roberts M^, Maddern G*

*Discipline of Surgery, School of Medicine, The University of Adelaide and Basil Hetzel Institute for Medical Research, The Queen Elizabeth Hospital
^Therapeutics Research Centre, School of Pharmacy and Medical Sciences, Division of Health Sciences, University of South Australia and Basil Hetzel Institute for Medical Research.

INTRODUCTION

Portosystemic shunts (PSS) are vessels that allow blood to bypass the liver without being filtered. Although commonly seen in cirrhotic livers, congenital and naturally acquired PSS are rare, but have been incidentally observed in healthy subjects (>256 case reports). Terayama *et al.*[1] found that 42 of 46 patients, without liver cirrhosis, had a form of a PSS.

PSS can complicate patient treatment by not allowing medication to metabolise at it's normal rate. The presence of a PSS in patients may therefore explain why some liver-metabolised drugs are more effective in some patients, while be less effective in others. A PSS can also change the pharmacokinetics of a particular drug, modifying the response to treatment in patients. Also, it can be speculated that PSS may be a reason for the distribution of secondary metastatic cancer cells beyond the liver. One study[2] diagnosed 2 patients, with pancreatic neuroendocrine tumours, to have secondary metastases in the lung a few months after they underwent a transjugular intrahepatic portosystemic shunt procedure. Typically, with this type of cancer, circulating metastases would be trapped in the liver.

Currently there are no validated clinical tests to detect or measure PSS. Hence, most PSS have only been found incidentally by radiological methods (Figure 1). Radiological methods such as x-ray, CT, MRI and ultrasound can be invasive, difficult to quantify them or may not detect small or microscopic PSS.

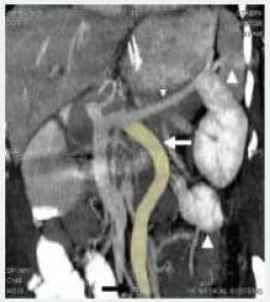

Figure 1: CT image of a large, naturally acquired, extrahepatic portosystemic shunt (large white arrow) connecting the splenic vein (thin white arrow) to the iliac vein. (Konstas *et al.*[3]).

AIMS

1: To develop a technique that can determine and measure portosystemic shunts in healthy or diseased livers.

2: To quantify portosystemic shunts by injecting highly extracted compounds into the portal system and measuring the rate of decay of each compound with and without the presence of a shunt.

METHODS

STAGE 1: The first stage is to re-create a vascular malformation in a pig. The simplest method is to create an anastomosis between the portal vein and the inferior vena cava using either polytetrafluoroethylene (PTFE, Figure 2) or iliac vein (Figure 3). This anastomosis mimics an extrahepatic Abernethy Type II PSS. Blood flow direction is then determined either by doppler sonography or by measuring venous pressure differences as fluid will always move from high pressure to low pressure. However, due to properties of PTFE, it is difficult to use doppler sonography. Therefore measuring the difference in pressure between portal vein and inferior vena cava is a better option.

STAGE 1: PORTOSYSTEMIC SHUNT CREATION

Figure 2: Shunt made from polytetrafluoroethylene (PTFE) connecting the portal vein to the inferior vena cava.

Figure 3: Shunt made from scavenged iliac vein connecting the portal vein to the inferior vena cava.

STAGE 2: TECHNIQUE DEVELOPMENT

STAGE 2: The second stage is to develop the appropriate test to measure PSS. A catheter is inserted into the inferior vena cava and guided up to the confluence with the hepatic veins for blood collection. A bolus of compounds (Table 1) that have a high extraction ratio and short half life are then injected into the portal venous system. Blood samples are collected over a 40 minute period. At the same time, breath samples are taken over a 60 minute period to measure for $^{13}CO_2$, a metabolite of ^{13}C-methacetin; and a LiMON® machine (PULSION®, Germany) will non-invasively measure indocyanine green via a spectrometer. This is then repeated with the shunt clamped.

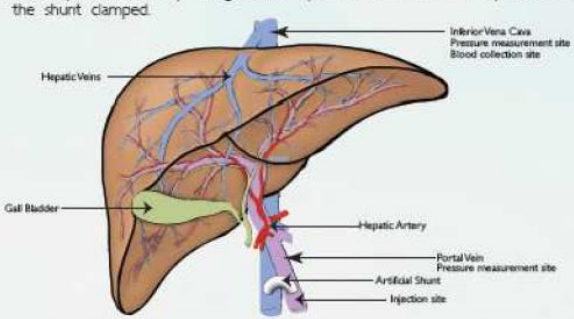

Figure 4: Schematic of a liver with an anatomosis attached between the portal vein and inferior vena cava.

Drug name	Uptake Transporter	Half Life	Extraction
Lignocaine	Passive	1.5hrs	99%
Sorbitol	GLUT4	~30mins	96%
Ethanol	Passive	-	*15mL/100mL/hr
Fructose	GLUT2/5	20mins	99%
13C-Methacetin	Passive	1hr	99%
3H-Taurocholate	NTCP, OATP, OAT2, OST	~30mins	90%
Indocyanine Green	OAT7	3mins	66%

*clearance rate

Table 1: List of compounds with a short half life (<2hrs) and a fast first pass hepatic uptake, with the exception of indocyanine green as it will be measured via the LiMON® system.

RESULTS

These pilot results (n=1) demonstrate differences between the presence of open PSS and the control situation in which the shunt has been clamped. The Indocyanine Green and methacetin blood results show a 31% and 23% larger area with the shunt, respectively (Fig. 5a & 5b). The breath test found a 9% decreased area with the shunt (Figure 5c).

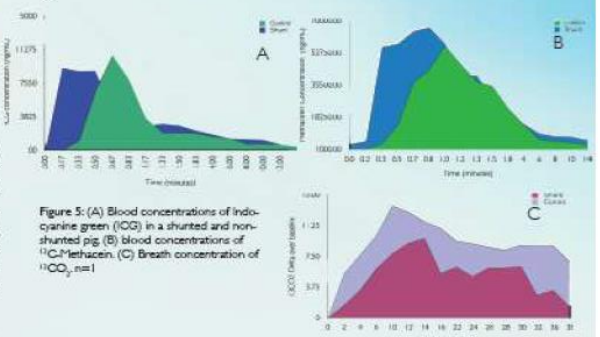

Figure 5: (A) Blood concentrations of Indocyanine green (ICG) in a shunted and non-shunted pig. (B) blood concentrations of ^{13}C-Methacetin. (C) Breath concentration of $^{13}CO_2$. n=1

DISCUSSION

We found that five of the seven compounds (Table 1) injected may be an effective marker for the determination and quantification of PSS. Fructose and ethanol were not used due to the poor sensitivity of their respective assays. ^{3}H-taurocholate is a possibility, however, due to it's high cost, it will not be used in this research. The pilot results show that Indocyanine green, ^{13}C-methacetin and its' metabolite $^{13}CO_2$ have clearly demonstrated a difference between shunted and control.

We also observed that the iliac vein or aortic artery is a preferable material to create a PSS. The shunt flow rate cannot be determined using a high sensitive probe in a PTFE shunt and is susceptible to occlusion. An alternative method is to measure the pressure differences between the portal vein and inferior vena cava. This will demonstrate flow direction as fluid will always move from high to low pressure.

Further experiments are ongoing to validate the use of the injected drugs (Table 1) and their metabolites in a clinical test demonstrating the presence and size of PSS.

REFERENCES

[1]Terayama, N., O. Matsui, et al. (2008). "Portosystemic shunt on CT during arterial portography: Prevalence in patients with and without liver cirrhosis." Abdominal Imaging 33(1): 80-86.
[2]Wallace, M. J., D. C. Madoff, et al. (2004). "Transjugular intrahepatic portosystemic shunts: Experience in the oncology setting." Cancer 101(2): 337-345.
[3]Konstas, A. A., S. R. Digumarthy, et al. (2010). "Congenital portosystemic shunts: Imaging findings and clinical presentations in 11 patients." European Journal of Radiology.

Appendix F – The Queen Elizabeth Hospital Research Day 2012 Abstract and Presentation

Abstract 22

Title:

A NOVEL NON-INVASIVE TECHNIQUE FOR THE DETECTION OF PORTOSYSTEMIC SHUNTS

Authors:

Matthews T*, Li P^, Hamilton M*, Trochsler M*, Wiess M^, Butler R#, Roberts M^, Maddern G*.

Departments(s):

*Discipline of Surgery, School of Medicine, The University of Adelaide and Basil Hetzel Institute for Medical Research, The Queen Elizabeth Hospital.

^Therapeutics Research Centre, School of Pharmacy and Medical Sciences, Division of Health Sciences, University of South Australia and Basil Hetzel Institute for Medical Research.

#Cancer Research, School of Pharmacy and Medical Sciences, Division of Health Sciences, University of South Australia and Basil Hetzel Institute for Medical Research.

Abstract

A portossystemic shunt (PSS) is defined as a congenital or acquired abnormal blood vessel that redirects blood around the liver without being filtered through hepatic parenchyme. The epidemiology of PSS are still unknown as there is yet to be a standardised clincial test for PSS detection. PSS are thought to be the reason behind the distribution of secondary metastases beyond the liver in 10-15% of all colorectal cancer patients without cirrhosis of the liver The aim of this study was to develop a cost effective, non-invasive technique that can detect and measure portosystemic shunts in a healthy liver.

An artificial PSS was created between the portal vein and the inferior vena in a pig model with a catheter inserted in the confluence of the hepatic veins for sample collection. A LiMON® spectrometer was attached to the pigs snout to detect indocyanine green dye via the LiMON® machine. Indocyanine green was injected into the portal vein with blood samples and LiMON® readings being collected simultaneously. The process was repeated with the PSS clamped as the control.

Results showed lag time and the time of the first peak were both significantly shorter in the shunted model. The data was modelled further to create a formula that estimates the percentage of blood bypassing the liver. This pilot study has developed a novel technique for the detection and quatification of PSS, and if implimented in a clinical setting, may be able to predict the chances of colorectal metastatic disease spreading beyond the liver.

Lay Description

There are patients with a healthy liver who have been diagnosed with abnormal blood vessels which allows blood to bypass the liver prior to filtering. It is thought that these blood vessels have the potential to spread colon cancer beyond the liver. Currently, there are no standardised tests to find these abnormal blood vessels leaving many cases undiagnosed. This study has developed a non-invasive test which can find and measure these liver bypassing blood vessels. Identifying these blood vessels will mean that cancer treatment in certain cases can be more aggressive, whereby reducing the chance of colon cancer spreading beyond the liver.

A NOVEL NON-INVASIVE TECHNIQUE FOR THE DETECTION OF PORTOSYSTEMIC SHUNTS

Matthews T*, Li P^, Hamilton M*, Trochsler M*, Weiss M^, Butler R#, Roberts M^, Maddern G*

^Therapeutics Research Centre, #Cancer Research, School of Pharmacy and Medical Sciences, Division of Health Sciences, University of South Australia and Basil Hetzel Institute for Medical Research.

*Discipline of Surgery, School of Medicine, The University of Adelaide and Basil Hetzel Institute for Medical Research, The Queen Elizabeth Hospital

INTRODUCTION

A portossystemic shunt (PSS) is defined as a congenital or acquired abnormal blood vessel that redirects blood around the liver without being filtered through hepatic parenchyma. The prevelance of PSSs are still unknown as there is yet to be a standardised clincial test for PSS detection. PSSs are thought to be the reason behind the distribution of secondary metastases beyond the liver in some colorectal cancer patients who do not have cirrhosis of the liver.

AIM

To develop a cost effective, non-invasive technique that can detect and measure portosystemic shunts in healthy livers.

METHODS

An 8mm diameter artificial PSS was created in a pig model between the portal vein and inferior vena cava to mimic this vascular anomaly. A dye, Indocyanine Green was injected into the portal system and its rate of metabolisation was measured non-invasively using an ear spectrometer with a LiMON® machine (Pulsion®, Germany) for 15 minutes. This data was then sent to Germany for modeling by a pharmacologist (MW) using the software ADAPT (Biomedical Simulations Resource, University of Southern California). Each pig was used as its own control with the shunt being occluded.

Figure 1:A) Locate inferior vena cava and portal vein (not shown). **B)** Attach 8mm diameter graft to inferior vena cava and portal vein. **C)** Patent shunt stabilised for 5 minutes.

RESULTS

A double peak was seen in each of the shunted pigs within 2 minutes post Indocyanine Green Dye injection(figure 2). A significant difference was seen in the lag time, time where the concentration maintained >0.01ug/L (figure 3), and also time of the first peak against its control.

The LiMON data was modelled, and the fraction of blood flowing through the shunt could be predicted and compared against the expected shunted ratio (table 1).

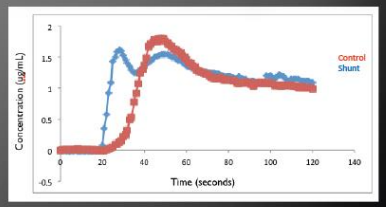

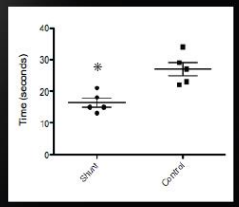

Figure 2 (left): Example of double peak of indocyanine green in a shunted and control model, n=1. **Figure 3** (right): Time lag (Indocyanine green plasma concentration threshold >0.01ug/L) between shunted and control. n=6, p=0.016

Table 1. Predicted fraction of blood bypassing the liver using the ADAPT software with expected range of diverted blood.

Pig	Shunted Blood Predicted from Model (%)	Expected Shunted Blood (%)
1	-	32 - 45.7
2	33.2	34.7 - 49.6
3	37.9	34.7 - 49.6
4	46.4	35.6 - 50.8
5	52.6	44.9 - 64.1
6	61.6	55.1 - 78.7
Mean	52.6	39.5 - 56.4
sd	11.6	8.8 - 12.6

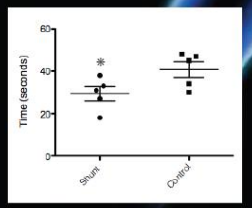

Figure 4: Time of first peak between shunted and control. n=6, p=0.019

CONCLUSION

This pilot study has developed a novel technique for the detection and quantification of PSSs, and if implemented in a clinical setting, may be able to predict the chances of colorectal metastatic disease spreading beyond the liver. Further study is required for smaller size shunts.

Appendix G – Three Minute Thesis Competition Poster

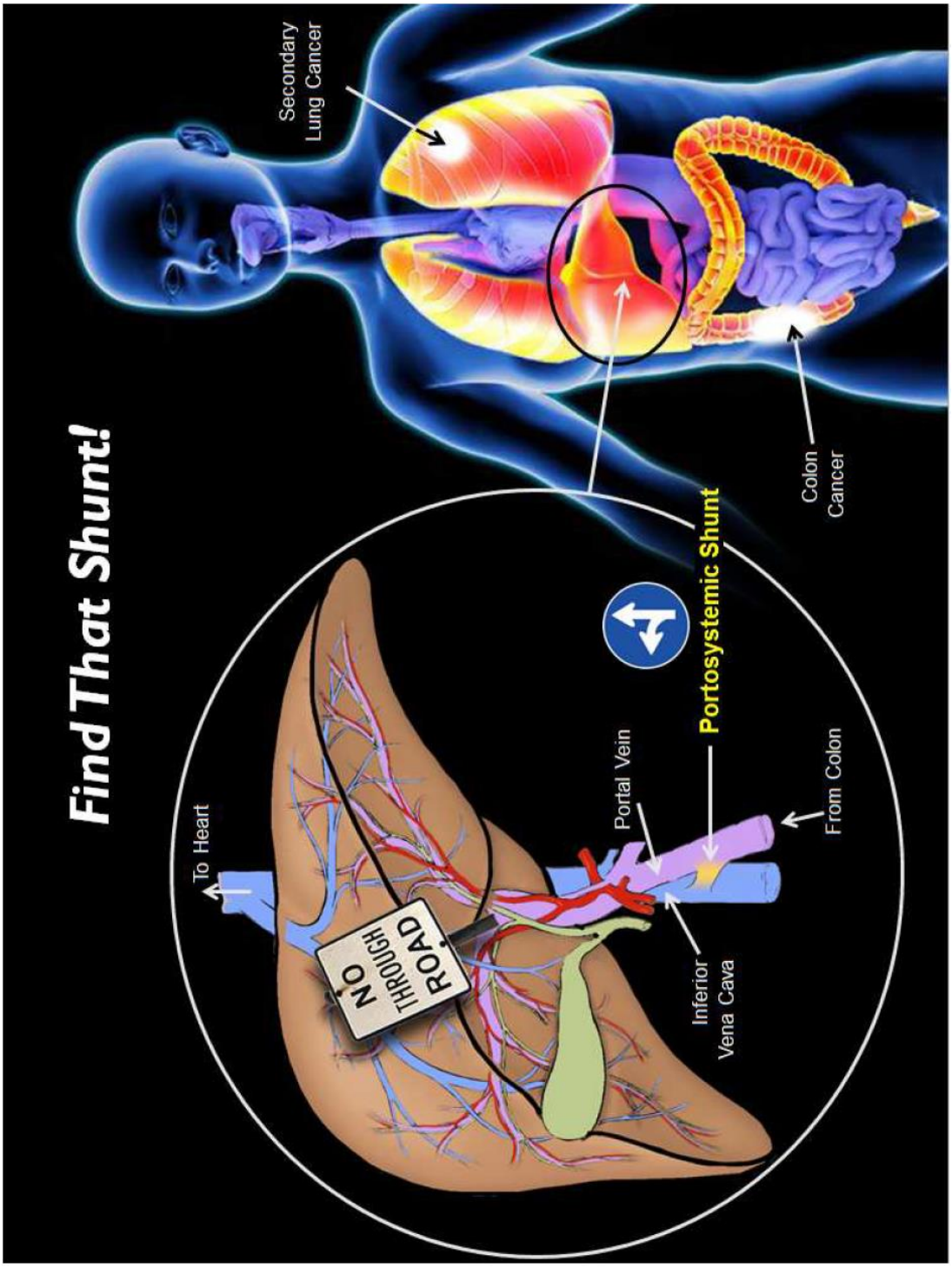

Appendix H – Review of Incidentally Diagnosed Congenital and Acquired Portosystemic Shunts in Patients Without Cirrhotic Liver Disease: *A Need for a Standardised Clinical Test*

Statement of Authorship

Title of Paper	Review of Incidentally diagnosed congenital and acquired portosystemic shunts in patients without cirrhotic liver disease: a need for a standardised clinical test
Publication Status	○ Published, ○ Accepted for Publication, ◉ Submitted for Publication, ○ Publication style
Publication Details	Submitted to British Journal of Surgery on 31/10/2013

Author Contributions

By signing the Statement of Authorship, each author certifies that their stated contribution to the publication is accurate and that permission is granted for the publication to be included in the candidate's thesis.

Name of Principal Author (Candidate)	Todd Matthews		
Contribution to the Paper	Performed search and analysis of data, and wrote manuscript.		
Signature		Date	31/10/2013

Name of Co-Author	Markus Trochsler		
Contribution to the Paper	Reviewed analyzed data and manuscript.		
Signature		Date	31/10/2013

Name of Co-Author	Guy Maddern		
Contribution to the Paper	Supervised development of work and acted as corresponding author.		
Signature		Date	31/10/13

Name of Co-Author			
Contribution to the Paper			
Signature		Date	

Review of Incidentally diagnosed congenital and acquired portosystemic shunts in patients without cirrhotic liver disease: *a need for a standardised clinical test*

AUTHORS:

Matthews T, Trochsler M, Maddern GJ,

DEPARTMENTS AND INSTITUTIONS

Discipline of Surgery, The Queen Elizabeth Hospital, University of Adelaide, Woodville South, South Australia.

CORRESPONDING AUTHOR:

Prof. G.J Maddern
University of Adelaide Discipline of Surgery
The Queen Elizabeth Hospital
28 Woodville Road
Woodville South
SA 5011
Australia
Ph: +61 8 8222 6756
Fax: +61 8 8222 6028
Email: guy.maddern@adelaide.edu.au

AUTHOR EMAILS

todd.matthews@adelaide.edu.au
markus.trochsler@health.sa.gov.au

MANUSCRIPT TYPE:

Review

Abstract

INTRODUCTION: Portosystemic shunts (PSSs) are rarely seen in healthy individuals or patients with non-cirrhotic liver disease. Portosystemic shunts may play a significant role in hepatic metabolism as well as in the spread of gastrointestinal metastatic tumors to specific organs. Small PSSs may be more common than generally thought. However, epidemiological data on PSSs is scarce and inconclusive. Commonly used radiological methods, used to detect PSSs are generally too invasive and costly to be used in these circumstances. Clinicians need a simple, accurate diagnostic tool to detect their presence.

METHODOLOGY: Articles were critically reviewed for adult patients, with normal liver function and a congenital or acquired portosystemic shunt, and what was the most frequently used diagnostic procedure. We identified eligible studies by searching the relevant databases, including PUBMED, EMBASE, MEDLINE and Cochrane Library. The selection of eligible articles was carried out using a predefined question, inclusion criteria (adult, non-surgical PSS) and a set of search terms that were established before the articles were identified.

RESULTS AND CONCLUSIONS: We reviewed 80 clinical studies describing 112 patients with congenital or acquired PSS, of which the majority were incidentally diagnosed while undergoing imaging tests for various reasons. Doppler ultrasound scanning and computed tomography were the most commonly used, with 49 extrahepatic PSS, 61 intrahepatic and two unspecified PSS diagnosed. This review

highlights the need for development of safe, cost-effective and easy to use technologies for detection, quantification and characterization of the naturally acquired PSS.

Introduction

A portosystemic shunt (PSS) is defined as a congenital or acquired abnormal blood vessel that diverts a portion or all of the hepatic portal blood into the systemic venous system. Consequently the diverted blood does not pass through the liver sinusoidal parenchyma. Portosystemic shunts developing after birth may develop *de novo*, as a consequence of disease or as a result of human intervention, but still little is known about them. Normal human vascular anatomy does not contain any venous connections between intrahepatic portal branches and hepatic veins, nor are there any connections between superior mesenteric veins, splenic veins, extrahepatic portal veins and other systemic veins [1, 2]. PSS are often seen in patients with cirrhosis of the liver, but have also surprisingly been viewed in patients with functionally healthy liver, including patients without cirrhosis, fibrosis or hepatitus.

Classification

Portosystemic shunts are anatomically divided into two groups – extrahepatic and intrahepatic (Figure 1). The English surgeon, John Abernethy FRS, first described extrahepatic vascular anomalies consistent with a PSS in the post mortem examination of a 10 month old infant in 1793 [3]. Consequently, these PSSs are now

described as being of an "Abernethy" Type. Bellah *et al.* [4] were the first to image extrahepatic PSS, with more recent work by Morgan and Superina [5] resulting in the description of Abernethy Types I and II (Figure 1). An Abernethy Type I PSS diverts all blood from the portal vein into the inferior vena cava and the intrahepatic portal vein is absent. An Abernethy Type II PSS diverts a portion of the blood into the inferior vena cava with the portal vein being tortuous.

Few Abernethy Type I cases have been reported in detail with pathological examination, and therefore it is possible that an underdeveloped hypoplastic portal vein may still be present [6]. It is therefore suggested that the Abernethy classifications show variability, rather than definite clinical representation [2].

Doehner *et al.*[7] initially reported intrahepatic PSSs, however Mori *et al.* [8] was the first to image them and Park *et al.*[9] later categorised them into four types (Figure 1) based on their location in Coinaud's segments (Figure 3)[10, 11]. Park Type I is a single, constant diameter shunt from the intrahepatic portal vein to the inferior vena cava. In Park Type II, single or multiple shunts can be found between the intrahepatic portal branches and the hepatic veins within the same segment. Park Type III is a shunt, which has formed via a portal system aneurysm connecting to a hepatic vein, and in Park Type IV, there are multiple shunts between the portal branches and the hepatic veins in multiple segments.

There are several different classifications to describe PSSs. For the purpose of this thesis and to encourage standardisation of PSS classification, the Abernethy and Park descriptions will be used.

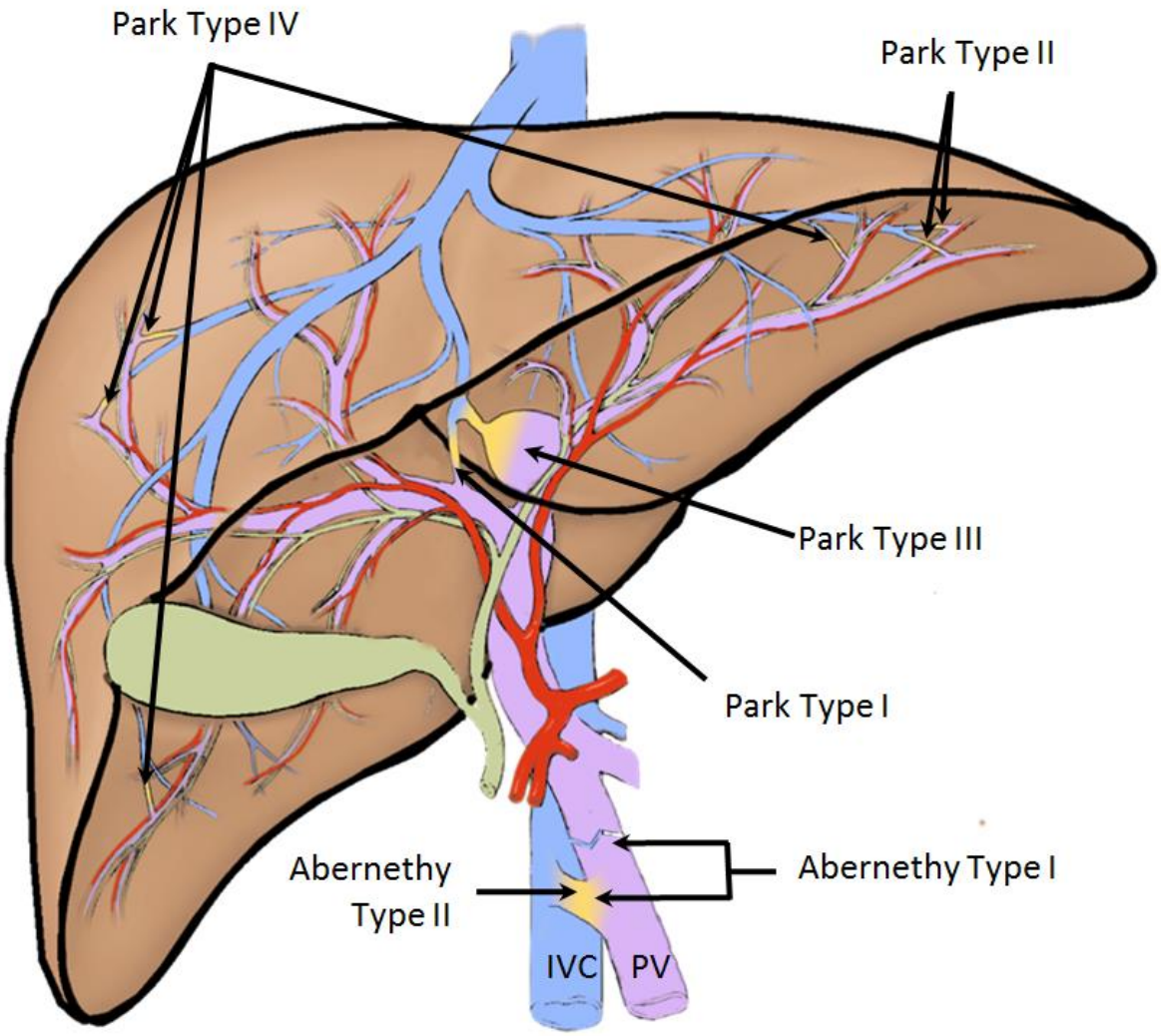

Figure 1: Extrahepatic Abernethy portosystemic shunts. Type I: All blood from the portal vein (PV) is diverted into the inferior vena cava (IVC). Type II: a portion of blood diverted into the IVC with the PV being patent, but tortuous. Park classification: Type I has a single, constant diameter shunt from the intrahepatic PV to the IVC. In Park Type II, single or multiple shunts and be found between the intrahepatic portal branches and the hepatic veins within the same segment. Park Type III has a shunt, which has formed via a portal system aneurysm connecting to a hepatic vein, and in Park Type IV, there are multiple shunts between the portal branches and the hepatic veins in multiple segments.

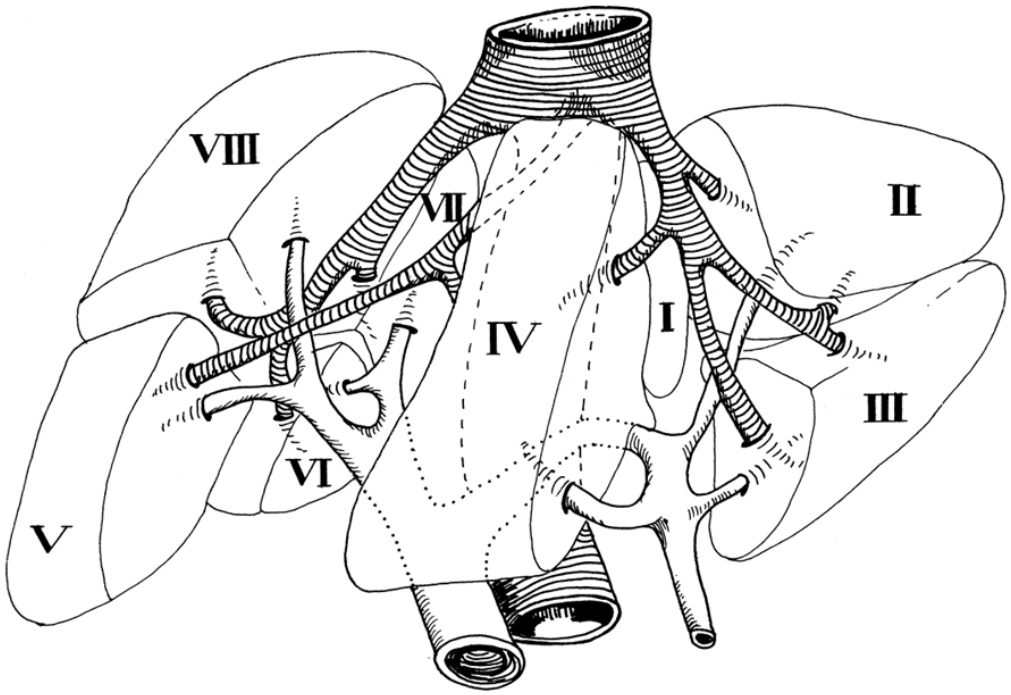

Figure 2: Human liver divided into segments according to Couinaud's nomenclature. The left lobe consists of segments I-IV, while the right lobe consists of segments V-VIII.

Portosystemic Shunt Variability Within The Classifications

Five types of classifications have been proposed for PSSs [12]. The Park and Abernethy classification is the most commonly used with some slight additions and variations. However, within the classification definitions, there is still some room for interpretation.

Abernethy and Banks [3] reported an abnormal inferior vena cava (IVC), however in most cases, the IVC is normal. A PSS may typically drain into the IVCa anywhere between the level of the renal veins [13] to the confluence of the hepatic veins [14]. There are reports of a portal vein formed from the splenic and superior mesenteric veins ascending retrohepatically and connecting to the IVC above the confluence of the hepatic veins [15, 16]. There is also an additional report of a Type I PSS connecting directly the right atrium [5]. Other Type I variation include cases reporting with either the splenic or superior mesenteric vein join to another systemic vein [2], or similarly the portal vein connects directly into a systemic vein other than the IVC. Other systemic veins may include left or right renal veins, or azygos vein [6, 17-19]. Although rare, there are several reports of a shunt between the inferior mesenteric vein, or the superior rectal tributaries with the common left or right internal iliac vein [14, 20, 21].

In a typical Type II PSS, portal blood is partially shunted via the IVC posteriorly to the liver [22-24] and the intrahepatic portal vein is of normal appearance or hypoplastic [24-26]. However, the shunt has been noted to be partly intrahepatic when

traversing the caudate lobe [27]. Most cases note the hepatic artery and its' intrahepatic branches are enlarged [14, 23, 28], while the portal venules are small or not present [14, 15, 20]. However, some liver biopsies were reported as normal in appearance [29].

Incidence

Acquired PSSs are commonly recognised in patients with cirrhotic liver disease as a compensatory mechanism for the associated portal hypertension [30]. In contrast, congenital and naturally acquired PSSs are thought to be rarely recognised in healthy individuals or in patients with non-cirrhotic liver disease. It is speculated that PSSs only occur in 1/30,000 people, however this is based purely on a nationwide screening for galactosemia [12, 31]. Hypergalactosemia is a rare genetic disorder known to be associated with PSSs [32, 33]. Such PSSs have usually been serendipitously detected and more may be detected if there was a standardised clinical prognostic test. Neither the true incidence, the cause, nor the clinical effect of a PSS in healthy individuals or in patients with non-cirrhotic liver disease is known. The absence of a standard, simple, diagnostic procedure to detect and evaluate the entity contributes to this ignorance.

Abernethy Type I PSSs are more common in females [14, 23]. Abernethy Type II are thought to be more prevalent in males [23, 25], but this is not universally accepted [6].

From 1971 to 2003, 61 cases of Abernethy extrahepatic PSS were found, with a majority of Type I more commonly occurring in females [4-6, 13, 14, 16, 18, 20, 23, 34-53]. Although Type II extrahepatic PSSs were not as common in these cases, the prevalence in both males and females is equal. PSS have been reported at ages ranging from 31 weeks intrauterine life to 76 years (Type I) and 28 weeks intrauterine life to 69 years (Type II) [6].

Park Types I and II are far more common than Types III and IV [2]. A study by Glitzelmann *et al.* [54] in 145,000 infants demonstrated that congenital PSSs in infants are rare. A PSS was evident in only five infants through biochemical and ultrasound findings. Of these five infants, only one was documented in a case study. Although still rare, 34 Park Type PSS and 17 Abernethy Type PSSs were identified [55]. However, more infants have been diagnosed with PSSs in Japan than anywhere else in the world and it thought that the prevalence of congenital PSSs is higher here as infants are routinely screened for hypergalactosemia [2, 25, 55].

Associated Malformations

Several congenital malformations are described in children with Abernethy PSSs. Cardiovascular anomalies including ventriculoseptal defect, coarctation of the aorta and atrioseptal defect are most prevalent in Abernethy Type I [5, 6, 13, 23, 25]. There are several further cases which report biliary atresia, some of which included splenic malformation syndrome (polysplenia, situs inversus and intestinal malrotation) [5, 23].

Other uncommon associated conditions include multicystic dysplastic kidney, oculoauriculovertebral dysplasia, choledochal cysts, skeletal anomalies and cutaneous haemangiomas [14-16, 56, 57].

Congenital malformations associated with Park Type PSSs are rarely seen, but biliary atresia, cutaneous haemangioma and congenital cardiac disease have been reported [54, 55, 58-60]. Congenital cardiac disease especially is thought to be linked to long durational PSS patency and aetiology [25, 61]. There are some reports that suggest there may be a general angiogenesis abnormality causing PSSs. Two patients with PSSs were reported, in association with multiple coronary artery fistulae, [62] a left internal carotid-basilar anastomosis and absent vertebral arteries [60].

Fewer associated abnormalities and conditions have been reported in relation to Abernethy Type II, although they are similar to the associated conditions related to Type I [2]. These include pulmonary valve atresia, patent ductus arteriosus, oculoauriculovertebral dysplasia, polysplenia with IVC anomalies and Cornelia de Lange syndrome [6, 23-25, 63].

Symptoms and Complications

Few symptoms have been associated with Park Type PSSs, many cases of which are asymptomatic [2]. On occasion neonatal jaundice has been reported [2]. Two main complications can occur as a result of PSS. Firstly, hepatic encephalopathy is often a

symptom of large PSS, and secondly PSSs may influence the development of intrahepatic tumours.

Hepatic encephalopathy is caused from circulating toxins affecting the cerebrum. These toxins are typically removed by the liver in a single pass, however a PSS avoids the metabolisation of the toxins. There can also be an increased concentration of bile acids, postprandial glucose, galactose, ammonia and nitrogenous substances, which may have an affect on the brain [55, 64]. Long standing PSSs can cause hypergalactosemia, which then may lead to cataract formation [64]. Often encephalopathy is related to the size and duration of the PSS [55], however, the vulnerability to hepatic encephalopathy increases with age [2].

The lack of, or severe reduction in intrahepatic portal blood flow may cause over arterialisation of the liver. This therefore can increase levels of hepatic growth factors such as insulin, glucagon or hepatocyte growth factor [65]. Any combination of these factors may encourage growth of benign hepatic tumours, such as focal nodular hyperplasia, nodular regenerative hyperplasia and adenoma [6, 14, 16, 20, 24, 41], or malignant hepatic tumours including hepatocellular carcinoma or hepatoblastoma [13, 56]. It is possible that these tumours may regress if PSSs are occluded, especially in patients with Abernethy Type II PSSs [2].

Experimental models and human patients have shown that reduced portal venous flow may cause some liver atrophy [66-68]. Animal models have also demonstrated that congenital PSSs in rats have developed hyperplastic nodules and hepatic atrophy [69, 70]. Portal venous blood supplies hepatotrophic factors from the digestive

system including insulin and glucagon, which may cause decreased liver size due to a congenital PSS. However, other factors may be at play including an imbalance between liver regeneration and apoptosis [65, 67].

Other less common complications have been noted such as hyperandrogenism and hyperinsulinism due to an Abernethy Type I PSSs [71]. Hepatopulmonary syndrome was also seen in patients with Abernethy Type II [26, 72]. Some reports suggest that PSSs may cause fatty liver features, as these features disappeared after the PSS was occluded [73, 74].

Pathogenesis

Three different hypotheses have been proposed as a cause of extrahepatic shunts and two potentially for intrahepatic shunts. The congenital theory proposes that during the initial stages of foetal development, there are connecting venous networks between the subcardinal and vitelline venous systems, as well as between the portal branches and the caval tributaries, which may later form a PSS [75], similar to the intra-uterine circulation through the ductus venous. Most congenital PSSs will spontaneously self-occlude during the first 12 - 24 months of life, however it is unknown how often this occurs [54, 58, 61, 64, 76, 77]. If the PSS does not occlude further complications can occur in adolescence and adulthood.

PSSs often occur in neonatal infants with a patent ductus venosus connecting the left portal vein to left hepatic vein via the umbilical recess of the liver [2]. Typically, this would start to occlude directly after birth with the liver being fully functional after 17 days [78-80]. It is thought that delayed closure may be the result of higher venous pressure and congenital heart disease [2]. The ductus venosus later forms the ligamentum venosum within the fissure between the caudate lobe and segment 3. Persistent patency of the ductus venous has only been diagnosed in 15 cases and was seen more in males than females [81]. Persistent patency is thought to be caused from or associated with either a genetic disorder [73, 82], or hypoplasia of the intrahepatic portal vein [81-83].

Development of Abernethy Type I has been associated with excessive involution of the periduodenal vitelline veins [15]. However, it is unknown if a PSS is the cause of lack in development of the portal vein or if the lack of a portal vein causes the development of a PSS [2].

Moncure *et al.* [84] proposed the adhesion theory after a PSS was found at the site of intra-abdominal adhesion in a patient with mesenteric varices. A third theory proposed by Akahoshi *et al*. [29] argues that PSSs are the natural result of idiopathic portal hypertension.

Detection and Assessment

Computed tomography (CT) and Doppler ultrasound scanning are the most frequently used imaging modalities for assessing the liver in adults, and therefore may account for the detection of most PSSs. These methods are commonly used to obtain images of vascular structures and there is considerable expertise required in their interpretation. However, there are several significant problems relating to the use of these techniques for the purpose of PSS detection. Both CT and Doppler ultrasound scanning can be time consuming when searching for a PSS. Furthermore, a simple CT scan of the abdomen has a similar amount of radiation (10mSv) to nine abdominal x-rays or 200 chest x-rays, [85, 86]and therefore carries a coincidental radiation burden. Although Doppler ultrasound scanning does not involve any radiation, it can have a low sensitivity for some PSSs, especially if they are small. The efficacy of Doppler ultrasound scanning is dependent on the transducer used to identify the location and size of the PSSs and the skill of the operator [87]. Lisovsky *et al.* [88] reported that Doppler ultrasound scanning was unreliable in detecting PSSs, and suggested that PSSs are commonly undiagnosed.

It is possible that the lack of a portal vein is unseen via ultrasound due to decreased intrahepatic vascular visibility and decreased liver size [64]. Indications of an Abernethy Type I PSS include an enlarged hepatic artery and common bile duct at the hepatic hilum [64]. Similarly, a liver biopsy may indicate the presence of an Abernethy Type I or possibly Type II PSS, with demonstration of absent portal venules, bile duct proliferation, arterialisation, and periportal fibrosis [82, 88].

However, these histological factors are not conclusive alone for a PSS [88]. With several indications, a CT would then be required to locate the Type I PSS.

Treatment

Surgical ligation or radiological occlusion can be used to treat PSS if it is surgically accessible [2]. Treatment is especially required if the PSS is the cause of hepatic encephalopathy or if there is a high risk of a benign hepatic tumour developing. Occlusion of PSS may not be safe in all cases especially if the portal vein is hypoplastic. Occlusion of the PSS may cause portal hypertension or hepatofugal flow. In some cases it may be deemed appropriate to surgically narrow the PSS and allow acclimatisation before occlusion [25]. For patients with an Abernethy Type I PSS, a liver transplant is currently the only viable treatment [5, 23, 89]. However, it is advised that treatment should be assessed separately for each patient.

Patients who are asymptomatic may not need treatment. In these cases, patients can be treated with a protein-free diet and regular administration of branched-chain amino acids and lactulose if any metabolic abnormalities occur [90].

Gastrointestinal Cancers

Colorectal cancer and associated secondary cancers are the third most common gastrointestinal cancer worldwide and the fourth most common cause of death. Before the primary tumour has been discovered, between 15 - 20% of patients will have secondary metastases [91]. The most common sites for secondary cancer are the liver and lung [92, 93]. Over a four year period, 754 patients were diagnosed with gastrointestinal cancer, including 12% being diagnosed colorectal cancer. Interestingly, 6% of the colorectal cancer patients were also diagnosed with isolated secondary lung metastases[94]. It is estimated that between 1.7% to 7.2% of patients have isolated secondary lung metastases originating from either colon or rectal cancer [94]. Veins from the gastrointestinal organ drain into the portal system [95] and is therefore clearly understood as to how cancer may spread beyond the liver, without the liver obtaining metastases itself. Theoretically, cancers spreading via the bloodstream should be trapped by the liver, rather than progress further and generate distant metastases. One possible theory to this obscure metastatic distribution phenomenon is that PSSs play a role in facilitating the distribution of cancer, however this remains to be investigated.

Circulating Tumour Cells

Circulating tumour cells (CTC) are cancer cells that have originated from a primary tumour and circulating through the vascular system or lymphatic system [96]. Metastases resulting from CTC are the most common reason for cancer related death with colorectal cancer being the second most common form of primary cancer [92, 93]. CTC have been shown to initiate secondary metastases, however it is thought that only 0.01% of these cells will actually form metastases [97]. The quantity of CTC that are released into the blood stream from a primary cancer is unknown [98] as their detection is difficult given there are only 1 - 10 CTC per millilitre of whole blood as compared to the millions of white blood cells and red blood corpuscles. However a number of established techniques, including PCR, have been developed to allow for the detection of CTC [99, 100].

For a CTC to form a metastasis, malignant cells must detach from the primary tumour and be able to migrate, invade and move through the extracellular matrix of the surrounding tissue towards the lymphatic or vascular system [101]. The cascade of events includes transmission through the epithelium and mesenchyme, invasion of surrounding tissue, entrance into the microvascular lymph and/or blood systems, survival through the circulation to the microvessels of another organ, crossing the mesenchyme and epithelial barrier, to attachment and proliferation within new tissue-specific area [98, 102]. Two alternative, time-dependant models of metastatic distribution, conflicting on whether CTC display haematogenous spread or lymphogenous spread, are still under scrutiny [101]. Haemotangeous spread is directly

into the vascular system of the primary tumour and lymphogenous spread is the spread of CTC into the lymphatic system, where they lie dormant in the lymph node before metastasising further [98, 101].

It is speculated that metastatic distribution mostly occurs from hematogenous dissemination [103, 104]. Dissemination into surrounding lymphatics of the primary tumour is often a dead end rather than the route of CTC metastasising and further spreading CTC [105].

Metastases Distribution

A hypothesis, first proposed in 1958 by Lore *et al.* [106] and later studied by Saitoh *et al.* [107], suggested that PSSs could be one of the routes responsible for the distribution of gastrointestinal metastases to distant organs, for example colorectal metastases into the lung rather than the liver. Theoretically, CTC from colorectal carcinomas should be 'trapped' by the liver, without further dissemination. However, according to this hypothesis, a PSS may act as a direct or indirect route for metastatic cancer cells to reach the pulmonary vascular system. If this hypothesis is correct, it is possible that detection and elimination of a naturally occurring PSS in cancer patients could prevent some forms of metastatic disease, or provide a prognostic indicator.

Wallace *et al*. [108] noted secondary metastases in two of their patients who had been implanted with artificial PSSs. Implantation of a transjugular intrahepatic

portosystemic shunt (TIPS) was successfully performed in 37 patients. TIPS is an artificial shunt that has been more widely used within the last decade to treat portal hypertension and other complications [108]. Two of these patients who were previously diagnosed with pancreatic neuroendocrine tumours had been identified with thoracic metastases and <5 mm nodules in the lung ten months after the TIPS procedure without hepatic metastases. The TIPS is most similar to Park Types I or II PSSs, depending on the site of the stent. Although, PSS diameters may be different to that of TIPS, the effects remain similar. The report by Wallace *et al.* [108] is an example of cancer patients that are later diagnosed with pulmonary nodules (secondary tumours) which may be due to TIPS. Therefore, it is possible that metastases beyond the liver may occur via a PSS.

CTC may still pass through the liver without a PSS provided they are not detected by the hepatic immune system. CTC must pass via the vascular bed within the sinusoid wall, which contains phagocytes, called Kupffer cells and liver-resident macrophages. These Kupffer cells and the macrophages are the first line of defence in removing unwanted cells and particles, including CTC [109-111]. For a CTC to be undetected and disseminate further ligands on the CTC membrane need to be modified through a multi-step process to give the 'appearance' of a normal cell.

The biophysics of endothelial cell and CTC interaction is still not entirely understood [112]. CTC undergo several stresses including shear hemodynamic stress, immune-surveillance and anchorage-dependent survival signalling [113] during movement through the extracellular matrix and vascular system. With these stresses, CTC roll and adhere along the epithelium via selectins and their specific binding selectin-

ligand. There are three types of selectins, L-, E- and P-selectin which are a type of glycoprotein found in the transmembrane that bind to corresponding glyconjugates or ligands on other cell membranes [112-115]. As the CTC move through the extracellular matrix and vascular system, they interact with different haemeopotoeic and endothelial cells, which consequently modifies their selectin ligands. This allows the CTC to acquire the potential to create site specific metastases [113]. Notably, colorectal carcinomas CTC injected into the portal system of E- and P-selectin knockout mice caused 84% fewer lung metastases as compared with normal mice [116]. This suggests that some CTC dispatched from colorectal carcinomas particularly acquire E- and P-selectin ligands, which are specific for the lung and still bypass the hepatic immune system

Notwithstanding the strategies that CTC's may employ to circumvent hepatic surveillance, the presence of a PSS may increase the concentration of colorectal carcinoma CTC reaching the lungs.

Summary

Naturally occurring and congenital PSSs are not a widely understood area especially when found in patients without cirrhosis. Although, believed to be rare, it is possible that microscopic Park Type PSSs maybe still present in some patients. Gastrointestinal cancers are far more common in adults, and it is debatable as to how these cancer patients have metastatic dissemination beyond the liver, without

metastases in the liver itself. It is possible that PSSs may be one factor that increase the risk of secondary metastases, and microscopic PSS maybe more prevalent than currently understood. However, there are no standardised clinical tests to detect PSS, which therefore limit the number of PSS studies.

A literature search was performed regarding: (a) congenital or naturally acquired PSSs in adult patients with functionally healthy livers (without cirrhosis, hepatitis or fibrosis.); and (b) the allied methods used to diagnose and characterize these PSSs. Reports regarding surgical PSSs and children under the age of 18 years old were excluded from this review.

Objectives

4. To review the occurrence of congenital or acquired PSSs in adult patients, with normal liver function.
5. Explore similarities between patients including age at diagnosis and symptoms.
6. What methods have been able to incidentally detect these PSSs and which are the most prevalently used methods.

Question

In adults, with normal liver function and congenital or naturally acquired PSSs and no plausible associated cause, what is the most frequently used diagnostic procedure?

Methodology

Search Strategy

Inclusion and exclusion criteria were defined. Articles were included if the patient was human, patient(s) had a natural PSS, functionally healthy liver, were equal to or older than 18 years and the article was in English. Articles were excluded if the patient(s) had a surgical PSS, diseased liver including cirrhosis, fibrosis or hepatitis, were younger than 18 years, animals, or the article was not written in English.

PUBMED, EMBASE, MEDLINE and Cochrane Library searches were performed using the terms “portosystemic shunt, portocaval shunt, portasystemic shunt, portacaval shunt, mesocaval shunt and splenorenal shunt”. The search was then limited to English language articles, and human subjects of 18+ years of age. Due to the numerous articles containing a surgical PSS, PSSs caused by liver disease, PSSs found in children and animals, a ‘NOT’ section was included in the search term, “surgical portosystemic shunt, transjugular intrahepatic shunt, cirrhosis and fibrosis”. If the patient could not be determined as an adult or the state of the patient's liver could not he clearly defined, the article was not included for review.

Results

Search Results

A total of 429 articles were identified from PubMed and Medline, from which 114 articles were included after reviewing the abstracts. An Embase search of the same keywords found a total of 266 articles. Following a review of the abstracts, 53 articles were included. A search for the term 'aneurysmal spontaneous portosystemic shunts' yielded 14 additional articles, of which eight were included. No articles were identified in the Cochrane Library. A total of 175 articles were selected for full text review. After reading through full texts, 80 of the 175 were deemed appropriate for inclusion in this review. Articles that were still found to contain patients with cirrhotic liver disease, patients who had a surgical PSSs or where data could not be clearly identified such as age were excluded from this review (Figure 4).

All but ten articles, which were retrospective cohort studies, were case studies. Data extracted from these 80 articles included age, sex, symptoms, medical history, PSS detection method, treatment, blood test results including ammonia levels and indocyanine green dye retention at 15 minutes (ICG R15) and Abernethy or Park type of shunt. If the article did not explicitly specify the type of PSS, it was categorised into one of the Abernethy or Park Types according to its description. Splenorenal and gastro-renal shunts were categorised under Abernethy Type II.

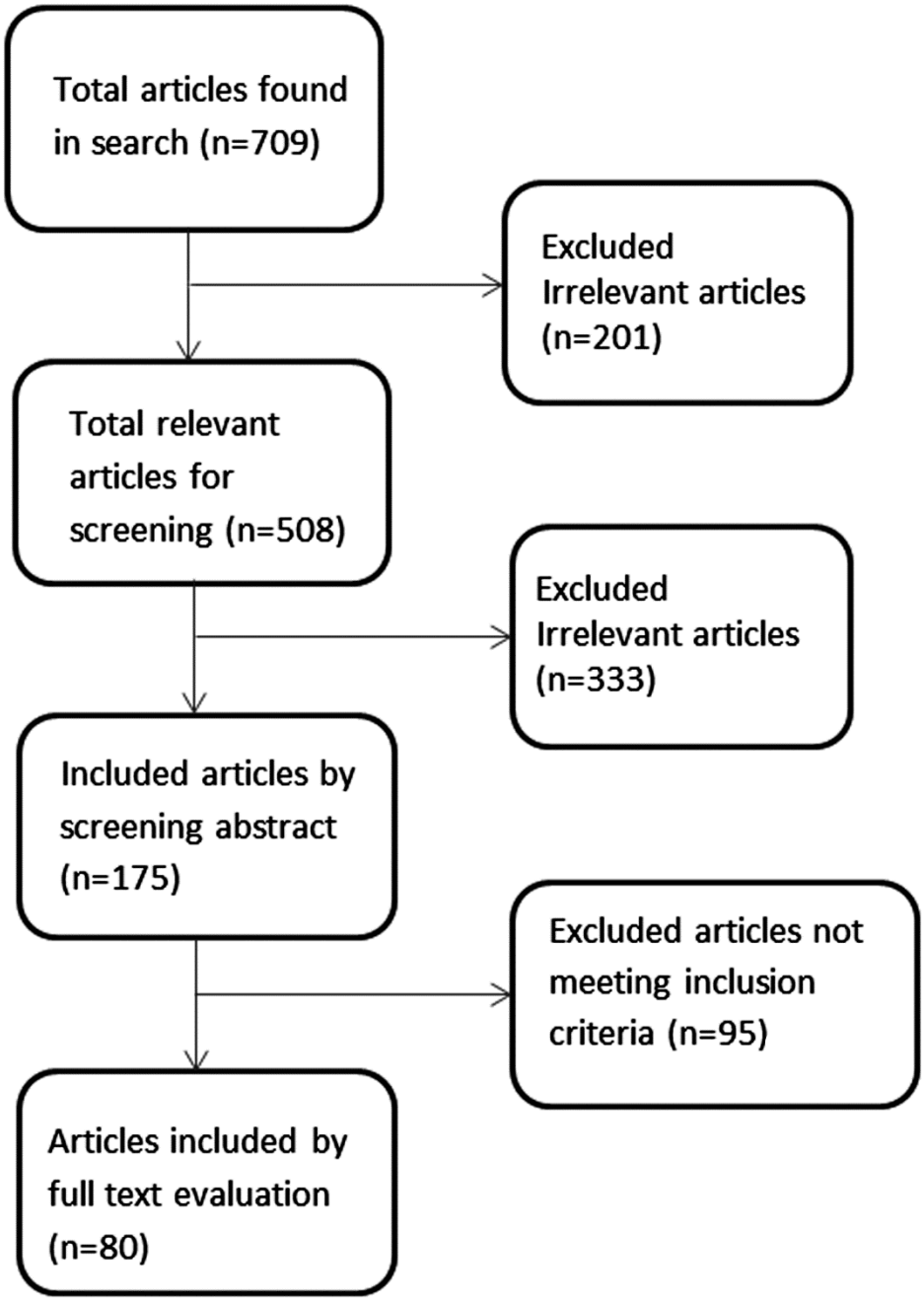

Figure 4. Flow chart of the systematic search strategy.

Demographics

In 80 clinical research articles, our analysis revealed that 112 patients were diagnosed with either an extrahepatic (Abernethy) or intrahepatic (Park) PSS. With regards to PSS sub-type, of these 112 PSS cases a total of 49 patients (43.8%) presented with extrahepatic Abernethy PSS and 61 patients (54.5%) were found to have intrahepatic Park PSS. In two patients the shunt type could not be specified (Table 1). Overall, PSSs were more prevalent in women than men (69 and 41 respectively). The exception to this finding was in the Abernethy Type I subset, where there were six males and two females.

Patients were commonly diagnosed with a PSS at a median age of 51 years, ranging 18 to 87 years for males and 55 years, ranging 18 to 90 years for females (Table 2). The median age of patients with an Abernethy PSS was 50 years ranging 18 to 84 years, while the median age in patients with a Park PSS was 57 years, ranging 18 to 90 years.

Frequency of Diagnostic Procedures

PSSs were detected and confirmed in 81 of the 112 patients (72.3%) using a single imaging method (Table 3). Doppler ultrasound scanning, computed tomography and computed tomography angiography (CT/A) were the most common with 26 and 24 patients respectively.

In 31 patients (27.6%) two or more imaging methods were required to confirm the presence of a PSS (Table 3). Of these combined methods, Doppler ultrasound and CT were the most commonly used conjointly in 15 patients of the 26 patients that required a combination of two methods.

Symptomatology and Associated Conditions

Only 72 cases report on symptoms and associated conditions. The majority of the symptoms reported were neurological symptoms including encephalopathy, disorientation/ataxia, dysarthria and nausea (Table 4). Encephalopathy was the most common and reported in 27 cases. The next most common symptom and complaint were hyperammonemia in 18 patients and abdominal pain in 16 patients, while five patients did not report any symptoms.

Idiopathic portal hypertension and Osler-Weber-Rendu syndrome, also known as hereditary haemorrhagic telangiectasia, are both believed to be associated with PSSs, and were seen in eight and five patients respectively. However, in 34% of cases PSSs were an incidental finding while testing for indirect or non-associated diseases. Some of these diseases included ovarian, oesophageal, mammary, gastric, colon, urinary tract and rectal carcinomas.

Other Investigations:

Other clinical investigations reviewed included, blood ammonia levels, ICG R15 and reported PSS flow rates. Analysis of included studies revealed 26 patients (23.2%) with reported ammonia levels, ranging from 41.9 to 424 μg/dL. Of these 26 cases, 18 patients had above normal levels, 30 to 85 μg/dL with a median of 130 μg/dL, ranging from 89 to 424 μg/dL [117].

One study reported on ICG R15 in 14 patients, which is commonly used as a liver function test. A normal ICG R15 after 15 minutes is <10% [118]. In 11 cases, the ICG R15 was remarkably high, even though their liver was classified as 'healthy'. Normal ICG R15 is described in three patients, while the remaining 11 patients showed an elevated IGC R15 ranging from 13 to 47.5%, with a median of 39%. Of the three patients with normal ICG R15 levels, two were found to have a Park Type II PSS with a low shunting ratio of <9%. The third patient had a Park Type III PSS with a large 11 cm aneurysm with turbulent flow. The slow flow in the shunt may account for the normal ICG R15 results.

Seven cases reported the shunt ratio and/or flow rate as measured by Doppler ultrasound (Table 5). The shunted ratio ranged from 15.7 to 39.5%, with a median of 25.5% and the shunt flow rate ranged from 0.17 to 1.2 L/min with a median of 0.33 L/min. Three cases with Park Type III PSSs demonstrated 6 mmHg, 8 mmHg and 17 mmHg pressure gradients between the portal branches and hepatic veins [119-121].

Table 1: Prevalence of the type of shunt in male and female patients.

Shunt Type	Abernethy		Park					
	Type I	Type II	Type I	Type II	Type III	Type IV	Unknown	Total
Males	6	17	1	6	9	2	-	41
Females	3	23	5	17	14	7	-	69
Total	9	40	6	23	23	9	2	112

Table 2: Median age at diagnosis of shunts n=104 (no data reported in eight patients)

Shunt Type		Median (years)	Range (years)
Abernethy Type I			
	Male	51.5	24 - 63
	Female	33	28 - 42
	Both	42	24 - 63
Abernethy Type II			
	Male	48	20 - 67
	Female	51	18 - 84
	Both	50.5	18 – 8 4
Park Type I			
	Male	68	68
	Female	58	43 - 69
	Both	62.5	43 - 69
Park Type II			
	Male	53.5	24 - 67
	Female	59	22 - 90
	Both	56	22 - 90
Park Type III			
	Male	53	18 - 87
	Female	59	27 - 89
	Both	57	18 - 89
Park Type IV			
	Male	54.5	43 - 66
	Female	47	34 - 68
	Both	47	34 - 68

Table 3: Different methods used for detection of naturally occurring portosystemic shunts in patients without hepatic cirrhosis. CT/A – Computed tomography/angiography. MRI/A-Magnetic resonance imaging/angiography. n=number of patients.

PSS Type	**Abernethy**		**Park**						
Method	**Type I**	**Type II**	**Type I**	**Type II**	**Type**	**Type I**	**Unknown**	**Total**	**Reference**
Doppler Ultrasound	1	4	2	7	10	2		26	118, 119, 122-136
CT/A	1	10	1	5	2	3	2	24	19, 75, 86, 137-153
Angiography/X-ray		13		2	1	3		19	8, 51, 117, 154-169
Scintigraphy		6		1		1		8	170-174
MRI/A	1	2		1				4	175-178
Combination of 2 methods	3	5	3	6	8			25	118, 121, 126, 134, 143, 167, 179-187
Combination of 3 methods	2	1			1			4	120, 143, 188, 189
Combination of 4 methods				1	1			2	25, 190
Total single method	3	35	3	16	13	9	2	81	
Total combinations	5	6	3	7	10			31	
Total	8	41	6	23	23	9	2	112	

Table 5: Symptoms and pre-existing conditions

Shunt Type	Abernethy		Park				
Symptom	**Type I**	**Type II**	**Type I**	**Type II**	**Type III**	**Type IV**	**Total**
Neurological symptoms							
Encephalopathy	1	18	1	3	3	1	27
Disorientation/Ataxia		4	2	1	2	2	11
Dysarthria		3	1		1		5
Non-neurological symptoms							
Hyperammonemia	1	10	2	2	2	1	18
Abdominal pain	2	5	1	3	4	1	16
Fatigue		1		1	3		5
Jaundice	1	1			1		3
Other pain	1	2					3
Dyspnoea		1					1
Flapping tremor					1		1
Nausea		1					1
No symptoms		1	1	1	2		5
Not reported		2		4	2		8
Associated Conditions							
Osler-Weber-Rendu				1		4	5
Hypertension		6	1		2		9
Non-associated conditions							
Neoplastic diseases	1	1		5	4		11
Other	2	14		3	3	1	23

Table 6: Shunt flow rate and shunted ratio.

Patient	Shunt Type	Shunt flow rate (L/min)	Shunted ratio (%)	Reference
1	Park Type III	0.17	14.7	118
2	Park Type III	0.08	9	118
3	Park Type III	0.33	22	118
4	Park Type III	0.36	29	118
5	Park Type III	1.2	-	119
6	Park Type IV	-	68.1	171
7	Abernethy Type II	-	39.5	129

Discussion

Over a 29 year period (1982-2011), 112 adult patients were incidentally diagnosed with PSS, emphasizing the rarity of this vascular malformation. This rarity in PSS diagnosis may be due to the lack of a standardised, cost-effective, and safe clinical test given that most cases of PSSs in patients with functionally healthy livers remain unnoticed. Therefore, the frequency of PSSs could be higher than currently thought, either due to patients not being tested for PSS or the limitations of the available diagnostic techniques. The clinical implications of PSSs, including the effect on reduced rate of drug metabolism and questionable tumour metastases distribution, highlight a need for the development of a diagnostic technique.

There are several limitations with this review mainly due to the inconsistency of PSS terminology and how they are categorised [12]. It is also questionable as to what constitutes a congenital PSS and a spontaneous PSS. Congenital implies that the PSS is present from birth, however there are some articles which use it with a definition that is actually 'acquired PSS' or 'natural PSS'. Most PSSs are 'naturally acquired' unless there is a congenital vascular malformation from birth. Similarly with 'spontaneous PSSs', which implies that a PSS suddenly appears without cause, most articles reference 'spontaneous' as secondary to another problem, for example, an aneurysm. We have categorised the PSSs into Abernethy and Park Types as a means to encourage a standardised PSS categorisation system.

Eighty articles were reviewed describing 112 patients with PSSs, of which the majority were incidental findings while undergoing imaging tests. The pathogenesis of the PSSs in these adult patients remains still largely unknown, except in those with Park Type III PSS, and some patients with Park Type IV who have Osler-Weber-Rendu Syndrome. The hypothesis originally posed by Lore *et al.* [106] that PSSs could be one of the routes responsible for the distribution of gastrointestinal metastases to distant organs, deserves additional attention. Therefore the question can be asked "What is the frequency of PSSs in patients with pulmonary metastases from colorectal origin without liver metastasis?" Although there are still yet to be any studies which directly link metastatic distribution with PSSs, it has been reported that two pancreatic neuroendocrine cancer patients, who had a TIPS inserted, were diagnosed with pulmonary metastases several weeks after the intervention [108]. A plausible explanation is that the artificial shunt acted as a route for circulating tumour cells to bypass the liver. Therefore, PSSs may be a plausible explanation for patients present with pulmonary metastases from pulmonary origin and no secondary liver metastases [191].

The 112 patients included in this review, Doppler ultrasound scanning and CT scans were singularly the most frequently used methods to detect PSSs (23% and 21% respectively; Table 3). However, 31 patients required two or more different

methods to confirm a PSS. Of these, 15 were diagnosed using a combination of both CT and Doppler ultrasound. This indicates that PSSs may be difficult to detect with just one method, or need confirmation with an additional imaging modality, thus supporting the need for new detection techniques. Other methods, such as MRI, MRA, CTA, venography and angiography procedures can be used for validation, however these methods can be costly and sometimes more time consuming than using Doppler ultrasound or CT alone.

CT scanning is a commonly used procedure in many medical fields, but is associated with a significant radiation burden, particularly, abdominal scans where patients are susceptible to a large exposure of radiation [85, 86]. It is therefore advisable that the amount of received radiation a patient can have at any one time should be kept at a minimum.

Doppler ultrasound scanning, MRI and MRA do not have the same radiation hazard as CT, angiography or venography, but could be time consuming and expensive. Although Doppler ultrasound scanning is more commonly used, PSSs are extremely difficult to find unless they are large. Small PSSs could quite easily be missed with the wrong transducer [87], or if they are intrahepatic and without the use of a contrast [192]. MRI or MRA is a better choice for determining the presence of PSSs as there is no radiation. Although standard MRI cannot visualise

blood flow in veins or arteries, the addition of a contrast dye makes it easier for the MRI to demonstrate the vein [193].

An additional concern with radiological PSS detection techniques is their sensitivity and specificity, which may be insufficient to detect small or microscopic PSSs. Angiography, CTA, and similarly scintigraphy may be better in detecting the smaller intrahepatic shunts as they can be visualised with a contrast dye or radioactive dye respectively [194]. Even if the PSS cannot be clearly identified by the dye, the connecting veins may still be visible, indicating the presence of a PSS. This may be especially useful for the detection of Park Type IV shunts.

Not all PSSs will have a similar size even across the different types. Many cases have reported the PSS to be 'large' or to have a diameter between 0.2 – 5 cm [8, 19, 51, 117, 129, 132, 134, 138, 144, 149, 154, 163, 169, 177, 178, 180, 181, 187]. There were ten Abernethy cases where the PSS was reported to be between 1 – 5 cm in diameter or as large/giant [19, 51, 117, 129, 144, 154, 163, 177, 180, 181], whereas there were eight Park cases that reported the PSS diameter to range between 2 – 7 mm in diameter and large or enormous in size[8, 132, 134, 138, 149, 169, 178, 187]. The larger diameter will increase the volume of flow to the heart, however this is not necessarily related to the severity of any associated symptoms.

Several reports using Doppler ultrasound scanning and scintigraphy went further to measure an associated shunt rate (Table 5). It has been suggested that encephalopathy is not associated with PSS, even in patients with cirrhotic livers if the shunted fraction is less than 24 – 30%. [118, 129] Although, children are less likely to have hepatic encephalopathy even with shunt ratio of 60%. Elderly patients with a shunting ratio larger than 60% have the greatest risk of hepatic encephalopathy. [15, 29, 73]

Few risk factors are actually distinguishable between age, sex, symptoms and pre-existing disease. Since the discovery of PSSs is often serendipitous, no clear conclusions can be made about the age it is acquired. Large PSS can be associated with a few symptoms, such as encephalopathy, disorientation or other neural and psychiatric disorders, [195] idiopathic portal hypertension and Osler-Weber-Rendu disease. [124, 138] Pain itself has not been directly associated with PSSs. Disregarding patients with a pre-existing disease, what is interesting is the lack of symptoms in several cases. If a person is asymptomatic, then the chance of a PSS being discovered would be low. However, it is also possible that some symptoms may be attributed to the pre-existing condition and therefore it is still unlikely that a PSS will be discovered. Consequently, it is impossible to provide an incidence of PSSs in patients without cirrhosis.

Twenty patients reported to have high serum levels of ammonia. This is comparable to the findings in patients with cirrhotic liver disease and one of the known associations of PSS is high serum ammonia. [30] Ammonia plasma levels alone are not conclusive enough to determine the presence of a PSS, but it can be used as an indication of a PSS to indirectly determine the severity of the shunt. [30, 195] Fourteen patients were also tested for ICG R15. Eleven had retention up to four times higher than normal (<10%) ICG. These levels are similar to those seen in a cirrhotic patient. Typically, high ICG R15 levels indicate severe liver dysfunction, but if other tests, such as liver biochemistry blood test and biopsies, show no sign of liver failure, ICG R15 may well be a strong indicator of a PSS. Issues with both ammonia and ICG R15 tests are that, alone, they are neither conclusive nor quantitative. However, if the ammonia serum test is used in conjunction with ICG R15 test, integration of these two biomarkers could serve as a more conclusive test for a PSS, and would be indicative of the need for further imaging tests.

Depending on the severity and/or Type of PSS, treatment options may be limited. If the patient shows no symptoms and is in good health, then there may not be any need for treatment. In most cases, patients were treated for their symptoms of encephalopathy and pain, and not for the actual PSS. In some extreme cases, where a PSS was having a serious effect on the patient, the patient underwent surgical treatment for either an occlusion, ligation or embolization procedure. [117, 142, 153, 160, 163, 164, 166, 177, 180]

Conclusion

Over 29 years, there were 112 cases of PSSs in adult patients with functionally healthy livers, which were critically reviewed. Most PSSs were serendipitously found with a high prevalence in middle aged patients and especially in women. Doppler ultrasound and CT were more commonly used in the detection of PSSs. However these methods are not guaranteed to find a PSS and they could be easily missed. It is suggested that a combination of methods is used, which may decrease the chance of a PSS being missed, although more attention to this research area is required. Microscopic PSSs could easily be missed using any of the current techniques available, and therefore answering the question if PSS has a role in metastatic distribution is currently not possible. A novel technique is needed that can quantify PSSs and is less susceptible to the downfalls and limitations of radiological techniques is needed future study, in order to provide evidence in answering what role PSSs may play in metastatic distribution.

References

1. Hales MR, Allan JS, Hall EM. Injection-corrosion studies of normal and cirrhotic livers. The American journal of pathology. 1959;35:909-41
2. Stringer MD. The clinical anatomy of congenital portosystemic venous shunts. Clin Anat. 2008;21(2):147-57
3. Abernethy J, Banks J. Account of Two Instances of Uncommon Formation, in the Viscera of the Human Body. Philosophical Transactions of the Royal Society of London. 1793;83:59-66
4. Bellah RD, Hayek J, Teele RL. Anomalous portal venous connection to the suprahepatic vena cava: sonographic demonstration. Pediatr Radiol. 1989;20(1-2):115-7
5. Morgan G, Superina R. Congenital absence of the portal vein: two cases and a proposed classification system for portasystemic vascular anomalies. J Pediatr Surg. 1994;29(9):1239-41
6. Murray CP, Yoo SJ, Babyn PS. Congenital extrahepatic portosystemic shunts. Pediatr Radiol. 2003;33(9):614-20
7. Doehner GA, Ruzicka FF, Jr., Rousselot LM, Hoffman G. The portal venous system: on its pathological roentgen anatomy. Radiology. 1956;66(2):206-17
8. Mori H, Hayashi K, Fukuda T, Matsunaga N, Futagawa S, Nagasaki M, et al. Intrahepatic portosystemic venous shunt: Occurrence in patients with and without liver cirrhosis. American Journal of Roentgenology. 1987;149(4):711-4
9. Park JH, Cha SH, Han JK, Han MC. Intrahepatic portosystemic venous shunt. American Journal of Roentgenology. 1990;155(3):527-8
10. Couinaud C. Bases anatomiques des hépatectomies gauche et droite réglées. Journal de Chirurgie. 1954;70:933-66
11. Couinaud C. Le fouie: études anatomiques et chirurgicales. Masson. 1957:74-5
12. Guerin F, Blanc T, Gauthier F, Abella SF, Branchereau S. Congenital portosystemic vascular malformations. Semin Pediatr Surg. 2012;21(3):233-44
13. Joyce AD, Howard ER. Rare congenital anomaly of the portal vein. British Journal of Surgery. 1988;75(10):1038-9
14. Grazioli L, Alberti D, Olivetti L, Rigamonti W, Codazzi F, Matricardi L, et al. Congenital absence of portal vein with nodular regenerative hyperplasia of the liver. European Radiology. 2000;10(5):820-5
15. Altavilla G, Cusatelli P. Ultrastructural analysis of the liver with portal vein agenesis: A case report. Ultrastructural Pathology. 1998;22(6):477-83
16. Kinjo T, Aoki H, Sunagawa H, Kinjo S, Muto Y. Congenital absence of the portal vein associated with focal nodular hyperplasia of the liver and congenital choledochal cyst: A case report. Journal of Pediatric Surgery. 2001;36(4):622-5
17. Kim SZ, Marz PL, Laor T, Teitelbaum J, Jonas MM, Levy HL. Elevated galactose in newborn screening due to congenital absence of the portal vein [4]. European Journal of Pediatrics. 1998;157(7):608-9
18. Shinkai M, Ohhama Y, Nishi T, Yamamoto H, Fujita S, Take H, et al. Congenital absence of the portal vein and role of liver transplantation in children. J Pediatr Surg. 2001;36(7):1026-31
19. Bonington SC, Hodgson DI, Mehta S, Lynch N, Chalmers N. A congenital venous anomaly, with a portal-systemic shunt into a previously undescribed intra-thoracic vein. Clin Radiol. 2002;57(7):658-60

20. Arana E, Martí-Bonmatí L, Martínez V, Hoyos M, Montes H. Portal vein absence and nodular regenerative hyperplasia of the liver with giant inferior mesenteric vein. Abdominal Imaging. 1997;22(5):506-8
21. Goo HW. Extrahepatic portosystemic shunt in congenital absence of the portal vein depicted by time-resolved contrast-enhanced MR angiography. Pediatric Radiology. 2007;37(7):706-9
22. Mboyo A, Lemouel A, Sohm O, Gondy S, Destuynder O, De Billy B, et al. Congenital extra-hepatic portocaval shunt. Concerning a case of antenatal diagnosis. European Journal of Pediatric Surgery. 1995;5(4):243-5
23. Howard ER, Davenport M. Congenital extrahepatic portocaval shunts - The Abernethy malformation. Journal of Pediatric Surgery. 1997;32(3):494-7
24. Kanamori Y, Hashizume K, Kitano Y, Sugiyama M, Motoi T, Tange T. Congenital extrahepatic portocaval shunt (Abernethy type 2), huge liver mass, and patent ductus arteriosus--a case report of its rare clinical presentation in a young girl. J Pediatr Surg. 2003;38(4):E15
25. Ikeda S, Sera Y, Ohshiro H, Uchino S, Uchino T, Endo F. Surgical indications for patients with hyperammonemia. J Pediatr Surg. 1999;34(6):1012-5
26. Tercier S, Delarue A, Rouault F, Roman C, Bréaud J, Petit P. Congenital portocaval fistula associated with hepatopulmonary syndrome: Ligation vs liver transplantation. Journal of Pediatric Surgery. 2006;41(2):E1-E3
27. Takayama Y, Moriura S, Nagata J, Akutagawa A, Hirano A, Ishiguro S, et al. Embolization of the left portal vein to inferior vena cava shunts for chronic recurrent hepatic encephalopathy via the mesenteric vein. Journal of Gastroenterology and Hepatology. 2001;16(12):1425-8
28. Akita H, Suzuki H, Ito K, Kinoshita S, Sato N, Takikawa H, et al. Characterization of bile acid transport mediated by multidrug resistance associated protein 2 and bile salt export pump. Biochimica et Biophysica Acta - Biomembranes. 2001;1511(1):7-16
29. Akahoshi T, Nishizaki T, Wakasugi K, Mastuzaka T, Kume K, Yamamoto I, et al. Portal-systemic encephalopathy due to a congenital extrahepatic portosystemic shunt: three cases and literature review. Hepatogastroenterology. 2000;47(34):1113-6
30. Tarantino G, Citro V, Esposito P, Giaquinto S, de Leone A, Milan G, et al. Blood ammonia levels in liver cirrhosis: a clue for the presence of portosystemic collateral veins. BMC Gastroenterol. 2009;9:21
31. Sakura N, Mizoguchi N, Eguchi T, Ono H, Mawatari H, Naitou K, et al. Elevated plasma bile acids in hypergalactosaemic neonates: a diagnostic clue to portosystemic shunts. Eur J Pediatr. 1997;156(9):716-8
32. Kono T, Hiki T, Kuwashima S, Hashimoto T, Kaji Y. Hypergalactosemia in early infancy: diagnostic strategy with an emphasis on imaging. Pediatr Int. 2009;51(2):276-82
33. Nishimura Y, Tajima G, Dwi Bahagia A, Sakamoto A, Ono H, Sakura N, et al. Differential diagnosis of neonatal mild hypergalactosaemia detected by mass screening: clinical significance of portal vein imaging. J Inherit Metab Dis. 2004;27(1):11-8
34. Marois D, Van Heerden JA, Carpenter HA, Sheedy Ii PF. Congenital absence of the portal vein. Mayo Clinic Proceedings. 1979;54(1):55-9
35. Laverdiere JT, Laor T, Benacerraf B. Congenital absence of the portal vein: Case report and MR demonstration. Pediatric Radiology. 1995;25(1):52-3

36. Yonemitsu H, Mori H, Kimura T, Kagawa K, Tsuda T, Yamada Y, et al. Congenital extrahepatic portocaval shunt associated with hepatic hyperplastic nodules in a patient with Dubin-Johnson syndrome. Abdom Imaging. 2000;25(6):572-5
37. Massin M, Verloes A, Jamblin P. Cardiac anomalies associated with congenital absence of the portal vein. Cardiology in the Young. 1999;9(5):522-5
38. Kitagawa S, Gleason WA, Jr., Northrup H, Middlebrook MR, Ueberschar E. Symptomatic hyperammonemia caused by a congenital portosystemic shunt. J Pediatr. 1992;121(6):917-9
39. Mizoguchi N, Sakura N, Ono H, Naito K, Hamakawa M. Congenital porto-left renal venous shunt as a cause of galactosaemia. J Inherit Metab Dis. 2001;24(1):72-8
40. Woodle ES, Thislethwaite JR, Emond JC, Whitington PF, Vogelbach P, Yousefzadeh DK, et al. Successful hepatic transplantation in congenital absence of recipient portal vein. Surgery. 1990;107(4):475-9
41. Nakasaki H, Tanaka Y, Ohta M, Kanemoto T, Mitomi T, Iwata Y, et al. Congenital absence of the portal vein. Annals of Surgery. 1989;210(2):190-3
42. Ikeda H, Aotsuka H, Nakajima H, Sawada M. Portosystemic shunt with polysplenia and hypoplastic left heart syndrome. Pediatr Cardiol. 2005;26(4):446-8
43. Olling S, Olsson R. Congenital absence of portal venous system in a 50 year old woman. Acta Medica Scandinavica. 1974;196(4):343-5
44. Morse SS, Taylor KJW, Strauss EB. Congenital absence of the portal vein in oculoauriculovertebral dysplasia (Goldenhar syndrome). Pediatric Radiology. 1986;16(5):437-9
45. Guariso G, Fiorio S, Altavilla G, Gamba PG, Toffolutti T, Chiesura-Corona M, et al. Congenital absence of the portal vein associated with focal nodular hyperplasia of the liver and cystic dysplasia of the kidney. European Journal of Pediatrics. 1998;157(4):287-90
46. Wakamoto H, Manabe K, Kobayashi H, Hayashi M. Subclinical portal-systemic encephalopathy in a child with congenital absence of the portal vein. Brain Dev. 1999;21(6):425-8
47. Motoori S, Shinozaki M, Goto N, Kondo F. Case report: Congenital absence of the portal vein associated with nodular hyperplasia in the liver. Journal of Gastroenterology and Hepatology. 1997;12(9-10):639-43
48. Matsuoka Y, Ohtomo K, Okubo T, Nishikawa J, Mine T, Ohno S. Congenital absence of the portal vein. Gastrointestinal Radiology. 1992;17(1):31-3
49. Shah R, Ford EG, Woolley MM. Congenital portocaval shunt. Pediatric Surgery International. 1992;7(3):216-7
50. Usuki N, Miyamoto T. A case of congenital absence of the intrahepatic portal vein diagnosed by MR angiography. Journal of Computer Assisted Tomography. 1998;22(5):728-9
51. Ohwada S, Hamada Y, Morishita Y, Tanahashi Y, Takeyoshi I, Kawashima Y, et al. Hepatic encephalopathy due to congenital splenorenal shunts: report of a case. Surg Today. 1994;24(2):145-9
52. Tanano H, Hasegawa T, Kawahara H, Sasaki T, Okada A. Biliary atresia associated with congenital structural anomalies. Journal of Pediatric Surgery. 1999;34(11):1687-90
53. Ji EK, Yoo SJ, Kim JH, Cho KS. Congenital splenorenal venous shunt detected by prenatal ultrasonography. Journal of Ultrasound in Medicine. 1999;18(6):437-9
54. Gitzelmann R, Forster I, Willi UV. Hypergalactosaemia in a newborn: Self-limiting intrahepatic portosystemic venous shunt. European Journal of Pediatrics. 1997;156(9):719-22

55. Uchino T, Matsuda I, Endo F. The long-term prognosis of congenital portosystemic venous shunt. Journal of Pediatrics. 1999;135(2 I):254-6
56. Barton Iii JW, Keller MS. Liver transplantation for hepatoblastoma in a child with congenital absence of the portal vein. Pediatric Radiology. 1989;20(1-2):113-4
57. Pohl A, Jung A, Vielhaber H, Pfluger T, Schramm T, Lang T, et al. Congenital atresia of the portal vein and extrahepatic portocaval shunt associated with benign neonatal hemangiomatosis, congenital adrenal hyperplasia, and atrial septal defect. Journal of Pediatric Surgery. 2003;38(4):633-4
58. Valls E, Ceres L, Urbaneja A, Muñoz R, Alonso I. Color doppler sonography in the diagnosis of neonatal intrahepatic portosystemic shunts. Journal of Clinical Ultrasound. 2000;28(1):42-6
59. Yamagami T, Nakamura T, Tokiwa K, Ohno K, Itoh H, Maeda T. Intrahepatic portosystemic venous shunt associated with biliary atresia: Case report. Pediatric Radiology. 2000;30(7):489-91
60. Komaba Y, Nomoto T, Hiraide T, Kitamura S, Terashi A. Persistent Primitive Hypoglossal Artery Complicated by Atrial Septal Defect and Congenital Intrahepatic Shunts. Internal Medicine. 1998;37(1):60-4
61. Ono H, Mawatari H, Mizoguchi N, Eguchi T, Sakura N. Clinical features and outcome of eight infants with intrahepatic porto- venous shunts detected in neonatal screening for galactosaemia. Acta Paediatrica, International Journal of Paediatrics. 1998;87(6):631-4
62. Mori K, Dohi T, Yamamoto H, Kamada M. An enormous shunt between the portal and hepatic veins associated with multiple coronary artery fistulas. Pediatric Radiology. 1990;21(1):66-8
63. Kalifa G, Brunelle F, Chaumont P. Congenital porto-caval fistula. FISTULE PORTO-CAVE CONGENITALE. 1978;21(2-3):183-6
64. Gallego C, Miralles M, Marín C, Muyor P, González G, García-Hidalgo E. Congenital hepatic shunts. Radiographics. 2004;24(3):755-72
65. Starzl TE, Francavilla A, Halgrimson CG, Francavilla FR, Porter KA, Brown TH, et al. The origin, hormonal nature, and action of hepatotrophic substances in portal venous blood. Surgery Gynecology and Obstetrics. 1973;137(2):179-99
66. Chiu B, Melin-Aldana H, Pillai S, Chu F, Superina RA. Factor VII transcription correlates with hepatocyte proliferation and hepatocyte growth factor expression in a rodent extrahepatic portal vein obstruction model. J Am Coll Surg. 2007;205(2):277-83
67. Gandhi CR, Murase N, Subbotin VM, Uemura T, Nalesnik M, Demetris AJ, et al. Portacaval shunt causes apoptosis and liver atrophy in rats despite increases in endogenous levels of major hepatic growth factors. J Hepatol. 2002;37(3):340-8
68. Superina R, Bambini DA, Lokar J, Rigsby C, Whitington PF. Correction of extrahepatic portal vein thrombosis by the mesenteric to left portal vein bypass. Ann Surg. 2006;243(4):515-21
69. Vonnahme FJ, Dubuisson L, Kubale R. Ultrastructural characteristics of hyperplastic alterations in the liver of congenital portacaval-shunt rats. British Journal of Experimental Pathology. 1984;65(5):585-96
70. Bioulac-Sage P, Saric J, Boussarie L, Balabaud C. Congenital portacaval shunt in rats: Liver adaptation to lack of portal vein - A light and electron microscopic study. Hepatology. 1985;5(6):1183-9
71. Satoh M, Yokoya S, Hachiya Y, Hachiya M, Fujisawa T, Hoshino K, et al. Two hyperandrogenic adolescent girls with congenital portosystemic shunt. European Journal of Pediatrics. 2001;160(5):307-11

72. Kamata S, Kitayama Y, Usui N, Kuroda S, Nose K, Sawai T, et al. Patent ductus venosus with a hypoplastic intrahepatic portal system presenting intrapulmonary shunt: a case treated with banding of the ductus venosus. J Pediatr Surg. 2000;35(4):655-7
73. Uchino T, Endo F, Ikeda S, Shiraki K, Sera Y, Matsuda I. Three brothers with progressive hepatic dysfunction and severe hepatic steatosis due to a patent ductus venosus. Gastroenterology. 1996;110(6):1964-8
74. Hori T, Yonekawa Y, Okamoto S, Ogawa K, Ogura Y, Oike F, et al. Pediatric orthotopic living-donor liver transplantation cures pulmonary hypertension caused by Abernethy malformation type Ib. Pediatr Transplant. 2011;15(3):e47-52
75. Yoshidome H, Edwards MJ. An embryological perspective on congenital portacaval shunt: a rare anomaly in a patient with hepatocellular carcinoma. Am J Gastroenterol. 1999;94(9):2537-9
76. Santamaría G, Pruna X, Serres X, Inaraja L, Zuasnabar A, Castellote A. Congenital intrahepatic portosystemic venous shunt: Sonographic and magnetic resonance imaging. European Radiology. 1996;6(1):76-8
77. Caiulo VA, Presta G, Latini G, Mattioli G, Jasonni V. Diagnosis and follow-up of congenital intrahepatic portosystemic venous shunt by ultrasounds [2]. Acta Paediatrica, International Journal of Paediatrics. 2001;90(10):1209-10
78. Meyer WW, Lind J. The ductus venosus and the mechanism of its closure. Archives of disease in childhood. 1966;41(220):597-605
79. Loberant N, Barak M, Gaitini D, Herskovits M, Ben-Elisha M, Roguin N. Closure of the ductus venosus in neonates: Findings on real-time gray- scale, color-flow Doppler, and duplex Doppler sonography. American Journal of Roentgenology. 1992;159(5):1083-5
80. Fugelseth D, Lindemann R, Liestøl K, Kiserud T, Langslet A. Ultrasonographic study of ductus venosus in healthy neonates. Archives of Disease in Childhood: Fetal and Neonatal Edition. 1997;77(2):F131-F4
81. Yoshimoto Y, Shimizu R, Saeki T, Harada T, Sugio Y, Nomura S, et al. Patent ductus venosus in children: a case report and review of the literature. J Pediatr Surg. 2004;39(1):E1-5
82. Jacob S, Farr G, De Vun D, Takiff H, Mason A. Hepatic manifestations of familial patent ductus venosus in adults. Gut. 1999;45(3):442-5
83. Matsubara T, Sumazaki R, Saitoh H, Imai H, Nakayama J, Takita H. Patent ductus venosus associated with tumor-like lesions of the liver in a young girl. J Pediatr Gastroenterol Nutr. 1996;22(1):107-11
84. Moncure AC, Waltman AC, Vandersalm TJ. Gastrointestinal hemorrhage from adhesion related mesenteric varices. Annals of Surgery. 1976;183(1):24-9
85. Wall BF, Hart D. Revised radiation doses for typical X-ray examinations: Report on a recent review of doses to patients from medical X-ray examinations in the UK by NRPB. British Journal of Radiology. 1997;70(MAY):437-9
86. Afzal S, Nair A, Grainger J, Latif S, Rehman AU. Spontaneous thrombosis of congenital extrahepatic portosystemic shunt (abernethy malformation) simulating inguinal hernia incarceration. Vascular and Endovascular Surgery. 2010;44(6):508-10
87. Rizzatto G. Ultrasound transducers. Eur J Radiol. 1998;27 Suppl 2:S188-95
88. Lisovsky M, Konstas AA, Misdraji J. Congenital extrahepatic portosystemic shunts (abernethy malformation): A histopathologic evaluation. American Journal of Surgical Pathology. 2011;35(9):1381-90

89. Charre L, Roggen F, Lemaire J, Mathijs J, Goffette P, Danse E, et al. Hematochezia and congenital extrahepatic portocaval shunt with absent portal vein: Successful treatment by liver transplantation [1]. Transplantation. 2004;78(9):1404-6
90. Florio F, Nardella M, Balzano S, Giacobbe A, Perri F. Congenital intrahepatic portosystemic shunt. Cardiovasc Intervent Radiol. 1998;21(5):421-4
91. Ghetie C, Davies M, Cornfeld D, Suh N, Saif MW. Expectoration of a lung metastasis in a patient with colorectal carcinoma. Clin Colorectal Cancer. 2008;7(4):283-6
92. Pantel K, Brakenhoff RH. Dissecting the metastatic cascade. Nat Rev Cancer. 2004;4(6):448-56
93. Wolfrum F, Vogel I, Fandrich F, Kalthoff H. Detection and clinical implications of minimal residual disease in gastro-intestinal cancer. Langenbecks Arch Surg. 2005;390(5):430-41
94. Tan KK, Lopes Gde L, Jr., Sim R. How uncommon are isolated lung metastases in colorectal cancer? A review from database of 754 patients over 4 years. J Gastrointest Surg. 2009;13(4):642-8
95. Netter F. Portal Vein Tributaries: Portacaval Anastomoses. In: Colacino S, editor. Atlas of Human Anatomy. Basle, Switzerland: CIBA-GEIGY Limited; 1989.
96. Gupta GP, Massague J. Cancer metastasis: building a framework. Cell. 2006;127(4):679-95
97. Zhe X, Cher ML, Bonfil RD. Circulating tumor cells: finding the needle in the haystack. Am J Cancer Res. 2011;1(6):740-51
98. Steinert G, Scholch S, Koch M, Weitz J. Biology and significance of circulating and disseminated tumour cells in colorectal cancer. Langenbecks Arch Surg. 2012;397(4):535-42
99. Yu M, Stott S, Toner M, Maheswaran S, Haber DA. Circulating tumor cells: approaches to isolation and characterization. J Cell Biol. 2011;192(3):373-82
100. Miller MC, Doyle GV, Terstappen LW. Significance of Circulating Tumor Cells Detected by the CellSearch System in Patients with Metastatic Breast Colorectal and Prostate Cancer. J Oncol. 2010;2010:617421
101. Chaffer CL, Weinberg RA. A perspective on cancer cell metastasis. Science. 2011;331(6024):1559-64
102. Fidler IJ. The pathogenesis of cancer metastasis: the 'seed and soil' hypothesis revisited. Nat Rev Cancer. 2003;3(6):453-8
103. Chambers AF, Groom AC, MacDonald IC. Dissemination and growth of cancer cells in metastatic sites. Nat Rev Cancer. 2002;2(8):563-72
104. Hanahan D, Weinberg RA. The hallmarks of cancer. Cell. 2000;100(1):57-70
105. Joyce JA, Pollard JW. Microenvironmental regulation of metastasis. Nat Rev Cancer. 2009;9(4):239-52
106. Lore JM, Jr., Madden JL, Gerold FP. Pre-existing portacaval shunts: a hypothesis for the bizarre metastases of some carcinomas. Cancer. 1958;11(1):24-7
107. Saitoh H, Yoshida KI, Uchijima Y, Kobayashi N, Suwata J, Nakame Y. Possible metastatic routes via portacaval shunts in renal adenocarcinoma with liver metastasis. Urology. 1991;37(6):598-601
108. Wallace MJ, Madoff DC, Ahrar K, Warneke CL. Transjugular intrahepatic portosystemic shunts: Experience in the oncology setting. Cancer. 2004;101(2):337-45
109. Bayon LG, Izquierdo MA, Sirovich I, van Rooijen N, Beelen RH, Meijer S. Role of Kupffer cells in arresting circulating tumor cells and controlling metastatic growth in the liver. Hepatology. 1996;23(5):1224-31

110. Pearson HJ, Anderson J, Chamberlain J, Bell PR. The effect of Kupffer cell stimulation or depression on the development of liver metastases in the rat. Cancer Immunol Immunother. 1986;23(3):214-6
111. Ryden S, Bergqvist L, Hafstrom L, Hultberg B, Stenram U, Strand SE. Influence of a reticuloendothelial-suppressing agent on liver tumor growth in the rat. J Surg Oncol. 1984;26(4):245-51
112. Geng Y, Marshall JR, King MR. Glycomechanics of the metastatic cascade: tumor cell-endothelial cell interactions in the circulation. Ann Biomed Eng. 2012;40(4):790-805
113. Li J, King MR. Adhesion receptors as therapeutic targets for circulating tumor cells. Front Oncol. 2012;2:79
114. Kansas GS. Selectins and their ligands: current concepts and controversies. Blood. 1996;88(9):3259-87
115. Varki A. Selectin ligands: will the real ones please stand up? J Clin Invest. 1997;100(11 Suppl):S31-5
116. Kohler S, Ullrich S, Richter U, Schumacher U. E-/P-selectins and colon carcinoma metastasis: first in vivo evidence for their crucial role in a clinically relevant model of spontaneous metastasis formation in the lung. Br J Cancer. 2010;102(3):602-9
117. Nishie A, Yoshimitsu K, Honda H, Kaneko K, Kuroiwa T, Fukuya T, et al. Treatment of hepatic encephalopathy by retrograde transcaval coil embolization of an ileal vein-to-right gonadal vein portosystemic shunt. Cardiovasc Intervent Radiol. 1997;20(3):222-4
118. Kudo M, Tomita S, Tochio H, Minowa K, Todo A. Intrahepatic portosystemic venous shunt: Diagnosis by color Doppler imaging. American Journal of Gastroenterology. 1993;88(5):723-9
119. Bodner G, Gluck A, Springer P, Konig P, Perkmann R. Aneurysmal portosystemic venous shunt: A case report. Ultraschall in der Medizin. 1999;20(5):215-7
120. Fanelli F, Marcelli G, Bezzi M, Salvatori FM, Rossi M, Rossi P, et al. Intrahepatic aneurysmal portohepatic venous shunt: Embolization with a tissue adhesive solution. Journal of Endovascular Therapy. 2003;10(1):147-53
121. Komori A, Kataoka C, Okamura S, Tanoue K, Hashizume M, Ichiki Y, et al. Aneurysmal intraheptic portosystemic venous shunt associated with idiopathic portal hypertension: A lesion evaluated by a 3D image reconstructed from power doppler flow imaging. Journal of Medical Ultrasonics. 2000;27(2):131-7
122. Gheorghiu D, Leibowits O, Bloom RA. Asymptomatic aneurysmal intrahepatic porto-hepatic venous shunt - Diagnosis by ultrasound. Clinical Radiology. 1994;49(1):64-5
123. Cacciapaglia F, Vadacca M, Coppolino G, Buzzulini F, Rigon A, Zennaro D, et al. Spontaneous splenorenal shunt in a patient with antiphospholipid syndrome: The first case reported. Lupus. 2007;16(1):56-8
124. Matsuo M, Kanematsu M, Kato H, Kondo H, Sugisaki K, Hoshi H. Osler-Weber-Rendu disease: Visualizing portovenous shunting with three-dimensional sonography. American Journal of Roentgenology. 2001;176(4):919-20
125. Oktenli C, Gul D, Deveci MS, Saglam M, Upadhyaya M, Thompson P, et al. Unusual features in a patient with neurofibromatosis type 1: Multiple subcutaneous lipomas, a juvenile polyp in ascending colon, congenital intrahepatic portosystemic venous shunt, horseshoe kidney. American Journal of Medical Genetics. 2004;127(3):298-301
126. Lin ZY, Chen SC, Hsieh MY, Wang CW, Chuang WL, Wang LY. Incidence and clinical significance of spontaneous intrahepatic portosystemic venous shunts detected by

sonography in adults without potential cause. Journal of Clinical Ultrasound. 2006;34(1):22-6
127. Di Candio G, Campatelli A, Mosca F, Santi V, Casanova P, Bolondi L. Ultrasound detection of unusual spontaneous portosystemic shunts associated with uncomplicated portal hypertension. J Ultrasound Med. 1985;4(6):297-305
128. Leyendecker JR, Grayson DE, Good R. Transient postpartum portosystemic shunting revealed by MR venography. AJR American journal of roentgenology. 2002;178(5):1152-4
129. Konno K, Ishida H, Uno A, Ohnami Y, Masamune O. Large extrahepatic portosystemic shunt without portal hypertension. Abdom Imaging. 1997;22(1):79-81
130. Horiguchi Y, Kitano T, Takagawa H, Imai H, Itoh M, Miyakawa S, et al. A large inferior mesenteric-caval shunt via the internal iliac vein. Gastroenterol Jpn. 1988;23(6):684-7
131. Kerlan RK, Jr., Sollenberger RD, Palubinskas AJ, Raskin NH, Callen PW, Ehrenfeld WK. Portal-systemic encephalopathy due to a congenital portocaval shunt. AJR Am J Roentgenol. 1982;139(5):1013-5
132. Horiguchi Y, Kitano T, Imai H, Ohsuki M, Yamauchi M, Itoh M. Intrahepatic portal-systemic shunt: its etiology and diagnosis. Gastroenterol Jpn. 1987;22(4):496-502
133. Oguz B, Akata D, Balkanci F, Akhan O. Intrahepatic portosystemic venous shunt: Diagnosis by colour/power Doppler imaging and three-dimensional ultrasound. British Journal of Radiology. 2003;76(907):487-90
134. Shapiro RS, Winsberg F, Stancato-Pasik A, Sterling KM. Color Doppler sonography of vascular malformations of the liver. J Ultrasound Med. 1993;12(6):343-8
135. Wittich G, Jantsch H, Tscholakoff D. Congenital portosystemic shunt diagnosed by combined real-time and Doppler sonography. J Ultrasound Med. 1985;4(6):315-8
136. Chagnon SF, Vallee CA, Barge J, Chevalier LJ, Le Gal J, Blery MV. Aneurysmal portahepatic venous fistula: report of two cases. Radiology. 1986;159(3):693-5
137. Thakur SK, Dalai SS. Balloon retrograde transvenous occlusion of fundic varix. Indian J Gastroenterol. 2010;29(2):88-9
138. Matsumoto S, Mori H, Yamada Y, Hayashida T, Hori Y, Kiyosue H. Intrahepatic porto-hepatic venous shunts in Rendu-Osler-Weber disease: Imaging demonstration. European Radiology. 2004;14(4):592-6
139. Filik L, Boyacioglu S. Asymptomatic aneurysmal portosystemic venous shunt: a case report and review of the literature. Acta medica (Hradec Králové) / Universitas Carolina, Facultas Medica Hradec Králové. 2006;49(4):241-4
140. Crespin J, Nemcek A, Rehkemper G, Blei AT. Intrahepatic portal-hepatic venous anastomosis: A portal-systemic shunt with neurological repercussions. American Journal of Gastroenterology. 2000;95(6):1568-71
141. Machida H, Ueno E, Isobe Y, Nishimaki H, Fujimura M, Tomimatsu M, et al. Stent-graft to treat intrahepatic portosystemic venous shunt causing encephalopathy. Hepato-Gastroenterology. 2008;55(81):237-40
142. Lin YT, Chang CH, Chen WC. Asymptomatic congenital splenorenal shunt in a noncirrhotic patient with a left adrenal aldosterone-producing adenoma. Kaohsiung J Med Sci. 2009;25(12):669-74
143. Konstas AA, Digumarthy SR, Avery LL, Wallace KL, Lisovsky M, Misdraji J, et al. Congenital portosystemic shunts: Imaging findings and clinical presentations in 11 patients. European Journal of Radiology. 2011;80(2):175-81
144. Kuramitsu T, Komatsu M, Matsudaira N, Naganuma T, Niizawa M, Zeniya A, et al. Portal-systemic encephalopathy from a spontaneous gastrorenal shunt diagnosed

by three-dimensional computed tomography and treated effectively by percutaneous vascular embolization. Liver. 1998;18(3):208-12
145. Ortiz M, Cordoba J, Alonso J, Rovira A, Quiroga S, Jacas C, et al. Oral glutamine challenge and magnetic resonance spectroscopy in three patients with congenital portosystemic shunts. J Hepatol. 2004;40(3):552-7
146. Sawyer B, Dow C, Frank J, Lau E. Congenital portocaval shunt-associated liver lesions in a patient with cancer. ANZ J Surg. 2008;78(7):613-4
147. Ishii Y, Inagaki Y, Hirai K, Aoki T. Hepatic encephalopathy caused by congenital extrahepatic portosystemic venous shunt. J Hepatobiliary Pancreat Surg. 2000;7(5):524-8
148. Imamura H, Momose T, Kitabayashi H, Takahashi W, Yazaki Y, Takenaka H, et al. Pulmonary hypertension as a result of asymptomatic portosystemic shunt. Jpn Circ J. 2000;64(6):471-3
149. Senocak E, Oguz B, Edguer T, Cila A. Congenital intrahepatic portosystemic shunt with variant inferior right hepatic vein. Diagn Interv Radiol. 2008;14(2):97-9
150. Soyer P, Bluemke DA, Sitzmann JV, Hruban RH, Fishman EK. Hepatocellular carcinoma: findings on spiral CT during arterial portography. Abdom Imaging. 1995;20(6):541-6
151. Hekimoglu K, Ustundag Y. Cavernous hemangioma with arterioportal and portosystemic shunts: precise diagnosis with dynamic multidetector computed tomography imaging. Abdom Imaging. 2010;35(3):328-31
152. Eren S, Karaman A, Okur A. The superior vena cava syndrome caused by malignant disease. Imaging with multi-detector row CT. Eur J Radiol. 2006;59(1):93-103
153. Park SW, Kang HS, Kim YJ, Lee MW, Roh HG. Successful occlusion of spontaneous portosystemic shunts leading to encephalopathy in a non-cirrhotic patient by using the Amplatzer vascular plug. Acta Radiol. 2007;48(10):1077-81
154. Kimura N, Kumamoto T, Hanaoka T, Nakamura K, Hazama Y, Arakawa R. Portal-systemic shunt encephalopathy presenting with diffuse cerebral white matter lesion: an autopsy case. Neuropathology. 2008;28(6):627-32
155. Ito K, Takada T, Amano H, Toyota N, Yasuda H, Yoshida M, et al. Localization of islet-cell hyperplasia: value of pre- and intraoperative arterial stimulation and venous sampling. J Hepatobiliary Pancreat Surg. 2004;11(3):203-6
156. Handra-Luca A, Paradis V, Vilgrain V, Dubois S, Durand F, Belghiti J, et al. Multiple mixed adenoma-focal nodular hyperplasia of the liver associated with spontaneous intrahepatic porto-systemic shunt: a new type of vascular malformation associated with the multiple focal nodular hyperplasia syndrome? Histopathology. 2006;48(3):309-11
157. Raskin NH, Bredesen D, Ehrenfeld WK, Kerlan RK. Periodic confusion caused by congenital extrahepatic portacaval shunt. Neurology. 1984;34(5):666-9
158. Tanaka O, Ishihara K, Oyamada H, Harusato A, Yamaguchi T, Ozawa M, et al. Successful portal-systemic shunt occlusion with balloon-occluded retrograde transvenous obliteration for portosystemic encephalopathy without liver cirrhosis. J Vasc Interv Radiol. 2006;17(12):1951-5
159. Serrien B, Rigauts H, Marchal G, Lambrechts P. Congenital intrahepatic porto-systemic shunt. J Belge Radiol. 1992;75(6):492-4
160. Seyama Y, Sano K, Tang W, Kokudo N, Sakamoto Y, Imamura H, et al. Simultaneous resection of liver cell adenomas and an intrahepatic portosystemic venous shunt with elevation of serum PIVKA-II level. J Gastroenterol. 2006;41(9):909-12
161. Brandenburg VM, Krueger S, Haage P, Mertens P, Riehl J. Heterotaxy syndrome with severe pulmonary hypertension in an adult. South Med J. 2002;95(5):536-8

162. Momoo T, Johkura K, Kuroiwa Y. Spike-wave stupor in a patient with metabolic disorder. J Clin Neurosci. 2006;13(2):301-3
163. Nagino M, Hayakawa N, Kitagawa S, Katoh M, Komatsu S, Nimura Y, et al. Interventional embolization with fibrin glue for a large inferior mesenteric-caval shunt. Surgery. 1992;111(5):580-4
164. Shimono J, Tsuji H, Azuma K, Hashiguchi M, Fujishima M. Recurring encephalopathy abolished by gastrorenal shunt ligation in a diabetic hemodialysis patient. Am J Gastroenterol. 1998;93(2):270-2
165. Ohno T, Muneuchi J, Ihara K, Yuge T, Kanaya Y, Yamaki S, et al. Pulmonary hypertension in patients with congenital portosystemic venous shunt: A previously unrecognized association. Pediatrics. 2008;121(4):e892-e9
166. Takada K, Homma H, Takahashi M, Mezawa S, Miyanishi K, Sumiyoshi T, et al. A case of successful management of portosystemic shunt with autosomal dominant polycystic kidney disease by balloon-occluded retrograde transvenous obliteration and partial splenic embolization. Eur J Gastroenterol Hepatol. 2001;13(1):75-8
167. Yamagami T, Arai Y, Takeuchi Y, Nakamura T, Inaba Y, Matsueda K, et al. Increased hepatic arterial blood flow after decreased portal supply to the liver parenchyma owing to intrahepatic portosystemic venous shunt: Angiographic demonstration using helical CT. British Journal of Radiology. 2000;73(874):1042-5
168. Yoshimitsu K, Andou H, Kudo S, Matsuo Y, Matsumoto S, Nakao T, et al. Multiple intrahepatic portosystemic venous shunts: treatment by portal vein embolization. Cardiovasc Intervent Radiol. 1993;16(1):49-51
169. Yoshikawa K, Matsumoto M, Hamanaka M, Nakagawa M. A case of manganese induced parkinsonism in hereditary haemorrhagic telangiectasia. J Neurol Neurosurg Psychiatry. 2003;74(9):1312-4
170. Ito T, Ikeda N, Watanabe A, Sue K, Kakio T, Mimura H, et al. Obliteration of portal systemic shunts as therapy for hepatic encephalopathy in patients with non-cirrhotic portal hypertension. Gastroenterol Jpn. 1992;27(6):759-64
171. Suga K, Ishikawa Y, Matsunaga N, Tanaka N, Suda H, Handa T. Liver involvement in hereditary haemorrhagic telangiectasia: assessment with 99Tcm-phytate radionuclide angiography and 123I-IMP transrectal portal scintigraphy. Br J Radiol. 2000;73(874):1115-9
172. Nishida T, Okuda A. Case report: Diagnosis of cavo-portal shunt in inferior vena cava obstruction: Comparison between venography and dynamic scintigraphy. Clinical Radiology. 1991;43(4):274-5
173. Chu LS, Chang CP, Liu RS, Wynchank S, Sheu MH, Chiang JH, et al. The 'Fisherman's Waders' sign in a bone scan of inferior vena cava thrombosis associated with nephrotic syndrome. Annals of Nuclear Medicine. 1995;9(4):237-41
174. Ceylan Gunay E, Erdogan A. Incidentally diagnosed portosystemic shunt on 99mTc red blood cell gastrointestinal bleeding scintigraphy. Revista Espanola de Medicina Nuclear. 2011;30(5):329-30
175. Matsuura T, Morimoto Y, Nose K, Hara Y, Akiyama T, Kurita T. Venous abnormalities incidentally accompanied by renal tumors. Urol Int. 2004;73(2):163-8
176. Tanaka A, Morimoto T, Yamamori T, Moriyasu F, Yamaoka Y. Atypical liver hemangioma with shunt: long-term follow-up. J Hepatobiliary Pancreat Surg. 2002;9(6):750-4
177. Ali S, Stolpen AH, Schmidt WN. Portosystemic encephalopathy due to mesoiliac shunt in a patient without cirrhosis. J Clin Gastroenterol. 2010;44(5):381-3
178. Kanda T, Nogawa S, Muramatsu K, Koto A, Fukuuchi Y. Portal systemic encephalopathy presenting with dressing and constructional apraxia. Intern Med. 2000;39(5):419-23

179. Jeng LBB, Chen MF. Intrahepatic portohepatic venous shunt: A case report of successful surgical resection. Archives of Surgery. 1993;128(3):349-52
180. Sato T, Asanuma Y, Ishida H, Hashimoto M, Tanaka J, Andoh H, et al. A case of extrahepatic portosystemic shunt without portal hypertension treated by laparoscopically assisted embolization. Surgery. 1999;126(5):984-6
181. Yamaguchi Y, Okai T, Watanabe H, Motoo Y, Mai M, Matsui O, et al. Myxedema accompanied by huge portal-systemic shunt without portal hypertension. Intern Med. 2001;40(12):1200-4
182. De Gaetano AM, Rinaldi P, Barbaro B, Mirk P, Di Stasi C, Gui B, et al. Intrahepatic portosystemic venous shunts: Color Doppler sonography. Abdominal Imaging. 2007;32(4):463-9
183. Barchetti F, Pellegrino L, Al-Ansari N, De Marco V, Scarpato P, Ialongo P. Congenital absence of the portal vein in a middle-aged man. Surgical and Radiologic Anatomy. 2011;33(4):369-72
184. Yokota T, Tsuchiya K, Umetani K, Furukawa T, Tsukagoshi H. Choreoathetoid movements associated with a spleno-renal shunt. J Neurol. 1988;235(8):487-8
185. Kumar A, Kumar J, Aggarwal R, Srivastava S. Abernethy malformation with portal vein aneurysm. Diagn Interv Radiol. 2008;14(3):143-6
186. Teshima H, Hayashida N, Akashi H, Aoyagi S. Surgical treatment of a descending aortic aneurysm in a patient with noncirrhotic portal hypertension and a portal systemic shunt. Circ J. 2002;66(12):1176-7
187. Matsumoto S, Mori H, Yoshioka K, Kiyosue H, Komatsu E. Effects of portal-systemic shunt embolization on the basal ganglia: MRI. Neuroradiology. 1997;39(5):326-8
188. Collard B, Maleux G, Heye S, Cool M, Bielen D, George C, et al. Value of carbon dioxide wedged venography and transvenous liver biopsy in the definitive diagnosis of Abernethy malformation. Abdom Imaging. 2006;31(3):315-9
189. Chandler TM, Heran MK, Chang SD, Parvez A, Harris AC. Multiple focal nodular hyperplasia lesions of the liver associated with congenital absence of the portal vein. Magn Reson Imaging. 2011;29(6):881-6
190. Hanatate F, Matsuoka H, Mizuno Y, Kitamura T. Porto-hepatic venous shunt via portal vein aneurysm with splenomegaly. J Gastroenterol. 1995;30(6):786-9
191. Villeneuve PJ, Sundaresan RS. Surgical management of colorectal lung metastasis. Clin Colon Rectal Surg. 2009;22(4):233-41
192. Liu Y, Ren W, Liu C, Huang K, Feng Y, Wang X, et al. Contrast-enhanced ultrasonography of the rabbit VX2 tumor model: Analysis of vascular pathology. Oncol Lett. 2012;4(4):685-90
193. Sati P, George IC, Shea CD, Gaitan MI, Reich DS. FLAIR*: a combined MR contrast technique for visualizing white matter lesions and parenchymal veins. Radiology. 2012;265(3):926-32
194. Duddalwar VA. Multislice CT angiography: a practical guide to CT angiography in vascular imaging and intervention. Br J Radiol. 2004;77 Spec No 1:S27-38
195. Degos B, Daelman L, Huberfeld G, Meppiel E, Rabier D, Galanaud D, et al. Portosystemic shunts: an underdiagnosed but treatable cause of neurological and psychiatric disorders. J Neurol Sci. 2012;321(1-2):58-64

Appendix I – Creation of a Portocaval Shunt in Pigs With a Method for Estimating Shunt Fractions

Statement of Authorship

Title of Paper	Creation of a Portocaval Shunt in pigs, with a method to estimating shunt fractions
Publication Status	○ Published, ○ Accepted for Publication, ◉ Submitted for Publication, ○ Publication style
Publication Details	Submitted to Journal of Surgical Research on 31/10/2013

Author Contributions

By signing the Statement of Authorship, each author certifies that their stated contribution to the publication is accurate and that permission is granted for the publication to be included in the candidate's thesis.

Name of Principal Author (Candidate)	Todd Matthews		
Contribution to the Paper	Assisted with surgery, collected and analyzed data, and wrote manuscript.		
Signature		Date	31/10/2013

Name of Co-Author	Markus Trochsler		
Contribution to the Paper	Assisted with surgery and reviewed data and manuscript.		
Signature		Date	31/10/2013

Name of Co-Author	Mark Hamilton		
Contribution to the Paper	Designed and performed the surgical anastomosis.		
Signature		Date	31/10/13

Name of Co-Author	Guy Maddern		
Contribution to the Paper	Supervised development of work and acted as corresponding author.		
Signature		Date	31/10/13

TITLE:

Creation of a Portocaval Shunt in pigs, with a method for estimating shunt fractions

AUTHORS:

Todd Matthews BHthSc (Hons),

Markus Trochsler (MD)

Mark Hamilton (BhB.MBChB FRACS)

Guy J Maddern (MBBS, MS, MD, PhD, FRACS)

AFFILIATION:

Discipline of Surgery, The Queen Elizabeth Hospital, University of Adelaide, Woodville South, South Australia.

RUNNING TITLE:

Creation of a Portocaval Shunt in Pigs

SUBJECT CATEGORY:

Gastrointestinal

CORRESPONDING AUTHOR:

Prof. G.J Maddern
University of Adelaide Discipline of Surgery
The Queen Elizabeth Hospital
28 Woodville Road
Woodville South
SA 5011
Australia
Ph: +61 8 8222 6756
Fax: +61 8 8222 6028
Email: guy.maddern@adelaide.edu.au

Abstract

Introduction

Grafts are used for a wide range of surgical procedures. Validation of blood flow through the graft would typically be measured using Doppler ultrasound. However, there can be large difficulties in measuring the portion of blood diverted in the graft. If equipment is not available, another method may be required. There are several methods that can measure blood flow including Doppler ultrasound, contrast CT, and angiography. However, these were not available and a simple expedient method was employed to measure the volume ratio in relation to a portosystemic shunt.

Methods

An 8mm diameter shunt was created between the portal vein and the inferior vena cava in five female pigs. Flow rate through the shunt was attempted to be measured Doppler ultrasound, and flow direction was determined using pressure difference between the portal vein and inferior vena cava. Evans blue was administered into the portal vein with the shunt open and closed to determine the mean transit time and therefore shunted fraction. The ratio of the portal vein to the shunt was compared to shunted fraction.

Results and Conclusions

Flow rates were not obtainable using the Doppler ultrasound transducer available. The shunt is large enough to allow adequate flow into the inferior vena cava, but still allow hepatopetal flow in the portal vein as confirmed by

pressure gradient. The total volume ratio between the portal vein and shunt can show a sound estimate in fraction of blood shunted that is comparable to pharmacokinetic methodology.

KEY TERMS:

Portosystemic shunt, portocaval shunt, portal vein, graft, inferior vena cava, shunt fraction

Introduction

Artificial grafts were first used experimentally in 1947, in an animal model, to replace the aorta [2]. Today, grafts are used for a wide range of surgical procedures for example aneurysm repair, vascular trauma, hypertension or chronic ischemia [1]. Validation of blood flow through the graft would typically be measured using Doppler ultrasound. In an artificial graft or even a naturally acquired shunt, a physician's primary concern is the flow of oxygenated blood. However, there can be large difficulties in measuring this, and therefore another method may be used if not all equipment is available. There are several other methods that can measure blood flow including Doppler ultrasound, contrast CT, and angiography. If these techniques are not available contrast MRI, thermodilution, blood pressure or even Doppler cuffs can be used.

Typical graft material is made from Polyethylene terephthalate (Dacron) or Polytetrafluoroethylene (PTFE) as they are durable and perform well provided the diameter of the graft is >6 mm [3]. When the graft is attached to tissue, many serum proteins including, albumin, fibrinogen and immunoglobulin, are absorbed into the graft immediately after it is exposed to blood flow and line the graft. The interaction between blood and the graft surface is dependent on surface charge, surface energy and friction. Positive surface charge will allow platelet adhesion, while negative charge will reduced the platelet affinity for adhesion. PTFE shunts are commonly used for vascular procedures

in human medicine as they allow better tissue adhesion than other synthetic materials, and as the surface is negatively charged, it reduces the chance of thrombosis [3]. The patency of PTFE has been demonstrated to last long-term [4-6] and has also been used to create an artificial PSSs for portal hypertension relief [7, 8].

Natural shunts are known to occur commonly in patients with cirrhotic livers, but have also been known to occur in patients with healthy livers. The size and length of these natural portosystemic shunts can range dramatically between patients and also shunt type. In many cases of natural PSSs, blood flow has been hepatopetal, normal flow direction with the pressure difference between the portal vein and inferior vena cava being greatly different [9-26]. There are some cases with Park Type III PSSs that have shown a pressure gradient of 6 to 17 mmHg between the portal branches and hepatic veins [27-29]. It is known that fluid direction is always from high pressure to low pressure, however the rate of flow within the portal vein can change dramatically depending on heart rate, breathing rate, food consumption or even body position. There have been some case studies in both Park and Abernethy PSS that also show the fraction of blood flowing through the PSS. The mean fraction between these cases is 30.4%, ranging from 9% to 68.1% and the shunt flow rate mean was 0.428L/min with a range of 0.08 L/min to 1.2 L/min [24, 27, 30, 31]. Several studies have also shown the size of PSSs found in patients to be <7mm diameter [9-26].

Earlier portocaval shunt animal models have been used to treat hypercholesterolemia [32] or measure cholesterol metabolism [33]. However, appropriate equipment required is not always available to determine flow through the shunt. This study reports an alternative method for determining blood flow through a portocaval shunt when typical blood flow measuring equipment is not available. A swine model was chosen as they have similar sized blood vessels and liver function to humans. A pig's portal vein and inferior vena cava have a similar diameter between 14-16mm and similar flow rates to that of humans with the liver size (~1500cm^3).

Materials & Methods

This study was approved by the University of Adelaide Animal Ethics Committee and the Institute of Medical and Veterinary Science Animal Ethics Committee. Five pathogen free domestic female pigs were used in this study and an extrahepatic portosystemic shunt was created between the portal vein, to the inferior vena cava (IVC), startng approximately 5 – 10 cm below the liver. Each shunt had a diameter of 8 mm and was made of PTFE.

The median weight of the animals was 45 kg, ranging 35 to 55 kg. Each pig was anesthetised by a trained veterinary technician with 0.5 mg/kg ketamine followed by a continuous dose of 1.5% isoflurane in oxygen via an endotracheal tube for the duration of the surgery. After the surgery was

completed and all samples collected the animal was euthanized with a lethal dose 100 mg/kg of sodium pentobarbitone.

Surgical Procedure

A 10 cm incision was made on the lower right side of the neck and the jugular vein was dissected and mobilised. A 16G x 1.25" Braun Introcan Safety® intravenous catheter was inserted into the jugular vein to allow for a 0.9% sodium chloride drip line. The catheter and drip line were secured to nearby epithelium. A midline laparotomy was performed with an incision of approximately 40 cm. The infrahepatic vena cava was exposed via visceral rotation and then mobilised in a cephalad fashion to a level at the confluence of the liver substance and the adventitia of the cava (Figure 1A). The portal vein was then identified and mobilised with separation of lymphatics and lymphatic nodes that surround the portal vein (Figure 1B). Each pig was initially heparinised with a weight appropriate dose of 80 units/kg of intravenous heparin, immediately followed by 5000 units added to each 1 L 0.9% saline bag.

The inferior vena cava (IVC) was partially clamped using a side biting Satinsky clamp and a longitudinal venotomy was performed with local heparin/saline irrigation. An end-to-side anastomosis of the portosystemic shunt was performed using continuous 6/0 polypropylene suture (Ethicon™) and 8 mm diameter by 10-15 cm PTFE (Figure 1C). The portal vein and IVC were

prepared with a 16 mm elliptical excision and the shunt material, PTFE was bevelled at each end for an acute angled connection to reduce turbulence. The anastomosis is first started at the 'heel' end with a suture running along each side to the middle. The 'toe' end is then started with sutures running along each side, meeting the other suture from the heel in the middle with any excess trimmed before the join is complete (Figure 1E) [1]. The shunt was flushed with heparinised saline and clamped. The portal vein anastomosis was similarly completed with partial occlusion clamping and end to side anastomosis using 6/0 suture material in continuous fashion (Figure 1D).

The portal system and shunt were flushed with heparinised saline and the suture line was completed and haemostasis achieved. Antegrade portal circulation was achieved prior to release of the clamp on the shunt. A dual lumen Turbo-Flo® 4 French catheter (Cook Medical) was flushed with saline and inserted into the portal vein inferior to the liver, approximately 10 cm below the shunt. Another tri-lumen 5 French catheter was inserted into the IVC and guided up to the confluence of the hepatic veins. Each catheter has surrounding 6/0 purse string sutures to secure and avoid tearing of the veins. The shunt was then left to stabilise for five minutes.

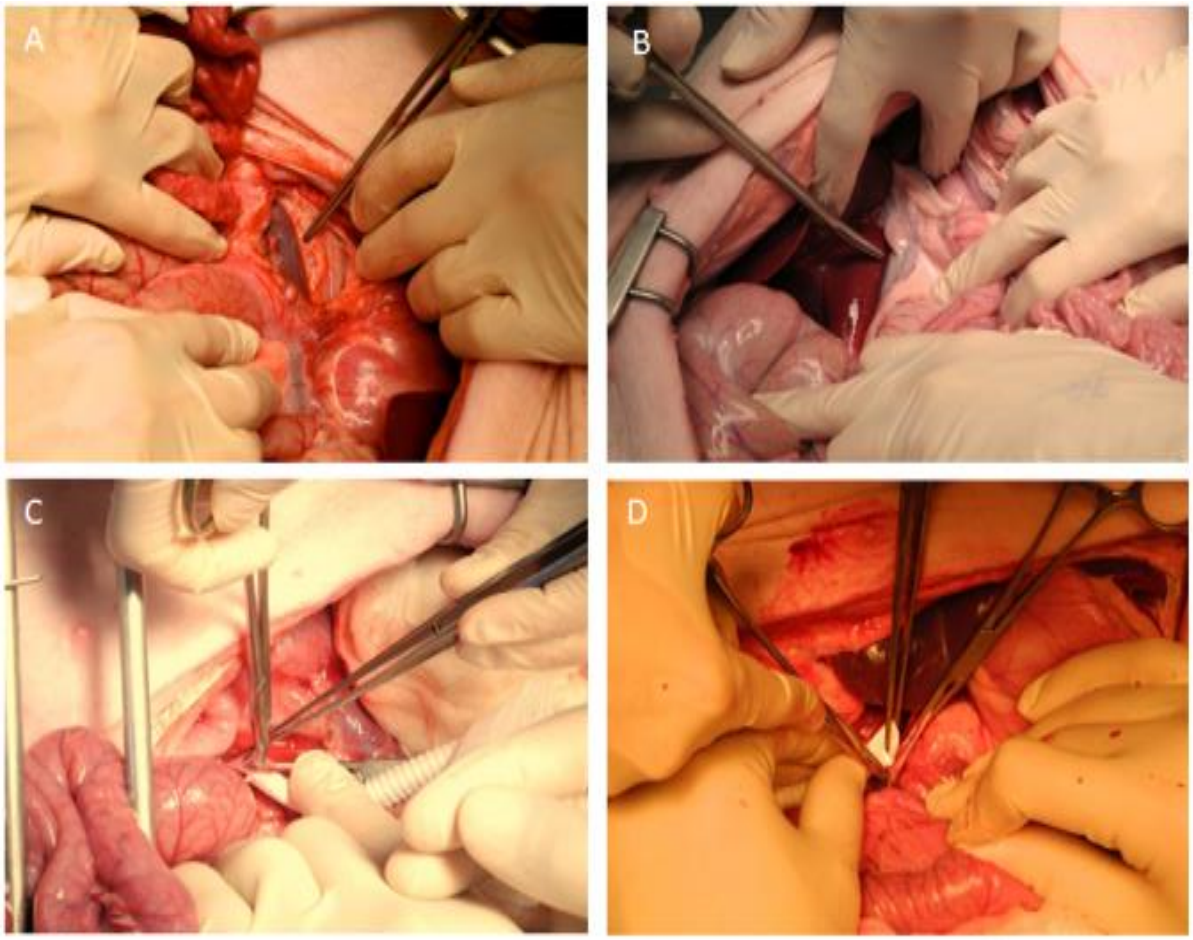

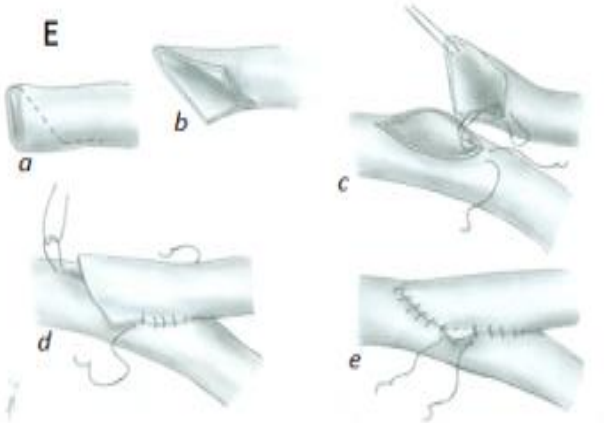

Figure 1: A) The inferior vena cava (arrow) is located **B)** The portal vein (solid arrow) was identified and mobilised with separation of lymphatics (hollow arrow). **C**) A longitudinal venotomy was performed to the inferior vena cava. An end to side anastomosis of the portosystemic shunt is performed using PTFE tubing. **D**) The portal vein anastomosis was similarly completed with partial occlusion clamping and end-to-side anastomosis. **E**) Schematic of an end-to-side anastomosis. (**a** and **b**)The graft material is trimmed. (**c**) A 16 mm elliptical excision is made into the portal vein or inferior vena cava with the suture starting at the 'heel'. (**d**) The 'heel' is sutured until half way, along both sides and then suturing is started from the toe. (**e**) Suture from the toe is joined in the middle with any excess edges removed. (From Rutherford RB. [1]).

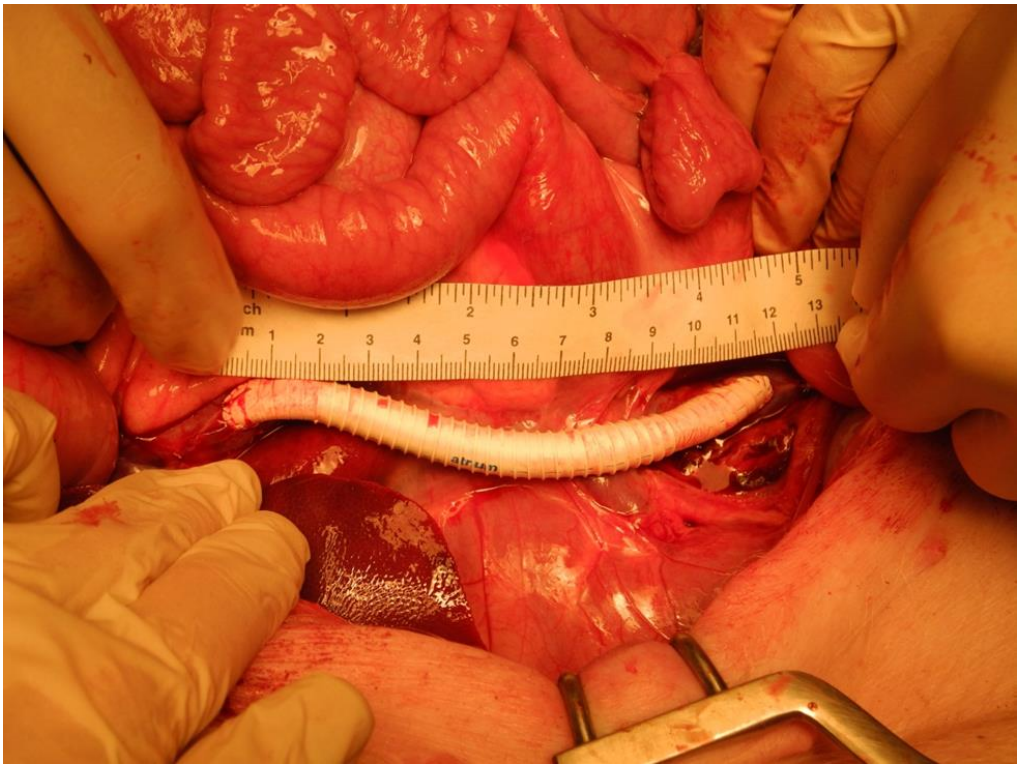

Figure 2: The complete end-to-side portocaval shunt.

Shunt Flow Direction

Typically flow direction and velocity can be determined using Doppler ultrasound scanning with the appropriate transducer. A thermodilution technique could also be used to measure flow, however, there is a 19 cm distance between the sensor and injection port on the catheters. Therefore, each shunt would need to be >19 cm for thermodilution to be accurate. Thermodilution was not deemed a viable option for this study.

Doppler ultrasound was conducted with a SonoSite® Micromaxx and a HEFL38 13-6 Mhz transducer. This type of transducer is typically used in vascular surgery and for vascular imaging. After the anastomosis described in the previous section had stabilised, the transducer was placed directly on top of the shunt, portal vein and inferior vena cava. Due to the type, size and weight of the transducer and the microporous structure of PTFE, there was a tendency for the veins to collapse, hence imaging the vein and calculating velocity of flow was difficult. Further PSSs were soaked in 0.9% saline solution, in a modified vacuum container. However, the blood flow could still not be determined with a soaked PTFE anastomosis. This was believed to be due to a low flow rate and the type of transducer. It is generally understood that fluids will always flow from high to low pressure, provided there are no obstructions. With this knowledge of fluid dynamics, we can be certain the flow direction in the anastomosis if the portal vein pressure is higher than the IVC pressure. In humans, a typical portal vein pressure is 23 - 25 mmHg and

the IVC pressure is 0 - 3 mmHg. Due to the animal being in supine position with an open abdominal cavity for the shunt procedure, there are no external forces on the portal vein and IVC, the pressure will be much less and will be mostly due to the force of the blood within the vessel. An ARGON® DTXPlus™ central venous pressure transducer was connected to the catheters previously inserted in the portal vein and in the IVC. The pressure transducer was fixed at the same height as the midline of the animal and connected to a 1 L bag of 0.9% saline solution in a pressure bag set to 300 mmHg. The lines were flushed of any air and the pressure is zeroed to atmospheric pressure via a three way tap. The line was then connected to the catheter in the portal vein or IVC and allowed to stabilise for one minute. Pressure measurements were taken for portal vein with shunt open and shunt closed, IVC with shunt open and closed, and in the portal vein with a clamp above the shunt for 100% shunting.

Shunted Blood

Since neither suitable Doppler ultrasound transducer nor thermodilution equipment was available, an exact calculation of blood flow through the shunt could not be obtained. Theoretically, flow rate can be calculated using a rearranged Hagan Poiseuille equation (Equation 1). Also, a new simplified

equation developed in dogs was used to calculate PSS fraction (Equation 2)[34].

Kudo *et al.* [30] measures shunt ratio by dividing the blood flow volume of the shunt by that of the portal vein using Doper ultrasound. However, as Doppler ultrasound was not available, the PSS fraction was calculated using the ratio of total volume between the portal vein and the total volume of the anastomoses (Equation 3).The volume of each vessel can be calculated by π x radius^2 x length. Photographs were used to measure the length of the shunt and the diameter of the portal vein. Due to the difficulty of measuring the length of the portal vein, average length of 6.5 ± 1.5 cm was used.

As a comparator for shunt flow and shunted fraction, Evans blue dye was injected into the shunt and control models to determine the flow rates by its pharmacokinetic properties. Blood samples were taken every 10 seconds for two minutes, then every 20 seconds till three minutes had elapsed. The mean transit time (MTT) of Evans blue was calculated and then applied to Equation 4 to determine the relative flow rate through the portal vein and shunt. The shunted fraction can then be calculated by dividing the shunt flow rate by the portal vein flow rate.

$$Flow\ rate = \frac{\text{pressure difference}.\ \pi.\ \text{diameter of shunt\^{}4}}{128.\ \text{blood viscosity}.\ \text{length of shunt}}$$

Equation 1: Hagan Poiseuille equation rearranged to find the flow rate of the portosystemic shunt.

$$PSS\ fraction\ (\%) = 100 - \frac{100\ .\ \text{PVP (shunt)}}{\text{PVP (control)}}$$

Equation 2: A simplified equation to calculate the portosystemic shunt (PSS) fraction using the Portal vein Pressure (PVP) when the shunt is open and closed. Adapted from Washizu *et al.* [34].

$$PSS\ fraction\ (\%) = 100\ .\frac{\text{PSS volume}}{\text{Portal vein volume}}$$

Equation 3: Ratio of blood volume between the portosystemic shunt (PSS) volume and the portal vein volume.

$$Flow\ rate = \frac{\text{volume}}{\text{MTT}}$$

Equation 4: Pharmacokinetic equation to calculate flow rate using the volume of the vessel and the mean transit time (MTT) of the injected compound.

Results

Photographs of each pig shunt were taken to record the length. The PTFE shunt lengths ranged from 9 to 13.5 cm, with a mean of 10.1 cm (Table 1). The shortest length possible was used, but was dependant on the visual location of the portal vein and IVC. The diameter of the portal vein was also recorded, with a mean of 14 mm, to calculate its volume. The ratio of the anastomosis volume to the portal vein volume estimates the expected amount of blood bypassing the liver, with a mean of 47.9 ± 11.96% (assuming portal vein length 6.5 ± 1.5 cm)(Table 1). This is not significantly different to the shunted fraction as calculated from Evans blue of 55.2 ± 11.96% (p=0.4).

Table 1: Length of each anastomosis that was inserted into each pig with the ratio between the portal vein (PV) and shunt (PSS) volumes. A range is given as the portal vein length was assumed of 6.5 ± 1.5cm. The shunted fraction as determined by Evans blue is shown as a comparator.

Pig	Shunt Length (cm)	PV:PSS Ratio (%)	Shunt Fraction (%)
1	8.5	42.15 ± 10.6	41
2	8.5	42.2 ± 10.5	71
3	10	43.2 ± 10.7	47
4	11	54.5 ± 13.6	59
5	13.5	66.9 ± 16.7	58
Mean ± SD	10.1 ± 1.9	47.9 ± 11.96	55.2 ± 11.96

Pressure Gradients

There was a significant pressure difference between the IVC from the portal vein when the shunt is closed of 7 ± 2.1 mmHg ($p<0.001$) and also when the shunt is open of 6 ± 1.1 mmHg ($p<0.001$). It therefore can be assumed that flow direction is from the portal vein to the IVC. Due to the hemodynamic properties of blood, that is the different viscosity of each component of blood, actual flow rate is difficult to be calculated using the Hagan-Poiseuille equation (Equation 1). Another simple equation was used to estimate the fraction of blood shunted, based on the difference on portal venous pressure when the shunt is open and closed (Equation 2)[34]. However, this equation requires a minimum of 1 mmHg pressure difference and fails to take into account the portal vein can expand, thus reducing pressure.

The portal vein was clamped above the anastomosis to allow 100% shunting. Pressure difference was recorded in the portal vein with 100% shunting and was compared against portal vein pressure with the shunt open. The mean pressure of 100% shunting was 4.5 mmHg, ranging from 1 to 7 mmHg and is significantly higher than normal flow with shunt open, mean of 1.83 mmHg, ranging 1 to 3 mmHg ($p=0.02$). This is to be expected as more blood is now forced through the shunt.

Discussion

An extrahepatic Abernethy Type II PSS was successfully recreated in a swine model. Due to the sheer size of the PSS, it can be classified as 'enormous' as it is 8 mm in diameter and slightly larger than what's been previously reported in patients with PSSs and without cirrhosis [9-16]. The surgical PSS procedure used is similar to what would be used for a liver transplant or any other type of shunt surgery and the end-to-side anastomosis is commonly used for vein and artery reconstructive vascular surgery [1].

PTFE was originally marketed in 1937 by DuPont as Teflon® [3]. The compound itself is hydrophobic, however through a process of heating, stretching and extruding, a microporous structure can be formed. Due to this microporous structure of PTFE, containing 'air pockets' ultrasound is poorly transmitted from air to water due to impedance mismatching and the ultrasound wave is virtually reflected. Ideally, a more appropriate transducer may be a smaller 'hockey stick' shaped probe, for example the SonoSite® SLA 13-6MHz. This probe is lighter, smaller and therefore unlikely to collapse the vein, the transducer would have better spatial resolution due to a smaller scanning area. Due to the high costs of Doppler ultrasound transducers, the 'hockey stick' probe could not be obtained for animal use.

A limitation with using pigs in this model is that they are known to be susceptible to anaesthetics and may prematurely die. Although no animals prematurely died, it is possible that independent breathing may occur against the respirator can affect the venous blood flow, by increasing the pressure and heart rate, and also cause possible suffocation. This can have some erratic flow rates through the shunt.

Measuring the pressure difference between the portal vein and inferior vena cava would ideally been more appropriate if the measurement was taken within either end of the anastomosis. However, for this to occur, two more catheters would need to be inserted into the portal vein and IVC. Although theoretically possible, due to the fragile nature of the vascular system, there is a high risk of tearing and bleeding and therefore was not practical. As a consequence, pressures of the portal vein and IVC were measured and using Bernoulli's principle, it can be concluded that flow is from portal vein to IVC.

At any given point in time, the ratio of blood shunted is the same irrespective of actual flow rate, which can change. The total volume of the portal vein and the total volume of the shunt is a similar ratio as the percentage shunted. Although this technique is not completely accurate, it is similar to the known shunted fractions as determined by the pharmacokinetics of Evans blue. Therefore, measuring volume ratio can show a good estimate of shunting rate and somewhat severity and can be used when other equipment is not available.

Conclusion

Using techniques based from human surgery, it was possible to create and mimic a PSS in a swine model. The anastomosis is large enough to allow adequate flow into the IVC, but still allow hepatopetal flow in the portal vein. When no equipment is available to measure vascular flow or shunt flow, the total volume ratio between the primary vessel and shunt will show a sound estimate in fraction of blood shunted.

References

1. Hufnagel CA. Permanent intubation of the thoracic aorta. Archives of Surgery. 1947;54(4):382-9
2. Rutherford R. Basic Vascular Surgical Techniques. In: Rutherford R, editor. Vascular Surgery. 1. 6th ed. Philadelphia, Pennsylvania: Elsevier Saunders; 2005. p. 661-71.
3. Xue L, Greisler H. Prosthetic Graphs. In: Rutherford R, editor. Vascular Surgery. 1. 6th ed. Philadelphia: Elsevier Saunders; 2005. p. 723-40.
4. Landry GJ, Moneta GL, Taylor LM, Jr., Porter JM. Axillobifemoral bypass. Annals of Vascular Surgery. 2000;14(3):296-305
5. Berce M, Sayers RD, Miller JH. Femorofemoral crossover grafts for claudication: a safe and reliable procedure. European Journal of Vascular and Endovascular Surgery. 1996;12(4):437-41
6. Christenson JT, Broome A, Norgren L, Eklof B. The late results after axillo-femoral bypass grafts in patients with leg ischaemia. Journal of Cardiovascular Surgery. 1986;27(2):131-5
7. Sarfeh IJ, Rypins EB, Mason GR. A systematic appraisal of portacaval H-graft diameters. Clinical and hemodynamic perspectives. Annals of Surgery. 1986;204(4):356-63
8. Collins JC, Ong MJ, Rypins EB, Sarfeh IJ. Partial portacaval shunt for variceal hemorrhage: longitudinal analysis of effectiveness. Archives of Surgery. 1998;133(6):590-2; discussion 2-4
9. Yoshikawa K, Matsumoto M, Hamanaka M, Nakagawa M. A case of manganese induced parkinsonism in hereditary haemorrhagic telangiectasia. Journal of Neurology, Neurosurgery and Psychiatry. 2003;74(9):1312-4
10. Matsumoto S, Mori H, Yamada Y, Hayashida T, Hori Y, Kiyosue H. Intrahepatic porto-hepatic venous shunts in Rendu-Osler-Weber disease: Imaging demonstration. European Radiology. 2004;14(4):592-6
11. Mori H, Hayashi K, Fukuda T, Matsunaga N, Futagawa S, Nagasaki M, Mutsukura M. Intrahepatic portosystemic venous shunt: Occurrence in patients with and without liver cirrhosis. American Journal of Roentgenology. 1987;149(4):711-4
12. Horiguchi Y, Kitano T, Imai H, Ohsuki M, Yamauchi M, Itoh M. Intrahepatic portal-systemic shunt: its etiology and diagnosis. Gastroenterologia Japonica. 1987;22(4):496-502
13. Matsumoto S, Mori H, Yoshioka K, Kiyosue H, Komatsu E. Effects of portal-systemic shunt embolization on the basal ganglia: MRI. Neuroradiology. 1997;39(5):326-8
14. Kanda T, Nogawa S, Muramatsu K, Koto A, Fukuuchi Y. Portal systemic encephalopathy presenting with dressing and constructional apraxia. Internal Medicine. 2000;39(5):419-23
15. Shapiro RS, Winsberg F, Stancato-Pasik A, Sterling KM. Color Doppler sonography of vascular malformations of the liver. Journal of Ultrasound in Medicine. 1993;12(6):343-8

16. Senocak E, Oguz B, Edguer T, Cila A. Congenital intrahepatic portosystemic shunt with variant inferior right hepatic vein. Diagnostic and Interventional Radiology. 2008;14(2):97-9
17. Ohwada S, Hamada Y, Morishita Y, Tanahashi Y, Takeyoshi I, Kawashima Y, Nakamura S, Iino Y, Miyamoto Y, Hirato J. Hepatic encephalopathy due to congenital splenorenal shunts: report of a case. Surgery Today. 1994;24(2):145-9
18. Kimura N, Kumamoto T, Hanaoka T, Nakamura K, Hazama Y, Arakawa R. Portal-systemic shunt encephalopathy presenting with diffuse cerebral white matter lesion: an autopsy case. Neuropathology. 2008;28(6):627-32
19. Ali S, Stolpen AH, Schmidt WN. Portosystemic encephalopathy due to mesoiliac shunt in a patient without cirrhosis. Journal of Clinical Gastroenterology. 2010;44(5):381-3
20. Nishie A, Yoshimitsu K, Honda H, Kaneko K, Kuroiwa T, Fukuya T, Irie H, Ninomiya T, Yoshimitsu T, Hirakata H, Okuda S, Masuda K. Treatment of hepatic encephalopathy by retrograde transcaval coil embolization of an ileal vein-to-right gonadal vein portosystemic shunt. Cardiovascular and Interventional Radiology. 1997;20(3):222-4
21. Yamaguchi Y, Okai T, Watanabe H, Motoo Y, Mai M, Matsui O, Nakanuma Y, Sawabu N. Myxedema accompanied by huge portal-systemic shunt without portal hypertension. Internal Medicine. 2001;40(12):1200-4
22. Nagino M, Hayakawa N, Kitagawa S, Katoh M, Komatsu S, Nimura Y, Shionoya S. Interventional embolization with fibrin glue for a large inferior mesenteric-caval shunt. Surgery. 1992;111(5):580-4
23. Sato T, Asanuma Y, Ishida H, Hashimoto M, Tanaka J, Andoh H, Yasui O, Kurokawa T, Komatsuda T, Konno K, Heianna J, Koyama K. A case of extrahepatic portosystemic shunt without portal hypertension treated by laparoscopically assisted embolization. Surgery. 1999;126(5):984-6
24. Konno K, Ishida H, Uno A, Ohnami Y, Masamune O. Large extrahepatic portosystemic shunt without portal hypertension. Abdominal Imaging. 1997;22(1):79-81
25. Kuramitsu T, Komatsu M, Matsudaira N, Naganuma T, Niizawa M, Zeniya A, Yoshida T, Toyoshima I, Chiba M, Masamune O. Portal-systemic encephalopathy from a spontaneous gastrorenal shunt diagnosed by three-dimensional computed tomography and treated effectively by percutaneous vascular embolization. Liver. 1998;18(3):208-12
26. Bonington SC, Hodgson DI, Mehta S, Lynch N, Chalmers N. A congenital venous anomaly, with a portal-systemic shunt into a previously undescribed intra-thoracic vein. Clinical Radiology. 2002;57(7):658-60
27. Bodner G, Gluck A, Springer P, Konig P, Perkmann R. Aneurysmal portosystemic venous shunt: A case report. Ultraschall in der Medizin. 1999;20(5):215-7
28. Fanelli F, Marcelli G, Bezzi M, Salvatori FM, Rossi M, Rossi P, Passariello R. Intrahepatic aneurysmal portohepatic venous shunt: Embolization with a tissue adhesive solution. Journal of Endovascular Therapy. 2003;10(1):147-53

29. Komori A, Kataoka C, Okamura S, Tanoue K, Hashizume M, Ichiki Y, Takasaki T, Shigematsu H, Hayashida K, Ishibashi H. Aneurysmal intraheptic portosystemic venous shunt associated with idiopathic portal hypertension: A lesion evaluated by a 3D image reconstructed from power doppler flow imaging. Journal of Medical Ultrasonics. 2000;27(2):131-7
30. Kudo M, Tomita S, Tochio H, Minowa K, Todo A. Intrahepatic portosystemic venous shunt: Diagnosis by color Doppler imaging. American Journal of Gastroenterology. 1993;88(5):723-9
31. Suga K, Ishikawa Y, Matsunaga N, Tanaka N, Suda H, Handa T. Liver involvement in hereditary haemorrhagic telangiectasia: assessment with 99Tcm-phytate radionuclide angiography and 123I-IMP transrectal portal scintigraphy. British Journal of Radiology. 2000;73(874):1115-9
32. Dupont J, Lumb WV, Nelson AW, Seegmiller JP, Hotchkiss D, Chase HP. Portacaval shunt as treatment for hypercholesterolemia. Metabolic and morphological effects in a swine model. Atherosclerosis. 1985;58(1-3):205-22
33. Chase HP, Morris T. Cholesterol metabolism following portacaval shunt in the pig. Atherosclerosis. 1976;24(1-2):141-8
34. Washizu M, Torisu S, Kondo Y, Shimizu N, Washizu T, Takemura N, Kinoshita G. A simple calculation for obtaining shunt fractions of portosystemic shunts. Journal of Veterinary Medical Science. 2004;66(4):449-51

Appendix J – Detrimental effect of isoflurane in gas chromatography

Statement of Authorship

Title of Paper	Detrimental effect of isoflurane in gas chromatography
Publication Status	○ Published, ○ Accepted for Publication, ◉ Submitted for Publication, ○ Publication style
Publication Details	Submitted to Journal of Breath Research

Author Contributions

By signing the Statement of Authorship, each author certifies that their stated contribution to the publication is accurate and that permission is granted for the publication to be included in the candidate's thesis.

Name of Principal Author (Candidate)	Todd Matthews		
Contribution to the Paper	Designed study, analysed data and wrote manuscript draft.		
Signature		Date	21/11/2013

Name of Co-Author	Simon Barry		
Contribution to the Paper	Analysed data and reviewed manuscript draft.		
Signature		Date	21/11/2013

Name of Co-Author	Betty Zacharakis		
Contribution to the Paper	Analysed samples and data.		
Signature		Date	21/11/2013

Name of Co-Author	Guy Maddern		
Contribution to the Paper	Supervised development of work and acted as corresponding author		
Signature		Date	21/11/13

TITLE: Detrimental Effect of Isoflurane in Gas Chromatography

Authors: Matthews T*, Barry S#, Zacharakis B#, Maddern G*

*Discipline of Surgery, The Queen Elizabeth Hospital, University of Adelaide, Woodville South, South Australia.

#Department of Gastroenterology, Women's and Children's Health Network; North Adelaide, South Australia.

Email:

todd.matthews@adelaide.edu.au

simon.barry@health.sa.gov.au

betty.zacharakis@health.sa.gov.au

guy.maddern@adelaide.edu.au

CORRESPONDING AUTHOR:

Prof. G.J Maddern

University of Adelaide Discipline of Surgery

The Queen Elizabeth Hospital

28 Woodville Road

Woodville South

SA 5011

Australia

Ph: +61 8 8222 6756

Fax: +61 8 8222 6028

Email: guy.maddern@adelaide.edu.au

Abstract

There are numerous experimental and surgical scenarios where breath sampling studies using stable isotopes would be useful. Currently breath test samples are not routinely collected while patients or animals are under general anaesthesia as there may be an impact of the inhaled anaesthetic agents on the sample analysis. Only nitrous oxide (N_2O) has known issues with contamination of CO_2 breath analysis in isotope ratio mass spectrometry (IRMS). In an animal liver function study, it was noted that the $^{13}CO_{2,}$ analysed by IRMS, showed a peak time decrease.

Six pathogen female pigs were used in a study regarding liver function tests (weight of 45.2 ±6 .7 kg). Each pig was anesthetised with 0.5 mg/kg ketamine followed by a continuous dose of 1.5% isoflurane in oxygen. A further three pigs were used in a follow on study and anaesthetised via continuous intravenous administration of alfaxalone, diazepam and ketamine. Two intravenous injections of ^{13}C-methacetin (2 mg/kg) and breath samples were collected every two minutes for 40 minutes after each dose. Breath samples were analysed using an IRMS.

The $^{13}CO_2$ peak gradually drifted outside of the analysis window as more samples were analysed from the first six pigs. It was hypothesised that the general anaesthetic isoflurane contaminated the samples and was adsorbed by the gas chromatography column consequently causing the retention time of $^{13}CO_2$ to decrease. The three pigs in the follow on study without isoflurane showed no drift in the analysis window, suggesting that isoflurane has an effect on the chromatography process during analysis. It is recommended that any future stable

isotope breath testing studies, that require sedation, the use of intravenous general anaesthetics minimises the risk of perturbations in sample chromatography.

Introduction

Non-invasive breath testing with stable isotopes is becoming a more widely used to test metabolic processes especially in pre-clinical studies. Also, [^{13}C] labelled compounds are being used in a number of large animal experiment models [1-3]. Breath sampling has not yet been widely used while the animal or patient is under general anaesthesia due to sampling difficulty. The hesitation to use breath testing in a clinical setting and animal research also maybe due to limited understanding of the metabolic process, and some machinery may not be sensitive enough to determine small changes [4]. However, future studies involving surgery may require the use of breath testing while the animal or patient is under general anaesthesia.

[^{13}C] Breath testing has been used for a range of tests including detection of *Helicobacter pylori* using ^{13}C-urea [5-7], lung cancer detection [8-10], gastric emptying using ^{13}C-acetic acid and ^{13}C-lactose ureide [11] and liver function using ^{13}C-phenylaline, ^{13}C-leucine or ^{13}C-methacetin [12, 13]. In particular ^{13}C-methacetin has been used to predict liver failure posthepatectomy [14] and graft failure post-transplant [15]. For this study ^{13}C-methacetin is used as it is exclusively taken up and metabolised by the liver, and its metabolite $^{13}CO_2$ can be collected from exhaled breath samples and assayed with an isotope-mass spectrometer (IRMS).

^{13}C-methacetin has been used as a liver function assessment method by measuring

the ratio and decay of $^{13}CO_2$ in the breath. Methacetin is passively taken up into hepatocytes and entirely metabolised by cytochrome 1A2 (CYP1A2) [16]. CYP1A2 metabolises methacetin into acetaminophen (paracetamol) and CO_2 [13]. The $^{13}CO_2$ breathed out, as measured in liver function tests, may not correlate with the amount of ^{13}C-methacetin injected, and this could be due to either the diffusion process in the blood [17] or from the presence of a portosystemic shunt (PSS), allowing methacetin to directly bypass the hepatocytes.

Volatile organic compounds (VOCs) are commonly used for general anaesthesia in both patient and animal surgical procedures. Current inhalational general anaesthetic compounds used include isoflurane, desflurane and sevoflurane, which can also be combined with nitrous oxide (N_2O). However, isoflurane is used more routinely for animal surgery. To date, the only known issues with ^{13}C isotope breath analysis and volatile organic compound (VOCs) is with N_2O. N_2O has a mass overlap with $^{13}CO_2$ when using IRMS, such that variable amounts of N_2O in the sample will cause large variability in peak composition for the $^{13}CO_2$ analysis window [18, 19]. This study describes an observed impact of the anaesthetic during an animal study of liver function analysis, where ^{13}C-methacetin was intravenously administered into six female pigs anesthetised with isoflurane. During the breath sample analysis, it was noted that the expected $^{13}CO_2$ peak time gradually drifted and escaped the analysis window. As N_2O was not being used in this study, it was unknown what was causing the peak shift in the IRMS.

Materials & Methods

This study was approved by the University of Adelaide Animal Ethics Committee and the Institute of Medical and Veterinary Science Animal Ethics Committee. Six pathogen free domestic female pigs were used with a mean weight of 45.2 ± 6.7 kg. Each pig was anesthetised with 0.5 mg/kg ketamine followed by a continuous dose of 1.5% isoflurane in oxygen via an endotracheal tube for the duration of the surgery. The animals were continuously monitored for change in heart rate and oxygen saturation for the duration of the procedure. After the surgery was completed and all breath samples collected the pig was euthanized with a lethal dose 100 mg/kg of sodium pentobarbitone.

Four intravenous doses of ^{13}C-methacetin (dose 2 mg/kg) were rapidly made into either the portal vein or jugular vein. Breath samples were collected for 40 minutes following ^{13}C-methacetin dose. Which each pig was under general anaesthesia, breath samples were collected in duplicate every two minutes until 40 minutes had elapsed. Samples were collected in 12 mL Exetainer® vials with a rubber septa (Labco®, Ceredigion, United Kingdom), through a blood transfer device connected to a three-way tap via the sample line. The three-way tap allowed the sample line to also be used for monitoring the end tidal CO_2. Samples were collected using the blood transfer device, piercing the septa at the same time as the pig exhaled.

Analysis

Breath samples were sent to the Gastroenterology Department at the Women's and Children's Hospital (North Adelaide, South Australia) for analysis. Breath samples were analysed using an isotope ratio mass spectrometer (IRMS). The machine used was an Automated Breath ^{13}Carbon Analyser (ABCA, SerCon®, Crewe, England), an ABCA auto-sampler and Carbosieve G 60/80 mesh packed gas chromatography column. The IRMS was first calibrated with 5 ± 0.5% CO_2 in nitrogen. The breath samples in the exetainers were then loaded into the auto-sampler with a 5 ± 0.5% quality control reference gas placed in every 10th position. The data was then analysed using the provided software, with the integration analysis window set at 75 – 85 seconds with a five second buffer (SerCon®, ABCA ^{13}Carbon Isotope Ratio Analyser: Version 500.7.4 2004).

Results

Breath samples were analysed from a trial pig showing typical $^{13}CO_2/^{12}CO_2$ ratios. The quality control (QC) reference gas of 5 ± 0.5% was tracked throughout which showed a decrease in $^{13}CO_2/^{12}CO_2$ ratio and thus a drift in the expected transit time of the mass peak. As this sample is from an independent QC stock, not exhaled air, the drift in peak transit time was further investigated. (Figure 1). Raw data from the samples was digitally re-analysed and the analysis window time lag was systematically decreased for each sample set until the QC was near linear and

consistent within each set (Figure 2). The analysis window has a normal lag time of approximately 80 second. Each sample set was rerun with the analysis window lag time shortened in five seconds increments, until all QC ratios were consistent.

In a follow on study, three pigs were anaesthetised via continuous administration of Alfaxalone. No isoflurane was used during the testing. Breath samples were taken at similar time points as the first group of pigs. The QC ratio was tracked throughout the analysis and was consistent, with no observable drifting of the analysis window (Figure 3).

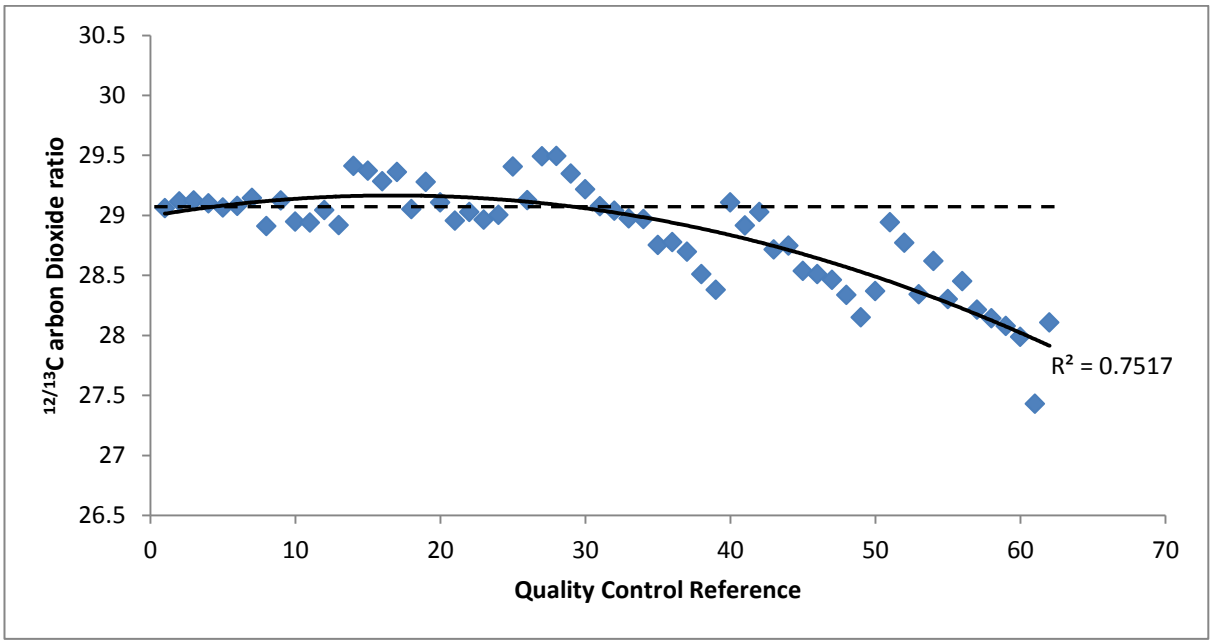

Figure 1: Series of quality control references throughout sampling for $^{13}CO_2$ in the presence of isoflurane. Each quality control should maintain similar ratio of 29.1 ± 0.2 (dashed line), however a drift occurs (solid line) as more isoflurane contaminated samples are analysed. The black dash line shows the standard deviation of the drift.

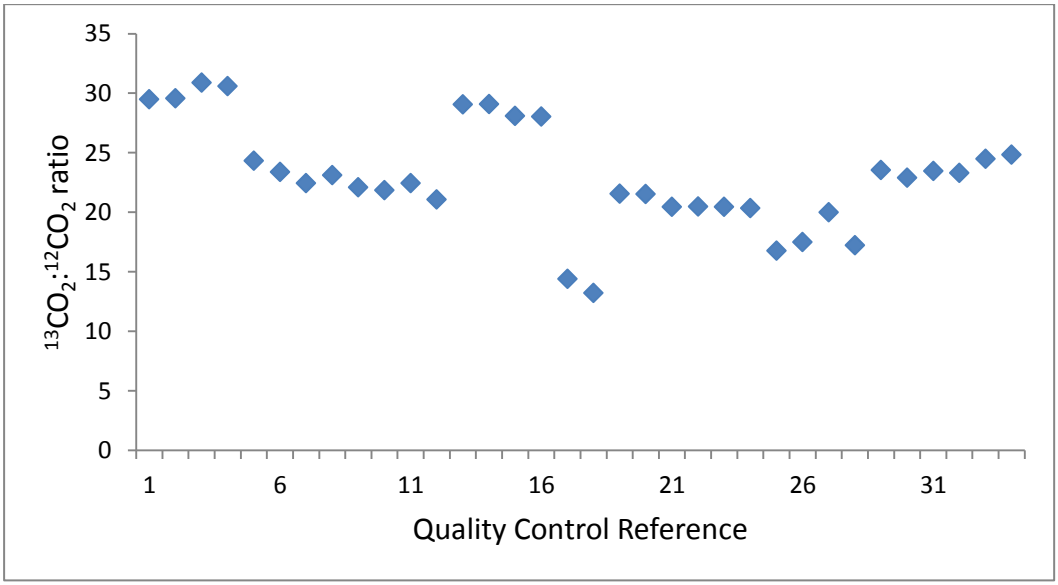

Figure 2: Groups of corrected quality control (QC) references throughout sampling for $^{13}CO_2$ in the presence of isoflurane. Digital raw sample data were rerun in sample sets of 20 and 4 QC samples. The analysis window was changed in each group to correct for the drift.

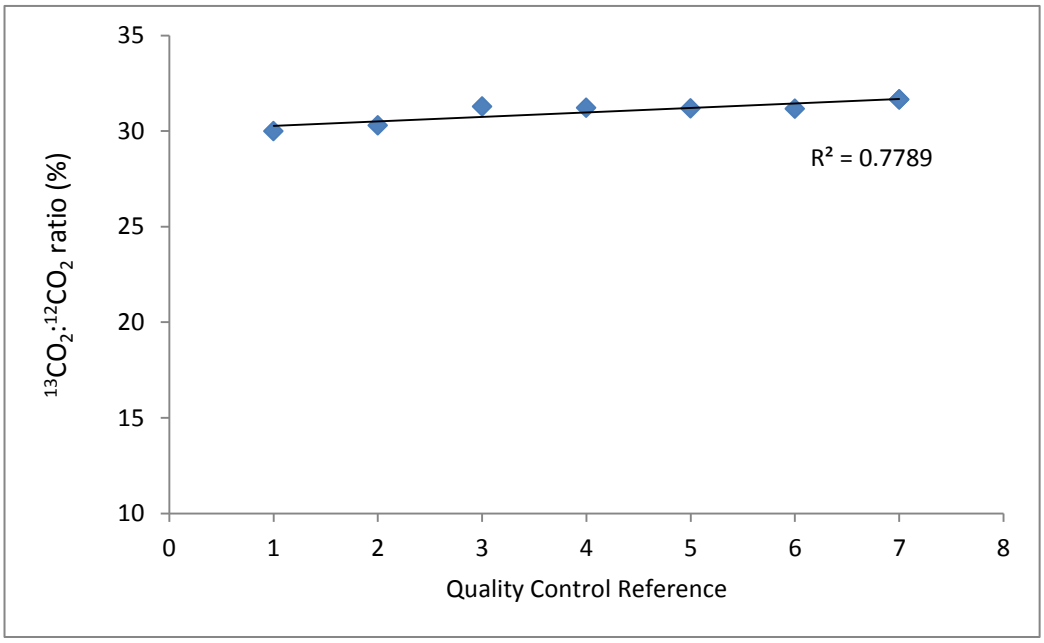

Figure 3: Series of quality control references samples that were collected in the absence of isoflurane. Each quality control maintained similar ratio of 31.1 ±0.6%.

Discussion

Breath collection for large animals is difficult as they are currently not sedated. For example, a pig must be restrained and breath samples taken using a modified mask [1]. This is not only dangerous for the technician taking the breath samples, but can also be harmful and stressful for the animal. For this reason, breath testing while patients or animals are anaesthetised may be beneficial for future research. However, here we describe a previously unknown issue with inhalational anaesthetics affecting the IRMS separating column. This issue using breath sampling in the presence of isoflurane is different to the previous known issue of N_2O contaminating breath samples. In this case, the mass overlap of N_2O and CO_2 caused non-linearity and consequently skewed results [18].

The absence of isoflurane in the follow on study, where there was no effect of the IRMS column suggests that isoflurane may contaminate the breath samples during analysis as. The IRMS column is used to separate gas compounds according to their molecular size. The column contains a molecular sieve called Carbosieve G that allows low molecular weight gas compounds such as CO_2 to pass through the sieve with a longer transit time, compared with large molecular weight gases. However, this study proposes that isoflurane gradually binds to the Carbosieve G and consequently reduces the porosity, such that the CO_2 now transits the column more rapidly. This therefore, decreases the retention time of $^{13}CO_2$. A previous study used Carbosieve G to adsorb the greenhouse gas tetrafluromethane (CF_4) [20]. Here, Carbosieve G was shown to adsorb a large amount (1.7 mol/kg) of CF_4 before saturation. The smaller sized pours within the Carbosieve G increase the adsorption

potential [20]. Isoflurane's chemical structure contains a trifluroethane group, similar to the active fluorine group in CF_4 which suggests it can also adsorb to Carbosieve G.

The QC gas sample is a fixed concentration of 5 ± 0.5% $^{13}CO_2$ which is used to determine the linearity and accuracy of the results and we routinely run QC tubes repeatedly throughout the experimental breath samples. When the peak of $^{13}CO_2$ drifts out of the analysis window, the apparent concentration of $^{13}CO_2$ reduces. The IRMS Carbosieve G. separating column was affected by continued presence of isoflurane, which caused the peak time to steadily reduce and consequently the mass spectroscopy peak appeared early and was not analysed within the programmed time window. Although the analysis window can be manually shifted according to the drift of the peak, this may increase the error margin. This correction is not ideal as the analysis window would be needed to be shifted after every five to ten samples and would be different for every machine. Alternative solutions include using a silica zeolite filter, however this also removes CO_2 from the breath [21], and heating the Carbosieve G. column to desorb the isoflurane from the Carbosieve G. However, no attempts have been successful and hence, no solution has yet been found when samples contains isoflurane. Other analytical techniques may include non-dispersive infrared spectroscopy (NDIRS), which has been used to detect $^{13}CO_2$ as an alternative to IRMS [22]. NDIRS does not use a filter or separating column, however, mechanical ventilation can cause a bias in $^{13}CO_2$ and $^{12}CO_2$ measurements due to additional O_2 [22, 23].

As inhalational general anaesthesia compounds desflurane and sevoflurane also have an active tetrafluroethane group, they may cause similar issues for gas chromatography. It is advisable that if breath testing is required in research or in patients under general anaesthesia, any gas analytical techniques that require a gas chromatography column for separation should not be used. It is recommended that in breath sampling studies that require sedation, intravenous general anaesthetics should be used.

Acknowledgements

The authors acknowledge Professor Ross Butler's guidance and assistance throughout this study. There are no conflicts of interests.

References

1. Terry R, van Wettere WH, Whittaker AL, Herde PJ, Howarth GS. Using the noninvasive (13)C-sucrose breath test to measure intestinal sucrase activity in swine. Comparative Medicine. 2012;62(6):504-7
2. Bauchart-Thevret C, Stoll B, Benight NM, Olutoye O, Lazar D, Burrin DG. Supplementing monosodium glutamate to partial enteral nutrition slows gastric emptying in preterm pigs. Journal of Nutrition. 2013;143(5):563-70
3. Danicke S, Diers S. Effects of ergot alkaloids in feed on performance and liver function of piglets as evaluated by the (1)(3)C-methacetin breath test. Archives of Animal Nutrition. 2013;67(1):15-36
4. Rubin T, von Haimberger T, Helmke A, Heyne K. Quantitative determination of metabolization dynamics by a real-time 13CO2 breath test. J Breath Res. 2011;5(2):027102
5. Klein PD. ^{13}C breath tests: visions and realities. Journal of Nutrition. 2001;131(5):1637S-42S
6. Braden B, Lembcke B, Kuker W, Caspary WF. 13C-breath tests: Current state of the art and future directions. Digestive and Liver Disease. 2007;39(9):795-805
7. Cutler AF, Havstad S, Ma CK, Blaser MJ, Perez-Perez GI, Schubert TT. Accuracy of invasive and noninvasive tests to diagnose Helicobacter pylori infection. Gastroenterology. 1995;109(1):136-41
8. Bajtarevic A, Ager C, Pienz M, Klieber M, Schwarz K, Ligor M, Ligor T, Filipiak W, Denz H, Fiegl M, Hilbe W, Weiss W, Lukas P, Jamnig H, Hackl M,

Haidenberger A, Buszewski B, Miekisch W, Schubert J, Amann A. Noninvasive detection of lung cancer by analysis of exhaled breath. Biomed Central Cancer. 2009;9:348

9. Phillips M, Cataneo RN, Cummin AR, Gagliardi AJ, Gleeson K, Greenberg J, Maxfield RA, Rom WN. Detection of lung cancer with volatile markers in the breath. Chest. 2003;123(6):2115-23
10. McCulloch M, Jezierski T, Broffman M, Hubbard A, Turner K, Janecki T. Diagnostic accuracy of canine scent detection in early- and late-stage lung and breast cancers. Integrative Cancer Therapies. 2006;5(1):30-9
11. Uchida M, Yoshida-Iwasawa K. Simultaneous measurement of gastric emptying and gastrocecal transit times in conscious rats using a breath test after ingestion of [1-13C] acetic acid and lactose-[13C] ureide. Journal of Smooth Muscle Research. 2012;48(4):105-14
12. Miura Y, Washizawa N, Urita Y, Imai T, Kaneko H. Evaluation of remnant liver function using 13C-breath tests in a rat model of 70% partial hepatectomy. Hepato-Gastroenterology. 2012;59(114):311-6
13. Stockmann M, Lock JF, Riecke B, Heyne K, Martus P, Fricke M, Lehmann S, Niehues SM, Schwabe M, Lemke AJ, Neuhaus P. Prediction of postoperative outcome after hepatectomy with a new bedside test for maximal liver function capacity. Annals of Surgery. 2009;250(1):119-25
14. Stockmann M, Lock JF, Malinowski M, Niehues SM, Seehofer D, Neuhaus P. The LiMAx test: a new liver function test for predicting postoperative outcome in liver surgery. HPB (Oxford). 2010;12(2):139-46
15. Stockmann M, Lock JF, Malinowski M, Seehofer D, Puhl G, Pratschke J, Neuhaus P. How to define initial poor graft function after liver transplantation? - a new functional definition by the LiMAx test. Transplant International. 2010;23(10):1023-32
16. Guengerich FP, Krauser JA, Johnson WW. Rate-limiting steps in oxidations catalyzed by rabbit cytochrome P450 1A2. Biochemistry. 2004;43(33):10775-88
17. Crandall ED, Bidani A. Effects of red blood cell HCO3Cl exchange kinetics on lung CO2 transfer: Theory. Journal of Applied Physiology Respiratory Environmental and Exercise Physiology. 1981;50(2):265-71
18. Sirignano C, Neubert RE, Meijer HA. N_2O influence on isotopic measurements of atmospheric CO_2. Rapid Communications in Mass Spectrometry. 2004;18(16):1839-46
19. Assonov SS, Brenninkmeijer CA. On the N_2O correction used for mass spectrometric analysis of atmospheric CO_2. Rapid Communications in Mass Spectrometry. 2006;20(11):1809-19
20. Kowalczyk P, Holyst R. Efficient adsorption of super greenhouse gas (tetrafluoromethane) in carbon nanotubes. Environ Sci Technol. 2008;42(8):2931-6
21. Doyle DJ, Byrick R, Filipovic D, Cashin F. Silica zeolite scavenging of exhaled isoflurane: a preliminary report. Canadian Journal of Anaesthesia. 2002;49(8):799-804

22. Vogt JA, Radermacher P, Georgieff M. $^{13}CO_2$ breath tests, a tool to assess intestinal and liver function in the ICU? Current Opinion in Critical Care. 2010;16(2):169-75
23. Riecke B, Neuhaus P, Stockmann M. Major influence of oxygen supply on 13CO2:12CO2 ratio measurement by nondispersive isotope-selective infrared spectroscopy. Helicobacter. 2005;10(6):620-2

Appendix K – Safe and Inexpensive Method for Breath Sampling and a Technique for Continuous Intravenous Anaesthesia in Pigs

Statement of Authorship

Title of Paper	Safe and inexpensive method for breath sampling and a technique for continuous intravenous anaesthesia in pigs
Publication Status	○ Published, ○ Accepted for Publication, ◉ Submitted for Publication, ○ Publication style
Publication Details	Submitted to Journal of Breath Research

Author Contributions

By signing the Statement of Authorship, each author certifies that their stated contribution to the publication is accurate and that permission is granted for the publication to be included in the candidate's thesis.

Name of Principal Author (Candidate)	Todd Matthews		
Contribution to the Paper	Designed study, assisted in surgery, analysed data and wrote manuscript draft.		
Signature		Date	7/11/13

Name of Co-Author	Timothy Kuchel		
Contribution to the Paper	Designed intravenous anaesthesia protocol, administered anaesthesia agents and monitored animal.		
Signature			6 NOV '13

Name of Co-Author	Guy Maddern		
Contribution to the Paper	Supervised development of work and acted as corresponding author.		
Signature		Date	21/11/13

Name of Co-Author			
Contribution to the Paper			
Signature		Date	

Title: Safe and inexpensive method for breath sampling and a technique for continuous intravenous anaesthesia in pigs

Running Title: Method for breath sampling and continuous intravenous anaesthesia in pigs

Authors and addresses:

T Matthews[1], T Kuchel[2], G Maddern[1].

[1]The Queen Elizabeth Hospital, Discipline of Surgery, The University of Adelaide, 28 Woodville Rd, Woodville South, South Australia 5011

[2] Institute of Medicine and Veterinary Science, 101 Blacks Road, Gilles Plains, Adelaide, South Australia 5086

Email:

todd.matthews@adelaide.edu.au

tim.kuchel@sahmri.com

guy.maddern@adelaide.edu.au

CORRESPONDING AUTHOR:

Prof. G.J Maddern
University of Adelaide Discipline of Surgery
The Queen Elizabeth Hospital
28 Woodville Road
Woodville South
SA 5011
Australia
Ph: +61 8 8222 6756
Fax: +61 8 8222 6028
Email: guy.maddern@adelaide.edu.au

Key words

Breath sampling, intravenous anaesthesia, pigs, alfaxalone, animal anaesthesia

Abstract

Breath testing with stable isotopes is becoming more common in large animal studies to test metabolic processes using [^{13}C] labelled compounds. However, this causes concern for the safety of the technician and also stress for large animals, unless the animal is sedated. This led to the designing of a device using common hospital equipment to sample breath from the respirator during a surgical procedure to then be analysed by an isotope-radio mass spectrometer (IRMS). However, some IRMS machines are susceptible to certain inhalational anaesthetising agents such as nitrogen oxide and isoflurane. So, a technique for continuous intravenous anaesthesia is also described.

Key words: Breath test method, intravenous anaesthesia method, pigs, breath sampling

Introduction

Breath testing in large animals will become an increasing need for future medical research. Safety for the technician becomes a concern especially for breath collection from large animals unless they are sedated. Currently, a pig must be restrained and breath samples taken using a modified mask [1]. It not only dangerous for the technician taking the breath samples, but can also be harmful and stressful for the animal.

Breath testing with stable isotopes are becoming a more widely method used to test metabolic processes using [^{13}C] labelled compounds in large animal experiment models [1-3]. Breath sampling while the animal is under general anaesthesia has not yet been used due to physical interference with the ventilator. Hence, why this is not a widely used method in a clinical setting it is a non-invasive breath test method. Therefore, for breath testing studies to occur in the future in a large animal model, general anaesthesia would be required to minimise safety risk for the technician and animal.

Typically, stable isotope [^{13}C] breath samples are analysed via isotope-ratio mass spectrometer (IRMS). [^{13}C] Breath testing has been used for a range of tests including detection of *Helicobacter pylori* [4-6], lung cancer detection [7-9], gastric emptying [10] and liver function [11, 12]. In particular ^{13}C-methacetin has been used to predict liver failure posthepatectomy [13] and graft failure [14]. However, some inhalational anaesthesia agents such as nitrous oxide (N_2O) [15, 16] and

isoflurane that are also present in the breath sample have been known to cause interference with the IRMS whereby producing inaccurate results. It is suggested that intravenous anaesthesia is used when breath sampling in large animals is required. To date, only propofol has been used for intravenous anaesthesia in pigs [17]. This study demonstrates the use of other intravenous anaesthetic agents including alfaxalone, ketamine and diazepam, all of which are safe for use in pigs and do not interfere with breath sampling and the IRMS results.

Methods

This study was approved by the University of Adelaide Animal Ethics committee and the Institute of Medical and Veterinary Science Animal Ethics Committee.

Intravenous Anaesthesia

Three pathogen free domestic female pigs were used with a mean (standard deviation) weight of 45.2 (6.7) kg. Each animal was initially sedated with 15 mg/kg of ketamine (Ketamil®, Ilium, Australia) administered intramuscularly. This was followed two minutes later by a secondary intramuscular injection of 2.5 mg/kg alfaxalone (Alfaxan®, Jurox Pty Ltd, Australia). Once the animal was sedated, it placed on the surgical table and another dose of 2.5 mg/kg alfaxalone was administered intravenously via an ear vein. An endotracheal tube was inserted and connected to the ventilator. A 16G x 13 cm intravenous catheter (Angiocath™, BD

Australia) was inserted into the external jugular vein and saline drip line attached and set at 500 mL/hr. To the same intravenous line, alfaxalone was administered at a rate of 500 mg per hour using a syringe pump (P3000 syringe pump, IVAC Medical Systems). It was noted that alfaxalone alone caused the heart rate to rise dangerously above 200 bpm, therefore 30 mg (3 mL) of Ketamine and Diazepam (Pamlin injection®, Parnell Laboratories, Australia) were administered intravenously, alternately every 30 minutes to maintain the heart rate at around 150 bpm. If the heart rate was less than 150 bpm at the 30 minute interval, no ketamine or diazepam was administered until the heart rate was above 150 bpm.

Breath Sampling Apparatus

Breath samples were collected in two vacuum sealed 12 mL Exetainer® vials with a rubber septa (Labco®, Labco®, Ceredigion, United Kingdom). As Exetainer® are the same diameter as standard blood collecting tubes, breath samples can be collected using a blood transfer device (BD® Vacutainer®). The blood transfer device is fitted to a three-way tap (BD Conneta™) using a double male leur lock adapter (Argon Medical Devices) (Figure 1). This can then be fitted between the filter and sampling line using the free ends of the three way tap (Figure 2). The Exetainers® were then manually pressed down in the transfer device, piercing the septa in time with the exhalation of the animal.

Liver Function Test

Each animal had an 8 mm diameter anastomoses was created between the portal vein and inferior vena cava to impair liver function. Liver function was measured by the production of [^{13}C] labelled carbon dioxide [$^{13}CO_2$] in the breath. Intravenous doses of ^{13}C-methacetin (dose 2 mg/kg) were rapidly made into the portal vein with the anastomoses open and then closed. Breath samples were collected in duplicate every two minutes until 40 minutes elapsed.

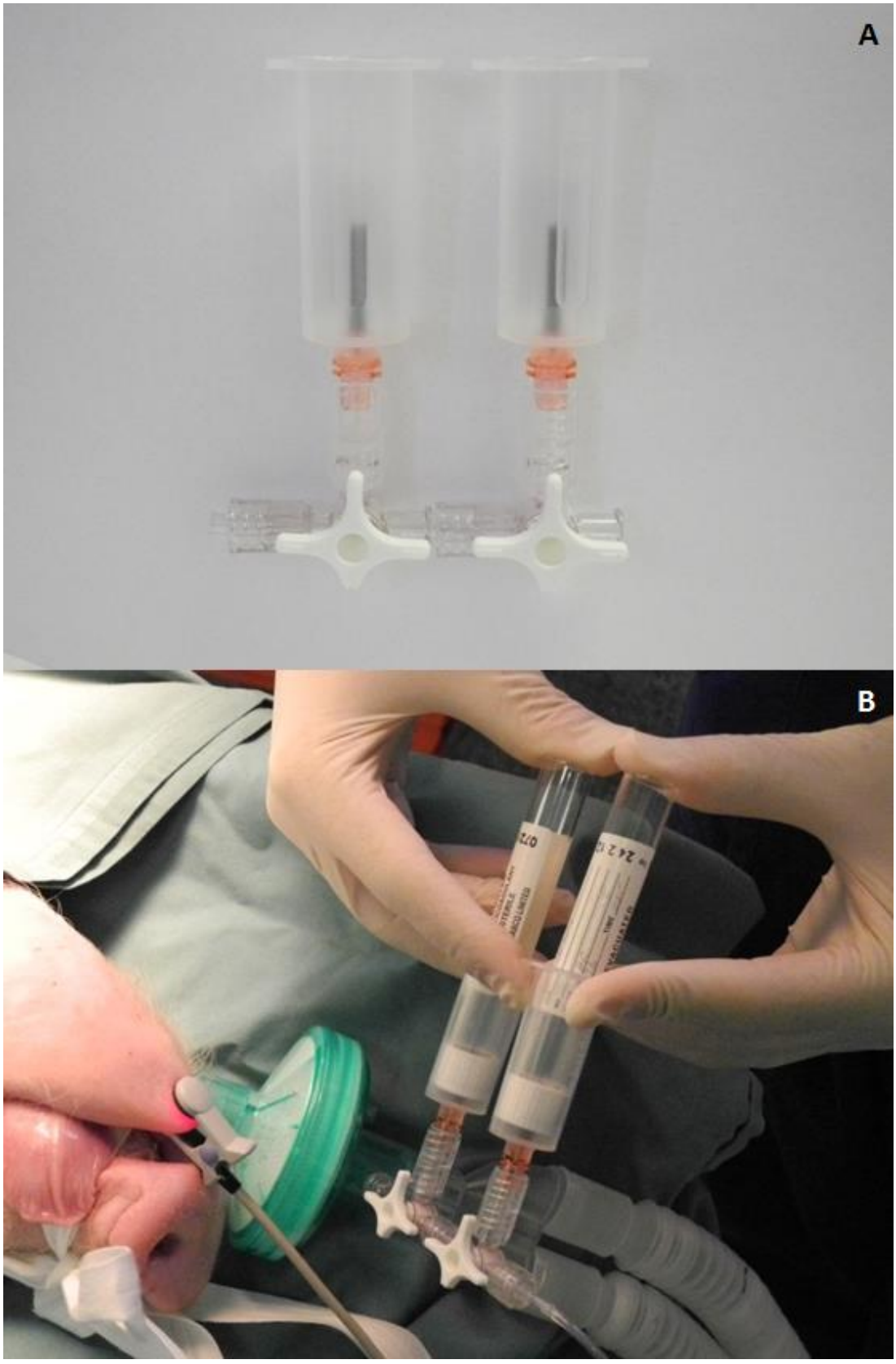

Figure 1: (**A**) Breath sample collecting apparatus consisting of two standard blood transfusers, a male to male luer lock adapter and two three way taps that (**B**) connect to the monitoring line of the anaesthesia machine. This allows uninterrupted air flow and non-invasive breath sampling.

Results

The breath sampling apparatus is a quick, inexpensive and efficient method for breath sampling while the animal is sedated. Each breath sample contained more than 2% CO_2 when the sample was timed with the ventilator. The $^{13}CO_2$ showed normal liver function in the control and a 43% reduction in liver function was observed when the liver function was impaired with the portocaval anastomoses. This demonstrates that the breath sampling apparatus designed is a sufficient tool for breath sampling when determining liver function.

Discussion

The materials for this particular setup are inexpensive and can be readily found in most clinics, hospitals or veterinary hospitals. The advantage of using this setup is that no stress is caused to the animal and it is safe for the technician to collect reliable breath samples at specific time points. Conscious animals may resist and therefore sampling at specific time points may not be physically possible. This is particularly important when using, large animals that weigh more than 30 kg as there are increased safety risks for the technician and animal if the animal is not properly restrained. General anaesthesia removes these risks, but the anaesthesia should only be performed by a veterinarian or trained technician. Previous studies [1] have used young pigs that weigh less than 10 kg and can be easily restrained and held.

Regardless of the weight of the animal, this breath sampling method is most useful for real time or continuous breath sampling analysis during a surgical procedure without having to interfere with the endotracheal tube and the air supply to the animal. However, sampling must be precisely timed with the respirator otherwise only pure oxygen inhaled will captured in the sampling tube. This apparatus and vial can only hold 12 mL vials, which is also suited for the IRMS. Other methods such as non-dispersive isotope-selective infrared spectrometry for breath analysis require larger or continuous samples, but are not suitable for breath sampling while the animal is under anaesthesia as oxygen can affect the results [18].

The main limitations with this breath sampling method is that inhalational anaesthetics cannot be used. In particular, N_2O has mass overlap at 44 g/mol with CO_2 and cannot be differentiated by the IRMS [15, 16]. Additionally, another inhalational anaesthetics were showen to rapidly degrade the gas chromatography column within the IRMS (unpublished data).

The anaesthesia agent alfaxalone is a common intravenous and intramuscular anaesthetic for cats and dogs, but does produce stable sedation in pigs when used in conjunction with ketamine and diazepam. Alfaxalone caused the heart rate to rise >200 bpm, hence the addition of ketamine and diazepam in alternating intervals to reduce the heart rate to approximately 150 bpm. The use of alfaxalone, diazepam and ketamine can be suitable anaesthesia agents for pigs when anaesthesia is required for either short or long periods. However this is a more expensive option than inhalational anaesthetics. Additionally, other continuous

intravenous anaesthetics that may be suitable either singularly or a combination are propofol, midazolam and sufentanil [17, 19, 20].

Conclusion

Breaths testing with stable isotopes is becoming more common in large animal studies. This causes concern for the safety of the technician and also stress for the animal, unless they are sedated. The breath sampling device was designed using common hospital equipment so the samples could be analysed by an IRMS. However, the gas chromatography column in the IRMS is susceptible to certain inhalational anaesthetic agents, therefore intravenous anaesthesia is required.

Acknowledgements

We acknowledge the staff at the Department of Gastroenterology, Womens and Children's Hospital, including Professor Simon Barry, Ms Betty Zacharakis and Ms Esther Burt for their assistance in analysing the breath samples. We also acknowledge Mr Matthew Smith for monitoring the pig's anaesthesia. There were no conflicts of interest.

References

1. Terry R, van Wettere WH, Whittaker AL, Herde PJ, Howarth GS. Using the noninvasive (13)C-sucrose breath test to measure intestinal sucrase activity in swine. Comparative Medicine. 2012;62(6):504-7
2. Bauchart-Thevret C, Stoll B, Benight NM, Olutoye O, Lazar D, Burrin DG. Supplementing monosodium glutamate to partial enteral nutrition slows gastric emptying in preterm pigs. Journal of Nutrition. 2013;143(5):563-70
3. Danicke S, Diers S. Effects of ergot alkaloids in feed on performance and liver function of piglets as evaluated by the (1)(3)C-methacetin breath test. Archives of Animal Nutrition. 2013;67(1):15-36
4. Klein PD. ^{13}C breath tests: visions and realities. Journal of Nutrition. 2001;131(5):1637S-42S
5. Braden B, Lembcke B, Kuker W, Caspary WF. 13C-breath tests: Current state of the art and future directions. Digestive and Liver Disease. 2007;39(9):795-805
6. Cutler AF, Havstad S, Ma CK, Blaser MJ, Perez-Perez GI, Schubert TT. Accuracy of invasive and noninvasive tests to diagnose Helicobacter pylori infection. Gastroenterology. 1995;109(1):136-41
7. Bajtarevic A, Ager C, Pienz M, Klieber M, Schwarz K, Ligor M, Ligor T, Filipiak W, Denz H, Fiegl M, Hilbe W, Weiss W, Lukas P, Jamnig H, Hackl M, Haidenberger A, Buszewski B, Miekisch W, Schubert J, Amann A. Noninvasive detection of lung cancer by analysis of exhaled breath. Biomed Central Cancer. 2009;9:348
8. Phillips M, Cataneo RN, Cummin AR, Gagliardi AJ, Gleeson K, Greenberg J, Maxfield RA, Rom WN. Detection of lung cancer with volatile markers in the breath. Chest. 2003;123(6):2115-23
9. McCulloch M, Jezierski T, Broffman M, Hubbard A, Turner K, Janecki T. Diagnostic accuracy of canine scent detection in early- and late-stage lung and breast cancers. Integrative Cancer Therapies. 2006;5(1):30-9
10. Uchida M, Yoshida-Iwasawa K. Simultaneous measurement of gastric emptying and gastrocecal transit times in conscious rats using a breath test after ingestion of [1-13C] acetic acid and lactose-[13C] ureide. Journal of Smooth Muscle Research. 2012;48(4):105-14
11. Miura Y, Washizawa N, Urita Y, Imai T, Kaneko H. Evaluation of remnant liver function using 13C-breath tests in a rat model of 70% partial hepatectomy. Hepato-Gastroenterology. 2012;59(114):311-6
12. Stockmann M, Lock JF, Riecke B, Heyne K, Martus P, Fricke M, Lehmann S, Niehues SM, Schwabe M, Lemke AJ, Neuhaus P. Prediction of postoperative outcome after hepatectomy with a new bedside test for maximal liver function capacity. Annals of Surgery. 2009;250(1):119-25
13. Stockmann M, Lock JF, Malinowski M, Niehues SM, Seehofer D, Neuhaus P. The LiMAx test: a new liver function test for predicting postoperative outcome in liver surgery. HPB (Oxford). 2010;12(2):139-46
14. Stockmann M, Lock JF, Malinowski M, Seehofer D, Puhl G, Pratschke J, Neuhaus P. How to define initial poor graft function after liver

transplantation? - a new functional definition by the LiMAx test. Transplant International. 2010;23(10):1023-32
15. Sirignano C, Neubert RE, Meijer HA. N_2O influence on isotopic measurements of atmospheric CO_2. Rapid Communications in Mass Spectrometry. 2004;18(16):1839-46
16. Assonov SS, Brenninkmeijer CA. On the N_2O correction used for mass spectrometric analysis of atmospheric CO_2. Rapid Communications in Mass Spectrometry. 2006;20(11):1809-19
17. Gaviria E, Restrepo J, Marin J, Arango G, Aramburo D, Franco F, Tintinago L. Evaluation of propofol as an anesthetic in swine tracheal transplant surgery. Revista Colombiana de Ciencias Pecuarias. 2007;20:447-54
18. Riecke B, Neuhaus P, Stockmann M. Major influence of oxygen supply on 13CO2:12CO2 ratio measurement by nondispersive isotope-selective infrared spectroscopy. Helicobacter. 2005;10(6):620-2
19. Hedenqvist P, Edner A, Fahlman A, Jensen-Waern M. Continuous intravenous anaesthesia with sufentanil and midazolam in medetomidine premedicated New Zealand white rabbits. Biomed Central Veterinary Research. 2013;9:21
20. Mistraletti G, Mantovani ES, Cadringher P, Cerri B, Corbella D, Umbrello M, Anania S, Andrighi E, Barello S, Di Carlo A, Martinetti F, Formenti P, Spanu P, Iapichino G. Enteral vs. intravenous ICU sedation management: study protocol for a randomized controlled trial. Trials. 2013;14(1):92

Appendix L – Portosystemic shunt fraction determination by pharmacokinetic modelling

Statement of Authorship

Title of Paper	Portosystemic shunt fraction determination by pharmacokinetic modelling
Publication Status	○ Published, ○ Accepted for Publication, ● Submitted for Publication, ○ Publication style
Publication Details	Intended for publication.

Author Contributions

By signing the Statement of Authorship, each author certifies that their stated contribution to the publication is accurate and that permission is granted for the publication to be included in the candidate's thesis.

Name of Principal Author (Candidate)	Todd Matthews		
Contribution to the Paper	Designed study, assisted with surgery procedure, performed experimental procedures, collected and analysed samples and data, wrote manuscript draft.		
Signature		Date	8/11/13

Name of Co-Author	Michael Weiss		
Contribution to the Paper	Assisted in design study, analysed data, developed pharmacokinetic model.		
Signature		Date	11-7-2013

Name of Co-Author	Peng Li		
Contribution to the Paper	Assisted in sampled collection and analysis		
Signature		Date	8/11/2013

Name of Co-Author	Markus Trochsler		
Contribution to the Paper	Assisted in surgical procedure and data analysis.		
Signature		Date	8/11/2013

Title: Portosystemic shunt fraction determination by pharmacokinetic modelling

Authors:

Matthews T[1], Weiss M[2], Li P[3], Trochsler M[1], Hamilton M[1], Roberts M[3], Maddern G[1]

[1] Discipline of Surgery, University of Adelaide, The Queen Elizabeth Hospital, Woodville South, South Australia.

[2] Section of Pharmacokinetics, Department of Pharmacology, Martin Luther University Halle-Wittenberg, Halle, Germany.

[3] School of Pharmacy and Medical Sciences, University of South Australia, Basil Hetzel Institute for Translational Health Research, Woodville South, South Australia

CORRESPONDING AUTHOR:

Prof. G.J Maddern
University of Adelaide Discipline of Surgery
The Queen Elizabeth Hospital
28 Woodville Road
Woodville South
SA 5011
Australia
Ph: +61 8 8222 6756
Fax: +61 8 8222 6028
Email: guy.maddern@adelaide.edu.au

AUTHOR EMAILS

todd.matthews@adelaide.edu.au
michael.weiss@medizin.uni-halle.de
peng.Li@unisa.edu.au
markus.trochsler@health.sa.gov.au
mark.hamilton@health.sa.gov.au
m.roberts@uq.edu.au
guy.maddern@adelaide.edu.au

ABSTRACT:

INTRODUCTION

A portosystemic shunt is defined as a congenital or acquired abnormal blood vessel that diverts a portion or all of the hepatic portal blood into the systemic system. Portosystemic shunts are commonly recognised in patients with cirrhotic liver disease as a compensatory mechanism for the associated portal hypertension. In contrast, some congenital and naturally acquired portosystemic shunts have been recognised in healthy individuals or in patients with non-cirrhotic liver disease. Such portosystemic shunts have mostly been serendipitously detected by computed tomography and Doppler ultrasound, however small and microscopic portosystemic shunts can easily be undetected. Therefore a diagnostic technique is needed to capture all portosystemic shunts. The LiMON® system is typically used to test liver function, but could be used as a plausible technique for the detection of portosystemic shunts. Therefore, this study aimed to develop a technique and model for detection and quantification of portosystemic shunts using the LIMON® system.

METHODOLOGY

An 8 mm diameter portocaval shunt was created in six pigs. Indocyanine green was injected into the portal vein with blood samples and LiMON® readings collected simultaneously. The process was repeated with the PSS clamped as the control. The data was then modelled using ADAPT 5® software (Biomedical Simulations Resource).

RESULTS AND CONCLUSIONS

Results depict significantly shorter transit times in the shunted model. This data was modelled further to create a formula that estimates the percentage of blood bypassing the liver. This pilot study presents a novel technique for the detection and quatification of PSS, however further validation is required.

Introduction

A portosystemic shunt (PSS) is defined as a congenital or acquired abnormal blood vessel that diverts a portion or all of the hepatic portal blood into the systemic system [1, 2]. Consequently the diverted blood does not pass through the liver sinusoidal parenchyma. Portosystemic shunts developing after birth may develop *de novo*, as a consequence of disease or as a result of human intervention, but still little is known about them.

Portosystemic shunts are anatomically divided into two groups – extrahepatic and intrahepatic. Additionally, extrahepatic PSS are known of Abernethy types I and II [3-5] and intrahepatic are known as Park types I to IV[6-8] depending on their location and number in the liver.

PSSs are commonly recognised in patients with cirrhotic liver disease as a compensatory mechanism for the associated portal hypertension [9]. In contrast, congenital and naturally acquired PSSs have been diagnosed in healthy individuals or in patients with non-cirrhotic liver disease [1, 2]. Such PSSs have usually been incidentally detected. As such, the true incidence, cause and pathological value of PSSs in both healthy patients.

It is also thought that PSS may have an impact on gastrointestinal cancer distribution, in particular colorectal cancer. Over a four year period, 754 patients were diagnosed with gastrointestinal cancer, including 12% being diagnosed colorectal cancer. Interestingly, 6% of the colorectal cancer patients were also diagnosed with isolated secondary lung metastases [10]. Tan *et al.* [10] estimated

that between 1.7 - 7.2% of colorectal cancer patients have isolated secondary lung metastases. Theoretically, cancers spreading via the bloodstream should be trapped by the liver, rather than progress further and generate distant metastases. One possible theory to this obscure metastatic distribution phenomenon is that PSSs play a role in facilitating the distribution of circulating tumour cells, however this remains to be investigated as there are no standardised clinical tests for PSS detection.

Current methods for PSS detection are radiological based with computed tomography (CT) and Doppler ultrasound, [1]. Current detection methods available can only detect large PSSs and can easily miss small PSSs, with microscopic PSS being not detectable at all. Therefore a PSS detection method that can also capture microscopic PSS would be greatly beneficial.

This study aimed to determine if PSSs can be detected using the transit times of Indocyanine green (ICG). ICG retention and elimination has been well established as a liver function test with the use of pulse spectrophotometry [11-14]. Currently, the LiMON® system (Pulsion®, Germany) is the only spectrophotometry device, for the use of detection ICG available in Australia [15]. Typically the LiMON® system is used to measure liver function [15-17], but more recently, it has been used for prediction of post-hepatectomy liver failure [18].

If viewed as a two compartment model, with different flow rates through each compartment (shunt and liver), a difference in lag time may demonstrate a PSS.

This decreased lag time, also known as arrival time has been viewed in cirrhotic patients with a large degree of shunting when using Doppler ultrasound with a microbubble contrast [19] and radiolabelled red blood cells [20].

Materials and Methods

Animal Study

This study was approved by the University of Adelaide Animal Ethics Committee and the Institute of Medical and Veterinary Science Animal Ethics Committee. Ethical guidelines were followed according the National Health and Medical Research Council (NHMRC, Australia) [21]. Six pathogen free domestic female pigs were used in this pilot study with median weight 45 kg (33 – 55 kg) to create an Abernethy Type II PSSs and assess the pharmacokinetics of ICG in the presences of a PSS. After the surgery was completed and all samples collected the pig was euthanized with a lethal dose of >100 mg/kg of sodium pentobarbitone.

Portosystemic Shunt Surgical Procedure

To represent all types of PSS, an Abernethy Type II PSS connecting the portal vein to the inferior vena cava (IVC) was performed. Briefly, under general anaesthesia, a midline laparotomy was performed. Intravenous access was gained by a central venous catheter. The pig was heparinised with a weight appropriate dose of heparin (80 units/kg). End-to-side anastomosis of the portosystemic shunt was

performed using 8 mm diameter polytetrafluoroethylene (PTFE) between the portal vein and infrahepatic vena cava. Cannulae are introduced into the portal circulation and infrahepatic vena cava. Flow direction was confirmed using pressure differences between the portal vein, mean of 1.8 (0.5) mmHg) and infrahepatic vena cava, mean of -4 (1.2) mmHg (p=0.001).

Indocyanine Green Detection

A LiMON® disposable sensor was attached to the bottom lip of the pig and reinforced with surgical tape. The LiMON® machine was left to stabilise for several minutes. The machine was then connected to a computer so the raw data files could be recorded using the supplied software (LIMONWin, version 1.x; Pulsion Medical Systems AG, Germany). ICG was administered through the large lumen (16G) catheter which was previously inserted into the portal vein. The LiMON® machine was then started with a 10 second count down and ICG was injected at the end of the countdown, followed by 5 mL of saline to flush the catheter.

Two ICG injections (dose 25mg/kg) were administered, in less than 2 seconds, in the portal system (portal vein) with he shunt open and then into the portal system with the shunt closed (control). An additional dose was administered into the IVC to determine the time between the confluence of the hepatic veins and the LiMON® sensor. After each dose, lines were immediately flushed with 3 mL saline solution.

To demonstrate the minimum and approximate transit times of the shunt and the control respectively, two doses of ICG was administered directly into the shunt and then into the portal vein above the shunt In three pigs.

The LiMON® machine rapidly takes sample points at a rate of 25 – 30 points per second. For consistency, only the first sample from each second was used. The LiMON® data was collaborated against the blood samples at the corresponding times. The average ratio between the LiMON® data and the blood samples is calculate, then applied to the LiMON® data to provide a relative blood concentration.

Plasma Sample Collection

Blood samples were collected from the large lumen catheter (16G) inserted into the IVC. Samples were rapidly collected at a rate of 1vmL every 10 seconds for two minutes, then every two minutes until 20 minutes elapsed, and then every five minutes until 40 minutes had elapsed. Blood samples were then transferred into 1.5 mL microtubes with 20 µL heparin. All samples were agitated for five seconds then centrifuged for ten minutes at 25000 x g. The supernatant was separated and placed in new 1.5 mL microtubes for storage at minus 80 degrees Celsius.

High Performance Liquid Chromatography (HPLC)

Indocyanine green was assayed via high-performance liquid chromatography (HPLC). The HPLC system consisted of a Shimadzu SCL-10A VP system controller, SPD-10A UV-VIS spectrophotometric detector, LC-10AT pump controller and Gastorr GT-102 pump and a Waters Symmetry C18 5 µm 3.9 x 150 mm steel cartridge column with a Securityguard™ (Phenomenex®) column guard.

Samples were prepared by adding 900 µL of methanol to 300 µL plasma sample in a micro centrifugation tube. The samples were agitated for 20 seconds to ensure complete coagulation of the proteins. The prepared sample was then centrifuged for 10 minutes at 15,000 rpm (25,000 x g). The 200 µL supernatant was then transferred to auto sampler vials for HPLC assay. A standard curve was similarly prepared using the same sample preparation for each of the compounds with known concentrations of 0, 5, 10, 20, 50, 100 µg/mL.

The HPLC method for ICG was based and modified from Soons *et al.* [22]. The optimised method used 45% acetonitrile and 55% phosphate buffer, pH6 as the mobile phase. The UV detector wavelength was set at 790 nm and the retention time of ICG was four minutes.

Control Marker

Evans blue dye (1 mg/kg) was administered post ICG administration as a control as it is not metabolised by the liver. This will enable accurate determination of shunt fraction. Samples were collected every 10 seconds for two minutes, then every 20

seconds till three minutes. Samples were assayed by absorption at 625 nm using a Flurostar Optima® (BMG Labtech).

Shunted fraction was calculated based on the ratio of shunted flow (Q_s) and the portal vein flow (Q_{pv}), where shunted fraction equals $Q_s / Q_{pv.}$ Relative flow rates were calculated by the volume (V) divided by the mean transit time (MTT) (Eq 1).

$$Q = \frac{V}{MTT} \quad \text{.....(Eq. 1)}$$

Results

A student's T-test was used to compare the lag time (threshold of >0.01 µg/mL). There was a significant decrease in the corrected lag time with a mean (standard deviation) of seven (3.3) seconds in the shunted model and 19 (3.7) seconds in the control (p=0.002, n=6) (Table 1). The minimum possible lag time was 3.3 (2.5) seconds for the shunt with an expected control lag time of 17.7 (15.3) (n=3).

The mean transit time (MTT) for ICG was also shorter, but not significant, in the shunted model 61.5 (14.5) seconds as compared to the control of 910.1 (44.1) seconds (p=0.286, n=6).

There was high variability for the MTT in Evans blue. The shunted model MTT was 86.7 (11.1) seconds and 93.0 (15.3) seconds in the control model, p=0.599.

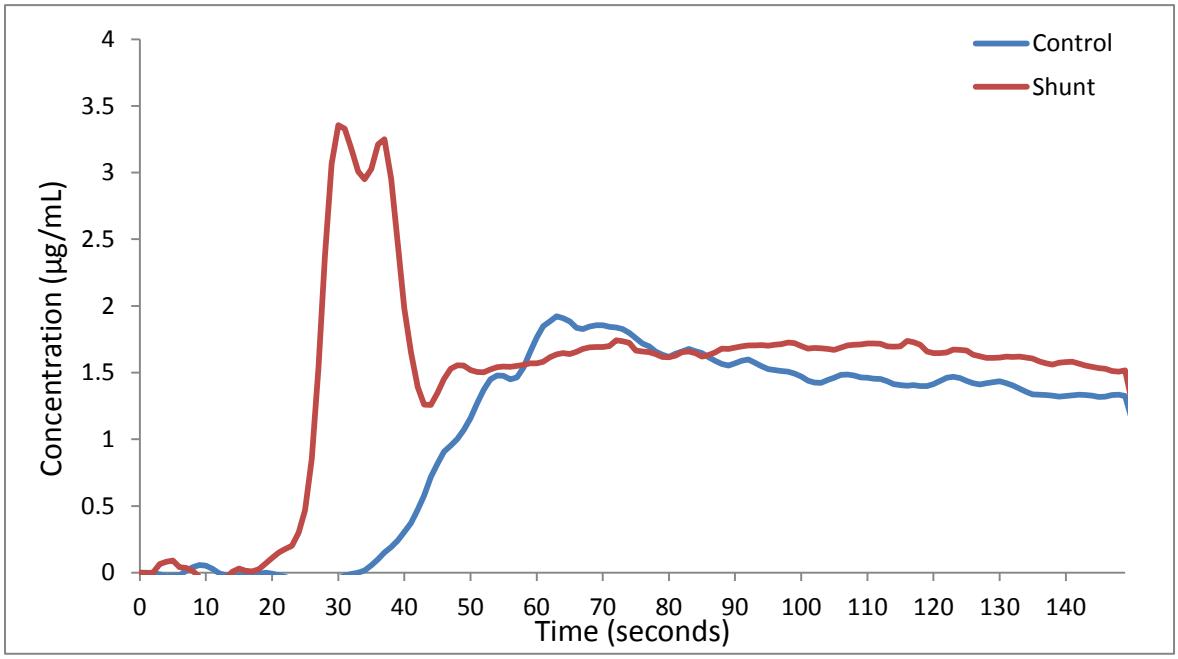

Figure 1: Indocyanine green dye (ICG) concentration the LiMON® (n=6) demonstrating an early peak and consequently a shorter transit time due to the shunt.

Table 1: Corrected Lag times (threshold > 0.01µg/L) and the mean transit times for indocyanine green.

	Lag time (s)			Mean Transit Time (s)		
Pig	**Shunt**	**Control**	**Difference**	**Shunt**	**Control**	**Difference**
1	8	20	12	32.1	179.9	147.8
2	5	18	13	65.4	76.6	11.2
3	10	13	3	68.0	72.5	4.5
4	6	18	12	67.2	69.4	2.2
5	11	24	13	69.1	73.2	4.1
6	2	21	19	67.3	68.7	1.4
Mean (SD)	7 (3.3)*	19 (3.7)*	12 (5.1)	61.5 (14.5)	90.1 (44.1)	28.5 (58.5)

*p=0.002

Pharmacokinetic Modelling

Model development was adapted as a single pass system from Weiss *et al* [23, 24] using the software ADAPT 5 (Biomedical Simulations Resource, University of Southern California). The shunted liver was modelled using an inverse Gaussian density function ($f_I\,(t)$), based on the first pass transit times (TTD) of ICG (Eq. 2).

$$f_{2IG}(t) = q\,f_1(t) + (1\text{-}q)\,f_2(t) \quad \text{..... (Eq. 2)}$$

Based on the experimental design shown in Figure 3, the data was truncated before there was a contribution by recirculation. First, the control data (no shunt) was fitted to a single TTD, (f_L (t)). The mean transit time, MTT_L, and relative dispersion (RD_L^2) of the liver could then be calculated. The fraction of blood flow of and the shunt (1-q) can be determined by the TTD through the shunt (f_S (t)). The total function ($f_{LS}(t)$) and ratio of blood bypassing the liver can then be determined by the collaboration of the liver and shunted functions (Eq. 3) (Figure 4).

$$f_i(t) = \sqrt{\frac{MTT_i}{2\pi RD_i^2 t^3}}\exp\left[-\frac{(t-MTT_i)^2}{2RD_i^2 MTT_i t}\right] \quad \text{.....(Eq. 3)}$$

The parameters of $f_L(t)$ were fixed to those obtained in the control after correcting them for the change in flow, i.e., $MTT_L \rightarrow MTT_L/q$ and $MTT_S \rightarrow MTT_S/q$. The estimated fractions of shunt flow, 1-q ($0 < q < 1$), and R^2 as measure of goodness of fit are 0.99. However, the model was not able to be validated as exact flow rates were not able to be taken at the time of the procedure. As a comparison the shunt fraction can be calculated from Evans blue (Table 3).

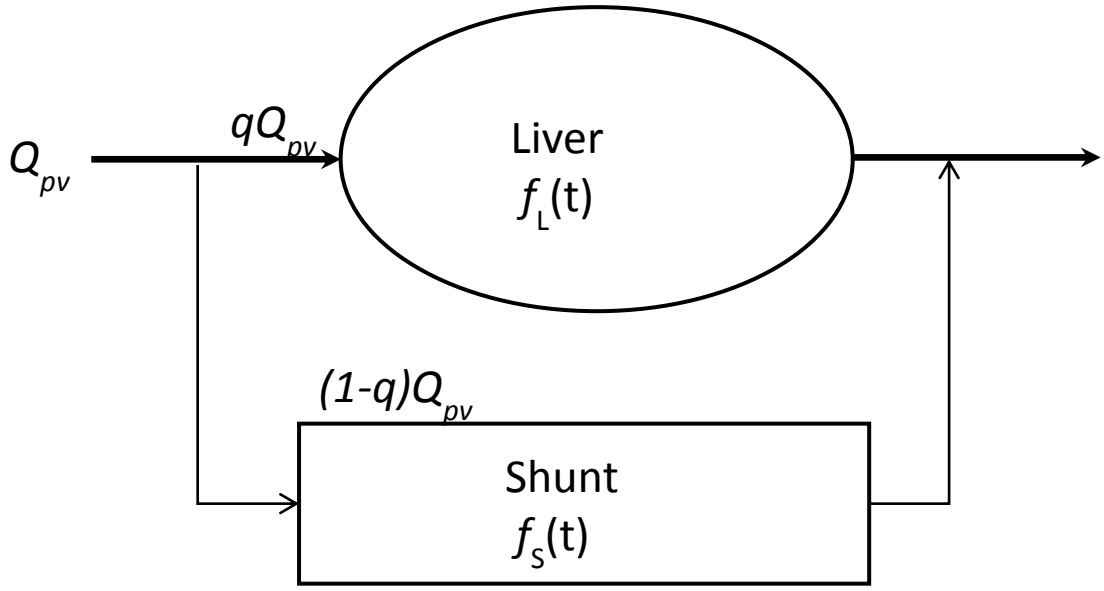

Figure 3: Single pass model of the liver in the presence of a portosystemic shunt. The liver and the shunt are in parallel with blood flows *qQ* and *(1-q)Q* respectively (*Qpv* is portal flow, and 0<*q*<1). The liver and body are individually characterised by inverse Gaussian transit time density functions shown as *fi*(t).

Table 3: Shunt fraction blood using the LiMON® data and its model compared to the ratio as depicted by the mean transit time of Evans blue.

Pig	MTT	Model	R^2
1	0.22	0.52	0.99
2	0.41	0.33	0.99
3	0.71	0.37	0.99
4	0.47	0.46	0.99
5	0.59	0.53	0.99
6	0.58	0.62	0.99
Mean (SD)	0.5 (0.17)	0.46 (0.12)	0.99 (0.01)

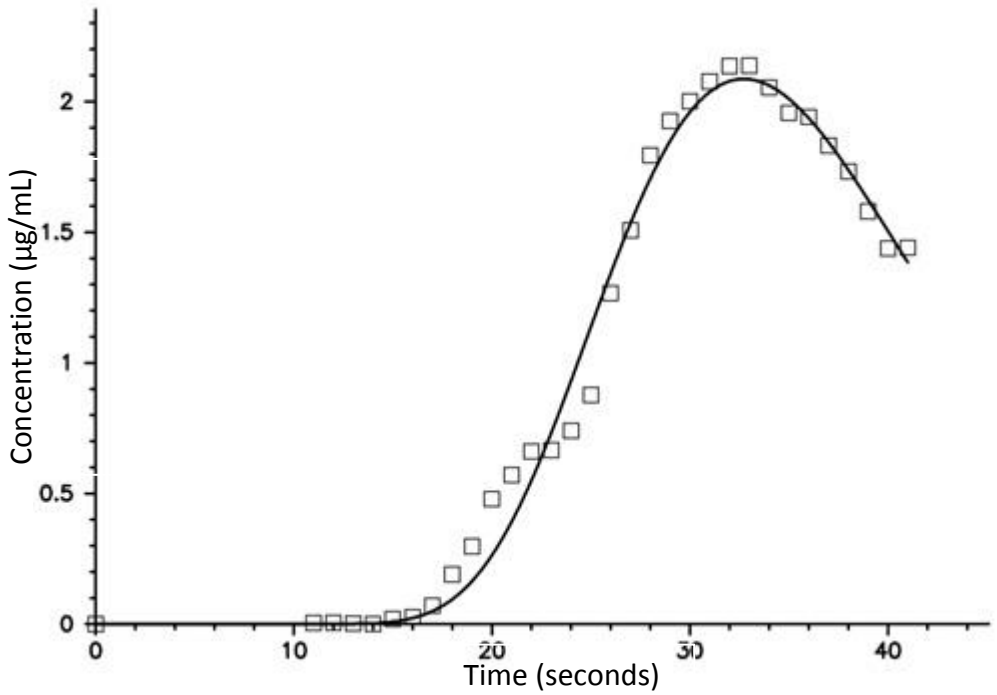

Figure 3: Example of shunt data being fitted to the model f2IG(t) with a 99% correlation coefficient.

Discussion

The two compartmental pharmacokinetic modelling is a necessary step in not only understanding the properties of PSSs, but also developing methods for detection. Upon further validation, the model will provide ways to determine the sensitivity and accuracy of different PSSs without the need for animals. Similarly, it will provide a clear characterisation of a PSS. In its current state, the model was able to provide predictive shunted fractions due to transit times for a large PSS.

ICG binds to plasma proteins [25] and ICG extraction would therefore be proportional to the extraction of the facilitating protein [26]. Therefore, the presence of a PSS would reduce the hepatic extraction of ICG. However, a perfused cirrhotic liver model demonstrated that the intrahepatic PSSs only accounted for a small portion of the decreased ICG extraction [27], thus concluding that reduced ICG extraction was due to impaired hepatocytes. PSSs, especially small PSSs were not clearly discernible using multiple indicator dilution technique, unless using large radio labelled microspheres are used [26, 28]. Despite a small difference of reduced ICG extraction from PSSs, transit times are able to discern differences in cirrhotic livers [19] and can detect PSSs.

Transit times of markers are a key feature that can distinguish hepatic hemodynamic changes in patients with and without shunting. As shown in patients with cirrhosis, there is a significantly shorter transit time compared to patients with

healthy livers using ultrasound [19, 20, 29]. This shift in transit time is similar to patients with known PSSs caused from cirrhosis. However, these studies did not go on to determine the shunted fraction of blood bypassing the liver sinusoids by means of determination by transit time.

The LiMON® system would be ideal for PSS detection as it is minimally invasive, time efficient (<15 minutes) and cost effective (AUD$80 per injection). Due to the LiMON® rapid sampling rate, accurate transit times can be calculated. The transit times of markers are a key feature that can distinguish hepatic hemodynamic changes in patients with and without shunting. As shown in patients with cirrhosis, there is a significantly shorter transit time compared to patients with healthy livers [19, 20]. Previous studies using ultrasound to determine transit times described a shortening in the transit time in the control patients who had liver metastases [19, 29]. This shift is similar to patients with known PSS caused from cirrhosis. The PSS provides a lower resistance, and therefore faster passageway than the liver and therefore reduces the transit times. However, this produces its own limiting factor in determining transit times. To know the transit time through the shunt and liver, ICG must be administered directly into the portal system. If, ICG is administered into the systemic system, the dye may reach the LiMON® sensor before passing through the liver and no transit time differentiation can be defined.

The model used in this study was based on previous work [23, 24, 30] and adapted to determine the fraction of shunted blood using the Adapt 5 software. It is based on inverse Gaussian distributions as TTD for ICG, showing estimated the fraction of shunted blood bypassing the liver. This density function particularly shows first pass time distribution [23] and has been used previously in tracer kinetics [31-33], modelling sorbitol disposition [34] and ICG [23, 24]. The model is simplified to the parameters of two compartments being the liver and the shunt, demonstrating the distribution kinetics of blood flow without recirculation. However, the model was not able to be validated as exact flow rates were not able to be taken at the time of the procedure (due to equipment not readily being available). Instead, the estimated shunted fraction was compared to the shunted fractions based on the MTT of Evans blue dye.

Conclusion

The model and transit times depict a reliable way of determining shunted fractions. By isolating the components of the liver and shunt, the maximum and minimum transit times can be demonstrated relating to the injected compound. Currently, this technique would be limited to colorectal cancer patients undergoing an initial resection, as there is easy access to the portal system for ICG administration. Further studies are required to show accuracy, specificity and limitations of detectable limits.

References

1. Konstas AA, Digumarthy SR, Avery LL, Wallace KL, Lisovsky M, Misdraji J, Hahn PF. Congenital portosystemic shunts: Imaging findings and clinical presentations in 11 patients. European Journal of Radiology. 2011;80(2):175-81
2. Lisovsky M, Konstas AA, Misdraji J. Congenital extrahepatic portosystemic shunts (abernethy malformation): A histopathologic evaluation. American Journal of Surgical Pathology. 2011;35(9):1381-90
3. Abernethy J, Banks J. Account of two instances of uncommon formation, in the viscera of the human body. Philosophical Transactions of the Royal Society of London. 1793;83:59-66
4. Bellah RD, Hayek J, Teele RL. Anomalous portal venous connection to the suprahepatic vena cava: sonographic demonstration. Pediatric Radiology. 1989;20(1-2):115-7
5. Morgan G, Superina R. Congenital absence of the portal vein: two cases and a proposed classification system for portasystemic vascular anomalies. Journal of Pediatric Surgery. 1994;29(9):1239-41
6. Park JH, Cha SH, Han JK, Han MC. Intrahepatic portosystemic venous shunt. American Journal of Roentgenology. 1990;155(3):527-8
7. Doehner GA, Ruzicka FF, Jr., Rousselot LM, Hoffman G. The portal venous system: on its pathological roentgen anatomy. Radiology. 1956;66(2):206-17
8. Mori H, Hayashi K, Fukuda T, Matsunaga N, Futagawa S, Nagasaki M, Mutsukura M. Intrahepatic portosystemic venous shunt: Occurrence in patients with and without liver cirrhosis. American Journal of Roentgenology. 1987;149(4):711-4
9. Tarantino G, Citro V, Esposito P, Giaquinto S, de Leone A, Milan G, Tripodi FS, Cirillo M, Lobello R. Blood ammonia levels in liver cirrhosis: a clue for the presence of portosystemic collateral veins. Biomed Central Gastroenterology. 2009;9:21
10. Tan KK, Lopes Gde L, Jr., Sim R. How uncommon are isolated lung metastases in colorectal cancer? A review from database of 754 patients over 4 years. Journal of Gastrointestinal Surgery. 2009;13(4):642-8
11. Sakka SG, Reinhart K, Meier-Hellmann A. Comparison of invasive and noninvasive measurements of indocyanine green plasma disappearance rate in critically ill patients with mechanical ventilation and stable hemodynamics. Intensive Care Medicine. 2000;26(10):1553-6
12. Iijima T, Aoyagi T, Iwao Y, Masuda J, Fuse M, Kobayashi N, Sankawa H. Cardiac output and circulating blood volume analysis by pulse dye-densitometry. Journal of Clinical Monitoring. 1997;13(2):81-9
13. Hsieh CB, Chen CJ, Chen TW, Yu JC, Shen KL, Chang TM, Liu YC. Accuracy of indocyanine green pulse spectrophotometry clearance test for liver function prediction in transplanted patients. World Journal of Gastroenterology. 2004;10(16):2394-6
14. Imai T, Takahashi K, Goto F, Morishita Y. Measurement of blood concentration of indocyanine green by pulse dye densitometry--comparison

with the conventional spectrophotometric method. Journal of Clinical Monitoring and Computing. 1998;14(7-8):477-84
15. Purcell R, Kruger P, Jones M. Indocyanine green elimination: a comparison of the LiMON and serial blood sampling methods. Australia and New Zealand Journal of Surgery. 2006;76(1-2):75-7
16. Nanashima A, Sumida Y, Morino S, Yamaguchi H, Tanaka K, Shibasaki S, Ide N, Sawai T, Yasutake T, Nakagoe T, Nagayasu T. The Japanese integrated staging score using liver damage grade for hepatocellular carcinoma in patients after hepatectomy. European Journal of Surgical Oncology. 2004;30(7):765-70
17. Wakabayashi H, Ishimura K, Izuishi K, Karasawa Y, Maeta H. Evaluation of liver function for hepatic resection for hepatocellular carcinoma in the liver with damaged parenchyma. Journal of Surgical Research. 2004;116(2):248-52
18. de Liguori Carino N, O'Reilly DA, Dajani K, Ghaneh P, Poston GJ, Wu AV. Perioperative use of the LiMON method of indocyanine green elimination measurement for the prediction and early detection of post-hepatectomy liver failure. European Journal of Surgical Oncology. 2009;35(9):957-62
19. Albrecht T, Blomley MJ, Cosgrove DO, Taylor-Robinson SD, Jayaram V, Eckersley R, Urbank A, Butler-Barnes J, Patel N. Transit-time studies with levovist in patients with and without hepatic cirrhosis: a promising new diagnostic tool. European Radiology. 1999;9 Suppl 3:S377-81
20. Syrota A, Vinot JM, Paraf A, Roucayrol JC. Scintillation splenoportography: hemodynamic and morphological study of the portal circulation. Gastroenterology. 1976;71(4):652-9
21. NHMRC. Australian code of practice for the care and use of animals for scientific purposes. 7th ed. Australia: National Health and Medical Research Council; 2004.
22. Soons PA, Kroon JM, Breimer DD. Effects of single-dose and short-term oral nifedipine on indocyanine green clearance as assessed by spectrophotometry and high performance liquid chromatography. Journal of Clinical Pharmacology. 1990;30(8):693-8
23. Weiss M, Krejcie TC, Avram MJ. Transit time dispersion in pulmonary and systemic circulation: effects of cardiac output and solute diffusivity. Am J Physiol Heart Circ Physiol. 2006;291(2):H861-70
24. Weiss M, Krejcie TC, Avram MJ. A physiologically based model of hepatic ICG clearance: interplay between sinusoidal uptake and biliary excretion. European Journal of Pharmaceutical Sciences. 2011;44(3):359-65
25. Baker KJ. Binding of sulfobromophthalein (BSP) sodium and indocyanine green (ICG) by plasma alpha-1 lipoproteins. Proceedings of the Society for Experimental Biology and Medicine. 1966;122(4):957-63
26. Huet PM, Goresky CA, Villeneuve JP, Marleau D, Lough JO. Assessment of liver microcirculation in human cirrhosis. Journal of Clinical Investigation. 1982;70(6):1234-44

27. Villeneuve JP, Huet PM, Gariepy L, Fenyves D, Willems B, Cote J, Lapointe R, Marleau D. Isolated perfused cirrhotic human liver obtained from liver transplant patients: a feasibility study. Hepatology. 1990;12(2):257-63
28. Varin F, Huet PM. Hepatic microcirculation in the perfused cirrhotic rat liver. Journal of Clinical Investigation. 1985;76(5):1904-12
29. Blomley MJ, Albrecht T, Cosgrove DO, Jayaram V, Eckersley RJ, Patel N, Taylor-Robinson S, Bauer A, Schlief R. Liver vascular transit time analyzed with dynamic hepatic venography with bolus injections of an US contrast agent: early experience in seven patients with metastases. Radiology. 1998;209(3):862-6
30. Weiss M. On the degree of solute mixing in liver models of drug elimination. Journal of Pharmacokinetics and Biopharmaceutics. 1997;25(3):363-75
31. Homer LD, Small A. A unified theory for estimation of cardiac output, volumes of distribution and renal clearance from indicator dilution curves. Journal of Theoretical Biology. 1977;64(3):535-50
32. Millard RK. Indicator-dilution dispersion models and cardiac output computing methods. American Journal of Physiology. 1997;272(4 Pt 2):H2004-12
33. Weiss M. A note on the role of generalized inverse Gaussian distributions of circulatory transit times in pharmacokinetics. Journal of Mathematical Biology. 1984;20(1):95-102
34. Weiss M, Hubner GH, Hubner IG, Teichmann W. Effects of cardiac output on disposition kinetics of sorbitol: recirculatory modelling. British Journal of Clinical Pharmacology. 1996;41(4):261-8

Appendix M – Figure 3.1 Grant of Permission

November 05, 2013

Grant of Permission

Dear Dr. Matthews,

Thank you for your interest in our copyrighted material, and for requesting permission for its use.

Permission is granted for the following subject to the conditions outlined below:

Figure 2, Li P, Wang GJ, Robertson TA, Roberts MS. Liver transporters in hepatic drug disposition: An update. Current Drug Metabolism. 2009;10(5):482-98

To be used in the following manner:

1. Bentham Science Publishers grants you the right to reproduce the material indicated above on a one-time, non-exclusive basis, solely for the purpose described. Permission must be requested separately for any future or additional use.

2. For an article, the copyright notice must be printed on the first page of article or book chapter. For figures, photographs, covers, or tables, the notice may appear with the material, in a footnote, or in the reference list.

Thank you for your patience while your request was being processed. If you wish to contact us further, please use the address below.

Sincerely,

AMBREEN IRSHAD

Permissions & Rights **Manager**
Bentham Science Publishers
Email: ambreenirshad@benthamscience.org
URL: www.benthamscience.com